RECLAMATION
Managing Water in the West

Sacramento and San Joaquin Rivers Basin Study

Basin Study Technical Appendices

U.S. Department of the Interior
Bureau of Reclamation

March 2016

APPENDIX 3A. CMIP3 AND CMIP5 DOWNSCALED CLIMATE MODEL PROJECTIONS

1. Introduction

This technical appendix outlines the salient differences between climate scenarios used in different phases for the Sacramento San Joaquin River Basins Study (SSJBS). The first phase of the study used climate scenarios based on climate model simulations from the Coupled Model Intercomparison Project Phase 3 (CMIP3) (IPCC 2007). These results were presented in the Sacramento and San Joaquin Basins Climate Impact Assessment (SSJBIA) report (Reclamation 2014). The CMIP3 climate model data was the basis for the Intergovernmental Panel on Climate Change (IPCC) Fourth Assessment Report (AR4) released in 2007 (IPCC 2007).

Future climate scenarios used in this phase of the SSJBS are based on climate model simulations from the Coupled Model Intercomparison Project Phase 5 (CMIP5) to ensure that the study reports the most current science available at the time of its release. The CMIP5 (Taylor et al. 2012) climate model data are the basis for the most recently released Intergovernmental Panel on Climate Change (IPCC) Fifth Assessment Report (AR5) (IPCC 2013).

The climate models in the CMIP5 (Taylor et al. 2012; Knutti and Sedlacek, 2012; Polade et al. 2013; Rupp et al. 2013; Seager et al. 2012; Pierce et al. 2013) were driven using a set of newly developed emission scenarios (called Representative Concentration Pathways; RCPs). There are four scenario pathways (RCP2.6, RCP4.5, RCP6.0 and RCP8.5) used in the CMIP5 (van Vuuren et al. 2011). Each Representative Concentration Pathway (RCP) defines a specific emissions trajectory and subsequent radiative forcing (a radiative forcing is a measure of the influence a factor has in altering the balance of incoming and outgoing energy in the Earth-atmosphere system). The RCPs pathways differ from the scenarios used in the IPCC 2007 report (IPCC 2001, 2007) which were developed based a range of possible future GHG emissions using assumptions of fossil fuel use, regional political and social conditions, technologies, population, and governance decisions. Both the current RCPs and the older emission scenarios, labeled as SRES (Special Report on Emission Scenarios) are shown on Figure 3A-1.
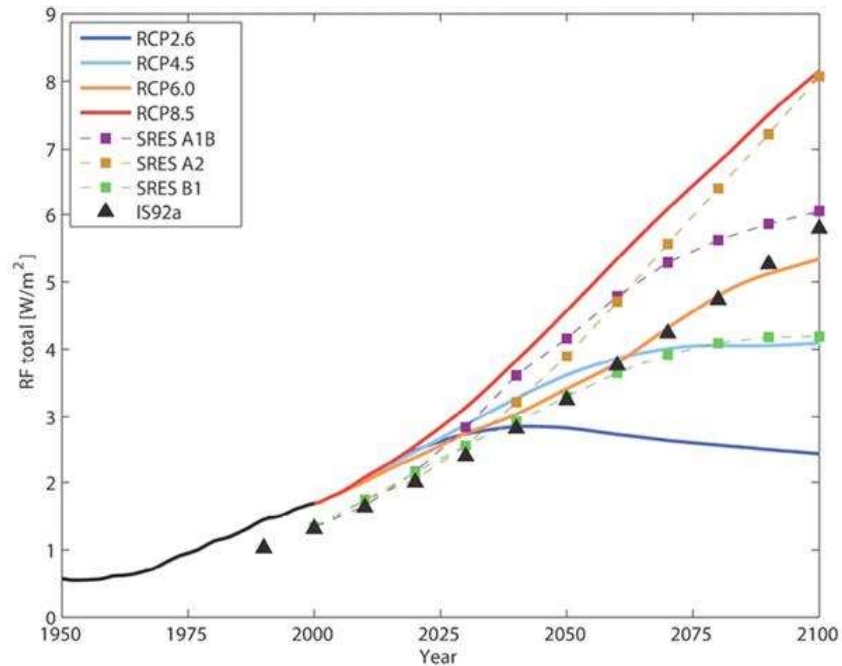
**Figure 3A-1. Comparisons of Total Radiative Forcing From Previous IPCC Assessments
(SAR IS92a, TAR/AR4 SRES A1B, A2 and B1) with RCP Scenarios**
Source IPCC AR5 (2013)

2. Climate Change Scenarios Used in Sacramento San Joaquin River Basins Impact Assessment and Sacramento San Joaquin River Basins Study

Incorporation of climate change in water planning continues to be an area of evolving science, methods, and applications. While precise prediction of future climate is impossible, in both SSJIA and the SSJBS studies, a total of 18 different climate scenarios were used to characterize a wide range of future hydroclimate uncertainties.

Five statistically representative climate scenarios (EI5) were developed using a transient "ensemble informed" approach. These five include one that represents the "central tendency" and four to capture the range of the ensemble uncertainty including: representing drier, less warming (WD); drier, more warming (HD); wetter, more warming (HW); and wetter, less warming (WW) conditions than the median projection (CEN). In addition, a simulation representing continuation of historical climate conditions was included for reference (RF).

Transient EI5 scenarios were developed for the Central Valley Project Integrated Resource Plan (CVP IRP) using the CMIP3 archive (Reclamation 2013). This method is a variant of the climate change scenarios method developed for incorporating climate change in Bay Delta Conservation Plan (BDCP) resource

impact assessments by CH2M HILL in collaboration with Reclamation, California Department of Water Resources (DWR), U.S. Fish and Wildlife Service, and National Marine Fishery Services, developed approaches (DWR 2014).

The EI5 approach maps projected changes in climate derived from an ensemble of downscaled climate model projections to a sequence of observed meteorology using a quantile method. Projected temperature and precipitation for selected 30-year future climatological periods are compared to a historical reference period and the changes are computed. The changes in temperature and precipitation are then mapped onto a historical observed meteorological pattern using a quantile mapping method which transforms the historical records into a modified sequence that incorporates the projections of future climate change. The result of the quantile mapping approach is a daily time series of temperature and precipitation that incorporates the natural variability observed in the historic record, but with statistical shifts that reflect the changes in climate properties (both mean and expanded variability) found in the downscaled climate projections. Since the sequence of future climate variability (wet/dry periods) is unknown, the transient ensemble informed method could be applied with any sequence of an observational, paleo-reconstructed, or synthetic "stationary" climate record.

In addition to the EI5 scenarios, twelve individual downscaled GCM projections were selected from six different GCMs and two different emission scenarios. One reference climate scenario was developed which included historical climate. Table 3A-1 summarizes the climate scenarios used in the SSJIA and SSJBS. Climate scenarios used in SSJIA was developed based on CMIP3, while the climate scenarios used in the SSJBS was generated based on CMIP5.

Table 3A-1. Climate Scenarios Used in the SSJIA and SSJBS

Scenario	Description	Emission Scenarios
Climate Scenarios Used in SSJIA (based on CMIP3)[1]		
RF	Reference Climate	This scenario was developed based on Livneh et al. (2013) reflecting the observed natural variability sequence for 1915-2003
WD	Drier and less warming	Derived from projections that include SRES A1B, A2, and B1
HD	Drier and more warming	Derived from projections that include SRES A1B, A2, and B1
HW	Wetter and more warming	Derived from projections that include SRES A1B, A2, and B1
WW	Wetter and less warming	Derived from projections that include SRES A1B, A2, and B1
CEN	Central tending climate scenario	Derived from projections that include SRES A1B, A2, and B1

Scenario	Description	Emission Scenarios
CAT Scenarios (Total 12 CAT scenarios) (Cayan et al. 2009)	California's CAT scenarios were developed to be used in the 2009 update of the California Water Plan.	The A2 scenario represents the higher emission levels, while the B1 represents lower emission levels
Climate Scenarios Used in SSJBS (based on CMIP5)[2]		
RF	Reference Climate	This scenario was developed using a newly developed historical climate daily data constructed based on monthly PRISM (Daly et al., 1994) and daily Livneh et al. (2013) reflecting the observed natural variability sequence for 1922-2010
WD	Drier and less warming	Derived from projections that include RCP4.5, RCP6.0 and RCP8.5
HD	Drier and more warming	Derived from projections that include RCP4.5, RCP6.0 and RCP8.5
HW	Wetter and more warming	Derived from projections that include RCP4.5, RCP6.0 and RCP8.5
WW	Wetter and less warming	Derived from projections that include RCP4.5, RCP6.0 and RCP8.5
CEN	Central tending climate scenario	Derived from projections that include RCP4.5, RCP6.0 and RCP8.5
CCTAG Scenarios (Total 12 CCTAG scenarios)	DWR CCTAG scenarios were developed to use in climate studies in California.	The RCP8.5 scenario represents the higher emission levels, while the RCP4.5 represents lower emission levels

Notes:

[1]EI5 for the SSJIA were developed using 112 climate projections from 16 different GCMs using the SRES emission scenarios A2, A1B, and B1, which had been bias-corrected spatially downscaled (BCSD) by Reclamation and others (Maurer et al., 2007). Projected changes in three future periods centered around 2025 (2011-2040), 2055 (2041-2070) and 2084 (2070-2099) were computed with respect to 1971-2000. The projected changes were mapped to the to the observed natural variability sequence over 1915-2003 in Livneh et al. (2013).

[2]EI5 for the SSJBS were developed from 175 climate projections generated from 36 different GCMs using the RCP emission scenarios RCP8.5, RCP6.0, and RCP4.5, which had been bias-corrected spatially downscaled (BCSD) by Reclamation and others (Reclamation, 2013). The climate projections simulated under RCP2.6 were not considered in the ensemble to develop EI5. RCP2.6 assumes drastic policy intervention; greenhouse gas emissions are reduced almost immediately, leading to a slight reduction on today's levels by 2100 (van Vuuren et al. 2011). Projected changes in three future periods centered around 2025 (2011-2040), 2055 (2041-2070) and 2084 (2070-2099) were computed with respect to 1981-2010. The projected changes were mapped to the observed natural variability sequence over 1922-2010 developed based on monthly PRISM (Daly et al., 1994) and daily Livneh et al. (2013).

3. Summary of Projected Changes in Temperature and Precipitation between CMIP3 and CMIP5 Archives

A set of graphs and tables were prepared to help illustrate the temperature and precipitation changes in the climate scenarios used in the SSJIA and SSJBS. The following sections discuss some of the results using the CEN climate change scenario developed based on the CMIP3 and CMIP5 ensembles.

3.1 Future Climate – Ensemble Informed Scenario

Figure 3A-2 shows the annual mean temperature and precipitation changes for California and Nevada derived from the CEN climate change scenario based CMIP3 and CMIP5 ensembles for the period of 2070-2099. While increased warming is consistent between CMIP3 and CMIP5 for entire region, inland valley and mountain ridges are projected to exhibit a larger degree of warming in the CMIP5 projections. The CMIP5 ensemble also suggest a significant reduction in the areas projected to be drier in the future as compared to the CMIP3 ensemble. The CMIP5 ensemble also provides greater clarity of wetter conditions in the Sacramento Valley, while suggesting more neutral (little change) projections for San Joaquin and Tulare Basins. The CMIP5 ensemble continues to project future drier conditions in the Southern California, but to a lesser degree as compared to the CMIP3 ensemble.

Tables 3A-2 and 3A-3 summarize future changes in mean annual temperature and precipitation in the Sacramento River, San Joaquin River, and Tulare Lake hydrologic regions for median climate change scenario (CEN) developed based on CMIP3 and CMIP5 archives. For both CMIP3 and CMIP5 based CEN climate scenario, air temperatures are projected to increase for all three hydrologic regions. The CEN suggests increase of air temperature between 1.8°C to 2°C by 2050 and between 2.5°C to 2.8°C by end of century. CEN based on CMIP5 projects slightly higher warming in the end of century.

While the median climate change scenario (CEN) developed based on the CMIP3 ensemble suggests only a slight increase in annual precipitation for Sacramento hydrologic region, the CEN based on the CMIP5 ensemble suggests an increase by about 2% by mid-century and about 4% by end of century (Table A-3). For San Joaquin and Tulare Lake hydrologic regions, the median climate change scenario (CEN) developed based on the CMIP3 ensemble suggests a slight decrease in precipitation be end of century, but the CEN based on the CMIP5 ensemble suggests an increase by about 2.5% and 1.5%, respectively.[1]

---

[1] These are quite small changes compared to California's large natural (historical) coefficients of variability. Note that CMIP5 models and ensemble are not on the whole more experienced nor longer in development than the CMIP3 models.

Temperature Change (CMIP3)
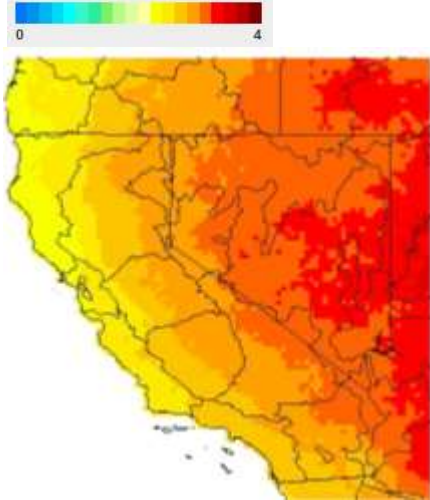
2084

Temperature Change (CMIP5)

2084

Precipitation Change (CMIP3)
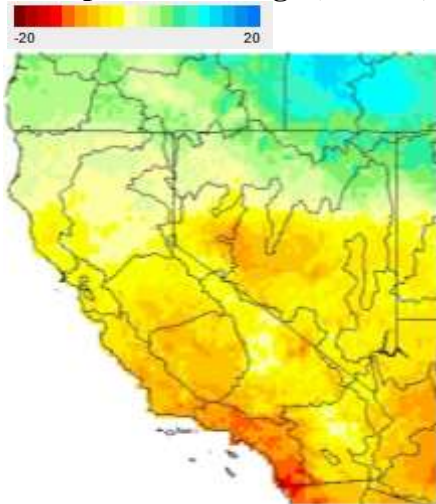
2084

Precipitation Change (CMIP5)
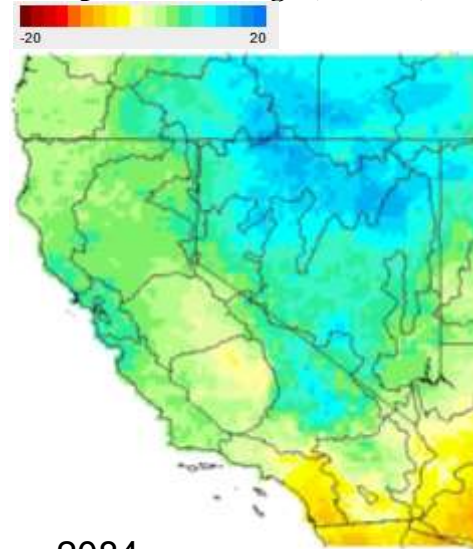
2084

Figure 3A-2. Comparison of Median Projected Changes in Annual Mean Temperature (°C) and Annual Precipitation (percent) for 2070-2099 (2084) for CEN Climate Scenario Developed Using CMIP3 and CMIP5 Ensembles

Notes:

Change compared to the 1971-2000 model simulated period for CMIP3, while for CMIP5 change compared to the 1981-2010 model simulated period. Mixtures of SRES A2, SRES A1B, and SRES B1 were considered for CMIP3, while for CMIP5 mixtures of RCP scenarios RCP8.5, RCP6.0, and RCP4.5 were considered for CEN climate change scenario

Top panel shows annual temperature change (°C). Bottom panel shows annual precipitation change (percent)

Table A-2. Annual Temperature Change (In Degrees C) in the Sacramento River, San Joaquin River, Tulare Lake Hydrologic Regions for CEN Climate Scenario Developed Based on CMIP3 and CMIP5 Archives for 2015–2039, 2040–2069, and 2070-2099

	Sacramento Hydrologic Region		San Joaquin Hydrologic Region		Tulare Lake Hydrologic Region	
	CEN (CMIP3)	CEN (CMIP5)	CEN (CMIP3)	CEN (CMIP5)	CEN (CMIP3)	CEN (CMIP5)
2015-2039	1.0	1.0	1.0	0.9	1.0	0.9
2040-2069	1.8	2.0	1.9	1.9	1.9	1.9
2070-2099	2.5	2.8	2.6	2.7	2.5	2.7

Notes:

Change compared to the 1971-2000 model simulated period for CMIP3, for CMIP5 change compared to the 1981-2010 model simulated period.

Table A-3. Annual Precipitation Change (percent) in the Sacramento River, San Joaquin River, and Tulare Lake Hydrologic Regions for CEN Climate Scenario Developed Based on CMIP3 and CMIP5 Archives for 2015–2039, 2040–2069, and 2070-2099

	Sacramento Hydrologic Region		San Joaquin Hydrologic Region		Tulare Lake Hydrologic Region	
	CEN (CMIP3)	CEN (CMIP5)	CEN (CMIP3)	CEN (CMIP5)	CEN (CMIP3)	CEN (CMIP5)
2015-2039	1.0	0.1	0.3	-0.2	-0.7	-0.3
2040-2069	0.4	2.1	-2.6	0.8	-5.2	-0.4
2070-2099	0.8	3.9	-1.5	2.5	-4.5	1.5

Notes:

Change compared to the 1971-2000 model simulated period for CMIP3, for CMIP5 change compared to the 1981-2010 model simulated period.

3.1 Generating Transient Climate Change Scenario Based on Ensemble Informed Scenario Method

In period-specific climate change scenarios, such as that applied in the BDCP, climate changes derived from one future period is used to transform a sequence of historical climate to an adjusted sequence reflective of future climate change. However, in the transient climate change scenario approach developed for the CVP IRP study and the SSJBS, the projected temperature and precipitation changes are mapped to a historical climate sequence based on an evolving pattern of change.

The projected future temperature and precipitation changes from all members in each sub-ensemble are compared to a historical period. The historical period of 1981-2010 was selected as the reference climate since it was the established climate normal used by National Oceanic and Atmospheric Administration (NOAA) at the time this work was conducted. Climate change is commonly measured over a 30-year period. The approach uses a technique called "quantile mapping" which maps the statistical properties of climate variables from one data subset with the time series of events from a different subset. In this fashion, the approach allows the use of a shorter period to define the climate state, yet maintains the variability of the longer historic record. The method uses the quantile map developed for each of these periods to redevelop a monthly time series of temperature and precipitation reflecting the observed natural variability sequence and the projected climate change (see Figure A-3).

The approach involves the following steps:

- 30-year slices of downscaled historical and future monthly precipitation and average temperature are extracted from the projects that make up the sub-ensemble of the scenario. The historical period was selected as 1981-2010 (1995 centering) and the three future 30 year periods were selected as centered on 2025 (2011-2040), 2055 (2041-2070), and 2084 (2070-2099) to representing early-, mid-, and late-21st century.

- Cumulative distribution functions (CDFs) of average temperature and precipitation change were developed. For each calendar month of the historical period (for e.g., 1981-2010) and future periods, cumulative distribution functions (CDFs) of average temperature and precipitation for each 1/8th degree grid cell were computed from the members of each sub-ensemble of interest. The change in the CDF was computed for each of the five sub-ensembles at each grid cell. The temperature and precipitation change quantities are not expected to shift uniformly across the range of conditions or months. For example, the climate shift could be larger for mid-range of temperature values and smaller at the extremes. While for precipitation, the projected shift could be larger at the extremes with little change at the lower values. Because this pattern may be different for each climate scenario, future period, spatial location, and month, it is important to map the full range of statistical climate shift to characterize the projected effects of climate change.

- The method applies the change for any particular year by interpolating linearly from the two CDFs that bracket the simulation year. This process adjusts the historic observed climate records by the climate shifts projected to occur in the future. The projected change in monthly average temperature was mapped to both historical monthly maximum and minimum temperature sequences.

- The projected change in monthly temperature and precipitation was then mapped to the historical climate sequence for 1922-2010 constructed based on monthly PRISM (Daly et al., 1994) and daily Livneh et al. (2013) data sources. This process adjusts the historical observed climate records by the climate shifts projected to occur in the future. An automated process was used to generate five scenarios for every grid cell within California.
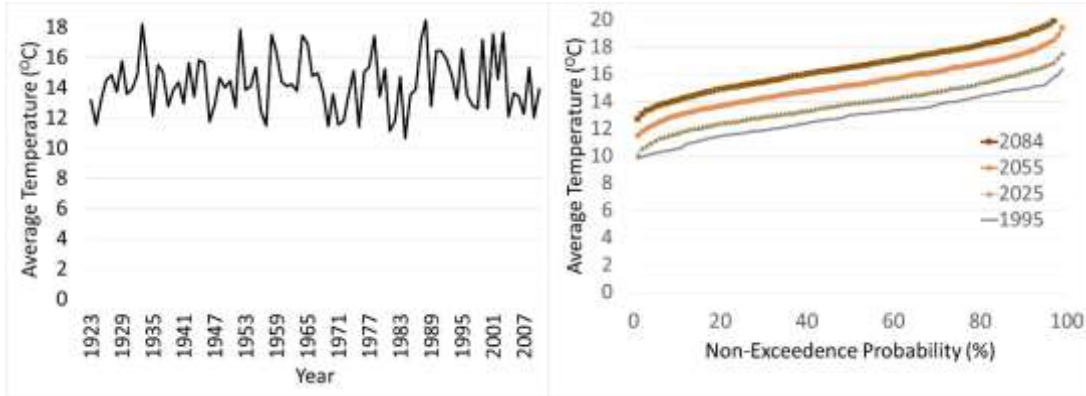
a) Historical natural variability sequence of Temperature or Precipitation

b) Climate shift (ΔT for temperature or Pf/Ph for precipitation) computed from month-specific CDF of T or P from downscaled climate projections
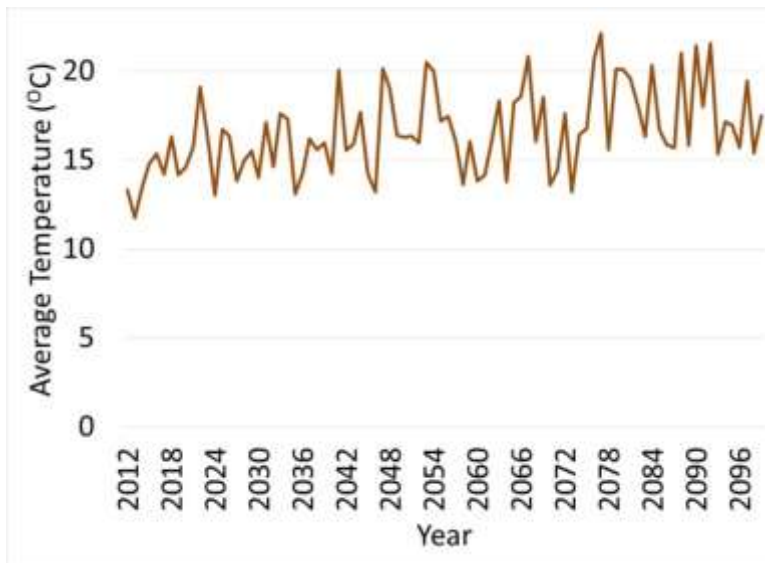
c) Future transient climate change scenario of T or P

Figure A-3. Schematic Methodological Diagrams for Developing Transient Future Climate Scenarios

3.3.   Future Climate – Downscaled Climate Projections

As indicated earlier in this appendix, in addition to the EI5, the SSJIA and SSJBS used twelve individual downscaled GCM projections derived from six GCMs and two emission scenarios. For the SSJBS, six GCMs were chosen from the 10 GCMs selected by the DWR CCTAG. The rationale in the selection of the six GCM projections was to obtain individual projections that had a similar mean and range as those for the complete 10 GCMs being considered by the CCTAG.

Figures A-4 and A-5 show the projected changes in annual average temperature and annual total precipitation computed from direct BCSD downscaled CMIP3 and CMIP5 climate model ensembles for the Sacramento region. The results are presented using the climate model projections from CMIP3 and CMIP5 simulated under 3 emission scenarios (SRES A1B, SRES A2, and SRES B1 for CMIP3; and RCP8.5, RCP6.0, and RCP4.5 for CMIP5). The plot also shows results from the CMIP3 GCMs selected by CAT (Cayan et al. 2009) and CMIP5 GCMs selected by DWR CCTAG for two bounded emission scenarios (SRES A2 and SRES B1 for CMIP3; RCP8.5 and RCP4.5 for CMIP5).

Under all available future climate projections, air temperatures are projected to increase in the Sacramento region. All projections are consistent in the direction of the temperature change (increase), but vary in terms of climate sensitivity (magnitude). Beyond the mid-century, the projections of warming are strongly dependent on the GHG emission pathway, while the CMIP5 based results suggests an expanded range of warming as compared to CMIP3 based results for the emission scenarios considered here. The median of the available climate model projections using the CMIP3 ensemble suggests about 1.9°C increase by 2050 and by about 2.7°C by end of century for the Sacramento region. Similarly, climate model projections using the CMIP5 ensemble suggests slightly higher warming; about 2.3°C increase by 2050 and by about 3.2°C by end of century. The CMIP5 climate models selected by the CCTAG include results of future warming results that span the degree of warming associated with the broader ensemble.

Projections of future precipitation are more uncertain than those for temperature. While the median of the future climate projections included in CMIP3 ensemble suggests a slight increase or no change in annual precipitation for the Sacramento region, the median of the projections in the CMIP5 ensemble suggests an increase by about 1.6% by mid-century and about 6% by end of century (Figure A-5). The CMIP5 climate models selected by the CCTAG include results of future precipitation changes that span the range associated with the broader ensemble.
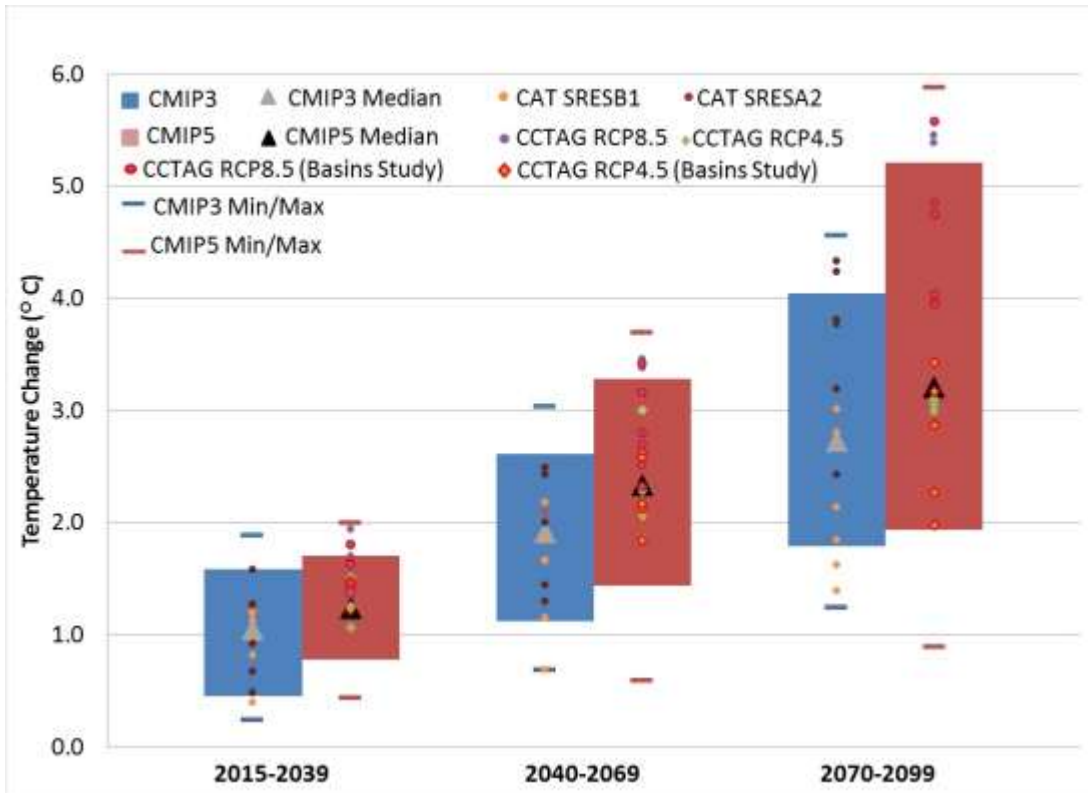
Figure A-4. Projected Changes in Mean Annual Temperatures (in degrees C) for the Sacramento Region based on CMIP3 and CMIP5 Projections

Notes:

The projected changes for CMIP3 and CMIP5 are computed using 112 (simulated under SRES emission scenarios A2, A1B, and B1) and 175 (simulated under RCP emission scenarios RCP8.5, RCP6.0, and RCP4.5) downscaled climate model projections used in the IPCC's AR4 and AR5, respectively. Changes are computed with respect to 1971-2000 model simulated period for both CMIP3 and CMIP5. Bars represent the range between the 10th and 90th percentiles. Circles represent the projections from the CMIP3 GCMs selected by CAT and the CMIP5 GCMs selected by DWR CCTAG for California climate and water assessments. CMIP3 and CMIP5 climate model projections have been bias-corrected and spatially downscaled (Maurer et al. 2007; Reclamation 2013). The downscaled CMIP3 and CMIP5 climate model projections were obtained from the Lawrence Livermore National Laboratory (LLNL) archive at http://gdo-dcp.ucllnl.org/downscaled_cmip_projections/.

GCMs Selected by CAT: CNRM CM3.0, GFDL CM2.1, MIROC3.2 (med), MPI ECHAM5, NCAR CCSM3, NCAR PCM1

GCMs Selected by CCTAG: ACCESS-1.0, CCSM4, CESM1-BGC, CMCC-CMS, CNRM-CM5, CanESM2, GFDL-CM3, HadGEM2-CC, HadGEM2-ES, MIROC5

GCMs Selected for SSJBS: CCSM4, CESM1-BGC, CNRM-CM5, GFDL-CM3, HadGEM2-ES, MIROC5

Figure A-5. Projected Changes in Mean Annual Precipitation for the Sacramento Region based on CMIP3 and CMIP5 Projections

Notes:

The projected changes for CMIP3 and CMIP5 are computed using 112 (simulated under SRES emission scenarios A2, A1B, and B1) and 175 (simulated under RCP emission scenarios RCP8.5, RCP6.0, and RCP4.5) downscaled climate model projections used in the IPCC's AR4 and AR5, respectively. Changes are computed with respect to 1971-2000 model simulated period for both CMIP3 and CMIP5. Bars represent the range between the 10th and 90th percentiles. Circles represent the projections from the CMIP3 GCMs selected by CAT and the CMIP5 GCMs selected by DWR CCTAG for California climate and water assessments. CMIP3 and CMIP5 climate model projections have been bias-corrected and spatially downscaled (Maurer et al. 2007; Reclamation 2013). The downscaled CMIP3 and CMIP5 climate model projections were obtained from the Lawrence Livermore National Laboratory (LLNL) archive at http://gdo-dcp.ucllnl.org/downscaled_cmip_projections/.

GCMs Selected by CAT: CNRM CM3.0, GFDL CM2.1, MIROC3.2 (med), MPI ECHAM5, NCAR CCSM3, NCAR PCM1

GCMs Selected by CCTAG: ACCESS-1.0, CCSM4, CESM1-BGC, CMCC-CMS, CNRM-CM5, CanESM2, GFDL-CM3, HadGEM2-CC, HadGEM2-ES, MIROC5

GCMs Selected for SSJBS: CCSM4, CESM1-BGC, CNRM-CM5, GFDL-CM3, HadGEM2-ES, MIROC5

Table A-4 summarizes statistics in future changes in mean annual temperature and precipitation from the 10 CCTAG GCMs, the six GCMs selected for the SSJBS, and CMIP5 ensemble for the Sacramento Region. The projected changes computed for the six GCMs selected for the SSJBS span appreciable range of the changes projected by the 10 CCTAG GCMs.

Table A-4. Annual Temperature Change (In Degrees C) and Annual Precipitation Change (percent) in the Sacramento Region Based CCTAG GCMs, the GCMS Selected for SSJBS and CMIP5 Archives for 2015–2039, 2040–2069, and 2070-2099

		Annual Precipitation Change (%)			Annual Temperature Change (%)		
		2015-2039	2040-2069	2070-2099	2015-2039	2040-2069	2070-2099
10 CCTAG GCMs (RCP8.5 and RCP4.5)	Mean	4.1	5.0	6.9	1.5	2.6	3.8
	Min	-11.1	-12.6	-15.8	1.1	1.8	2.0
	Max	24.4	26.3	41.5	1.9	3.5	5.6
6 CCTAG GCMs (RCP8.5 and RCP4.5)	Mean	4.8	3.6	7.3	1.5	2.5	3.6
	Min	-11.1	-12.6	-15.8	1.2	1.8	2.0
	Max	24.4	24.5	33.7	1.8	3.4	5.6
CMIP5 Ensemble (RCP8.5, RCP6.0, and RCP5)	Mean	1.3	1.9	6.6	1.2	2.3	3.4
	Min	-22.5	-23.2	-24.7	0.4	0.6	0.9
	Max	26.0	29.9	41.5	2.0	3.7	5.9

Notes:

The statistics of future changes are computed from 20 climate projections for the 10 CCTAG GCMs simulated under RCP emission scenarios RCP8.5 and RCP4.5 and from the 12 climate projections for the six GCMs selected for SSJBS simulated under RCP emission scenarios RCP8.5 and RCP4.5. For CMIP5 ensemble, changes are computed from 175 climate projections simulated under RCP emission scenarios RCP8.5, RCP6.0, and RCP4.5. Changes are computed with respect to 1971-2000 model simulated historical period.

GCMs Selected by CCTAG: ACCESS-1.0, CCSM4, CESM1-BGC, CMCC-CMS, CNRM-CM5, CanESM2, GFDL-CM3, HadGEM2-CC, HadGEM2-ES, MIROC5

GCMs Selected for SSJBS: CCSM4, CESM1-BGC, CNRM-CM5, GFDL-CM3, HadGEM2-ES, MIROC5

Acknowledgements

Intercomparison provides coordinating support and led development of software infrastructure in partnership with the Global Organization for Earth System Science Portals.

Twelve CMIP3 CAT scenarios were obtained from Scripps Institution of Oceanography. DWR Climate Change Advisory Technical Group (CCATG) provided the CCTAG CMIP5 GCM selection list.

Daily gridded historical climate data (Livneh et al. 2013) was obtained from the Surface Water Modeling Group at the University of Washington (http://www.hydro.washington.edu). PRISM monthly climate data (Daly et al., 1994) was obtained from PRISM Climate Group at Oregon State University (http://www.prism.oregonstate.edu/)

References

Bureau of Reclamation (Reclamation). 2013. Central Valley Project Integrated Resource Plan. Administrative Draft. Mid-Pacific Region. February.

Bureau of Reclamation (Reclamation). 2014. Sacramento and San Joaquin Basins Climate Risk Assessment Report. Mid-Pacific Region. September.

California Department of Water Resources (DWR). 2014. California Water Plan Update 2013. Bulletin 160-13. Sacramento, California.

Daly Christopher, Ronald P. Neilson, and Donald L. Phillips, 1994: A Statistical-Topographic Model for Mapping Climatological Precipitation over Mountainous Terrain. J. Appl. Meteor., 33, 140–158.

Intergovernmental Panel on Climate Change. 2001. Climate Change 2001: The Scientific Basis. Contribution of Working Group I to the Third Assessment Report of the Intergovernmental Panel on Climate Change.

IPCC (Intergovernmental Panel on Climate Change). 2007. Climate Change 2007: The Physical Science Basis. Contribution of Working Group I to the Fourth Assessment Report of the Intergovernmental Panel on Climate Change (Solomon, S., D. Qin, M. Manning, Z. Chen, M. Marquis, K. B. Averyt, M. Tignor and H. L. Miller [Eds.]). Cambridge University Press, Cambridge, United Kingdom and New York, NY, USA, 996 pp.

IPCC, 2013: Climate Change 2013: The Physical Science Basis. Contribution of Working Group I to the Fifth Assessment Report of the Intergovernmental Panel on Climate Change [Stocker, T.F., D. Qin, G.-K. Plattner, M. Tignor, S.K. Allen, J. Boschung, A. Nauels, Y. Xia, V. Bex and P.M. Midgley (eds.)]. Cambridge University Press, Cambridge, United Kingdom and New York, NY, USA, 1535 pp.

Knutti, R. and J. Sedlacek, 2013: Robustness and uncertainties in the new CMIP5 coordinated climate model projections. Nature Climate Change, 3, 369-373, doi:10.1038/nclimate1716

Livneh, B., E. A. Rosenberg, C. Lin, V. Mishra, K. Andreadis, E. P. Maurer, and D.P. Lettenmaier. 2013. A long-term hydrologically based data set of land surface fluxes and states for the conterminous U.S.: Update and extensions, Journal of Climate, doi: 10.1175/JCLI-D-12-00508.1.

Pierce, D. W., T. P. Barnett, H. G. Hidalgo, T. Das, C. Bonfils, B. D. Santer, G. Bala, M. D. Dettinger, D. R. Cayan, A. Mirin, A. W. Wood, and T. Nozawa. 2008. Attribution of Declining Western U.S. Snowpack to Human Effects. J. Climate, 21, 6425–6444.

Polade, S.D., A. Gershunov, D.R. Cayan, M.D. Dettinger and D.W. Pierce, 2013: Natural climate variability and teleconnections to precipitation over the Pacific-North American region in CMIP3 and CMIP5 models. Geophysical Research Letters, 40, 1-6. doi:10.1002/grl.50941

Rupp DE, Abatzoglou JT, Hegewisch KC, Mote PW. 2013. Evaluation of CMIP5 20th century climate simulations for the Pacific Northwest USA. Journal of Geophysical Research: Atmospheres. 118(19):10,884-10,906.

Seager, Richard, Mingfang Ting, Cuihua Li, Naomi Naik, Ben Cook, Jennifer Nakamura, Haibo Liu. 2012. Projections of declining surface-water availability for the southwestern United States. Nature Climate Change 3,482–486(2013)doi:10.1038/nclimate1787.

Karl E. Taylor, Ronald J. Stouffer, and Gerald A. Meehl, 2012: An Overview of CMIP5 and the Experiment Design. Bull. Amer. Meteor. Soc., 93, 485–498. doi: http://dx.doi.org/10.1175/BAMS-D-11-00094.1

van Vuuren DP, JA Edmonds, M Kainuma, K Riahi, AM Thomson, K Hibbard, GC Hurtt, T Kram, V Krey, J-F Lamarque, T Masui, M Meinshausen, N Nakicenovic, SJ Smith, and S Rose . 2011. The representative concentration pathways: an overview Climatic Change, 109: 5-31. DOI: 10.1007/s10584-011-0148-z. Available at: http://www.springerlink.com/content/f296645337804p75/.

APPENDIX 4B. CLIMATE INPUTS FOR THE WEAP-CV AGRICULTURAL DEMANDS

The analysis of the effects of potential future climate changes on agricultural water demands and productivity requires meteorological information beyond projections of future temperature and precipitation conditions. Crop growth, yield and evapotranspiration (ET) are also sensitive to solar radiation, atmospheric humidity, wind speed and carbon dioxide. In order to provide these additional data, several estimation methods using the temperature and precipitation projections were employed to obtain values for these meteorological conditions corresponding to the future climate projections.

In order to represent a reasonable range of spatial variability in these meteorological conditions, four locations were selected to characterize representative conditions in the Central Valley. These locations are shown on **Figure 4B-1**.
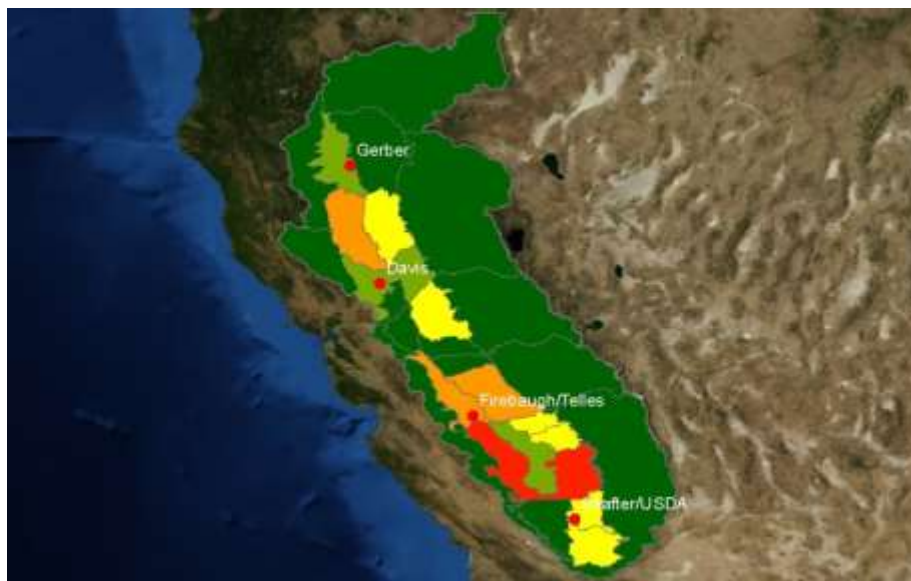
Figure 4B-1. Locations of the CIMIS station used in estimating meteorological conditions for Agricultural Demand and Productivity Analyses

The selected locations include existing California Irrigation Management Information System (CIMIS) stations located at Gerber, Davis, Firebaugh, and Shafter. These CIMIS stations were chosen because long term observations of daily maximum and minimum temperature (Tmax, Tmin), solar radiation (Rs), dew point temperature (Tdew), relative humidity (RH), and wind speed were available. All the historical data from the stations were also carefully checked for erroneous values prior to preparing the subsequent projections. In Figure 4B-2, an example of solar radiation (Rs) data from the CIMIS station located at Davis is presented. The top panel shows the observations prior to the elimination of values

in excess of the daily clear sky radiation, Rso maximum. The middle panel shows the same data with the extreme outliers eliminated. From this data, the ratio of daily Rs/Rso was calculated and the average ratio of the top 20% of values on a monthly basis was computed. The daily data were then adjusted by dividing by this adjustment factor to obtain the results shown in the bottom panel.
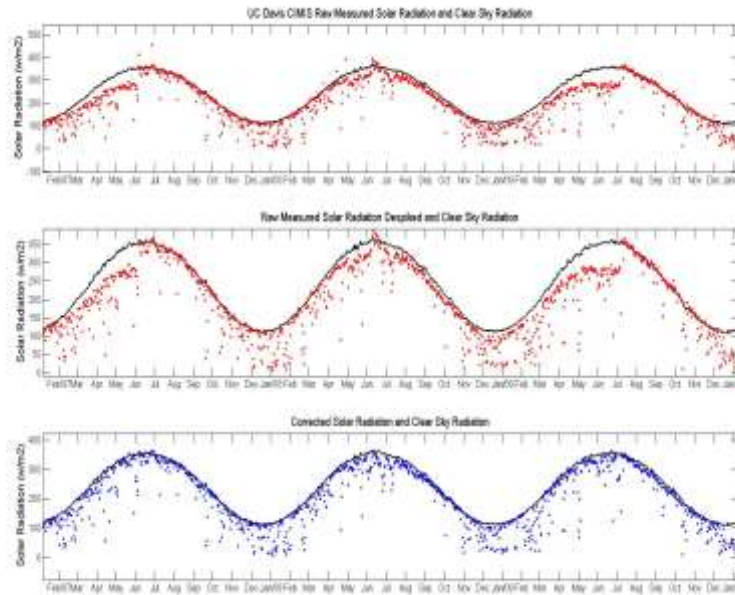
**Figure 4B-2. Adjustment of CIMIS daily solar radiation, Rs, values.
Top panel shows raw data; Middle Panel shows data after elimination of extreme values; Bottom panel shows the adjusted data.**

A similar analysis was performed on the relative humidity (RH) data. The top panel of **Figure B-3** shows the raw hourly RH data from the CIMIS located at Davis. As can be observed, the maximum RH values decline slowly over an extended period of time. This sensor drift was corrected by adjusting the values so that some of the values approach 100% RH during each year. The adjusted RH values are shown in the bottom panel of **Figure 4B-3**. After adjustment, any missing data values were estimated using methods described by Annaandale et al. (2002).
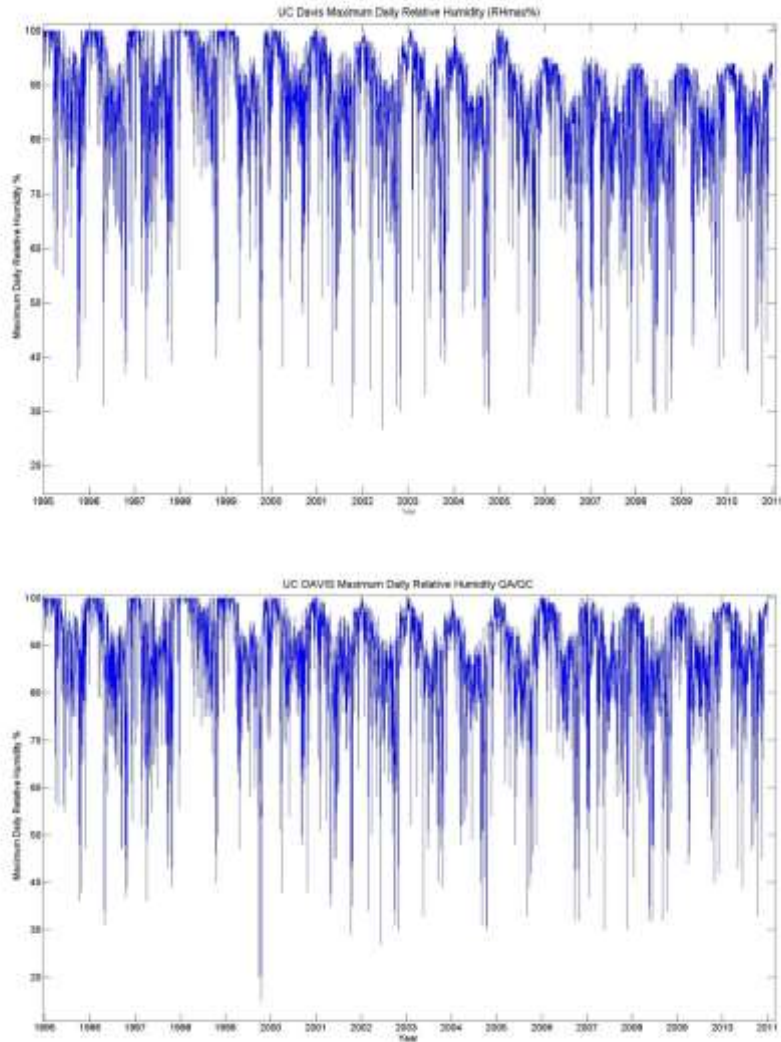
Figure B-3. Adjustment of CIMIS hourly relative humidity, RH, values.
Top panel shows raw data; Bottom panel shows the adjusted data.

Solar radiation is one of the factors affecting crop ET. It can be estimated from the Tmax and Tmin using the clear radiation (Ro) which only depends on latitude, day of the year and a site specific parameter (B). The CIMIS station historical records where used to calibrate B parameters and the climate projections of Tmax and Tmin were then used to compute Rs based on the Thornton and Running (1999) method for each of the EI climate projections.

Table 4B-1 shows the calibrated monthly B parameters at each of the four CIMIS stations. These values were computed from the following equation.

$$B = 0.031 + 0.201 * exp(-0.185 * (Tmax - Tmin)) \quad \text{Eqn. 1}$$

where Tmax and Tmin are the daily maximum and minimum temperatures respectively**.**

Table 4B-1. Average Monthly B parameters for the Central Valley CIMIS Stations

Station Name	Month											
	Jan	Feb	Mar	Apr	May	Jun	Jul	Aug	Sep	Oct	Nov	Dec
Davis	0.072	0.061	0.052	0.046	0.043	0.040	0.038	0.037	0.039	0.043	0.055	0.071
Firebaugh/Telles	0.067	0.056	0.049	0.045	0.042	0.040	0.039	0.039	0.040	0.043	0.051	0.065
Gerber	0.066	0.059	0.052	0.047	0.046	0.044	0.041	0.039	0.040	0.044	0.054	0.067
Shafter/USDA	0.060	0.051	0.046	0.042	0.040	0.039	0.039	0.038	0.038	0.039	0.045	0.056

Figure 4B-4 shows a comparison of the observed and estimated Rs at the CIMIS station located at U. C. Davis.
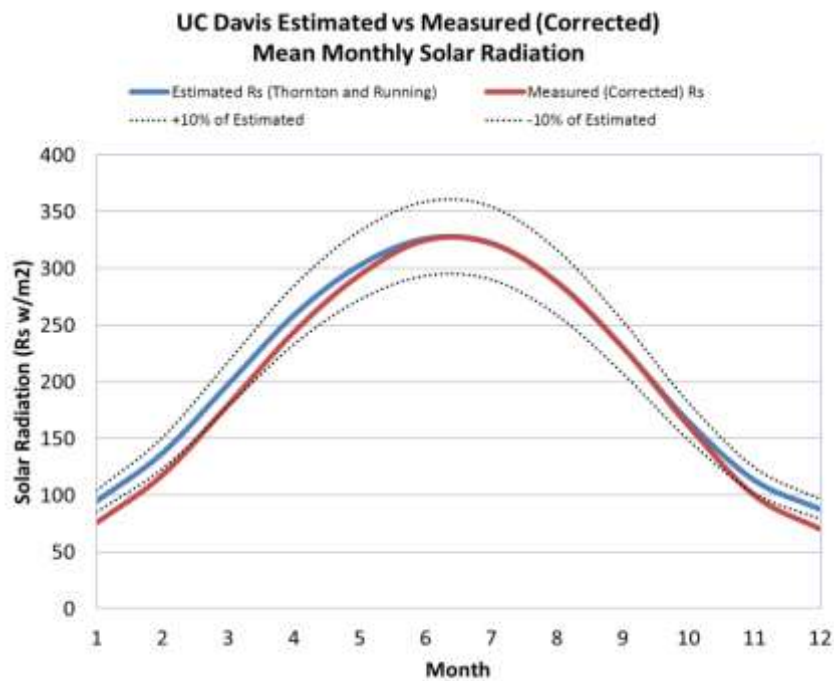
Figure 4B-4. Comparison of observed CIMIS and estimated Rs results at the U.C. Davis CIMIS station.

The average Tmax, Tmin and Rs results for the Baseline and each of the EI5 climate scenarios during the 2011-2040 (2025), 2041-2070 (2055), and 2070-2099 (2084) periods are presented in **Figure 4B-5** through **Figure 4B-7** respectively for the U.C. Davis CIMIS station.
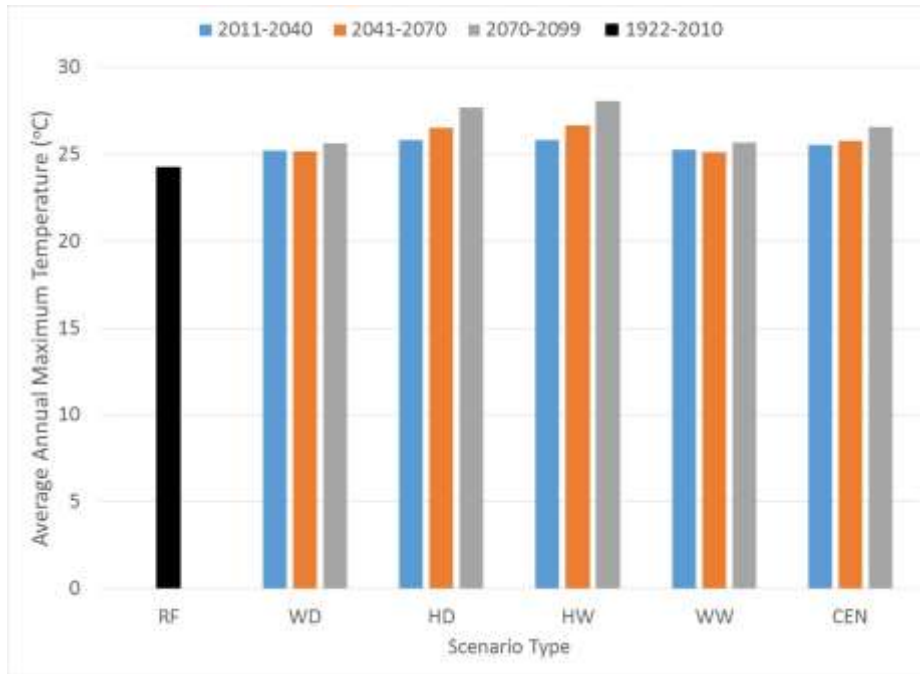
Figure 4B-5. Projected average daily maximum temperatures in degrees centigrade (ºC) for each climate scenario for 2011-2040 (2025), 2041-2070 (2055) and 2070-2099 (2084)

Notes: RF scenario was averaged over historical climate sequence for 1922-2010
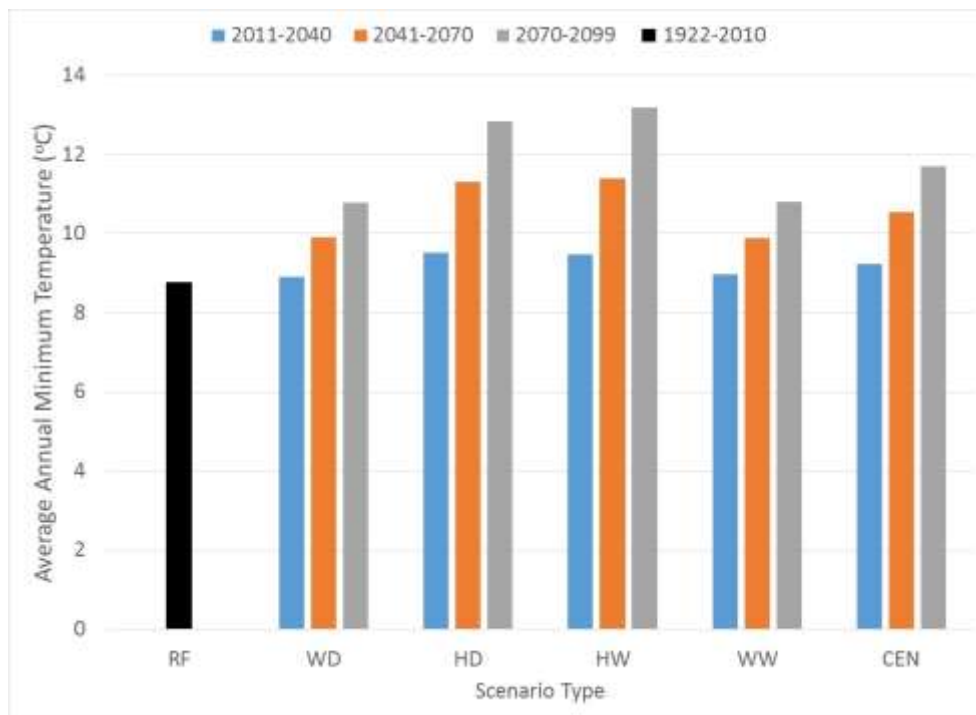
Figure 4B-6. Projected average daily minimum temperatures in degrees centigrade (ºC) for each climate scenario for 2011-2040 (2025), 2041-2070 (2055) and 2070-2099 (2084)

Notes: RF scenario was averaged over historical climate sequence for 1922-2010
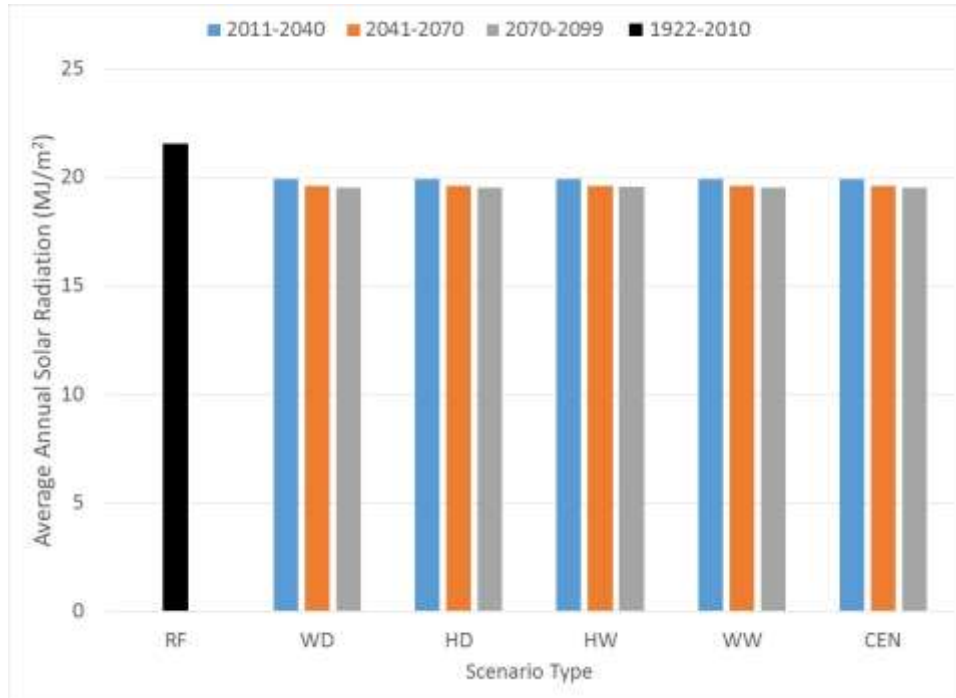
Figure 4B-7. Projected average solar radiation in mega-joules per square meter (MJ/m2) for each climate scenario for 2011-2040 (2025), 2041-2070 (2055) and 2070-2099 (2084)

Notes:RF scenario was averaged over historical climate sequence for 1922-2010

Atmospheric humidity also has a significant effect of crop ET. As the air becomes drier, ET generally increases. The dew point temperature (Tdew) is an indicator of the moisture content of the air. As the atmospheric humidity increases, Tdew also increases. The daily minimum temperature is a good indicator of Tdew. Cloudiness and high humidity reduce the amount of heat loss from the surface to the atmosphere which is generally reflected in higher Tmin values. To estimate projected changes in atmospheric humidity, an analysis of the CIMIS station records was performed to determine the monthly average differences between the observed Tmin and Tdew values. This difference is referred to as the dew point depression (Ko). Average monthly Ko values computed for each of the four CIMIS stations are presented in Table 4B—2 below.

Table 4B-2. Average monthly Ko values for each Central Valley CIMIS station

Station Name	Month											
	Jan	Feb	Mar	Apr	May	Jun	Jul	Aug	Sep	Oct	Nov	Dec
Davis	-1.91	-1.56	-0.40	0.85	2.25	2.48	1.34	1.79	3.19	2.34	-0.51	-1.72
Firebaugh/Telles	-1.23	-0.51	0.86	2.81	4.40	5.13	3.89	2.99	3.40	2.69	-0.11	-1.40
Gerber	0.46	1.06	1.52	2.27	2.61	4.06	4.07	3.51	3.96	3.37	0.56	-0.20
Shafter/USDA	-1.38	-0.46	0.40	2.07	3.63	3.91	3.14	2.92	3.18	1.61	1.09	1.56

To estimate projected changes in Tdew, these monthly average observed Ko values were subtracted for the projected Tmin values. The average Tdew results for the Baseline and each of the EI5 climate scenarios for 2011-2040 (2025), 2041-2070 (2055) and 2070-2099 (2084) are presented in Figure 4B-8.
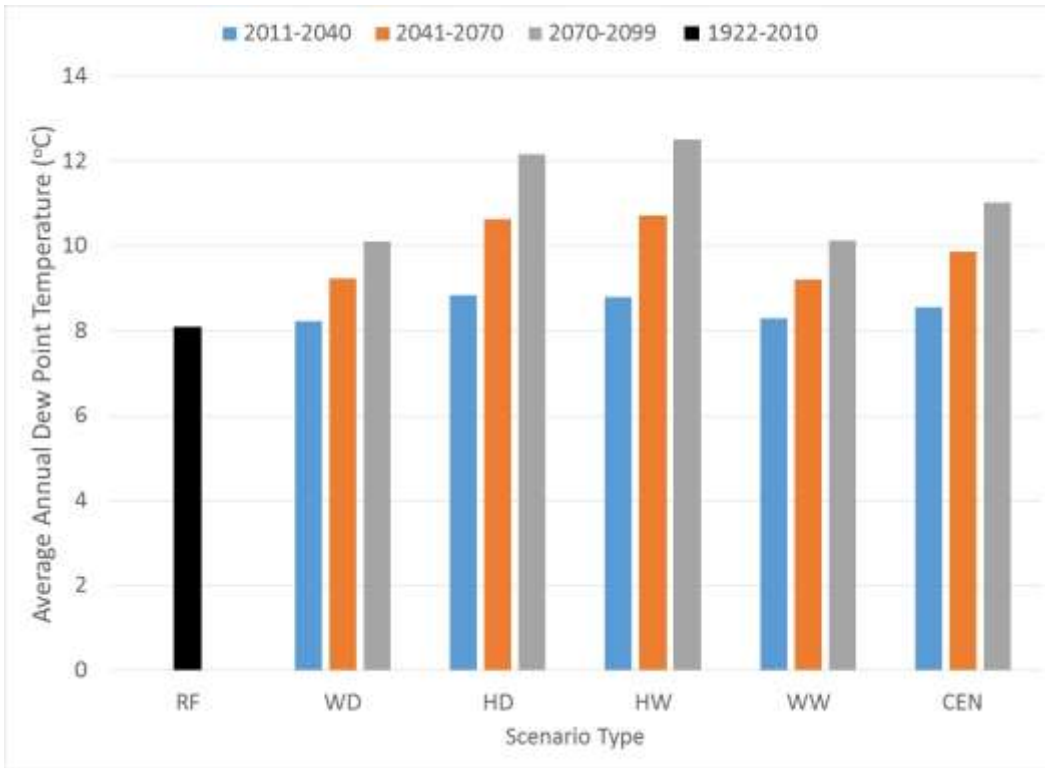
Figure 4B-8. Projected average daily dew point temperatures in degrees centigrade (ºC) for each climate scenario for 2011-2040 (2025), 2041-2070 (2055) and 2070-2099 (2084)

Notes: RF scenario was averaged over historical climate sequence for 1922-2010

The effects of atmospheric humidity are reflected in ET calculations by the difference between the saturated vapor pressure (es) in the moist plant leaves and the typically drier surrounding atmosphere (ea). This difference is referred to as the vapor pressure deficit (VPD). As the VPD increases, crop ET generally increases. Because the saturation vapor pressure is a function of temperature, projections of VPD can be computed from the projections of daily Tmax, Tmin and Tdew using methods described by Walter et al. (2005). Figure B-9 shows the projected VPD results for the RF and each of the EI5 climate scenarios during the 2011-2040 (2025), 2041-2070 (2055) and 2070-2099 (2084).
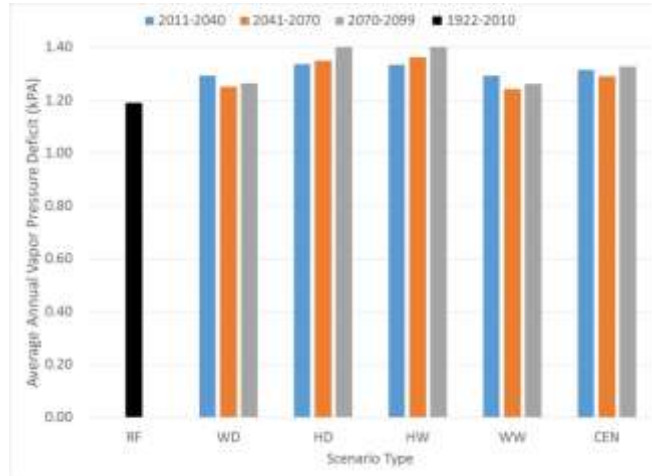
Figure B-9. Projected average daily vapor pressure deficits in kilo Pascals (kPa) for each climate scenario for 2011-2040 (2025), 2041-2070 (2055) and 2070-2099 (2084)

Notes: RF scenario was averaged over historical climate sequence for 1922-2010

In addition to the annual period averages presented in **Figure B-9** above, **Figure B-10** through **Figure B-21** present monthly period averages of VPD. VPD varies considerably on a monthly basis. Elevated values during the growing season exert important effects on crop ET and yield (see Appendix D). As shown in the figures, under projected climate changes VPD may become significantly greater than under current climatic conditions especially in the hotter projections.
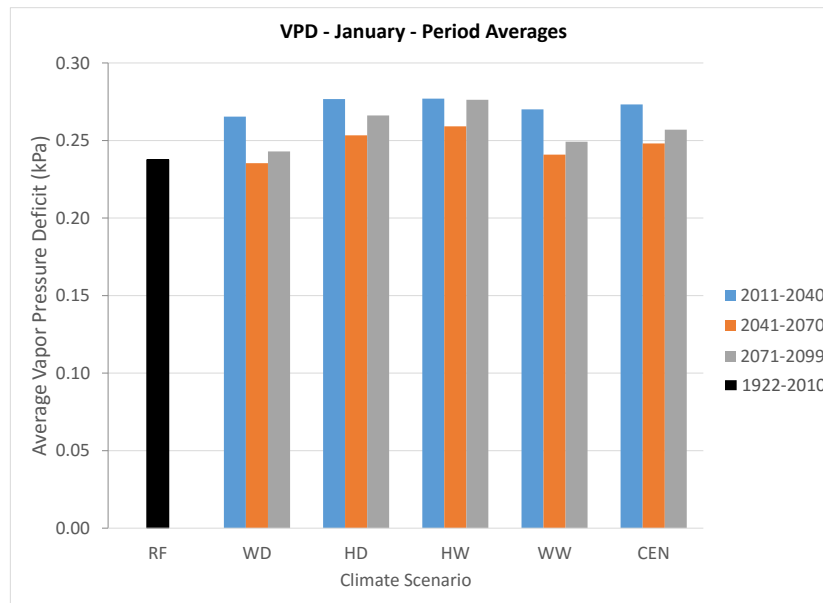
Figure 4B-10. Projected January monthly average vapor pressure deficits in kilo Pascals (kPa) for each climate scenario for 2011-2040 (2025), 2041-2070 (2055) and 2070-2099 (2084)

Notes: RF scenario was averaged over historical climate sequence for January from 1922-2010
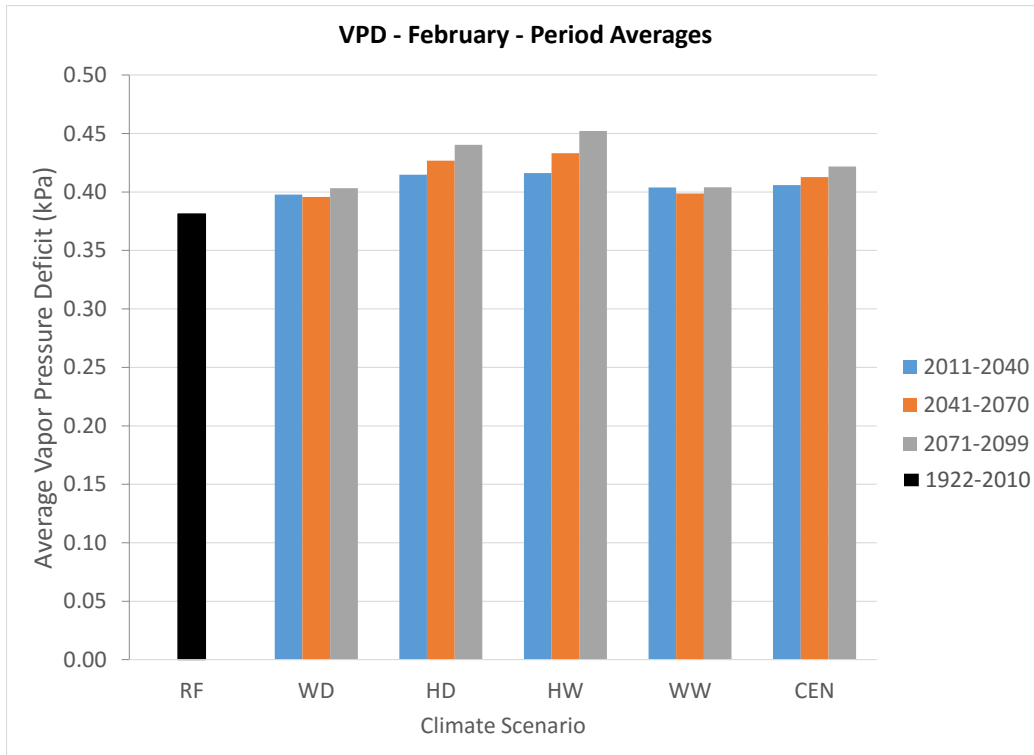
Figure 4B-11. Projected February monthly average vapor pressure deficits in kilo Pascals (kPa) for each climate scenario for 2011-2040 (2025), 2041-2070 (2055) and 2070-2099 (2084)

Notes: RF scenario was averaged over historical climate sequence for February from 1922-2010
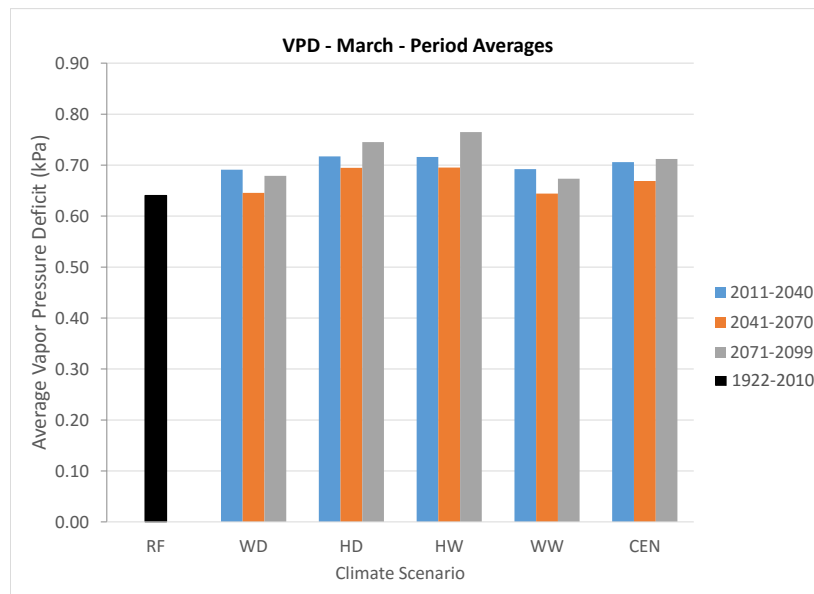
Figure 4B-12. Projected March monthly average vapor pressure deficits in kilo Pascals (kPa) for each climate scenario for 2011-2040 (2025), 2041-2070 (2055) and 2070-2099 (2084)

VPD - April - Period Averages
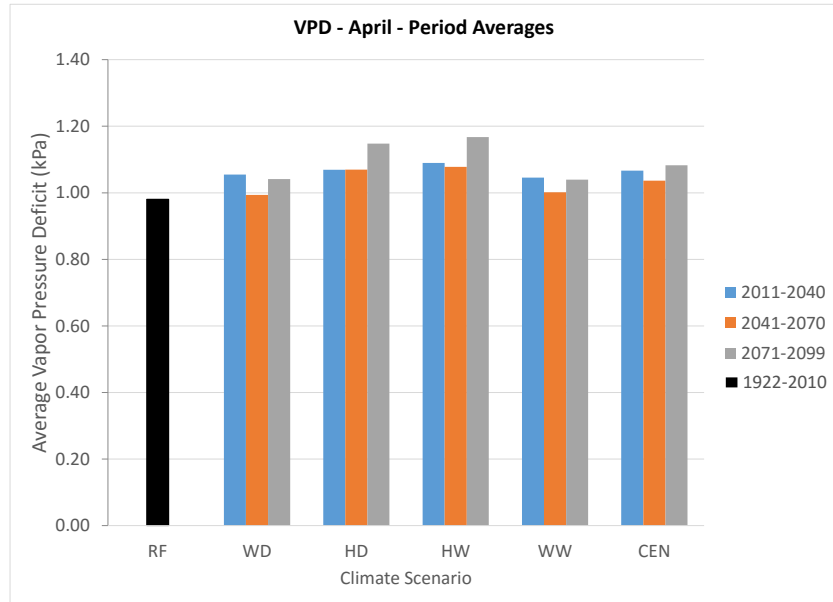
Figure 4B-13. Projected April monthly average vapor pressure deficits in kilo Pascals (kPa) for each climate scenario for 2011-2040 (2025), 2041-2070 (2055) and 2070-2099 (2084)

Notes: RF scenario was averaged over historical climate sequence for April from 1922-2010

VPD - May - Period Averages
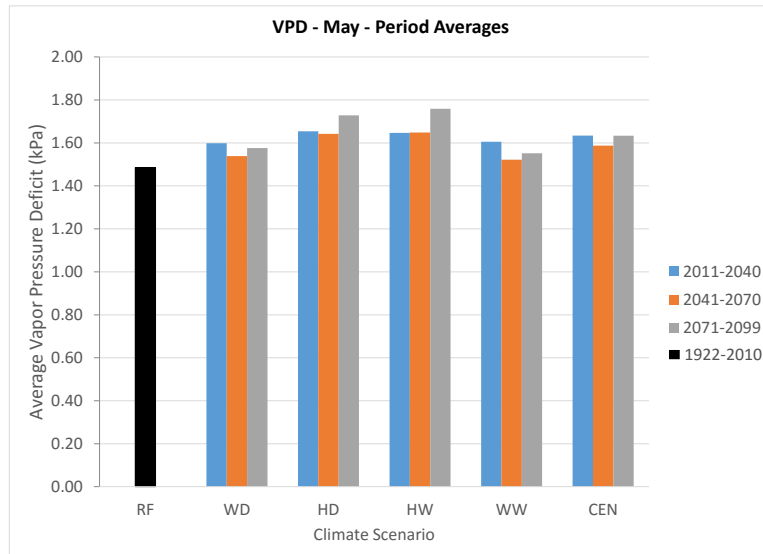
Figure 4B-14. Projected May monthly average vapor pressure deficits in kilo Pascals (kPa) for each climate scenario for 2011-2040 (2025), 2041-2070 (2055) and 2070-2099 (2084)

VPD - June - Period Averages
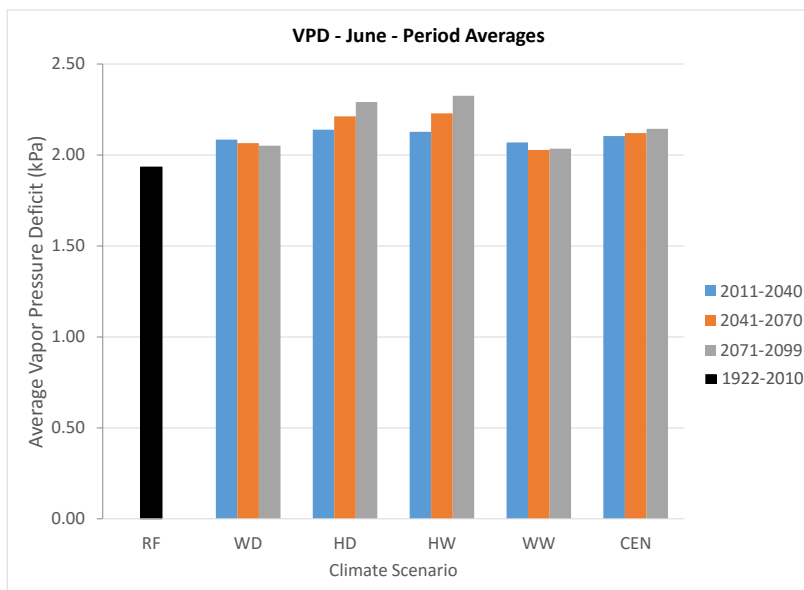
Figure 4B-15. Projected June monthly average vapor pressure deficits in kilo Pascals (kPa) for each climate scenario for 2011-2040 (2025), 2041-2070 (2055) and 2070-2099 (2084)

Notes: RF scenario was averaged over historical climate sequence for June from 1922-2010

VPD - July - Period Averages
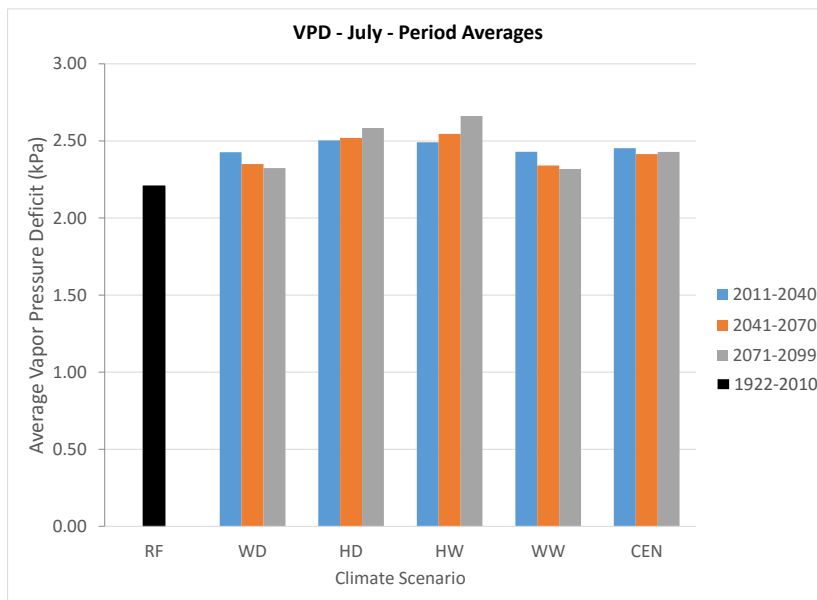
Figure 4B-16. Projected July monthly average vapor pressure deficits in kilo Pascals (kPa) for each climate scenario for 2011-2040 (2025), 2041-2070 (2055) and 2070-2099 (2084)

Notes: RF scenario was averaged over historical climate sequence for July from 1922-2010
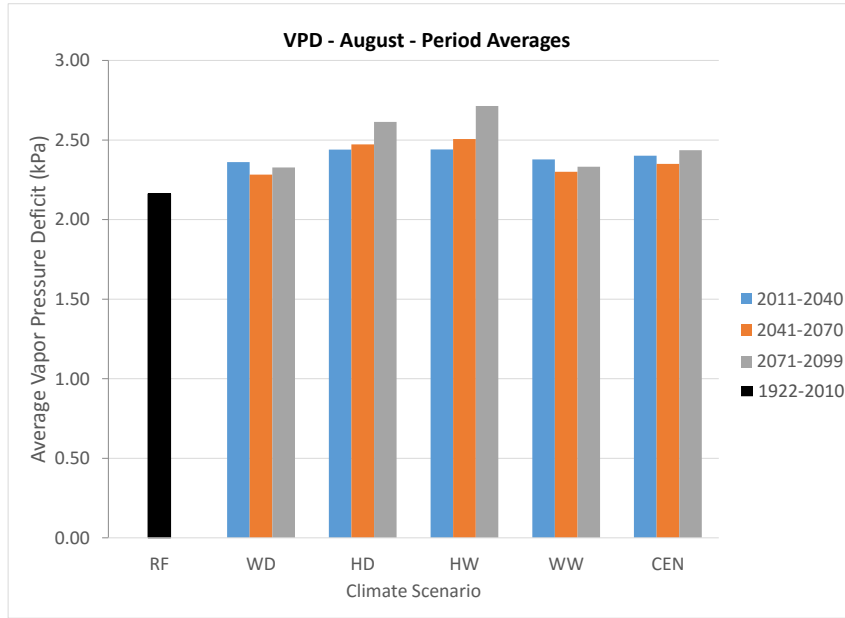
Figure 4B-17. Projected August monthly average vapor pressure deficits in kilo Pascals (kPa) for each climate scenario for 2011-2040 (2025), 2041-2070 (2055) and 2070-2099 (2084)

Notes: RF scenario was averaged over historical climate sequence for August from 1922-2010
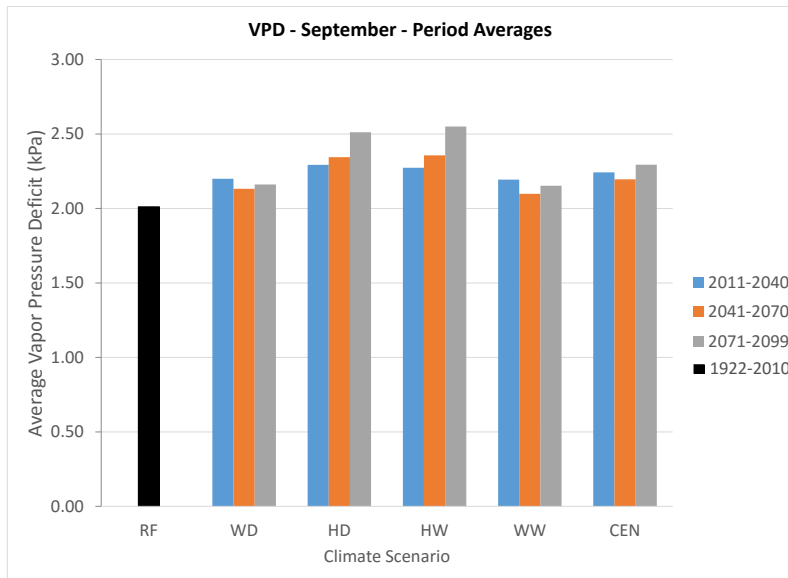
Figure 4B-18. Projected September monthly average vapor pressure deficits in kilo Pascals (kPa) for each climate scenario for 2011-2040 (2025), 2041-2070 (2055) and 2070-2099 (2084)

Notes: RF scenario was averaged over historical climate sequence for September from 1922-2010
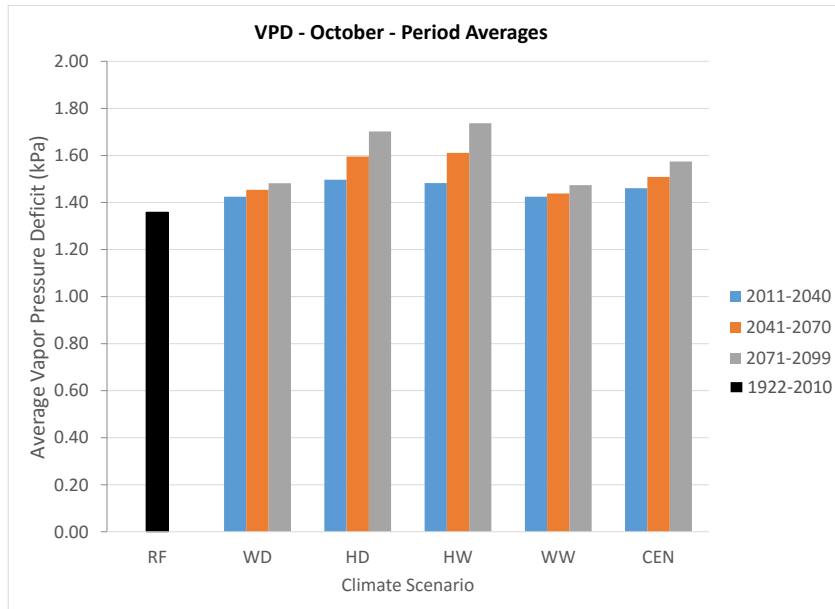
Figure 4B-19. Projected October monthly average vapor pressure deficits in kilo Pascals (kPa) for each climate scenario for 2011-2040 (2025), 2041-2070 (2055) and 2070-2099 (2084)

Notes: RF scenario was averaged over historical climate sequence for October from 1922-2010
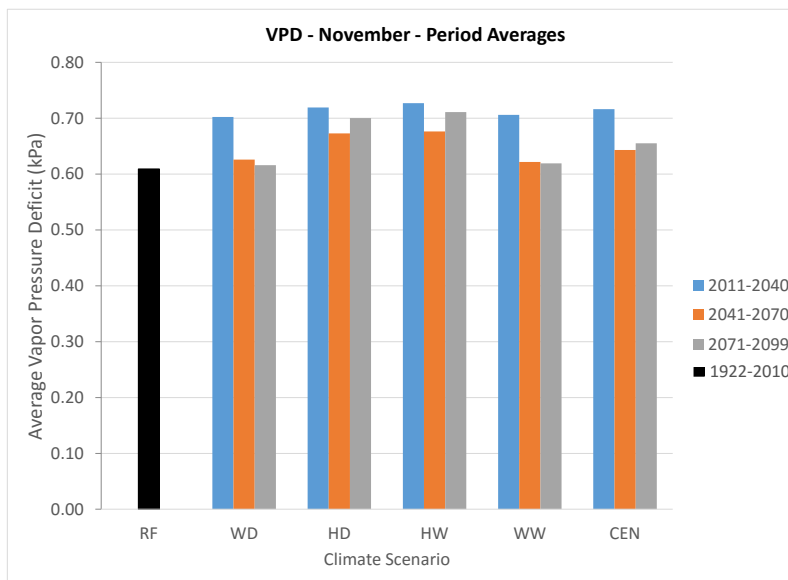
Figure 4B-20. Projected November monthly average vapor pressure deficits in kilo Pascals (kPa) for each climate scenario for 2011-2040 (2025), 2041-2070 (2055) and 2070-2099 (2084)

Notes: RF scenario was averaged over historical climate sequence for November from 1922-2010

VPD - December - Period Averages
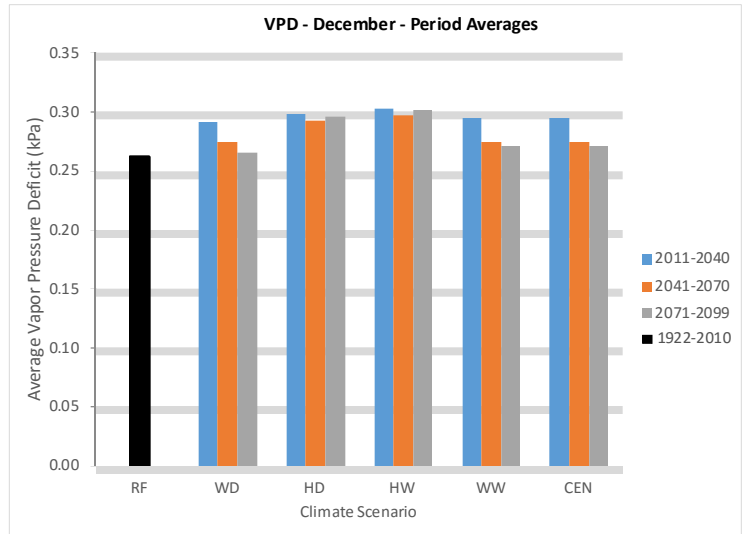
Figure 4B-21. Projected December monthly average vapor pressure deficits in kilo Pascals (kPa) for each climate scenario for 2011-2040 (2025), 2041-2070 (2055) and 2070-2099 (2084)

Notes: RF scenario was averaged over historical climate sequence for December from 1922-2010

Carbon dioxide (CO_2) has also been observed to exert a strong effect on crop ET and for some crop's yield (see Appendix D). As CO_2 concentrations increase, many crops have been observed to exhibit reductions ET. The representative concentration pathways (RCP) have associated CO2 concentrations (see Appendix A for details). Figure B-22 presents these values.
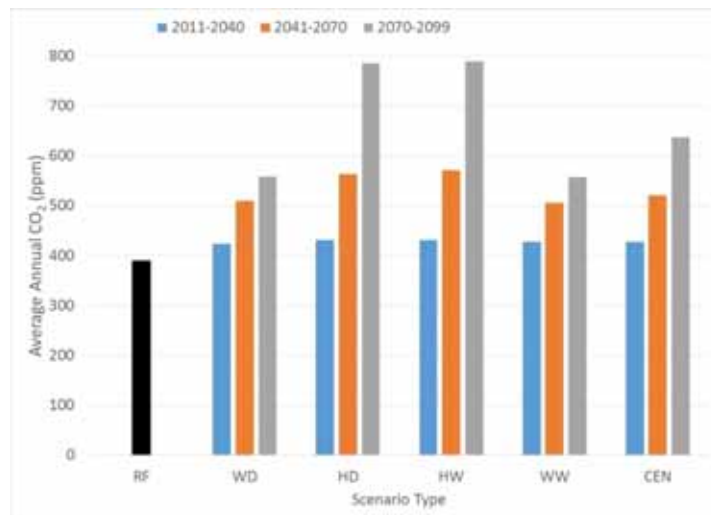
Figure 4B-22. Projected average daily average carbon dioxide concentrations (parts per million (ppm) of CO_2 by volume of air) for each climate scenario during for 2011-2040 (2025), 2041-2070 (2055) and 2070-2099 (2084).

APPENDIX 4C. WEAP-CV CALIBRATION OF THE PLANT GROWTH MODEL (PGM)

Abbreviations and Acronyms

θ_{FC}	soil moisture at field capacity
θ_{PWP}	soil moisture at permanent wilting point
BIS	Basic Irrigation Scheduling program
CIMIS	California Irrigation Management Information System
CO_2	carbon dioxide
CUP	Consumptive Use Program
WEAP-CV	Central Valley Planning Area model
D_e	cumulative depth of evaporation
DSIWM	Division of Statewide Integrated Water Management
DWR	California Department of Water Resources
ET	evapotranspiration
ET_c	crop evapotranspiration under standard conditions
ET_{cadj}	crop evapotranspiration under non-standard conditions
ET_o	reference crop evapotranspiration
FAO	Food and Agricultural Organization
HUI	heat unit index
ITRC	Irrigation Training and Research Center
K_c	crop coefficient
K_s	water stress coefficient
LAI	leaf area index
PGM	Plant Growth Model
PRISM	Parameter-Elevation Regressions on Independent Slopes Model
Reclamation	U.S. Department of the Interior, Bureau of Reclamation
REW	readily evaporable water
SIMETAW	Simulation of Evapotranspiration of Applied Water model
SSJBS	Sacramento-San Joaquin Rivers Basin Study
SWAT	Soil and Water Assessment Tool
TEW	total evaporable water
TM	Technical Memorandum
UC	University of California
USDA	U.S. Department of Agriculture
WEAP	Water Evaluation and Planning System
Z_e	Effective depth of soil over which evaporation will occur

Introduction

The Sacramento-San Joaquin Rivers Basin Study (SSJBS) undertaken by the U.S. Department of Interior, Bureau of Reclamation (Reclamation) in partnership with the California Department of Water Resources (DWR) and local water agencies will recommend various adaptation strategies in response to climate change. One of the principle analytical tools to support this study is the WEAP[2] Central Valley Planning Area (WEAP-CV) model.[3] The WEAP-CV model embeds watershed-based hydrologic routines in a systems operation model. One of the key components of the model is the dynamic calculation of crop water requirements under various climate change scenarios. In the WEAP-CV model crop water use is computed in the Plant Growth Model (PGM) which includes algorithms that compute evapotranspiration, biomass production and yield. In addition to these features, the PGM simulates important crop specific effects of elevated temperature, vapor pressure deficits (VPD) and carbon dioxide (CO_2) on crop water use that have not been included in many other studies.

The calibration of crop evapotranspiration (ET) was performed in two steps. First, daily ET values for 20 major crop types grown in the Central Valley were developed at four Central Valley locations for a recent, representative growing season. These daily ET values were subsequently used as target ET values in the calibration of the WEAP-CV PGM.

1. Evapotranspiration of Agricultural Crops in the Central Valley of California

1.1. Background
This section describes the procedures and models used to develop the ET data sets for the 20 major crop categories used as targets for the calibration of the WEAP-CV PGM. The methods and models employed were developed by the California Department of Water Resources (DWR) in conjunction with the University of California (UC), Davis and applied to data developed as part of California Water Plan, Update 2013.

1.2. Crop Evapotranspiration Under Standard Conditions
Reference crop evapotranspiration, ET_o is the rate of evaporation from an idealized grass crop with a fixed crop height of 0.12 meters, an albedo of 0.23, and a surface resistance of 69 seconds per meter (sm^{-1}) (ASCE-EWRI, 2005). It is used as the basis for computing crop evapotranspiration (ET) under standard conditions (ET_c) which is defined as the ET rate from disease-free, well-fertilized crops, grown in large fields, under optimum soil and water conditions, and

---

[2] The Water and Evaluation Planning (WEAP) System was developed by the Stockholm Environment Institute.
[3] The WEAP-CV model was initially developed for the Califonia Water Plan, Update 2009 and Update 2013 to evaluate the performance of alternative regional resource management strategies in meeting future water management objectives (DWR, 2010).

achieving full production under given weather conditions (Allen et al., 1998). ET_c can be related to ET_o through crop coefficients as follows:

$$ET_c = K_c * ET_o \qquad \text{Eqn. C1-1}$$

where:

ET_o = reference crop evapotranspiration [L/T]

ET_c = crop evapotranspiration under standard conditions [L/T]

K_c = crop coefficient [dimensionless]

In this appendix, ET_c refers to both crop transpiration during the growing season and bare soil evaporation during the growing and non-growing seasons.

A large number of empirical methods have been developed over the last 60 years to estimate ET_c under different meteorological conditions. Early studies related ET_c to pan evaporation data using a crop pan coefficient. Pan coefficients were published in Bulletin 113-3 (DWR, 1975) and Bulletin 113-4 (DWR, 1986). The procedure for determining ET_c from ET_o and crop coefficients was developed and presented in the FAO *Irrigation and Drainage Paper No 24, Crop Water Requirements* (Doorenbos and Pruitt, 1975). This procedure was later refined in *Irrigation and Drainage Paper No 56, Crop Evapotranspiration* (Allen et al., 1998). Grass-based crop coefficients for estimating ET_c were gradually adopted in California following the establishment of the California Irrigation Management Information System (CIMIS) agro-meteorological stations and readily available ET_o data. Over the last decades, crop coefficients for California have been gradually refined and also updated as crop management practices have changed and different crop varieties grown.

1.3 Crop Evapotranspiration under Nonstandard Conditions

ET rates from crops grown under field conditions may be less than under the standard conditions described above. Actual ET_c rates during the non-growing season and during the initial stage of crop growth are strongly influenced by soil moisture in the surface soil layers. Water stress and water salinity may reduce water uptake by plants and limit ET. Actual crop ET (ET_{cadj}) can be related to ET_o as follows:

$$ET_{cadj} = K_s * K_c * ET_o \qquad \text{Eqn. C1-2}$$

where:

ET_{cadj} = crop evapotranspiration under non-standard conditions [L/L]

K_s = water stress coefficient [dimensionless]

K_s can be determined as follows (Allen et al., 1998):

$$
K_s = \begin{cases} \dfrac{\theta_r}{p\theta_{f_c}} & \text{if } \theta_{pwp} \leq \theta_r \leq p\theta_{f_c} \\[3mm] 1 & \text{if } \theta_r > p\theta_{f_c} \end{cases}
$$

where:

θ_r = root zone soil mositure [L/L]

θ_{FC} = field capacity of the root zone [L/L]

θ_{PWP} = permanent wilting point [L/L]

p = fraction of field capacity that can be depleted from the root zone before water stress occurs (dimensionless), also known as the maximum allowable depletion

The factor p differs from one crop to another; varying from 0.3 for shallow-rooted plants to 0.7 for deep-rooted plants. A p value of 0.5 is commonly used for many crops (Allen et al., 1998).

To better account for the wetting and drying cycle driven by precipitation in the winter and spring, ET_c rates are typically determined using a daily soil water balance.

1.4 Bare Soil Evaporation

Bare soil evaporation is important during the non-growing season and during the initial growth stage for annual crops.[4] If the soil is wet, considerable amounts of evaporation may occur from the surface layer. However, as this top layer dries, the evaporation rate falls. Evaporation from bare soil can be divided into two stages (Allen et al., 2005). During the initial stage, actual evaporation is constant and equal to the potential evaporation rate, which is limited by the available energy. During the second stage, actual evaporation falls as the rate of transport of soil moisture to the ground surface falls below the potential evaporation rate.

Stage 1 stops when the cumulative depth of evaporation (D_e), measured since the last significant precipitation or irrigation event, is equal to the readily evaporable water (REW). During Stage 2, evaporation continues to fall until D_e becomes equal to the total evaporable water (TEW). Allen et al. (1998) assume that the REW is equal to the difference in soil moisture between field capacity (θ_{FC}) and mid-way between field capacity and the permanent wilting point (θ_{PWP}). Allen et al. also assume that evaporation will continue until soil moisture in the surface soil layer is mid-way between permanent wilting point and air-dry soil. The total evaporable water from bare soil can be calculated as:

$TEW = (\theta_{FC} - 0.5\ \theta_{PWP})^* Z_e$ Eqn. C1-4

---

[4] As defined in FAO *Irrigation and Drainage Paper No 24* (Doorenbos and Pruitt, 1977) and in FAO *Irrigation and Drainage Paper No 56* (Allen et al., 1998), the initial growth period for annual crops is the time between the planting date and the date of approximately 10 percent ground cover.

where:

$$TEW = \text{total evaporable water [L]}$$

θ_{FC} = soil moisture at field capacity [L/L]

θ_{PWP} = soil moisture at permanent wilting point [L/L]

Z_e = effective depth of soil over which evaporation will occur [L]

Allen et al. (1998) recommend values of Z_e between 4 and 6 inches. For a field capacity equal to 0.35 and permanent wilting point equal to 0.20 (typical values for a clay soil), TEW is equal to 1.5 inches.

The calculation of bare soil evaporation for the SSJBS follows the method of Snyder et al. (2000), Ventura et al. (2006), and as implemented in DWR's Consumptive Use Program[5] (CUP) (Orang et al., 2004; Orang et al., 2013). Allen et al., (1998) assumes that Stage 2 evaporation falls linearly with the cumulative depth of evaporation, once the readily evaporable water has evaporated. Snyder et al. (2000) assumes that Stage 2 evaporation falls linearly with the square root of the cumulative depth of evaporation following a significant wetting event. Bare soil evaporation is calculated using a daily soil water balance. Following precipitation events greater than twice the daily ET_o rate, soil moisture in the top 6-inch soil layer is assumed to be at field capacity. At this soil moisture, the bare soil evaporation coefficient is at its maximum rate, corresponding to Stage 1 evaporation, and can be expressed as follows (Snyder et al., 2000):

$$K_x = 1.22 - 0.04*ET_o \qquad\qquad \text{Eqn. C1-5}$$

where:

K_x = bare soil crop coefficient corresponding to maximum (potential) soil evaporation [dimensionless]

ET_o = reference crop evapotranspiration (mm/day)

Subsequently, daily evaporation falls as the soil surface dries, and evaporation corresponds to Stage 2. Ventura et al. (2006), using data from Doorenboos and Pruitt (1977), developed the following relationship for the bare soil crop coefficient:

$$K_{sx} = \frac{2.54}{\sqrt{CET_o}} \qquad\qquad \text{Eqn. C1-6}$$

where:

$$K_{sx} = \text{bare soil crop coefficient [dimensionless]}$$

CET_o = cumulative reference crop evapotranspiration (mm/day)

---

[5] The Consumptive Use Program was developed by DSIWM to determine ET_o and ET_c. DWR's Bay-Delta Office (BDO) has developed a Consumptive Use Program to calculate the depletion of precipitation and applied water through soil moisture storage and evaporation. These programs share the same name, but are otherwise different. This TM refers to the DSIWM developed program.

Figure 4C1-1 presents a graphical representation of the relationship between bare soil crop coefficient and cumulative reference crop evapotranspiration.
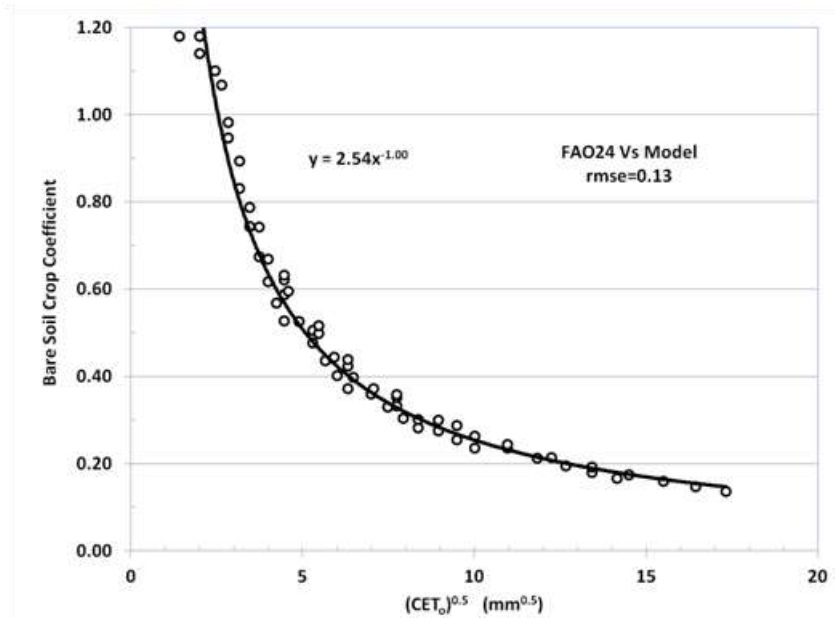
Figure 4C1-1. Relationship Between Bare Soil Crop Coefficient and Cumulative Reference Crop Evapotranspiration

2. ETo Data

Daily historical ET_o data are needed for the development of historical daily ET_c and subsequent calibration of the PGM. CIMIS was jointly developed in 1982 by DWR and UC Davis to assist California farmers use their water resources efficiently. Managed by DWR's Office of Water Use Efficiency, CIMIS consists of a network of over 120 automated weather stations throughout the State. One of the most important data sets provided by CIMIS is ET_o. Two models are used by DWR to determine CIMIS ET_o: Penman-Monteith and a version of Penman's equation modified by Pruitt and Doorenbos (1977). The modified Penman equation employs a wind function developed at UC Davis. The version of the equation used for CIMIS uses hourly weather data to calculate ET_o instead of daily weather data.

Figures 4C1-2 and 4C1-3 show the location of CIMIS stations in the Sacramento River, San Joaquin and Tuare Lake hydrologic regions in the domain covered by the WEAP-CV model. The figures also show the length of record, as indicated by the size of the location circle, and the year records began, as indicated by the value within the location circle. For example, records for the Durham station in the Sacramento River Hydrologic Region started in 1982. CIMIS stations with brown fill have been discontinued. **Figures 4C1-2 and 4C1-3** also delineate ET_o zones as developed for DWR by UC Davis (Jones et al, 1999). **Table 4C1-1** summarizes average monthly ET_o data for selected CIMIS stations located on the floor of the Central Valley.

Four CIMIS stations were selected for calibration of the PGM, based on length of record, locality, and reliability. The selected stations are: Gerber (stn #008), Davis (stn #006), Firebaugh/Telles (stn #007), and Shafter (stn #005). The selected period for PGM calibration was water year 2005.

The data used from the CIMIS stations included maximum and minimum temperature, relative humidity, solar radiation, and wind speed. These data were checked for errors by Justin Huntington of the Desert Research Institute during work on the Central Valley Project Integrated Resource Plan. The description of the error correction procedure provided below is paraphrased from the description given in Appendix B of this report.

The error checking procedures included removal of solar radiation outliers by comparison of daily observed data with daily clear sky radiation. Observed values in excess of the clear sky radiation were removed. Following that, a monthly average ratio of daily solar radiation and clear sky radiation was calculated for the top 20 percent daily values of the ratio. The daily values of solar radiation were then divided by this ratio to produce the final data.

A correction procedure was also applied to the relative humidity data. During this process it was observed that some of the CIMIS RH sensors suffered from "sensor drift" in which the maximum RH values decreased over a time span of seveal years. To correct this the observed RH values were adjusted so that the maximum values for each year approached 100 percent. Any missing values were estimated using the methods described in Annaandale et al. (2002).

Table 4C1-1. Reference Crop Evapotranspiration for Selected CIMIS Stations

CIMIS Station	Average Values, Water Years 1996–2005 Unless Noted Otherwise (inches)												
	Oct	Nov	Dec	Jan	Feb	Mar	Apr	May	Jun	Jul	Aug	Sep	Total
Sacramento River Hydrologic Region													
Browns Valley	3.9	1.7	1.1	1.0	1.7	3.5	4.6	6.3	7.5	8.3	7.4	5.6	52.6
Colusa	3.9	1.6	1.2	1.0	1.6	3.6	5.2	6.7	5.7	8.1	6.1	5.4	50.2
Davis	4.3	1.8	1.2	1.0	1.8	3.9	5.4	7.0	8.1	8.4	7.4	5.9	56.3
Dixon	4.1	1.8	1.2	1.0	1.8	3.8	5.2	6.8	7.9	8.4	7.3	5.6	54.8
Durham	3.4	1.5	1.0	1.0	1.9	3.6	4.8	6.4	7.4	7.7	6.8	5.2	50.9
FairOaks[1]	3.4	1.6	1.0	1.1	1.7	3.5	4.5	6.6	7.6	8.0	7.2	5.3	51.5
Gerber	4.1	1.7	1.1	1.1	1.8	3.7	4.9	6.7	8.0	8.3	7.3	5.6	54.4
Nicolaus	3.6	1.5	1.0	0.8	1.6	3.5	4.9	6.4	7.5	8.0	6.7	4.3	49.9
Orland	3.9	1.7	1.2	1.1	1.8	3.7	4.8	6.6	7.0	7.8	6.9	5.4	51.9
Zamora	3.9	1.7	1.2	1.0	1.8	3.8	5.0	6.6	7.4	7.8	6.9	5.4	52.3
San Joaquin River Hydrologic Region													
Brentwood	3.8	1.7	1.0	0.9	1.8	3.9	5.3	7.0	8.0	8.3	7.4	5.6	54.7
Firebaugh	4.0	1.8	1.1	1.0	1.9	4.0	5.6	7.7	8.2	8.2	7.5	5.7	56.8
Los Banos	3.8	1.7	1.1	1.0	1.8	3.8	5.4	7.4	8.3	8.5	7.5	5.7	56.0
Madera[1]	3.7	1.8	1.1	1.1	2.0	3.8	5.3	7.7	8.4	8.7	7.7	5.7	56.8
Merced[1]	3.7	1.8	1.1	1.2	1.9	3.7	4.9	7.1	8.0	8.5	7.7	5.6	55.1
Modesto	3.5	1.5	1.0	0.9	1.7	3.6	5.0	6.5	7.7	7.9	6.9	5.2	51.6
Panoche	4.0	1.7	1.2	1.1	2.0	4.1	5.8	7.9	8.6	8.4	7.3	5.7	57.8
Patterson[1]	4.1	2.0	1.3	1.3	2.1	4.3	5.5	8.0	8.7	8.4	7.4	5.8	58.9
Tulare Lake Hydrologic Region													
Blackwells Corner	4.1	1.8	1.3	1.4	2.1	4.2	5.8	7.8	8.8	9.5	8.5	6.3	61.5
Fresno State	3.6	1.7	1.0	1.0	1.7	3.7	5.3	7.4	8.3	8.6	7.7	5.6	55.8
Five Points	4.3	2.0	1.2	1.1	1.9	4.2	6.1	8.4	8.7	8.8	8.1	6.2	61.0
Kettleman	4.4	2.0	1.3	1.2	2.0	4.2	6.0	8.1	8.8	9.2	8.4	6.3	62.0
Lindcove	3.4	1.7	1.1	1.1	1.7	3.5	4.8	6.7	7.6	8.0	7.2	5.3	51.9
Parlier	3.4	1.6	1.0	0.9	1.7	3.7	5.2	7.1	7.8	8.1	7.2	5.3	53.0
Shafter	3.9	1.9	1.3	1.2	2.0	4.0	5.5	7.3	7.9	8.1	7.3	5.7	55.9
Stratford	4.1	1.8	1.1	1.1	1.9	4.0	5.7	8.0	8.7	8.9	8.0	6.1	59.4

Notes:

[1] Data are average of water years 2000 – 2009.

[2] Evapotranspiration for the 10-year period 2000 – 2009 is approximately 2 percent greater than for the 10-year period 1996–2005.

Key:

CIMIS=California Irrigation Management Information System
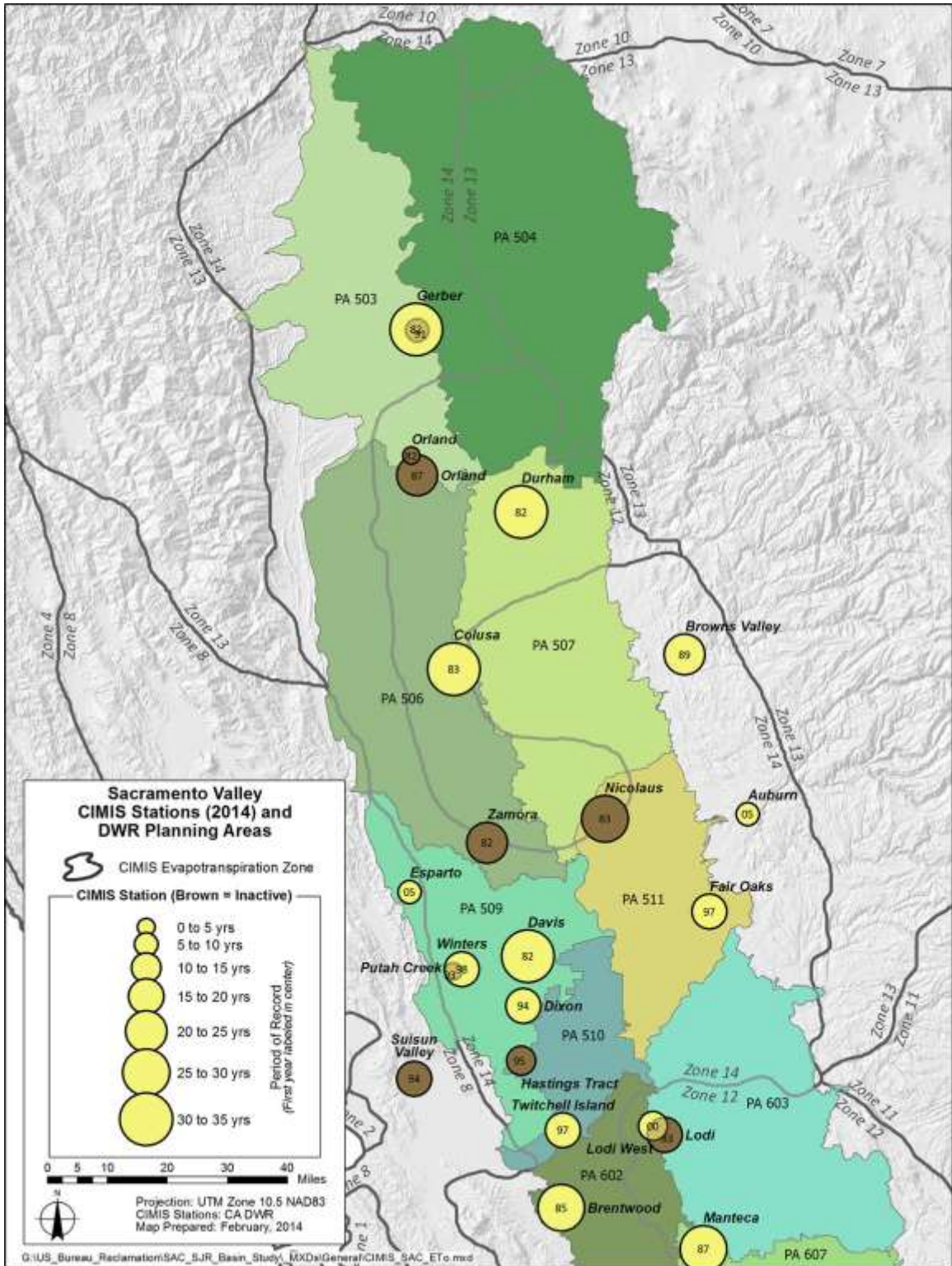
Figure 4C1-2. CIMIS Stations in Sacramento River Hydrologic Region
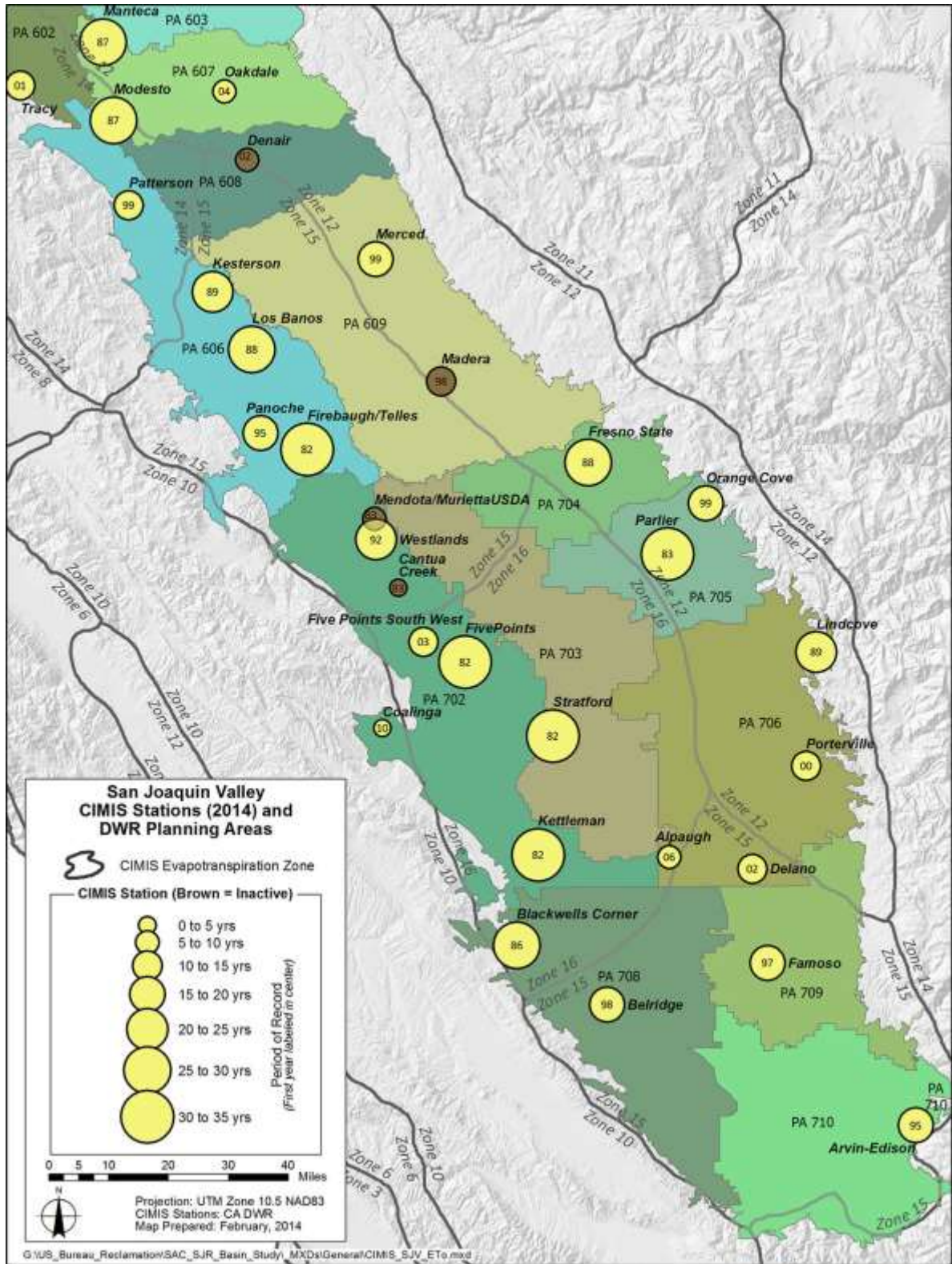
Figure C1-3. CIMIS Stations in San Joaquin and Tualre Lake Hydrologic Regions

2.1 Crop Type Categories

For the SSJBS, irrigated agricultural land is separated into 20 crop categories as used by the Division of Statewide Integrated Water Management (DSIWM) for the California Water Plan. **Table 4C1-2** presents the mapping of the 20 crop categories used by DSIWM to the 20 specific crops represented by the PGM.

Table 4C1-2. Mapping of Crop Type Categories

ID	Classification		ID	Classification	
	DSIWM	PGM		DSIWM	PGM
1	Alfalfa	Alfalfa	11	Other Truck	Cucumber/Lettuce[1]
2	Almonds/Pistachios	Almonds	12	Pasture	Pasture
3	Corn	Corn	13	Potatoes	Potatoes
4	Cotton	Cotton	14	Rice	Rice
5	Cucurbits	Melons	15	Safflower	Safflower
6	Dry Beans	Dry Beans	16	Subtropical	Oranges
7	Grain	Wheat	17	Sugar Beets	Sugar Beets
8	Onions and Garlic	Onions	18	Tomatoes Hand-Picked[2]	Tomatoes
9	Other Deciduous	Apples	19	Tomatoes Machine-Picked[3]	Tomatoes
10	Other Field	Corn - silage	20	Vineyards	Vines

Notes:

[1] Cucumber for the Sacramento Valley and Lettuce for the San Joaquin Valley.

[2] Hand-picked tomatoes are also known as fresh tomatoes.

[3] Machine-picked tomatoes are also known as processed tomatoes.

Key:

ID = identification number

DSIWM = Division of Statewide Integrated Water Management

PGM = Plant Growth Model

2.2. Crop Coefficients and Growth Stages

Crop coefficients relate ET_c to ET_o. ET_o accounts for variations in weather and is a measure of the evaporative energy. Difference between ET_c and ET_o are caused by light absorption of the plant canopy, canopy roughness and resulting turbulence, crop physiology, leaf age, and surface wetness. When not limited by water availability, ET is limited by the availability of energy to vaporize water. Therefore, solar radiation/light interception by the foliage has a large effect on the ET rate.

As a crop canopy develops, the ratio of transpiration from the plant to total ET increases until most of the ET is transpiration and evaporation from the soil surface is relatively small. Crop coefficients for field and row crops generally increase until the canopy ground cover reaches about 75 percent. For tree and vine crops the peak crop coefficient is reached when the canopy has reached about 63 percent ground cover (Snyder et al., 2007).

Crop coefficients for a specific crop vary by region, soil type, irrigation frequency, irrigation method, and many other factors. Coefficients for the non-

growing season (primarily to account for bare soil evaporation) vary with precipitation and resulting changes in soil moisture.

2.2.1. Annual Crops

Daily crop coefficients for a specific crop may be calculated from the standardized crop coefficient curve described in FAO *Irrigation and Drainage Paper 24* and illustrated in **Figure 4C1-4**. Seven parameters are used to define this standardized curve. Four parameters define the length of distinct growing periods (initial, development, mid-season, and late-season). Three values of K_c define the magnitude of the daily crop coefficients at particular stages of crop growth (initial stage, mid-season stage, and late stage). Crop coefficients for the initial growth stage are a function of the interval between wetting events, the evaporative energy (as indicated by ET_o), and the magnitude of the wetting events.
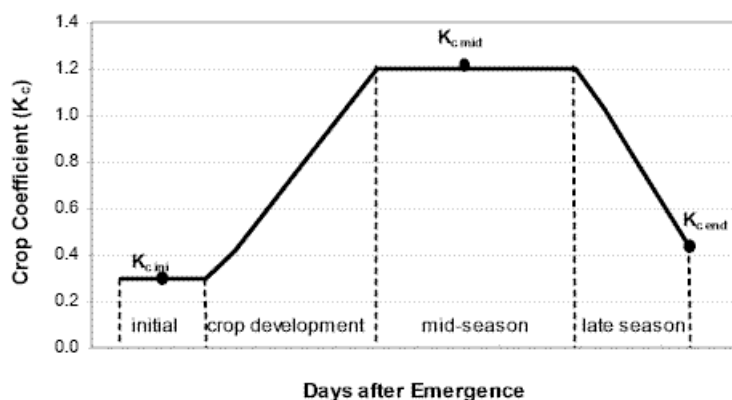
Figure 4C1-4. Standardized Crop Coefficient Curve

2.2.2. Deciduous Tree and Vines

In the absence of a cover crop, deciduous tree and vines have a similar K_c curve to annual crops, but without the initial growth period. The growing season begins with rapid growth at leaf out. The midseason period begins at approximately 60 percent ground cover. Subsequently, unless the crop is immature, the crop coefficient is constant until the onset of senescence. The crop coefficient begins to drop during late-season. At leaf drop, transpiration is near zero. At leaf out, the crop coefficient is equal to the bare soil evaporation.

When a cover crop is present, K_c values are higher depending on the amount of cover. The following are technical recommendations for analysis by Snyder et al. (2009):

During the growing season, the K_c value is increased by 0.35 over the value for a mature crop with no cover, but is capped at a maximum value of 1.15.

During the non-growing season, the K_c value is increased by 0.35 over the value for bare soil evaporation, but is capped at a maximum value of 0.90. This limit is imposed because of shading by tree trunk and branches.

Estimates for the area of trees and vines that have cover crops are presented in *Evaporation from Irrigated Agricultural Land in California* (ITRC, 2002). This report assumes that a cover crop exists on approximately 40 percent of the acreage of orchards and vineyards in the Sacramento Valley and the eastside of the San Joaquin Valley. On the westside of the San Joaquin Valley, the report assumes approximately 5 percent of orchards and vineyards have a cover crop. The lower value for the westside of the San Joaquin Valley is due to the scarcity of irrigation water in many years. The exception is citrus, which typically does not have a cover crop.

Immature deciduous tree and vines use less water than when mature. Snyder et al. (2009) give the following realtionships for modeling of immature trees and vines:

$$K_{c,\text{immature}} = K_{c,\text{mature}} * \text{minimum}(1.0, \sin\left(\frac{Cg}{70}.\frac{\pi}{2}\right))$$

And for citrus:

$$K_{c,\text{immature}} = K_{c,\text{mature}} * \text{minimum}(1.0, \sqrt{\sin\left(\frac{Cg}{70}.\frac{\pi}{2}\right)})$$

where:

Cg = percent ground cover

ITRC (2002) assumed that trees reach maturity after 6 years and vines after 3 years, and that both trees and vines have a 30-year life-span. These assumptions result in 17 percent of trees and 10 percent of vines being classified as immature.

2.2.3. Published Values

Typical values for crop coefficients and the length of crop growth stages are published in FAO *Irrigation and Drainage Paper 24* and *Irrigation and Drainage Paper Paper 56*. Values specific to California have been published by DWR (1986), the Cooperative Extension, University of California (1989, 1994), Division of Agriculture and Natural Resources (Schwankl et al., 2007), ITRC (2002), and Snyder et al., (2009).

Irrigation Training and Research Center

In 2002 and 2003, the Irrigation Training and Research Center (ITRC)[6] published reports on ET in California. *California Crop and Soil Evapotranspiration* (ITRC, 2003) presents monthly ET rates for a range of crops in 13 DWR-defined ET_o zones (Jones et al., 1999). Monthly values are for three types of precipitation years (typical, wet, and dry), which correspond to years 1997, 1998, and 1999, respectively. Crop transpiration and soil evaporation were determined based on the dual crop coefficient method developed by Allen et al. (1998) and daily simulation of soil moisture conditions in the root zone. Inputs to the daily simulation model are presented in *Evaporation from Irrigated Agricultural Land in California* (ITRC, 2002).

---

[6] The ITRC was established in 1989 at California Polytechnic State University, San Luis Obispo, as a center of excellence, to support California's irrigation industry.

University of California, Davis

The Basic Irrigation Scheduling (BIS) program was developed by Snyder (2000) to determine daily ET_c values for a range of crops based on monthly ET_o values. The program is an aid to irrigation scheduling. Input data for the program includes crop coefficients and growth stages assembled by Department of Land, Air, and Water Resources at UC Davis and the UC Cooperative Extension. The BIS program has been refined and released as CUP in collaboration with DWR (Orang et al., 2004). DWR has used identical crop coefficients and growth stages for the SIMETAW[7] and CALSIMETAW[8] models.

2.3. Crop Coefficients Used to Develop ETc Values for the Calibration

There are significant variations in published values for crop coefficients and growth stages. This is partly due to the effects of local climate and soil conditions on ETc, differences in crop varieties, and the effects of irrigation technology and management. The daily values of ETc used in the calibration of the WEAP-CV PGM were computed from the Kc and growth stage values developed by Snyder et al. for use in conjunction with BIS, CUP, and SIMETAW models. This choice provides greater consistency with DWR California Water Plan 2013 Update Study values. These values were obtained from Orang (2013) and are presented in Table C1-3. These values include revised Kc values for tree crops based on recent studies in the Central Valley reported by Consoli et al. (2006) and Sanden et al. (2012). Kc values reported in Table C1-3 do not include an 8 percent reduction to account for bare spots and reduced vigor.

Table 4C1-3. Parameters for Crop Coefficient Curves

Crop	Length of Season	Percent of Growing Season			Crop Coefficients		
		initial	development	mid-season	K_c ini	K_c mid	K_c end
Alfalfa (annual)	365	25	50	75	1.00	1.00	1.00
Almonds[1]	229	0	50	90	0.55	1.20	0.65
Apple	229	0	50	75	0.55	1.15	0.80
Asparagus	365	12	25	95	0.25	0.95	0.25
Barley	212	20	45	75	0.30	1.05	0.15
Beans (dry)	108	24	40	91	0.20	1.10	0.10
Broccoli	104	20	50	83	0.30	1.05	1.00
Carrots	121	20	50	83	0.85	0.95	0.80
Corn (grain)	153	20	45	75	0.20	1.05	0.60

---

[7] The Simulation of Evapotranspiration of Applied Water (SIMETAW) model simulates many years of daily weather data from monthly climate data and estimates ET_o and ET_c (Snyder et al., 2005). SIMETAW uses a soil water balance model that is similar to CUP.

[8] The CALSIMETAW computer model estimates ET_c and ET of applied water (ETAW) for use in California water resources planning (Rayej et al., 2011; Orang, 2013). The model includes spatial soil and climate information and uses historical crop category information to provide seasonal water balance estimates by combinations of detailed analysis units and county (DAU/County). The seasonal water balance is used to estimate the ETAW by crop and crop category for each DAU/County combination over the State.

Crop	Length of Season	Percent of Growing Season			Crop Coefficients		
		initial	development	mid-season	K_c ini	K_c mid	K_c end
Corn (silage)	107	20	45	100	0.20	1.05	1.00
Cotton	154	15	25	85	0.35	1.00	0.50
Cucumber	93	19	47	85	0.80	1.00	0.75
Eucalyptus	365	0	33	67	1.15	1.15	1.15
Flowers	184	33	67	92	0.80	1.00	0.80
Fig	229	0	50	90	0.55	1.20	0.65
Kiwifruit	184	0	22	67	0.35	1.10	0.80
Lettuce	73	32	80	90	0.40	1.00	1.00
Melon[3]	123	21	50	83	0.75	1.05	0.75
Oats	212	20	45	75	0.30	1.05	0.15
Olives[2]	365	0	33	67	0.90	0.90	0.90
Onion (dry)	215	13	42	72	0.55	1.20	0.55
Orange[1]	365	0	33	67	1.00	1.00	1.00
Pasture (improved)	365	25	50	75	0.95	0.95	0.95
Peppers (bell)	92	23	86	90	0.30	1.05	1.05
Pistachios[1]	271	0	33	78	0.70	1.15	0.50
Potato	123	20	45	78	0.70	1.15	0.50
Plum-Prune	229	0	50	90	0.55	1.15	0.65
Rice	139	24	37	86	1.20	1.05	0.80
Safflower	122	17	45	80	0.20	1.05	0.25
Sorghum	229	16	42	75	0.20	1.05	0.60
Squash	91	20	50	80	0.50	0.95	0.75
Strawberries	153	15	45	80	0.40	1.05	0.70
Stone fruits	229	0	50	90	0.55	1.20	0.65
Sudangrass	231	13	43	83	0.50	0.90	0.85
Sugarbeet	200	15	45	80	0.20	1.15	0.95
Sunflower	133	20	45	80	0.20	1.05	0.40
Sweet Potato	123	20	45	78	0.70	1.15	0.50
Tomato	153	25	50	80	0.20	1.20	0.60
Walnuts[1]	229	0	50	75	0.55	1.20	0.80
Wheat	212	25	60	90	0.30	1.05	0.15
Wine grapes	215	0	25	75	0.45	0.80	0.35

Notes:

[1] Mid-season crop coefficients for almonds and other tree crops may vary between 0.90 – 1.15 depending on whether a cover crop is present.

[2] The constant K_c value of 0.80 for olives is applicable to a mature orchard, and assumes no cover crop is present.

[3] The growing season for melons was revised from 229 days given in CUP to 123 days.

2.4. Growing Season Values Used to Develop ETc Values for the Calibration

For the WEAP-CV model calibration, the growing season lengths were based on typical crop planting and harvest dates published by the U.S. Department of Agriculture (USDA, 2010), ITRC (2003) and the DSIWM. More detailed information on planting dates available for each county through the agricultural cooperative extension services was also used in assessing the values to employ in

the calibration. Typical growing and irrigation seasons for the Central Valley are as follows (UC Davis 2013):

- **Alfalfa** seed is planted in September. Once established, Alfalfa is cut seven times per year. Cutting begins in March and continues through November. The crop is semi-dormant in December and dormant in January. Approximately 6 inches of water may be needed for seed germination. Once established, the crop is typically irrigated from April through September in seven irrigations totaling 3.5 feet.

- **Almonds/pistachios** category is predominantly almonds (90 percent). Almonds begin growing early February and bloom mid-February. Pistachios begin growing late March and bloom in April. Almonds and pistachios are harvested in September. Fields are typically irrigated from April through September and October (post-harvest). Almonds differentiate their fruiting buds during and after harvest, so it is important to reduce water stress immediately after harvest. Depending on the variety, almonds may require 5 to 10 inches of irrigation after harvest. Irrigation depths are typically 2 to 3 feet per year.

- **Corn** is typically planted March through April and harvested in August. It is irrigated April through July; irrigation depths are typically 3.5 feet per year. Corn for silage is planted in June and harvested from September through November.

- **Cotton** is planted in late March, April, and early May and harvested in October and early November. Irrigation is typically cut-off at the end of August. Crop plow-down in December and January is required for pest control. Irrigation depths are approximately 2.5 feet per year.

- **Cucurbits** include melons, squash, and cucumbers and have differing growing seasons and planting dates.

- **Dry beans** are typically planted mid-May to early July and harvested in August and September. They are irrigated May through August; irrigation depths are approximately 2.5 feet per year.

- **Grains** are typically planted October through mid-December and harvested May through July. For wheat, a 6-inch irrigation may be applied in April after the spring rains have finished.

- **Garlic** is planted mid-September through December and harvested June through August. Irrigation for fresh garlic typically ceases 1 month before harvest. Garlic for dehydration is harvested 2 months after end of irrigation.

- **Other deciduous** category is predominantly walnuts (32 percent), peaches and nectarines (25 percent), plums (12 percent), and prunes (9 percent). Walnuts are mechanically harvested September through October. However, irrigation is continued through November to prevent winter injury to mature trees. Irrigation depths are typically 3 feet per year.

- **Other field category** includes sorghum, sudan, and sunflower. Sorghum for grain is planted in late May through early July and harvested in September. Sunflower is primarily grown for seed production. It is planted in April and harvested in August/September. Approximately 2.5 feet are applied through the growing season.

- **Other truck** category covers a wide range of crops with differing planting dates. Particular crops may be planted at different times of the year. For example, carrots are planted December through March and harvested May through July. Alternatively, they may be planted July through September and harvested November through February.

- **Tomatoes** are planted over a 3-month period, late March to early June, to meet contracted delivery schedules at harvest. Tomatoes for processing are harvested late July through September. Irrigation depths are typically 3 feet per year.

- **Vines** leaf in March and are harvested August and September. The vines are typically irrigated May through October. Inadequate water after harvest may adversely affect spring growth. After harvest, grapevines continue to assimilate carbohydrates and mineral nutrients to maintain health during dormancy and new growth the following season. Late irrigation may be needed October through December when precipitation is less than 1 inch per month.

- **Wheat** is typically planted in December and harvested in June. Wheat may be planted into pre-irrigated soil or into dry soil and the seed germinated with an irrigation or impending rainfall. The first post-emergence irrigation for wheat is usually not needed until boot[9] (mid-April) in years of normal rainfall. The last irrigation should be applied at the beginning of soft dough[10] (mid-May).

---

[9] At the boot crop stage, the flag leaf is fully visible.
[10] The wheat kernel resembles soft dough during the final stage of weight accumulation.

Planting dates for calibration of the PGM are are based on values developed by DSIWM in conjunction with UC Davis (Snyder et al., 2013) and as part of the development of CUP and the SIMETAW and CALSIMETAW models. This approach provides greater consistency across DWR planning divisions. Planting dates were obtained from Orang (2013) and are presented in **Table 4C1-4**.

Table C1-4. Growing Season and Planting and Harvest Dates

Perennial Crop	Length of Growing Season	Start of Growing Season	End of Growing Season
Alfalfa (annual)	365	1-Jan	31-Dec
Almonds	229	1-Mar	15-Oct
Apple	229	1-Apr	15-Nov
Asparagus	365	1-Jan	31-Dec
Orange	365	1-Jan	31-Dec
Eucalyptus	365	1-Jan	31-Dec
Fig	229	1-Mar	15-Oct
Kiwifruit	184	1-May	31-Oct
Olives	365	1-Jan	31-Dec
Pasture (improved)	365	1-Jan	31-Dec
Pistachios	271	1-Mar	26-Nov
Plum-Prune	229	1-Mar	15-Oct
Stone fruits	229	1-Mar	15-Oct
Walnuts	229	1-Apr	15-Nov
Wine grapes	215	1-Apr	1-Nov
Annual Crop	**Length of GrowingSeason**	**Planting Date**	**Harvest Date**
Barley	212	1-Nov	31-May
Beans (dry)	108	15-Jun	30-Sep
Broccoli	104	20-Aug	1-Dec
Carrots	121	15-Jan	15-May
Corn (grain)	153	1-May	30-Sep
Corn (silage)	107	1-May	15-Aug
Cotton	154	15-May	15-Oct
Cucumber	93	15-May	31-Aug
Flowers	184	1-Apr	31-Aug
Lettuce	73	25-Aug	5-Nov
Melon	123	15-May	15-Sep
Oats	212	1-Nov	31-May
Onion (dry)	215	1-Mar	1-Oct
Peppers (bell)	92	25-Apr	25-Jul
Potato	123	15-Apr	15-Aug
Rice	139	15-May	30-Sep
Safflower	122	1-Apr	31-Jul
Sorghum	229	1-Apr	15-Nov
Squash	91	15-Jan	15-Apr
Strawberries	153	1-May	30-Sep
Sudangrass	231	1-Apr	17-Nov

Sugarbeet	200	15-Mar	30-Sep
Sunflower	133	1-May	10-Sep
Sweet Potato	123	15-Apr	15-Aug
Tomato	153	1-Apr	31-Aug
Wheat	212	1-Nov	31-May

2.5. Other Factors Affecting Evapotranspiration

The ITRC (2002) describe factors that affect ET and either increase or decrease the amount of ET compared to amounts determined using ET_o and crop coefficients. These factors are described below.

- Stubble, soil mulches, and no till practices can significantly decrease bare soil evaporation.

- Evaporation increases with the fraction of the soil surface that is wetted; this is primarily a function of irrigation method (surface, sprinkler, or drip).

- Evaporation from a wet canopy increases total ET, although this increase is partly offset by a decrease in transpiration; the increase in total ET may be over 50 percent.

- Evaporation from sprinkler spray, before droplets reaches the ground, are estimated to be between 1 and 4 percent of the applied water.

- Bare spots and decreased vigor, caused by uneven salinity, irrigation, and fertilizer distribution, pests and disease, and soil conditions, may reduce transpiration by 10 percent.

ITRC (2002) recommend that ET_c values used for water balance purposes should be decreased to account for bare spots and lack of vigor.[11] Research suggests that ET_c should be decreased by 7 to 8 percent (ITRC, 2003). For calibration of the PGM, crop coefficients were decreased by 8 percent from values presented in **Table C1-3** to account for these non-ideal conditions.

---

[11] ET_c values used for irrigation scheduling should not be decreased.

2.6. Simulation of Daily Crop Evapotranspiration

A spreadsheet model was constructed to simulate daily ETcadj. The spreadsheet model is an extension of CUP and can simulate soil moisture and ET for more than 50 different crop types using a daily time step and climate data from October 1921 through September 2009. The spreadsheet model was run for four sets of daily climate data (precipitation and ETo) corresponding to the four selected CIMIS stations for water year 2005. This water year was selected because it is fairly representative of long term climatological conditions (See Figure 3-3 and Figure 3-4). Table C1-5, C1-6, C1-7, and C1-8 present a summary of model results. ET values include both transpiration by the crop and evaporation from the soil surface during the growing and non-growing season.

Figure C1-5 presents model output for wheat for the two calendar years 2004 and 2005. The figure shows the Kc value, calculated as the ratio of ETc to ETo for the four selected CIMIS locations. The crop coefficient curve is most evident at Shafter because of the limited influence of precipitation. At Gerber, where precipitation is greatest, the standard crop coefficient curve is obscured by peak ET_c values following precipitation events.

Figure C1-6 presents model output for melons for the two calendar years 2004 and 2005. Similar to Figure 1-5, the figure shows the Kc value, calculated as the ratio of ETc to ETo for the four selected CIMIS locations. The standard crop coefficient curve is most evident than for wheat because of the limited influence of precipitation during the melon growing season.
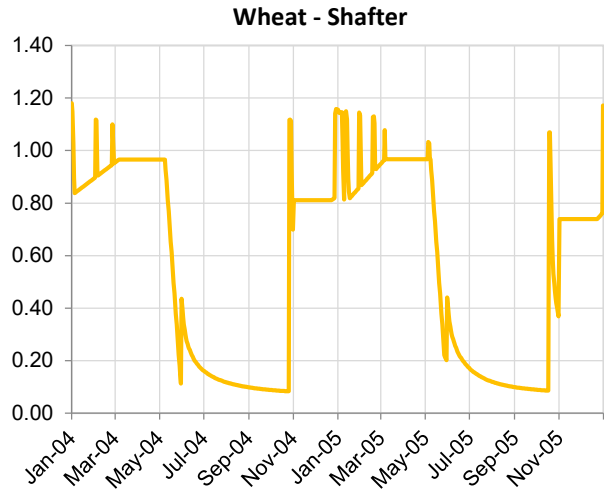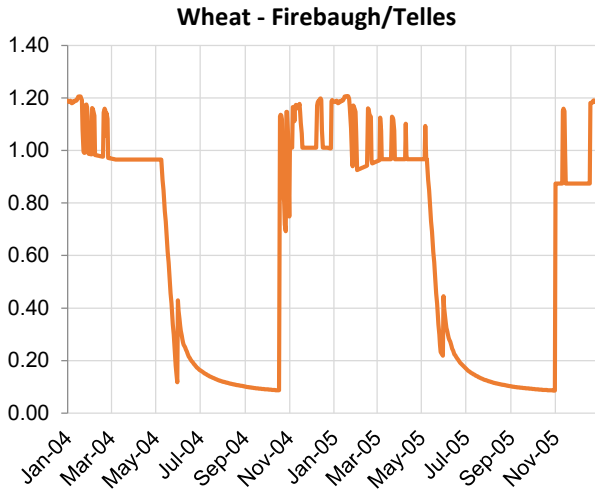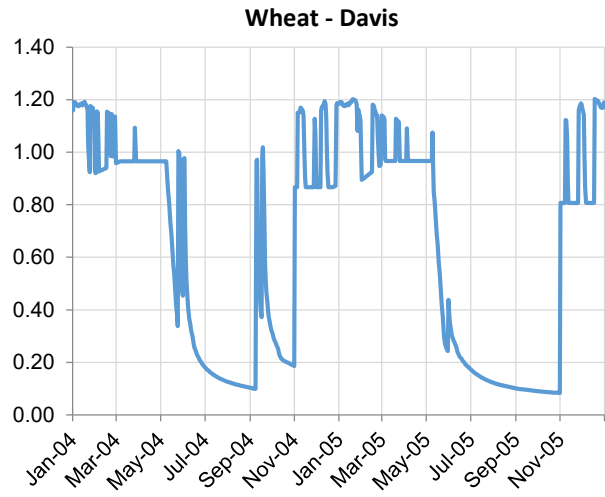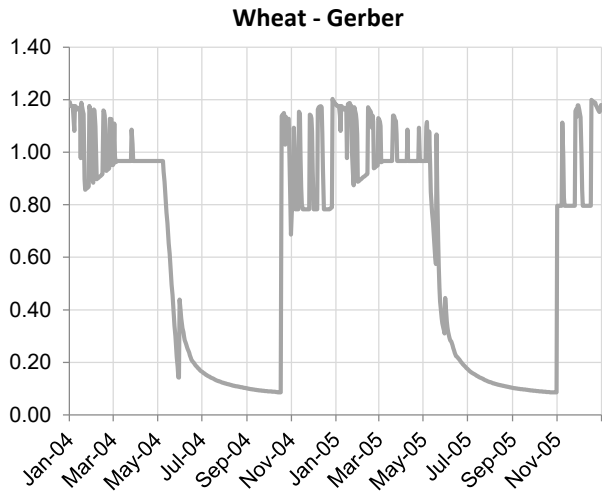
Figure C1-5. Ratio of ET$_c$ to ET$_o$ for Wheat at Four Different CIMIS Station Locations, Calender Years 2004-2005
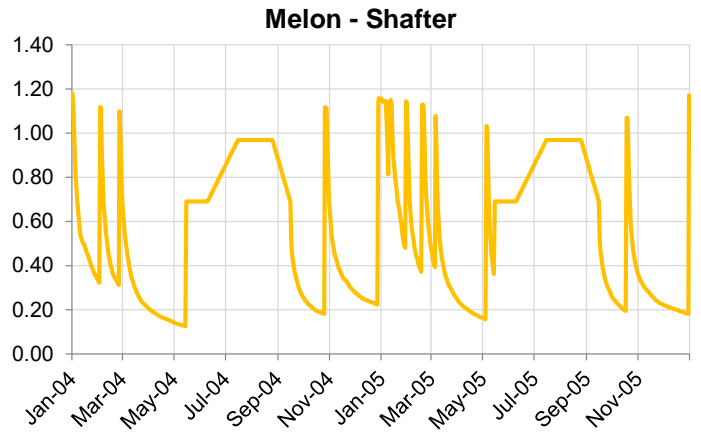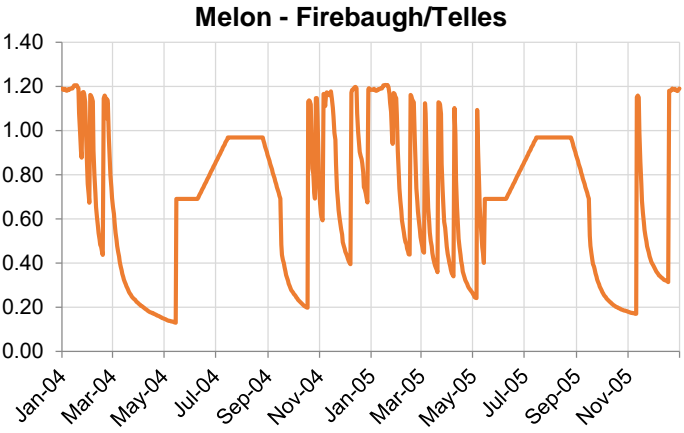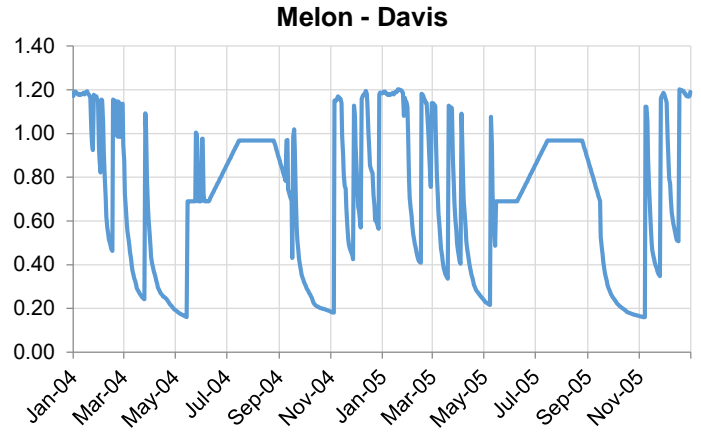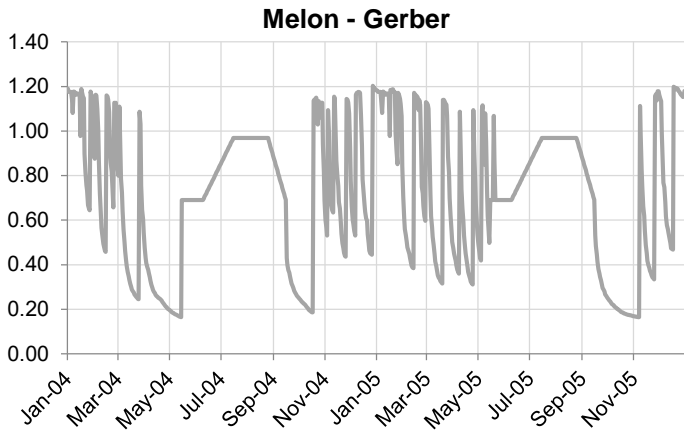
Figure C1-6. Ratio of ET$_c$ to ET$_o$ for Melon at Four Different CIMIS Station Locations, Calender Years 2004-2005

Table C1-5. Crop Evapotranspiration for Selected CIMIS Stations

CIMIS Station	Water Year 2005 (inches)												
	Oct	Nov	Dec	Jan	Feb	Mar	Apr	May	Jun	Jul	Aug	Sep	Total
Gerber													
ETo	4.6	2.8	2.1	1.6	2.5	4.0	4.5	5.4	6.9	8.1	7.8	6.2	56.4
Precipitation	4.0	1.7	6.7	5.1	2.4	2.4	1.5	2.7	0.3	-	-	-	26.7
Alfalfa	4.5	2.7	2.0	1.8	2.5	3.8	4.2	5.1	6.4	7.4	7.2	5.7	53.1
Almonds	3.7	2.1	1.5	1.8	1.8	2.9	3.5	5.1	7.3	8.9	8.6	6.6	53.9
Apples	4.5	2.3	1.5	1.8	1.8	2.5	2.9	4.3	6.0	8.2	8.2	6.4	50.5
Corn	2.5	2.1	1.5	1.8	1.8	2.5	2.4	3.5	4.9	7.7	7.4	4.4	42.4
Corn - silage	1.8	2.1	1.5	1.8	1.8	2.5	2.4	3.8	6.1	7.7	4.9	1.1	37.5
Cotton	3.3	2.1	1.5	1.8	1.8	2.5	2.4	3.2	5.0	7.6	7.3	5.6	44.2
Cucumber/Lettuce	1.5	1.8	1.2	1.4	1.6	2.1	2.0	3.3	4.7	6.1	5.4	1.4	32.6
Dry Beans	2.5	2.1	1.5	1.8	1.8	2.5	2.4	3.0	2.4	5.7	7.9	5.1	38.7
Melons	1.7	1.8	1.2	1.4	1.6	2.1	2.0	3.2	4.4	6.2	6.1	2.9	34.7
Onions	2.5	2.1	1.5	1.8	1.8	3.0	3.6	5.6	7.6	8.9	7.5	4.1	50.0
Oranges	4.5	2.7	2.0	1.8	2.5	3.8	4.2	5.1	6.4	7.4	7.2	5.7	53.1
Pasture	4.3	2.6	2.0	1.8	2.4	3.7	4.0	4.8	6.1	7.0	6.8	5.4	50.8
Potatoes	1.8	2.1	1.5	1.8	1.8	2.5	2.9	4.5	7.2	8.0	3.5	1.1	38.7
Rice	2.5	2.1	1.5	1.8	1.8	2.5	2.4	5.1	7.5	7.8	7.5	5.4	48.0
Safflower	1.7	2.1	1.5	1.8	1.8	2.5	2.9	4.9	6.7	5.1	1.9	0.9	34.0
Sugar Beets	2.5	2.1	1.5	1.8	1.8	2.8	3.3	5.0	7.2	8.5	8.2	5.8	50.5
Tomatoes	1.8	2.1	1.5	1.8	1.8	2.5	2.4	3.5	6.9	8.9	6.3	1.6	41.2
Vines	3.0	2.1	1.5	1.8	1.8	2.5	2.7	4.1	5.1	5.9	5.7	4.1	40.3
Wheat	1.3	2.1	1.5	1.5	2.2	3.2	3.7	3.0	1.4	1.0	0.7	0.5	22.1
Davis													
ETo	4.9	2.5	1.5	1.2	2.1	3.9	4.7	5.7	7.0	8.5	8.1	6.2	56.2
Precipitation	0.6	3.2	3.7	3.7	3.0	2.5	0.8	0.8	0.2	-	-	-	18.4
Alfalfa	4.5	2.5	1.5	1.4	2.1	3.8	4.4	5.2	6.4	7.8	7.4	5.7	52.7
Almonds	3.1	1.8	1.2	1.4	1.6	2.9	3.6	5.2	7.4	9.4	8.9	6.7	53.4
Apples	4.5	2.1	1.2	1.4	1.6	2.6	2.9	4.2	6.1	8.6	8.6	6.5	50.3
Corn	1.5	1.8	1.2	1.4	1.6	2.6	2.0	3.1	4.9	8.1	7.7	4.4	40.3
Corn - silage	1.1	1.8	1.2	1.4	1.6	2.6	2.0	3.5	6.2	8.2	5.0	1.1	35.6
Cotton	2.7	1.8	1.2	1.4	1.6	2.6	2.0	2.6	5.0	8.0	7.6	5.7	42.3
Cucumber/Lettuce	0.9	1.5	1.0	1.1	1.5	2.1	1.7	2.9	4.8	6.4	5.6	1.4	30.8
Dry Beans	1.5	1.8	1.2	1.4	1.6	2.6	2.0	2.1	2.3	5.8	8.1	5.1	35.5
Melons	0.9	1.5	1.0	1.1	1.5	2.1	1.7	2.8	4.4	6.6	6.3	2.9	32.9
Onions	1.6	1.8	1.2	1.4	1.6	3.0	3.8	5.8	7.7	9.4	7.8	4.1	49.2
Oranges	4.5	2.5	1.5	1.4	2.1	3.8	4.4	5.2	6.4	7.8	7.4	5.7	52.7
Pasture	4.2	2.4	1.4	1.4	2.0	3.6	4.2	5.0	6.1	7.4	7.1	5.5	50.3
Potatoes	1.1	1.8	1.2	1.4	1.6	2.6	2.9	4.5	7.2	8.5	3.7	1.1	37.6
Rice	1.5	1.8	1.2	1.4	1.6	2.6	2.0	4.8	7.6	8.2	7.8	5.5	46.0
Safflower	1.1	1.8	1.2	1.4	1.6	2.6	2.9	5.0	6.8	5.5	2.0	0.9	32.7
Sugar Beets	1.5	1.8	1.2	1.4	1.6	2.8	3.3	5.0	7.3	9.0	8.5	5.9	49.3
Tomatoes	1.1	1.8	1.2	1.4	1.6	2.6	2.0	2.9	7.0	9.4	6.6	1.6	39.1
Vines	2.2	1.9	1.2	1.4	1.6	2.6	2.7	4.0	5.1	6.2	5.9	4.2	39.0

Wheat	0.9	2.0	1.2	1.1	1.9	3.2	3.9	2.7	1.5	1.0	0.7	0.5	20.6
CIMIS Station	**Water Year 2005 (inches)**												
	Oct	Nov	Dec	Jan	Feb	Mar	Apr	May	Jun	Jul	Aug	Sep	Total
Firebaugh/Telles													
ETo	4.0	1.8	1.1	1.0	2.3	3.6	4.7	6.3	7.3	8.4	7.4	5.6	53.5
Precipitation	2.4	0.8	1.5	2.1	3.6	1.8	0.8	0.8	-	-	-	-	13.7
Alfalfa	3.8	1.8	1.1	1.1	2.2	3.4	4.3	5.9	6.7	7.7	6.8	5.2	50.0
Almonds	3.2	1.5	0.9	1.1	1.6	2.5	3.6	5.8	7.8	9.2	8.2	6.1	51.5
Apples	3.8	1.6	0.9	1.1	1.6	2.3	2.9	4.7	6.4	8.5	7.8	5.9	47.5
Corn	2.1	1.5	0.9	1.1	1.6	2.3	2.0	3.3	5.0	8.0	7.1	4.0	38.9
Corn - silage	1.5	1.5	0.9	1.1	1.6	2.3	2.0	3.6	6.4	8.0	4.7	1.1	34.7
Cotton	2.8	1.5	0.9	1.1	1.6	2.3	2.0	2.9	5.2	7.9	7.0	5.2	40.4
Cucumber/Lettuce	2.7	1.3	0.7	0.9	1.5	1.9	1.7	1.8	1.0	0.8	1.1	2.4	17.9
Dry Beans	2.1	1.5	0.9	1.1	1.6	2.3	2.0	2.3	2.3	5.6	7.5	4.7	33.8
Melons	1.4	1.3	0.7	0.9	1.5	1.9	1.7	3.2	4.7	6.5	5.8	2.8	32.3
Onions	2.1	1.5	0.9	1.1	1.6	2.7	3.8	6.5	8.1	9.2	7.2	3.7	48.6
Oranges	3.8	1.8	1.1	1.1	2.2	3.4	4.3	5.9	6.7	7.7	6.8	5.2	50.0
Pasture	3.6	1.8	1.1	1.1	2.1	3.3	4.1	5.6	6.4	7.3	6.5	4.9	47.8
Potatoes	1.5	1.5	0.9	1.1	1.6	2.3	2.8	5.0	7.6	8.3	3.5	1.1	37.2
Rice	2.1	1.5	0.9	1.1	1.6	2.3	2.0	5.6	7.9	8.1	7.1	5.0	45.2
Safflower	1.4	1.5	0.9	1.1	1.6	2.3	2.8	5.6	7.1	5.4	1.9	0.8	32.5
Sugar Beets	2.1	1.5	0.9	1.1	1.6	2.5	3.3	5.6	7.7	8.9	7.8	5.3	48.2
Tomatoes	1.6	1.5	0.9	1.1	1.6	2.3	2.0	3.3	7.4	9.2	6.1	1.6	38.5
Vines	2.5	1.5	0.9	1.1	1.6	2.3	2.6	4.5	5.4	6.1	5.4	3.8	37.7
Wheat	1.1	1.6	1.0	0.9	2.0	2.9	3.8	3.1	1.5	1.0	0.7	0.5	20.0
Shafter													
ETo	4.5	2.7	2.1	2.0	2.8	4.7	5.4	7.5	7.3	9.1	8.2	6.0	62.2
Precipitation	1.5	0.2	1.7	2.4	1.3	1.3	0.6	1.0	-	-	0.0	0.0	10.1
Alfalfa	4.2	2.5	2.0	2.1	2.6	4.3	5.0	6.9	6.7	8.3	7.6	5.5	57.7
Almonds	3.2	1.1	0.7	1.8	1.8	2.9	4.0	6.9	7.7	10.0	9.1	6.4	55.6
Apples	4.2	1.8	0.9	1.8	1.8	2.0	3.1	5.6	6.3	9.2	8.7	6.2	51.7
Corn	1.9	1.1	0.7	1.8	1.8	2.0	1.1	3.6	4.8	8.6	7.8	4.3	39.5
Corn - silage	1.1	1.1	0.7	1.8	1.8	2.0	1.1	4.0	6.3	8.7	5.2	1.1	34.8
Cotton	2.8	1.1	0.7	1.8	1.8	2.0	1.1	3.3	5.2	8.5	7.8	5.5	41.5
Cucumber/Lettuce	3.0	1.2	0.6	1.5	1.6	1.6	0.9	2.1	1.0	0.9	1.2	2.5	18.2
Dry Beans	1.9	1.1	0.7	1.8	1.8	2.0	1.1	2.5	2.2	6.1	8.3	5.0	34.5
Melons	1.2	0.9	0.6	1.5	1.6	1.6	0.9	3.7	4.6	7.0	6.5	2.9	33.0
Onions	1.9	1.1	0.7	1.8	1.8	2.9	4.0	7.5	8.0	10.0	8.0	4.0	51.6
Oranges	4.2	2.5	2.0	2.1	2.6	4.3	5.0	6.9	6.7	8.3	7.6	5.5	57.7
Pasture	4.0	2.3	1.9	2.0	2.5	4.1	4.7	6.6	6.4	7.9	7.2	5.2	54.9
Potatoes	1.1	1.1	0.7	1.8	1.8	2.0	2.4	5.9	7.6	9.0	3.8	1.1	38.3
Rice	1.9	1.1	0.7	1.8	1.8	2.0	1.1	6.4	7.9	8.8	7.9	5.3	46.6
Safflower	1.1	1.1	0.7	1.8	1.8	2.0	2.9	6.5	7.0	5.8	2.0	0.9	33.6
Sugar Beets	1.9	1.1	0.7	1.8	1.8	2.6	3.2	6.4	7.6	9.6	8.7	5.6	51.0
Tomatoes	1.2	1.1	0.7	1.8	1.8	2.0	1.1	3.8	7.3	10.0	6.7	1.6	39.2
Vines	2.4	1.1	0.8	1.8	1.8	2.0	2.7	5.3	5.3	6.6	6.0	4.0	39.9

Wheat	0.8	1.8	1.5	1.6	2.3	3.7	4.4	3.7	1.5	1.0	0.7	0.5	23.6

Tables C1-6 through C1-9 compare annual estimates of ET_c derived from the 2003 ITRC report[12] with ET_c values based on the CUP methods and agronomic data, but using the ITRC climate forcing (ET_o and precipitation).[13] Presented values are for DWR ET_o Zones 12, 14, 15, and 16, and calendar years 1997, 1998, and 1999. These 3 years represent typical, wet, and dry conditions, respectively. Values include soil evaporation for the entire year (other published values may ignore ET for annual crops during the non-growing season). ITRC values are for surface irrigation methods; values for sprinkler irrigation may be 1 to 4 percent higher and values for drip irrigation may be up to 6 percent higher. ET_c values adopted for PGM calibration are typically higher than values published in the 2003 ITRC report. Some of the reasons for adopting higher values for PGM calibration are discussed in the following sections.

Almonds

Traditionally, K_c values for California orchards have been derived from measurements of applied water, runoff, and soil water depletion. It was assumed that trees were transpiring at their full potential and that water supply was not restricted. The resulting midseason K_c value for almonds with no ground cover was 0.90. Recently, UC Davis and DWR conducted experiments to determine ET_c as the residual in an energy water balance (net radiation, less ground heat flux, less sensible heat flux). These experiments resulted in midseason K_c values of between 1.15 and 1.20. The lower K_c value (as used by ITRC) may be correct for the then existing management practices. However, almond orchards are less heavily pruned today, are treated with higher fertilizer rates, and have yields approximately 50 percent higher than 15 years ago (Sanden et al., 2012).

Tomatoes

During the 1970s, the *seasonal* ET_c for processing tomatoes in the Central Valley ranged from 25 to 28 inches depending on planting date (Fereres and Puech, 1981). Midseason K_c values derived from experimental data ranged from 1.05 under subsurface drip irrigation (Phene et al. 1985) to 1.25 under sprinkler irrigation (Pruitt et al,. 1972). More recently, the recommended midseason coefficients were 1.10 to 1.15 (Allen et al., 1998). Recently, UC Davis conducted experiments on the westside of the San Joaquin valley to update water requirements. Seasonal ET_c varied from 21 to 30 inches. Average mid-season crop coefficients varied year to year from 0.96 to 1.09 (Hansen and May, 2006), which is consistent with earlier studies. Crop coefficients for PGM calibration,

---

[12] Tables 8, 10, 11, and 12

[13] Daily precipitation and daily ET_o values used by ITRC for the calculation of ET_c were not available, so daily values were generated from monthly values published by ITRC (2002). Monthly precipitation was disaggregated to daily values using the observed daily pattern of precipitation at the the following gages: Colusa Bridge (for Zone 12), Marysville (for Zone 14), Fresno Yosemite International Airport (for Zone 15), and Los Banos (for Zone 16). Monthly ET_o was disaggregated to daily values using a cubic spline.

which are identical to those used in the CUP and SIMETAW models, may be high.

Table 4C1-6. Crop Evapotranspiration for Zone 12

Crop		Crop Evapotranspiration ETc (inches)							
		1997		1998		1999		Average	
Irrigation Training and Research Center (ITRC)	**SSJBS**	**ITRC**	**SSJBS**	**ITRC**	**SSJBS**	**ITRC**	**SSJBS**	**ITRC**	**SSJBS**
Alfalfa Hay and Clover	Alfalfa	45	49	39	41	43	47	42	46
Almonds	Almonds	39	50	37	44	40	48	39	47
Apple, Pear, Cherry, Plum, Prune	Apple	38	45	37	41	39	45	38	44
	Plum-Prune		48		42		47		46
Citrus (no ground cover)	Orange	38	49	33	41	36	47	36	46
Corn and Grain Sorghum	Corn (grain)	29	35	30	35	29	35	29	35
	Corn (silage)		32		30		32		31
	Sorghum		41		39		41		40
Cotton	Cotton	32	36	34	36	32	37	33	36
Flowers, Nursery, Christmas Tree	Flowers	37	35	36	34	38	35	37	35
Grain and Grain Hay	Wheat	19	13	15	16	16	14	17	14
	Barley		13		16		14		14
	Oats		13		16		14		14
Grape Vines with 80% canopy	Wine Grapes	28	36	29	32	28	35	28	34
Melons, Squash, and Cucumbers	Cucumber	18	33	22	31	19	33	20	33
	Melon		35		34		35		35
	Squash		17		16		14		16
Miscellaneous Subtropical	Olives	37	45	36	38	38	43	37	42
Miscellaneous Deciduous	Fig	37	50	36	44	38	48	37	47
Miscellaneous field crops	Sudangrass	26	38	26	34	26	37	26	37
Onions and Garlic	Onion (dry)	20	48	16	41	17	46	18	45
Pasture and Misc. Grasses	Pasture	45	47	40	39	44	45	43	44
Peach, Nectarine and Apricots	Stone fruits	38	50	37	44	39	48	38	47
Pistachio	Pistachio	35	52	36	44	35	50	35	49
Potatoes, Sugar beets, Turnip	Potato	35	36	28	31	33	35	32	34
	Sugarbeet		46		41		45		44
Rice	Rice[1]	39	42	38	39	40	42	39	41
Safflower and Sunflower	Safflower	26	32	22	27	27	31	25	30
	Sunflower		33		33		33		33
Small Vegetables	Carrots	19	22	17	18	18	19	18	20
	Lettuce		17		20		19		19

Crop		1997 ITRC	1997 SSJBS	1998 ITRC	1998 SSJBS	1999 ITRC	1999 SSJBS	Average ITRC	Average SSJBS
	Asparagus		47		39		45		44
	Sweet Potatoes		36		31		35		34
Strawberries	Strawberries	26	36	26	36	26	36	26	36
Tomatoes and Peppers	Tomatoes	24	35	25	34	25	35	25	35
Walnuts	Walnuts	42	47	40	42	42	46	41	45

Note:
[1] Evapotranspiration rates for rice assume bare soil during the non-growing season (i.e., no winter flooding)

Table 4C1-7. Crop Evapotranspiration for Zone 14

Crop		Crop Evapotranspiration ETc (inches)							
		1997		1998		1999		Average	
Irrigation Training and Research Center (ITRC)	SSJBS	ITRC	SSJBS	ITRC	SSJBS	ITRC	SSJBS	ITRC	SSJBS
Alfalfa Hay and Clover	Alfalfa	47	52	41	43	47	50	45	49
Almonds	Almonds	42	53	40	46	42	52	41	50
Apple, Pear, Cherry, Plum, Prune	Apple	42	49	40	43	43	48	42	46
	Plum-Prune		51		44		50		48
Citrus (no ground cover)	Orange	41	52	37	43	40	50	39	49
Corn and Grain Sorghum	Corn (grain)	31	38	31	37	30	38	31	37
	Corn (silage)		34		32		34		33
	Sorghum		44		41		43		43
Cotton	Cotton	34	38	37	38	35	39	35	38
Flowers, Nursery, Christmas Tree	Flowers	40	37	39	36	41	37	40	37
Grain and Grain Hay	Wheat	20	14	16	17	18	15	18	15
	Barley		14		17		15		15
	Oats		14		17		15		15
Grape Vines with 80% canopy	Wine Grapes	30	38	31	34	30	38	30	37
Melons, Squash, and Cucumbers	Cucumber	20	35	24	33	21	35	21	35
	Melon		37		35		37		37
	Squash		18		18		16		17
Miscellaneous Subtropical	Olives	40	48	39	39	41	46	40	44
Miscellaneous Deciduous	Fig		53	39	46	41	52	40	50
Miscellaneous field crops	Sudangrass		40	28	36	27	40	28	39
Onions and Garlic	Onion (dry)	21	50	17	43	18	49	19	48
Pasture and Misc. Grasses	Pasture		50	43	41	48	48	45	46
Peach, Nectarine and Apricots	Stone fruits	41	53	40	46	42	52	41	50
Pistachio	Pistachio	37	55	39	46	38	53	38	51
Potatoes, Sugar beets, Turnip	Potato	36	38	30	33	36	37	34	36

| Crop | | Crop Evapotranspiration ETc (inches) | | | | | | | |
| | | 1997 | | 1998 | | 1999 | | Average | |
Irrigation Training and Research Center (ITRC)	SSJBS	ITRC	SSJBS	ITRC	SSJBS	ITRC	SSJBS	ITRC	SSJBS
	Sugarbeet		49		43		48		47
Rice	Rice[1]	42	45	40	41	42	45	41	44
Safflower and Sunflower	Safflower	29	34	23	29	28	33	27	32
	Sunflower		36		34		35		35
Small Vegetables	Carrots	21	23	18	19	20	21	20	21
	Lettuce		19		22		20		20
	Asparagus		50		41		48		46
	Sweet Potatoes		38		33		37		36
Strawberries	Strawberries	27	39	28	37	27	39	28	38
Tomatoes and Peppers	Tomatoes	26	37	27	36	26	37	26	37
Walnuts	Walnuts	45	50	43	44	46	49	45	48

Note:
[1] Evapotranspiration rates for rice assume bare soil during the non-growing season (i.e., no winter flooding)

Table C1-8. Crop Evapotranspiration for Zone 15

| Crop | | Crop Evapotranspiration ETc (inches) | | | | | | | |
| | | 1997 | | 1998 | | 1999 | | Average | |
Irrigation Training and Research Center (ITRC)	SSJBS	ITRC	SSJBS	ITRC	SSJBS	ITRC	SSJBS	ITRC	SSJBS
Alfalfa Hay and Clover	Alfalfa	49	54	46	48	48	52	47	51
Almonds	Almonds	40	54	39	50	39	52	40	52
Apple, Pear, Cherry, Plum, Prune	Apple	42	49	42	46	41	49	42	48
	Plum-Prune		53		48		51		51
Citrus (no ground cover)	Orange	42	54	40	48	41	52	41	51
Corn and Grain Sorghum	Corn (grain)	31	37	33	39	29	37	31	38
	Corn (silage)		33		34		33		33
	Sorghum		44		43		45		44
Cotton	Cotton	34	38	37	40	34	39	35	39
Flowers, Nursery, Christmas Tree	Flowers	41	37	40	38	40	37	40	37
Grain and Grain Hay	Wheat	20	13	17	17	16	14	18	15
	Barley		13		17		14		15
	Oats		13		17		14		15
Grape Vines with 80% canopy	Wine Grapes	29	38	32	37	29	38	30	38
Melons, Squash, and Cucumbers	Cucumber	19	35	23	36	19	35	20	35
	Melon		37		38		37		37

Crop		1997		1998		1999		Average	
Irrigation Training and Research Center (ITRC)	SSJBS	ITRC	SSJBS	ITRC	SSJBS	ITRC	SSJBS	ITRC	SSJBS
	Squash		19		17		15		17
Miscellaneous Subtropical	Olives	41	49	40	43	40	47		47
Miscellaneous Deciduous	Fig	41	54	40	50	40	52	40	52
Miscellaneous field crops	Sudangrass	27	41	30	39	26	41	28	40
Onions and Garlic	Onion (dry)	21	52	17	47	17	50	18	50
Pasture and Misc. Grasses	Pasture	50	52	46	46	48	50	48	49
Peach, Nectarine and Apricots	Stone fruits	41	54	41	50	40	52	41	52
Pistachio	Pistachio	37	57	40	51	37	55	38	54
Potatoes, Sugar beets, Turnip	Potato	37	38	33	36	35	37	35	37
	Sugarbeet		50		47		49		48
Rice	Rice[1]	42	45	42	44	42	45	42	45
Safflower and Sunflower	Safflower	29	34	25	31	26	32	27	32
	Sunflower		35		36		35		35
Small Vegetables	Carrots	21	24	19	20	18	20	19	22
	Lettuce		18		21		20		19
	Asparagus		52		46		50		49
	Sweet Potatoes		38		36		37		37
Strawberries	Strawberries	27	38	30	40	26	39	28	39
Tomatoes and Peppers	Tomatoes	26	37	28	38	25	37	26	37
Walnuts	Walnuts	47	50	47	48	46	50	47	50

Note:
[1] Evapotranspiration rates for rice assume bare soil during the non-growing season (i.e., no winter flooding)

Table C1-9. Crop Evapotranspiration for Zone 16

Crop		1997		1998		1999		Average	
Irrigation Training and Research Center (ITRC)	SSJBS	ITRC	SSJBS	ITRC	SSJBS	ITRC	SSJBS	ITRC	SSJBS
Alfalfa Hay and Clover	Alfalfa	50	55	45	48	50	54	48	52
Almonds	Almonds	42	55	39	50	41	54	41	53
Apple, Pear, Cherry, Plum, Prune	Apple	44	50	41	47	43	51	43	49
	Plum-Prune		53		48		52		51
Citrus (no ground cover)	Orange	43	55	40	48	43	54	42	52
Corn and Grain Sorghum	Corn (grain)	31	36	32	38	31	38	31	38
	Corn (silage)		32		33		34		33

Crop		Crop Evapotranspiration ETc (inches)							
		1997		1998		1999		Average	
Irrigation Training and Research Center (ITRC)	SSJBS	ITRC	SSJBS	ITRC	SSJBS	ITRC	SSJBS	ITRC	SSJBS
	Sorghum		44		43		46		45
Cotton	Cotton	35	38	37	40	35	40	36	39
Flowers, Nursery, Christmas Tree	Flowers	42	36	40	37	42	38	41	37
Grain and Grain Hay	Wheat		12		18		16		15
	Barley	21	12	17	18	17	16	18	15
	Oats		12		18		16		15
Grape Vines with 80% canopy	Wine Grapes	31	39	31	36	31	39	31	38
Melons, Squash, and Cucumbers	Cucumber		34		35		36		35
	Melon	20	36	24	37	20	38	21	37
	Squash		17		19		15		17
Miscellaneous Subtropical	Olives	42	50	40	43	42	49		47
Miscellaneous Deciduous	Fig	42	55	40	50	42	54	41	53
Miscellaneous field crops	Sudangrass	28	41	29	39	28	42	28	41
Onions and Garlic	Onion (dry)	21	51	17	47	18	51	19	50
Pasture and Misc. Grasses	Pasture	52	53	46	45	50	52	49	50
Peach, Nectarine and Apricots	Stone fruits	42	55	41	50	42	54	42	53
Pistachio	Pistachio	39	57	40	51	39	56	39	55
Potatoes, Sugar beets, Turnip	Potato	39	37	31	35	36	38	35	37
	Sugarbeet		49		46		49		48
Rice	Rice[1]	-	45	-	43	-	47	-	45
Safflower and Sunflower	Safflower	32	33	23	30	27	33	27	32
	Sunflower		34		36		36		35
Small Vegetables	Carrots		23		21		20		21
	Lettuce		18		23		21		20
	Asparagus	21	53	20	45	19	52	20	50
	Sweet Potatoes		37		35		38		37
Strawberries	Strawberries	-	38	-	39	-	40	-	39
Tomatoes and Peppers	Tomatoes	28	36	26	37	27	38	27	37
Walnuts	Walnuts	49	51	46	48	49	52	48	50

Note:
[1] Evapotranspiration rates for rice assume bare soil during the non-growing season (i.e., no winter flooding).

3. WEAP-CV Plant Growth Model Calibration

In Section 2, the calibration of the WEAP-CV Plant Growth Model (PGM) based on the crop ET rates presented in Section 1 is described. One of the reasons WEAP-CV PGM was selected for use in the SSJBS is that the models described in Section 1 do not have the capability to explicitly simulate many important biological processes affecting crop ET. In addition, the WEAP-CV PGM has the capability to simulate the climatic effects on crops yields which is important to the analysis of the economic impacts of climate change on agriculture. This aspect of the model is described in Appendix D.

The WEAP-CV PGM was previously used by Reclamation to develop Central Valley crop water demands for the Central Valley Project Integrated Resource Plan (Reclamation, 2013). However, during that study it became evident that models of Central Valley crop water demands have been parameterized and calibrated using different standards. For instance, the PGM was calibrated to values published in the ITRC report "Evaporation from Irrigated Agricultural Land in Califorina" (ITRC, 2002). CalSim 3.0 was parameterized using crop ET values developed by DWR. While the Central Valley Planning Area model in WEAP used in the State Water Plan was calibrated to the crop water use values published in the State Water Plan Portfolios. For this reason the Basin Study authors deemed it desirable to calibrate the PGM using a widely accepted standard model recognized by Reclamation and DWR. This standard is the ET model CUP created by DWR. Although this model lacks some of the capabilities of the PGM, because it was appled only to develop a target calibration data set with 2005 data, the capabilities were not necessary.

Most previous modeling studies in the Central Valley have primarily simulated the effects temperature related climate change effects on crop water use. In these studies, increasing temperature typically results in increased crop ET. However, research has shown that there are several other bio-climate interactions that have effects on crop water use. These relationships include:

- Reduction in stomatal conductance caused by elevated atmospheric CO_2.

- Increase in radiation use efficiency caused by elevated atmospheric CO_2 (the CO_2 fertilization effect).

- Increase in leaf area caused by elevated atmospheric CO_2.

- Increase or decrease in plant temperature stress caused by elevated temperature.

- Earlier seasonal onset of plant gowth

- Accelerated accumulation of degree day heat units which shortens the crop growth period.

- Increase in the length of the growing season of perennial crops caused by elevated temperature.

- Reduction in stomatal conductance and radiation use efficiency caused by elevated vapor pressure deficit.

These processes are all discussed more detail in several publications (Kimball et al., 2002; Huntington, 2004; Neitsch, et al., 2005; Long et al., 2006; Ainsworth and Long, 2005; Hatfield et al., 2008; Kimball, 2010) and the reader is urged to consult them for more information.

The combined effects of these processes are complex and the degree to which they affect crop ET varies between crop types. Generally, an increase in temperature produces an increase crop ET. This is due to the increased temperature increasing the magnitude of the vapor pressure deficit (VPD) as well as increased soil evaporation. VPD is defined as the difference between the saturated vapor pressure, assumed to be the condition inside plant leaves, and the actual vapor pressure of the air surrounding the plant leaves. Typically, increased warming results in a larger VPD and increased crop ET. However, as described in Appendix B, the VPD in some of the projections did not increase over time despite warming because of the effects of increased atmospheric humidity on the actual vapor pressure. In addition, most plants will eventually respond to very high VPD by reducing their stomatal openings in order to survive. This biological mechanism is not represented in the standard Penman Montheith equation or in the crop coefficient method described above. These effects which are not simulated in the ASCE Penman Montieth and crop coefficient methods are simulated in the PGM.

The PGM also includes an algorithm that reduces leaf area development if the daily average temperature is in excess of the optimal growth temperature. This observed effect when it occurs will result in a reduction in leaf area which in turn will result in less crop ET. However, since the optimal temperature range varies between crops the magnitude of the effect will vary considerably both temporally and geographically. It may be that some of the difference in the bias between the CUP model and PGM at the four different sites may be in part due to these temperature stress effects.

The movement of moisture out of the leaves, and the movement of CO_2 into the leaves, is regulated by the stomata, which are small openings on the surface of the leaves. Many field and lab experiments have shown that crops reduce the size of the stomatal openings when CO_2 concentrations increase. This results in less water vapor loss (a reduction in transpiration) while maintaining the same inflow of CO_2 to support photosynthesis. The net effect of these phenomena is an increase in water use efficiency which is the ratio of biomass production to

transpiration. However, CO_2 also usually increases total leaf area and consequently the number of stomata which tends to counteract the effect of stomatal closure to varying degrees in different crops.

Finally, total crop ET is affected by the length of the growth period. For annual crops, increased temperatures typically shortens the growth period leading to potentially reduced crop ET. However, increased warming will generally increase the length of the growth period for perennial crops and thus increase overall crop ET.

4. **ET Calibration Approach**

Calibration of PGM crop water use was conducted using crop ET values produced by the CUP model values described in Section 1 as calibration targets. PGM parameters were adjusted until the growing season total crop ET was within 3 percent of the simulated values produced by the CUP model. Identical meteorological inputs were used in both the CUP and PGM models. These inputs were the same used in the CVP-IRP.

Within the PGM model there are several parameters that affect the crop evapotranspiration rate. At the leaf level, the movement of water vapor out of the leaf is regulated by leaf stomatal conductance. The development of the crop canopy is controlled by five parameters which determine the leaf area index (LAI). The combination of leaf stomatal conductance and crop canopy development results in canopy conductance. The development of LAI is illustrated in Figure C2-1. The development of LAI is a function of the accumulation of heat units, expressed in the figure as the Heat Unit Index (HUI). During plant development as the HUI increases the LAI increases. The rate at which LAI increases is defined by two user-specified points (LAI definition points #1 and #2) indicated on the figure where values of the HUI and corresponding values of LAI have to be provided. The fifth parameter that defines the development and decline of the LAI is the HUI at which LAI begins to decline as the growing season comes to an end (Start of LAI Decline).
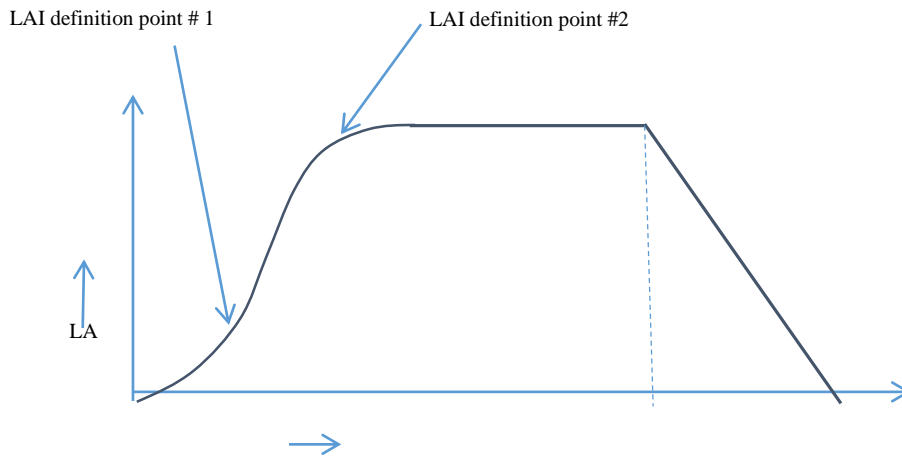
Figure C2-1. Illustration of Crop Leaf Area Index Development as a Function of Heat Unit Index.

The parameters described above were initially set at values found in the crop database for the SWAT model (Neitsch, et al. 2005). During calibration, adjustments were made to the parameters if the overall shape of the actual daily ET curve from the PGM did not match the curve from CUP. For instance, in some cases the early season ET was less in the PGM than the CUP model. To increase the early season ET the LAI definition points (see Figure C2-1) were adjusted to have the canopy develop more rapidly in the early season resulting in more early-season ET. In other cases the maximum daily ET during the full canopy portion of the season, typically July and August, did not match that computed by the CUP model. In those cases the leaf stomatal conductance was adjusted to bring the two models into agreement. In cases where there was disagreement between the models in the late-season ET, the "Start of LAI Decline" parameter was adjusted so that the decline started either earlier or later in the season.

Using the approach described above, a calibration was conducted for the 20 representative crops that were simulated in the Basin Study. This calibration was performed at four locations in the Central Valley in order to represent the variability in climatic conditions. The chosen locations were at Gerber, Davis, Firebaugh, and Shafter. These stations were also selected because they have long records of approropriate meteorological observations for computing ET. As described previously, the observations were adjusted to correct for sensor errors prior to performing the CUP simulations and PGM calibration. Results from the calibration are presented below.

5. ET Results

During calibration, PGM parameters were adjusted so that daily crop season ET from the PGM matched the values produced by the CUP model. The objective of the calibration effort was to obtain a seasonal ET within 3 percent of the CUP model value and on matching the shape of daily actual ET curve predicted by CUP. Seasonal ET from both models and the percent difference between them are presented in **Tables 4C2-1, 4C2-2, 4C2-3, and 4C2-4**. **Figures 4C2-2, 4C2-3, 4C2-4, and 4C2-5** provide a visual comparison of the daily ET values over the entire season.

5.1. Gerber

The results from the Gerber location are presented in **Table 4C2-1** and **Figures** 4**C2-2a** through **4C2-2g**.

Table 4C2-1. Seasonal ET totals from the CUP and PGM models for the Gerber location.

Crop	Period of Comparison	CUP ETc (mm)	PGM ETc (mm)	Percent Difference
Almonds/Pistachios	Apr 1 – Sep 30	1016	1024	0.8
Alfalfa	Apr 1 – Sep 30	898	911	1.4
Corn	May 1 – Sep 30	706	700	-0.9
Cotton	May 15 – Oct 15	740	747	1.1
Cucurbits – Melons	May 15 – Sep 15	634	648	2.3
Dry Beans	Jun 15 – Sep 30	512	511	-0.1
Grain – Wheat	Nov 1 – May 31	521	508	-2.6
Onions	Mar 1 – Sep 30	1024	1007	-1.5
Other Deciduous – Apples	Apr 1 – Sep 30	916	916	0.0
Other Field – Corn Silage	May 1 – Aug 15	538	540	0.3
Other Truck – Cucumber	May 15 – Aug 31	551	551	0.0
Pasture	Apr 1 – Sep 30	855	864	1.0
Potatoes	Apr 15 – Aug 15	603	611	1.2
Rice	May 15 – Sep 30	874	898	2.8
Safflower	Apr 1 – Jul 31	500	487	-2.3

Crop	Period of Comparison	CUP ETc (mm)	PGM ETc (mm)	Percent Difference
Subtropical – Olives	Apr 1 – Sep 30	823	815	-0.9
Sugar Beets	Mar 15 – Sep 30	1002	1015	1.4
Tomatoes	Apr 1 – Aug 31	712	688	-3.2
Vineyards	Apr 1 – Sep 30	700	713	1.8

Key:

CUP = Consumptive Use Program

ETc = crop evapotranspiration

mm = millimeters

PGM = Plant Growth Model

Almonds/Pistachios
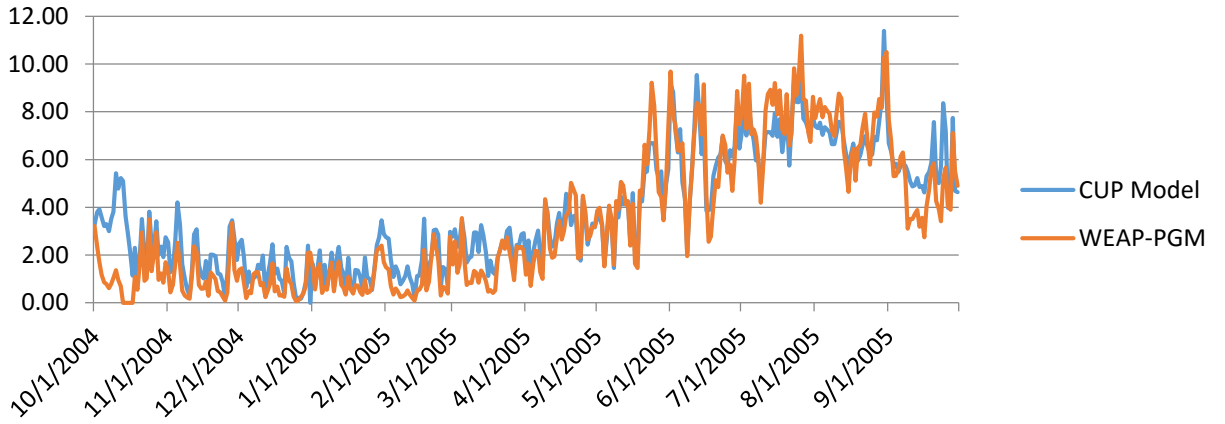
Alfalfa
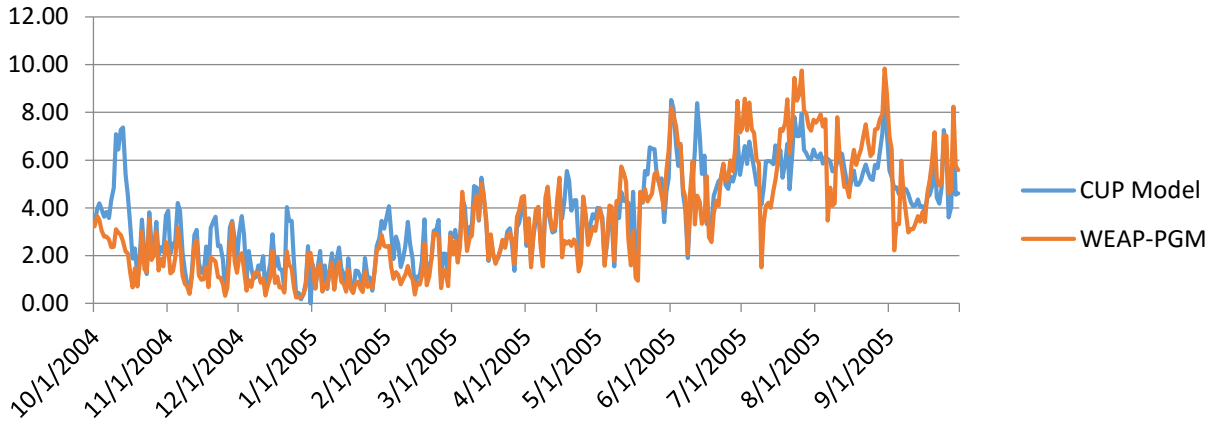
Corn
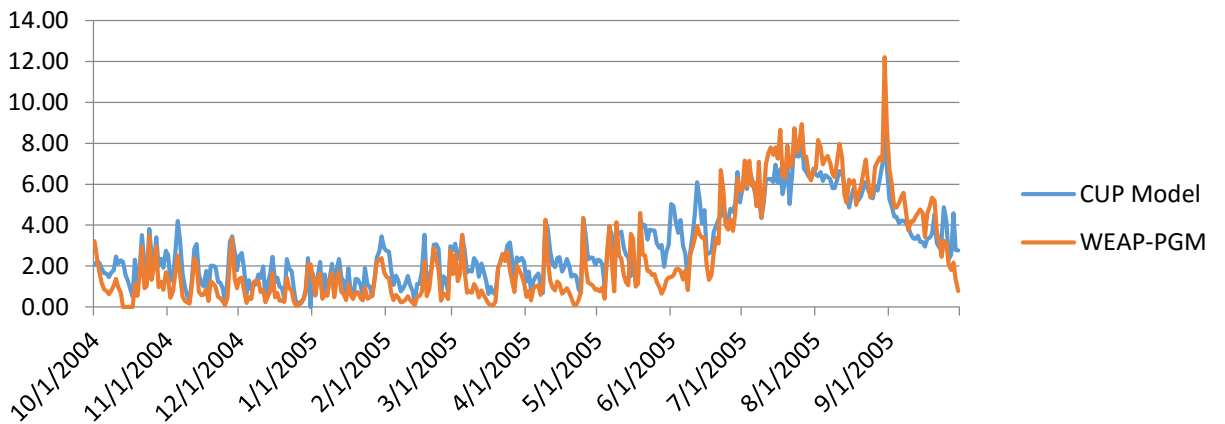
Figure C2-2a. Plots of Daily Evapotranspiration for 19 crops at the Gerber Location.

Cotton
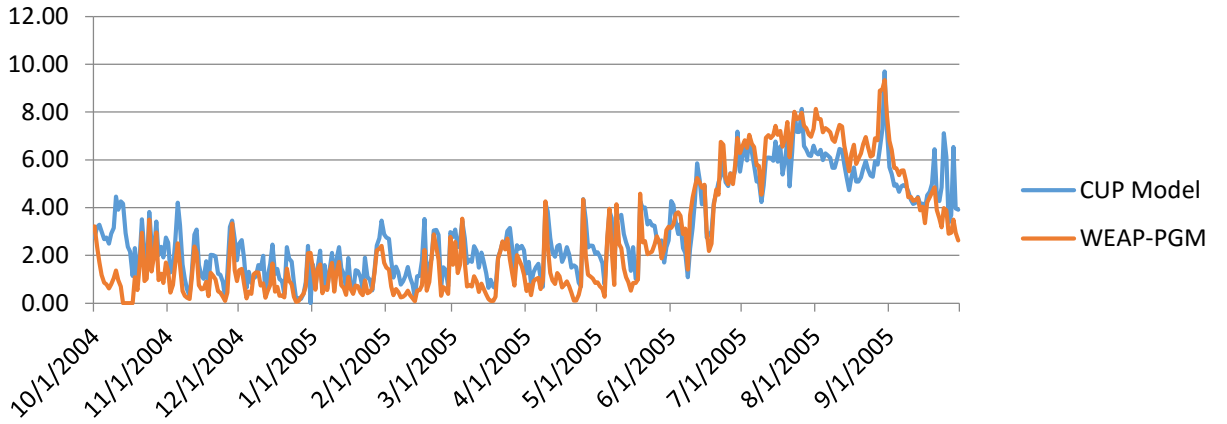
Cucurbits
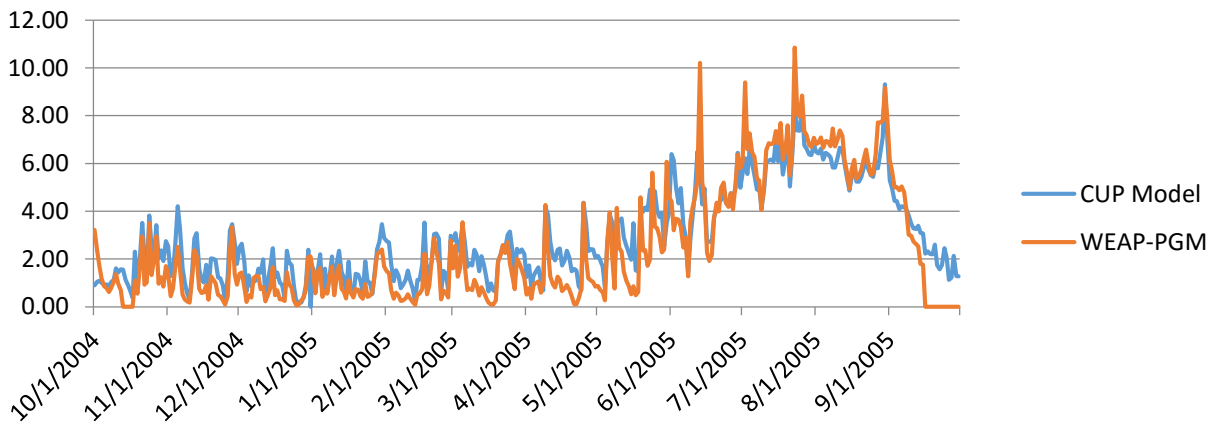
Dry Beans

Figure C2-3b. Plots of Daily Evapotranspiration for 19 crops at the Gerber Location.

Grain

Onions and Garlic

Other Deciduous
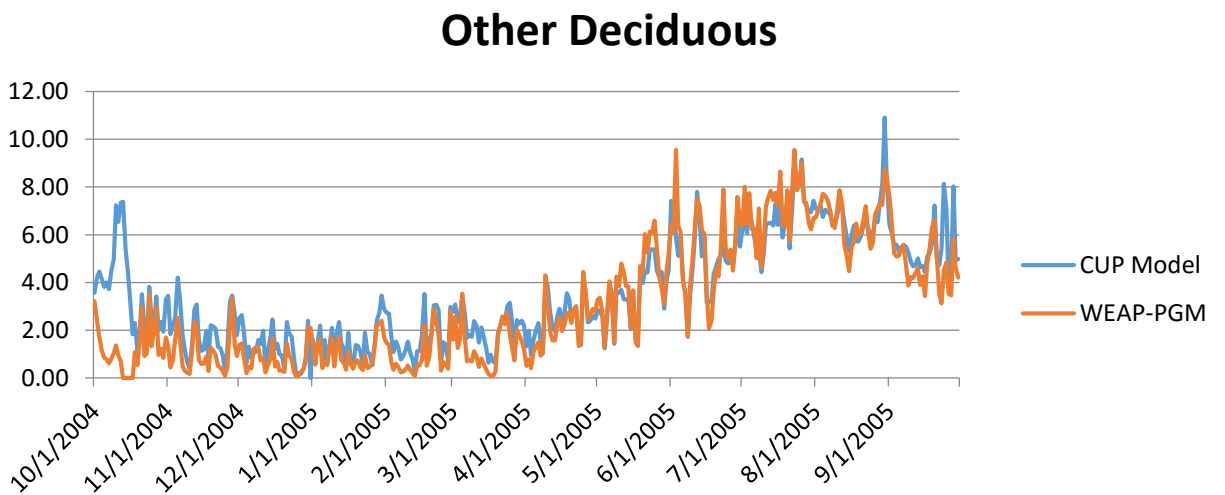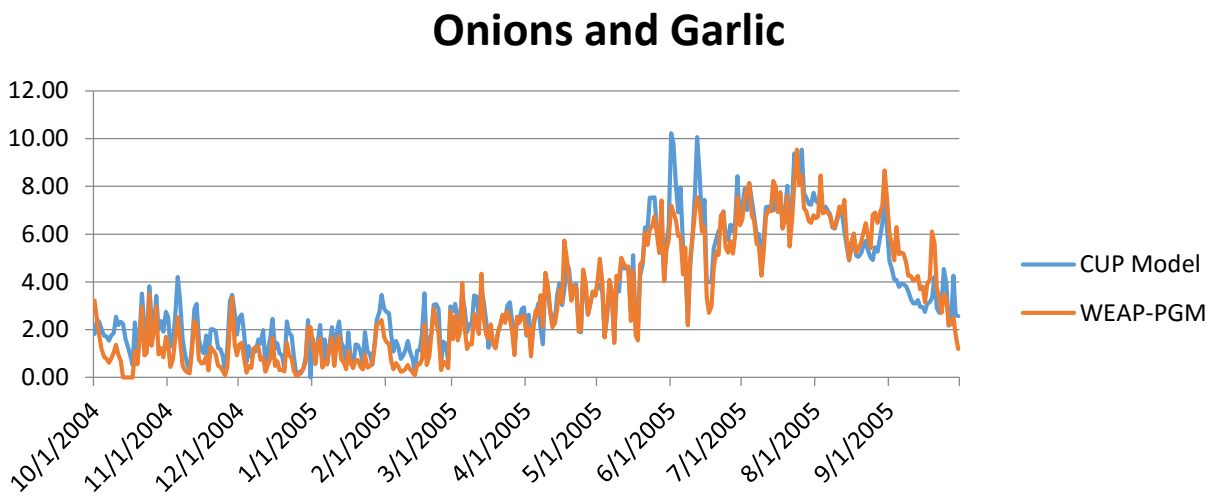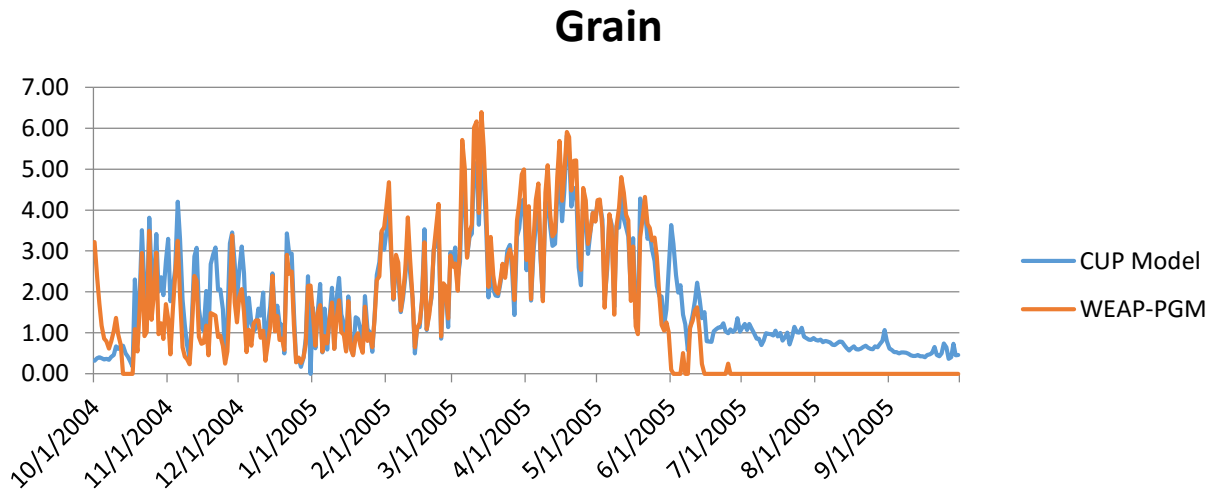
Figure C2-4c. Plots of Daily Evapotranspiration for 19 crops at the Gerber Location.

Other Field

Other Truck

Pasture

Figure C2-5d. Plots of Daily Evapotranspiration for 19 crops at the Gerber Location.

Potatoes
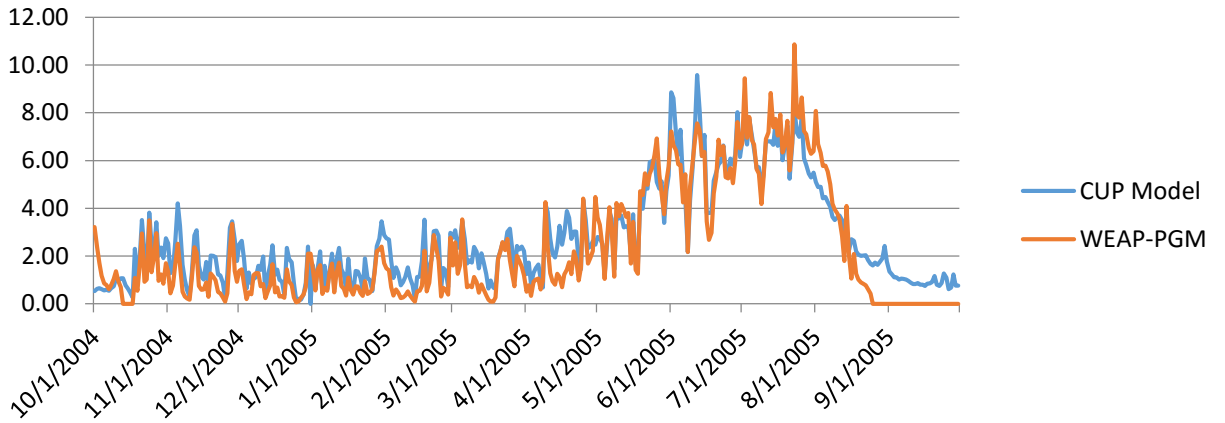
Rice
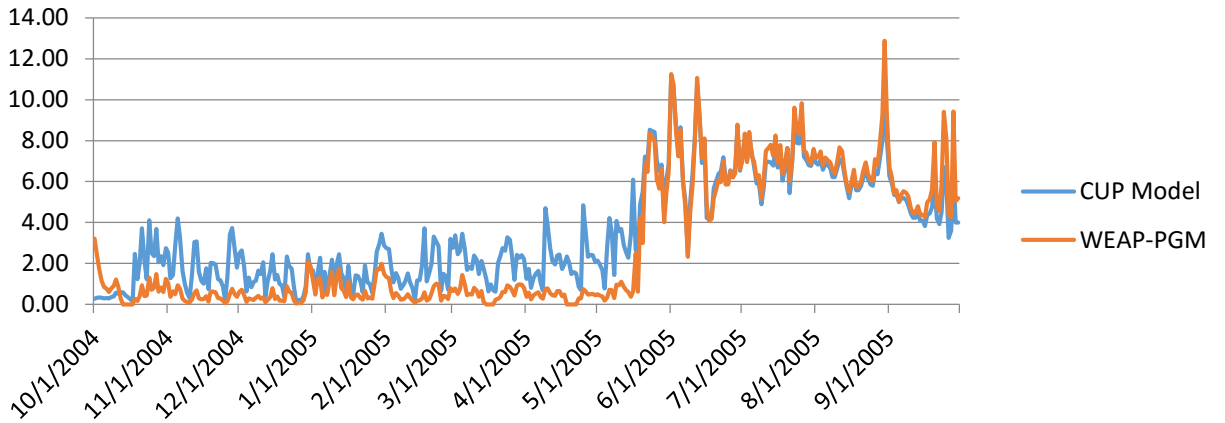
Safflower
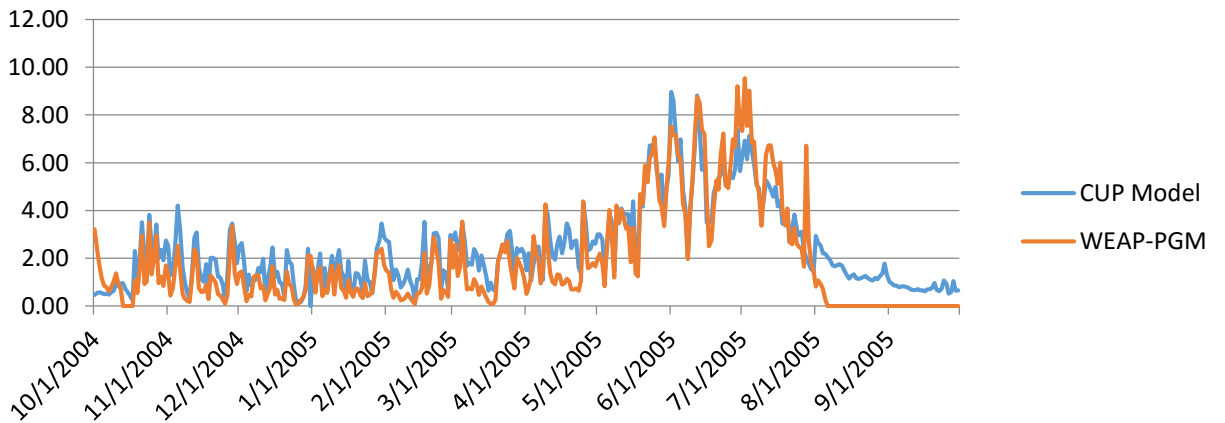
Figure C2-6e. Plots of Daily Evapotranspiration for 19 crops at the Gerber Location.

Subtropical

Sugar Beets

Tomatoes
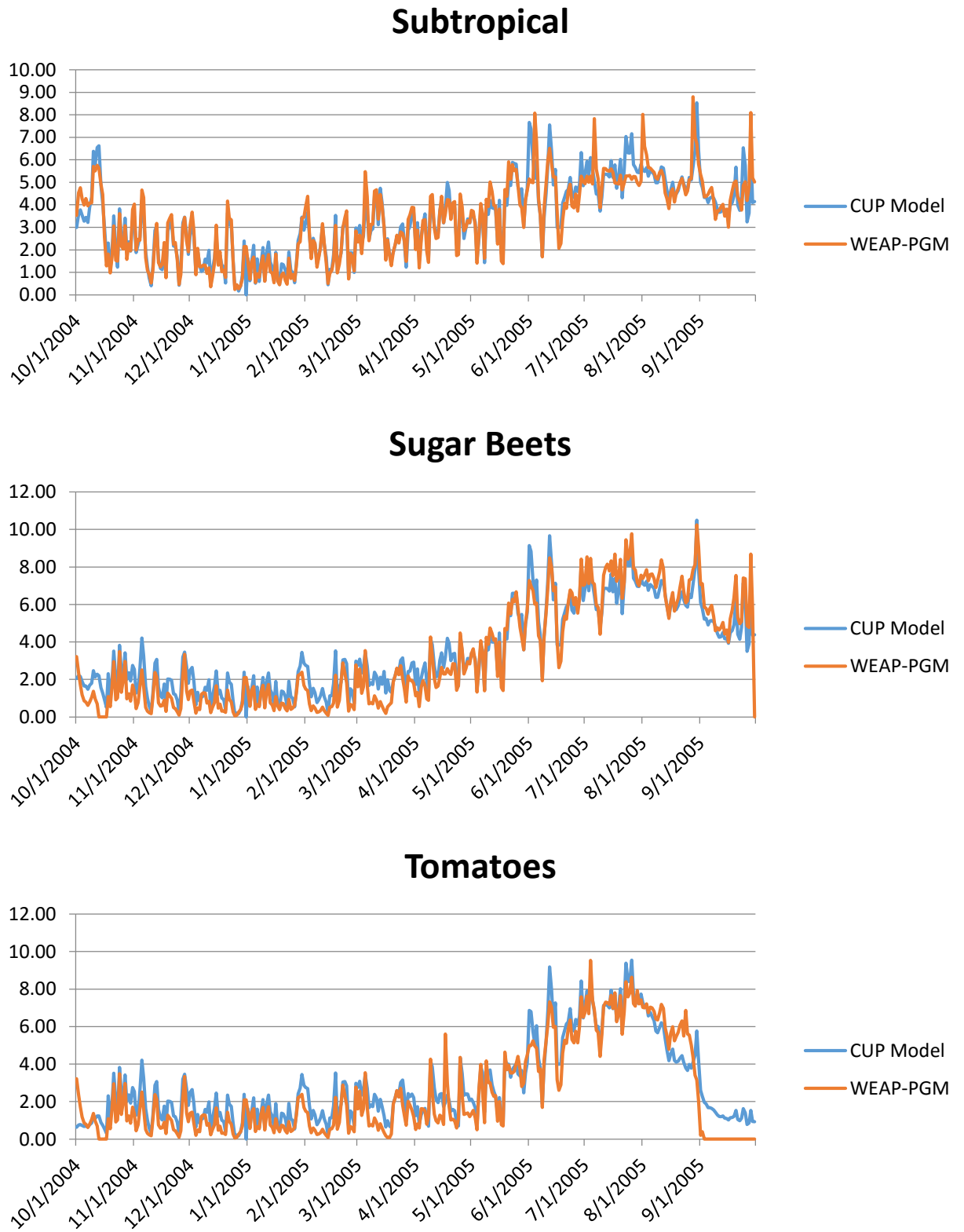
Figure C2-7f. Plots of Daily Evapotranspiration for 19 crops at the Gerber Location.
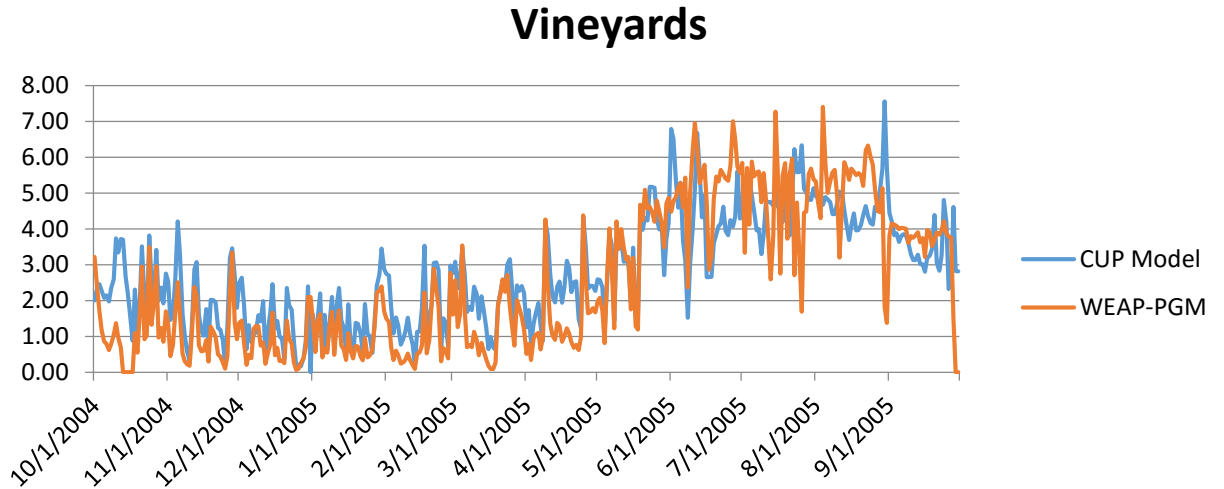
Figure C2-8g. Plots of Daily Evapotranspiration for 19 crops at the Gerber Location.

5.2. Davis

The results from the Davis location are presented in **Table 4C2-1** and Error! Reference source not found.**a** through **C2-2g**.

Table 2-2. Seasonal ET totals from the CUP and PGM models for the Davis Location.

Crop	Period of Comparison	CUP ETc (mm)	PGM ETc (mm)	Percent Difference
Almonds/Pistachios	Apr 1 – Sep 30	1034	1046	1.1
Alfalfa	Apr 1 – Sep 30	929	954	2.7
Corn	May 1 – Sep 30	717	725	1.2
Cotton	May 15 – Oct 15	758	780	2.9
Cucurbits – Melons	May 15 – Sep 15	653	639	-2.0
Dry Beans	Jun 15 – Sep 30	525	525	0.0
Grain – Wheat	Nov 1 – May 31	486	473	-2.5
Onions	Mar 1 – Sep 30	1057	1045	-1.1
Other Deciduous – Apples	Apr 1 – Sep 30	923	915	-0.9
Other Field – Corn Silage	May 1 – Aug 15	547	560	2.4

Crop	Period of Comparison	CUP ETc (mm)	PGM ETc (mm)	Percent Difference
Other Truck – Cucumber	May 15 – Aug 31	569	562	-1.3
Pasture	Apr 1 – Sep 30	883	865	-1.9
Potatoes	Apr 15 – Aug 15	617	624	1.2
Rice	May 15 – Sep 30	900	962	6.8
Safflower	Apr 1 – Jul 31	510	520	1.9
Subtropical – Olives	Apr 1 – Sep 30	837	854	1.9
Sugar Beets	Mar 15 – Sep 30	1029	1018	-0.9
Tomatoes	Apr 1 – Aug 31	706	688	-2.4
Vineyards	Apr 1 – Sep 30	706	702	-0.4

Key:
CUP = Consumptive Use Program
ETc = crop evapotranspiration
mm = millimeters
PGM = Plant Growth Model

Almonds/Pistachios
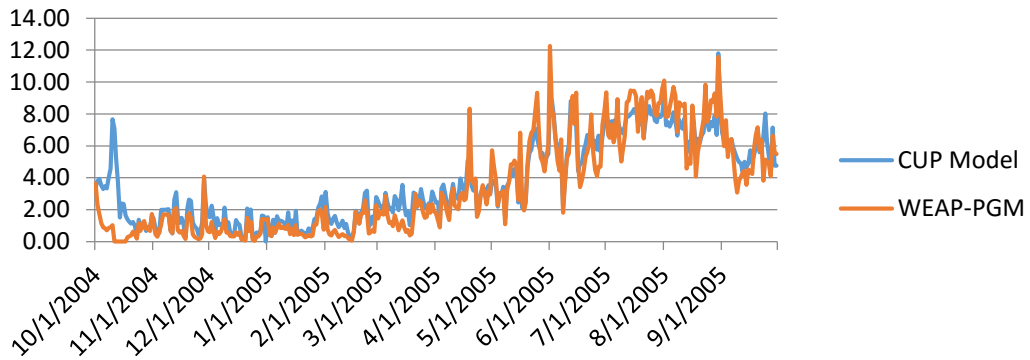
Alfalfa
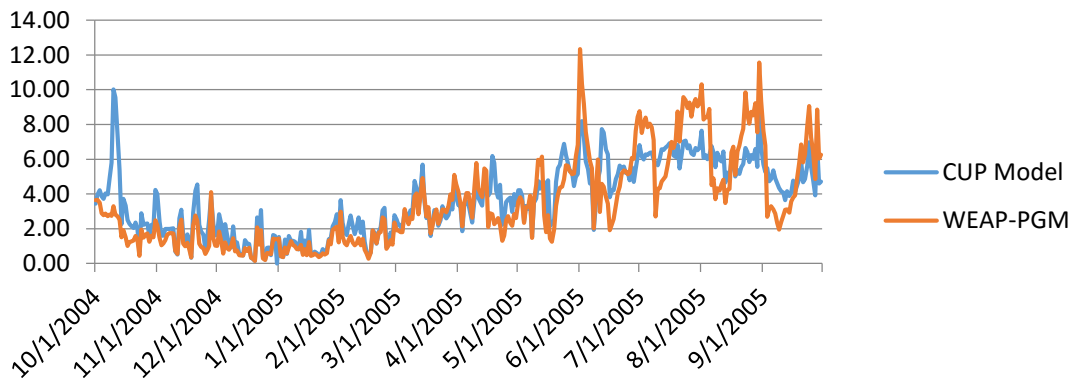
Corn
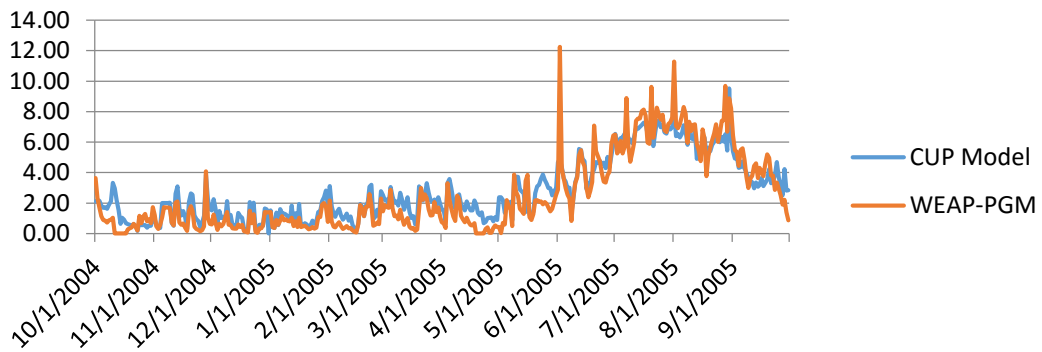
Figure C2-3a. Plots of Daily Evapotranspiration for 19 crops at the Davis Location.
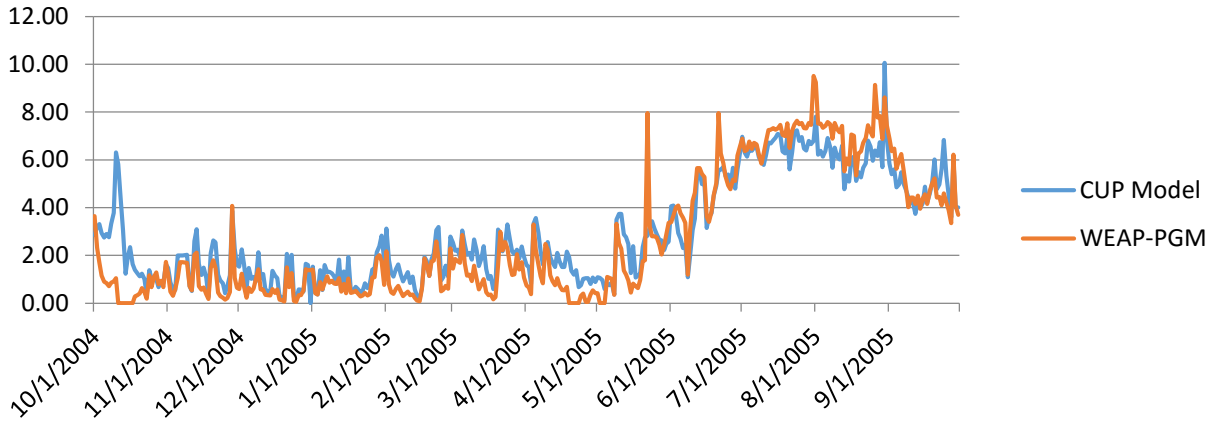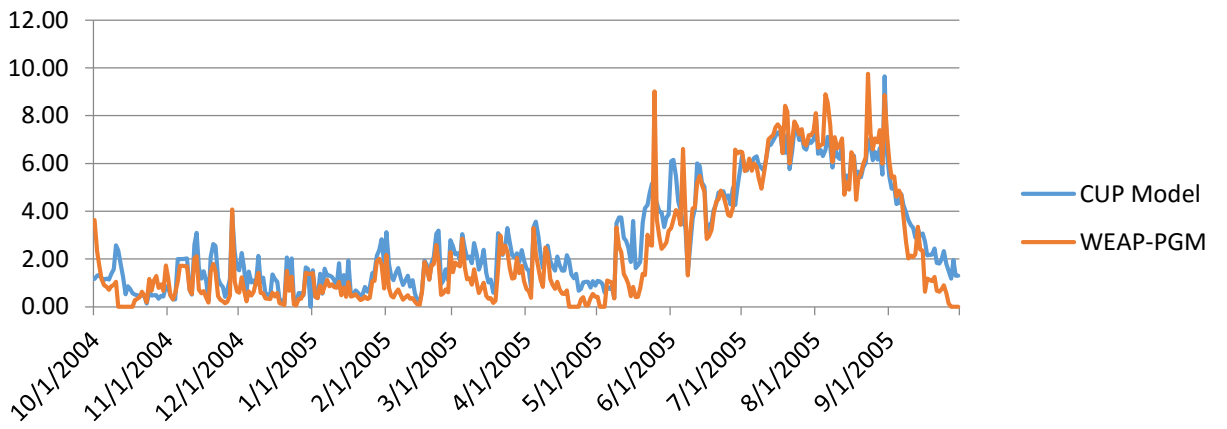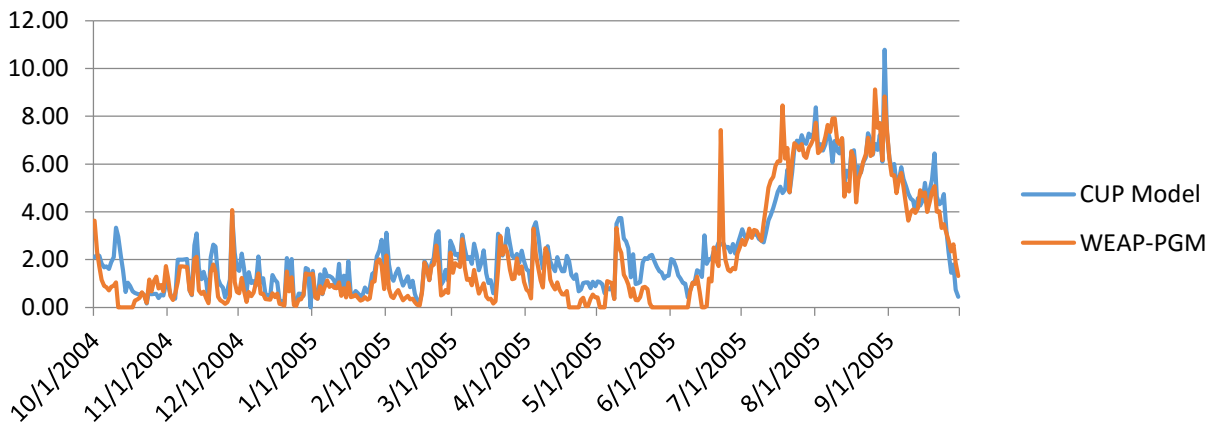
Figure C2-3b. Plots of Daily Evapotranspiration for 19 crops at the Davis Location.

Grain
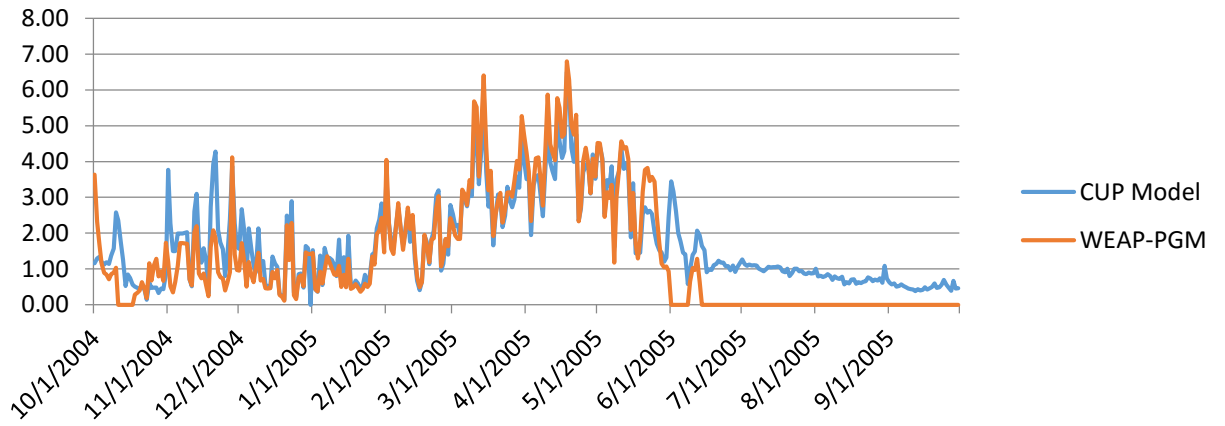
Onions and Garlic
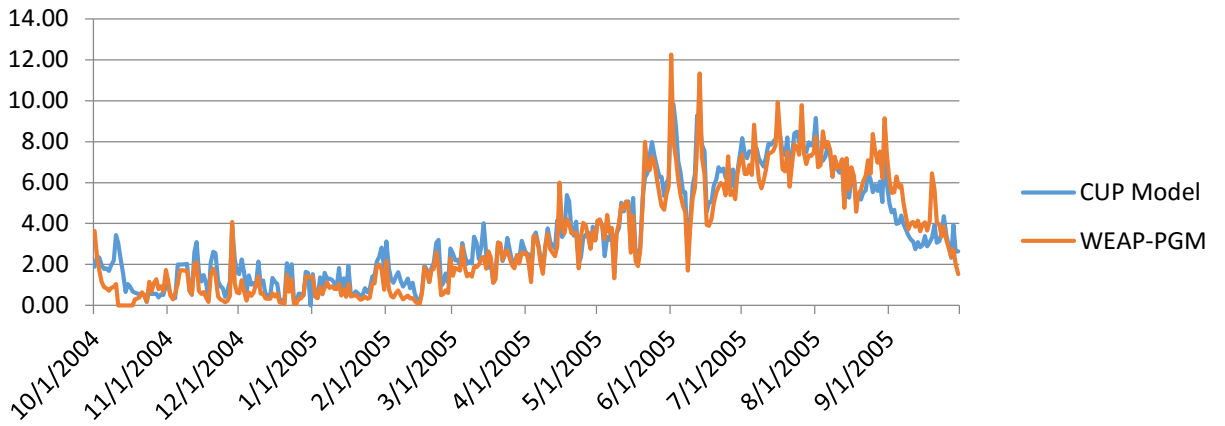
Other Deciduous
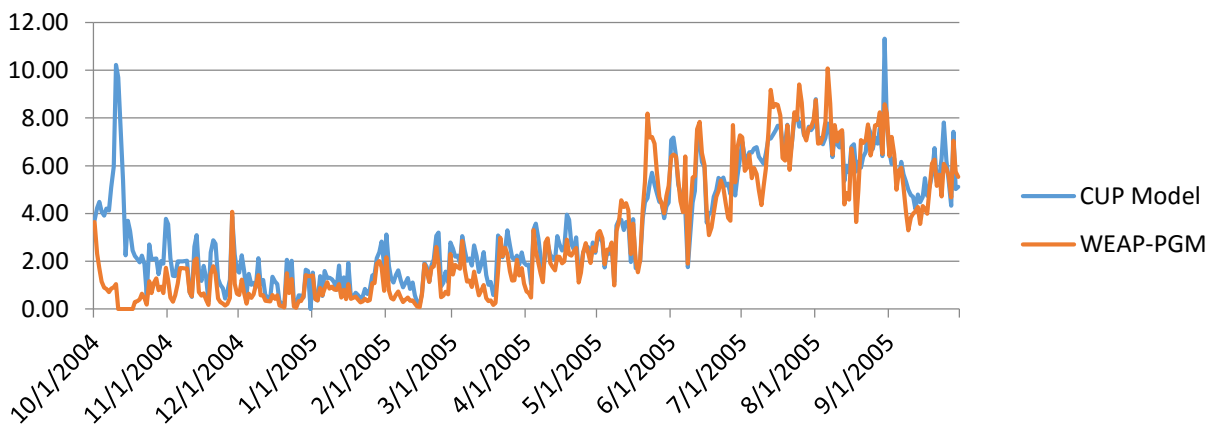
Figure C2-3c. Plots of Daily Evapotranspiration for 19 crops at the Davis Location.
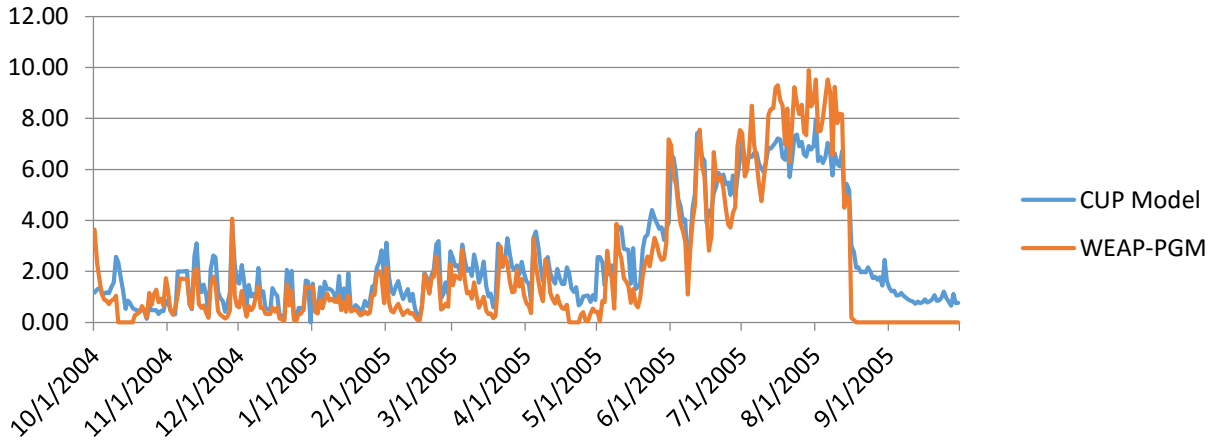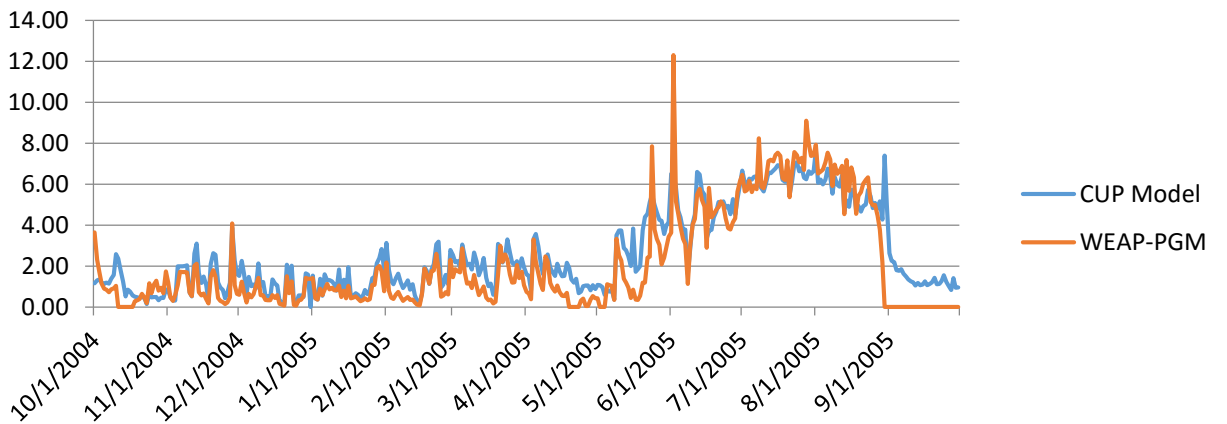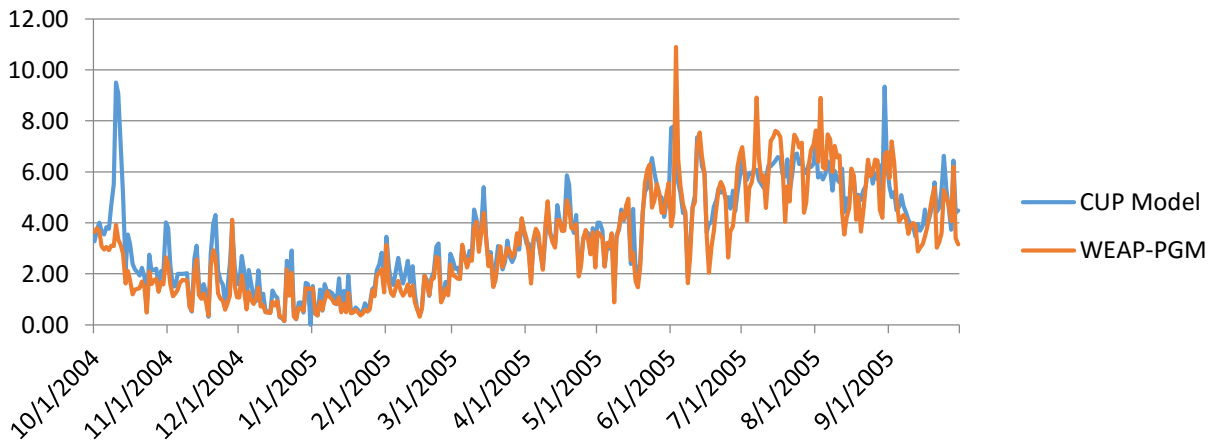
Figure C2-3d. Plots of Daily Evapotranspiration for 19 crops at the Davis Location.

Potatoes

Rice

Safflower
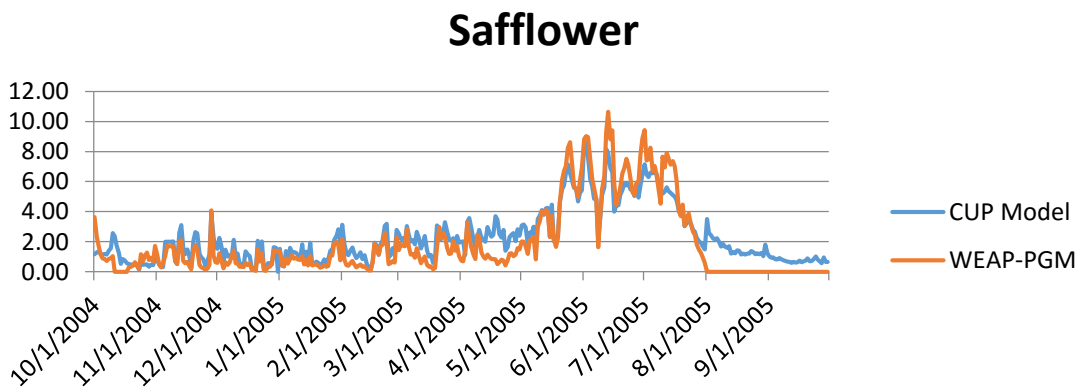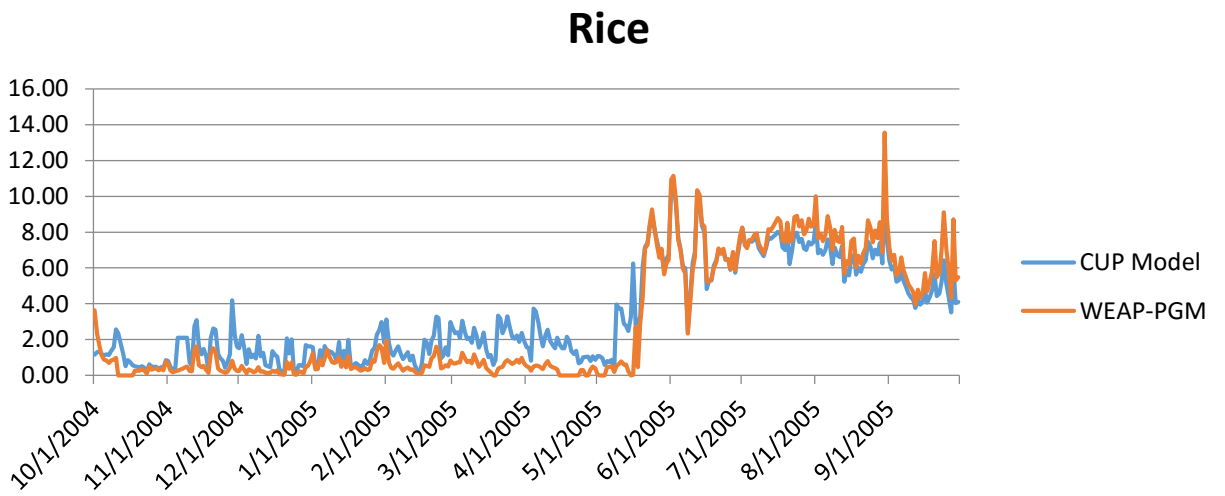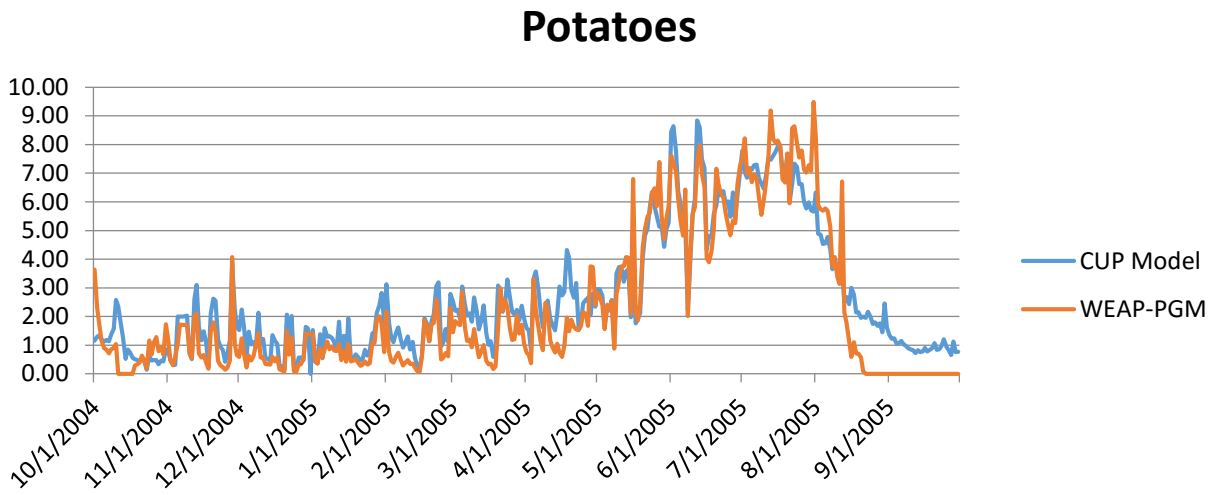
Figure C2-3e. Plots of Daily Evapotranspiration for 19 crops at the Davis Location.

Subtropical
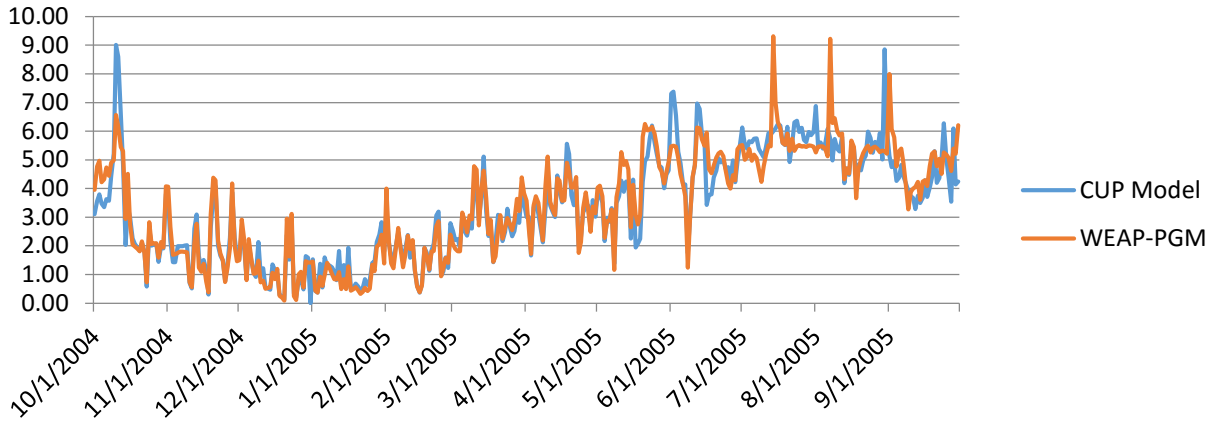
Sugar Beets
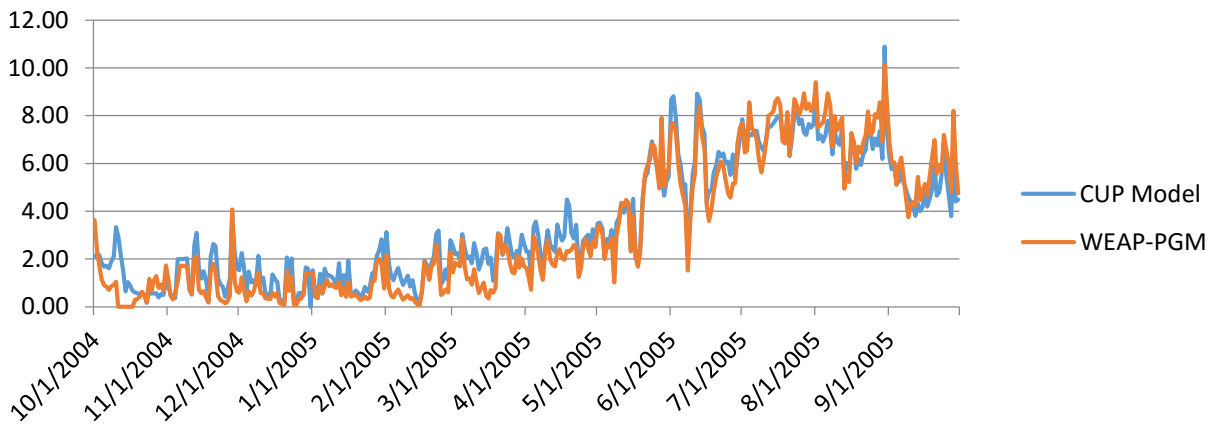
Tomatoes
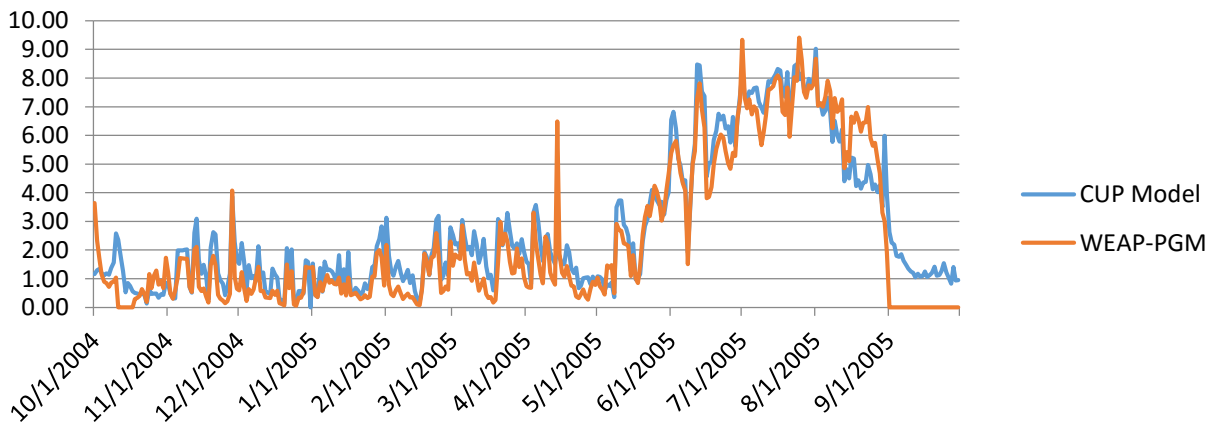
Figure C2-3f. Plots of Daily Evapotranspiration for 19 crops at the Davis Location.
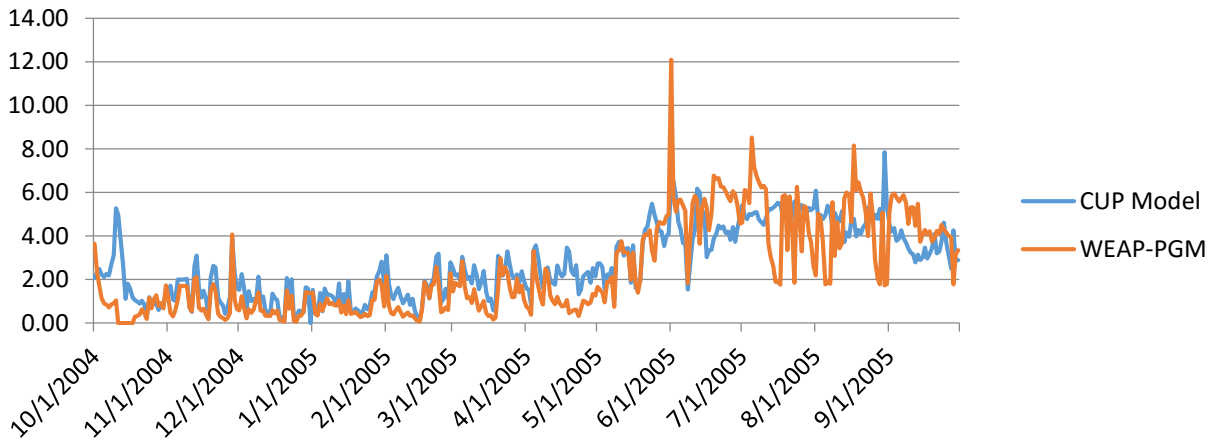
Figure C2-3g. Plots of Daily Evapotranspiration for 19 crops at the Davis Location.

5.3. Firebaugh

The results from the Firebaugh location are presented in **Table 4C2-13** and Error! Reference source not found.**4a** through **C2-2g**.

Table C2-3. Seasonal ET totals from the CUP and PGM models for the Firebaugh Location.

Crop	Period of Comparison	CUP ETc (mm)	PGM ETc (mm)	Percent Difference
Almonds/Pistachios	Apr 1 – Sep 30	1021	1001	-1.9
Alfalfa	Apr 1 – Sep 30	920	946	2.8
Corn	May 1 – Sep 30	695	698	0.5
Cotton	May 15 – Oct 15	725	726	0.1
Cucurbits – Melons	May 15 – Sep 15	650	659	1.5
Dry Beans	Jun 15 – Sep 30	493	495	0.3
Grain – Wheat	Nov 1 – May 31	467	456	-2.1
Onions	Mar 1 – Sep 30	1049	1067	1.7
Other Deciduous – Apples	Apr 1 – Sep 30	907	899	-0.8
Other Field – Corn Silage	May 1 – Aug 15	548	538	-1.6
Other Truck – Cucumber	May 15 – Aug 31	182	176	-2.8
Pasture	Apr 1 – Sep 30	875	890	1.7
Potatoes	Apr 15 – Aug 15	632	637	0.7
Rice	May 15 – Sep 30	891	931	4.5
Safflower	Apr 1 – Jul 31	533	544	2.1
Subtropical – Olives	Apr 1 – Sep 30	920	914	-0.6
Sugar Beets	Mar 15 – Sep 30	1013	1028	1.4
Tomatoes	Apr 1 – Aug 31	711	726	2.2
Vineyards	Apr 1 – Sep 30	700	709	1.3

Key:
CUP = Consumptive Use Program
ETc = crop evapotranspiration
mm = millimeters
PGM = Plant Growth Model
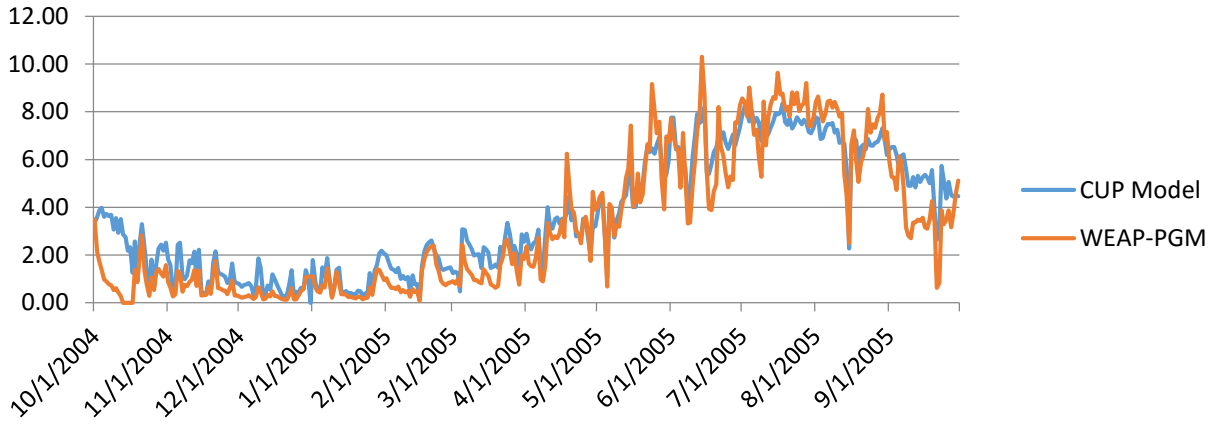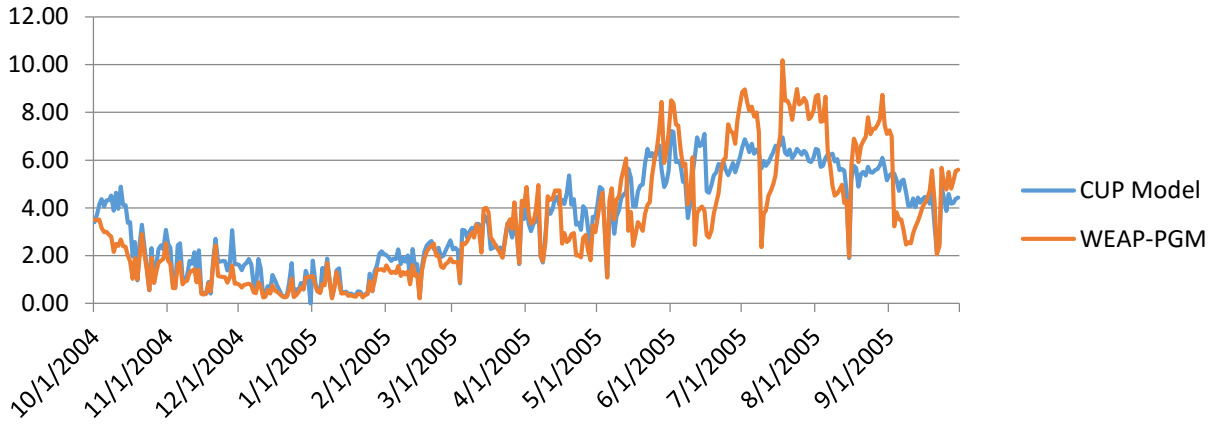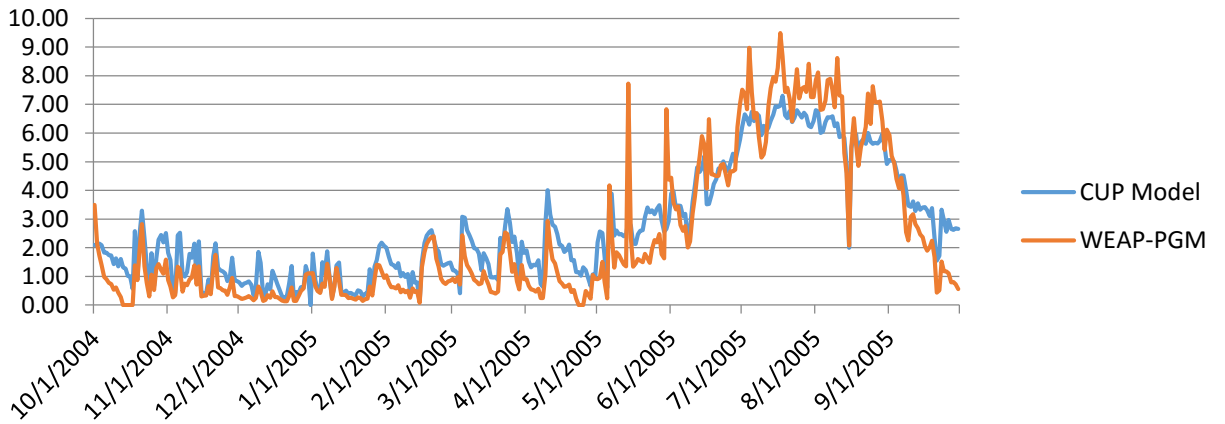
Figure C2-4a. Plots of Daily Evapotranspiration for 19 crops at the Firebaugh Location.

Cotton
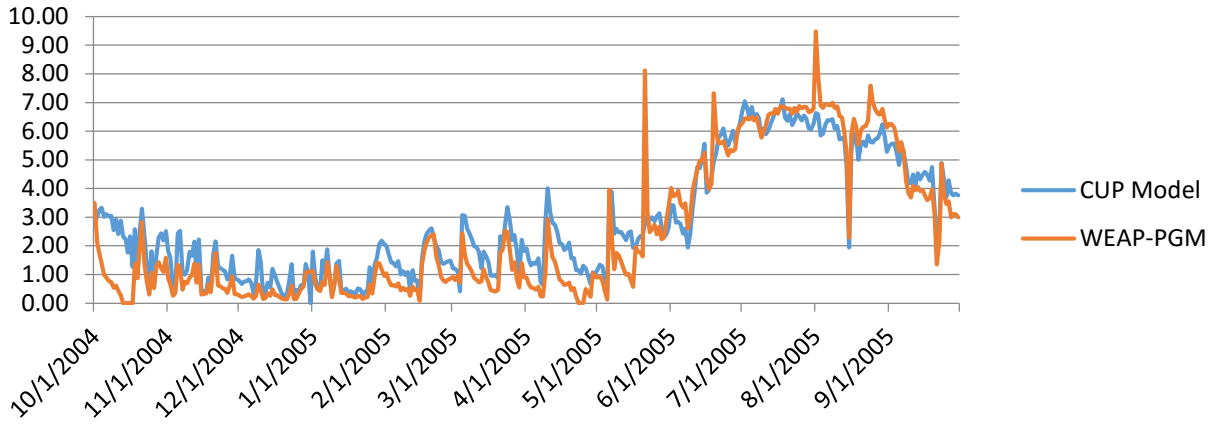
Cucurbits
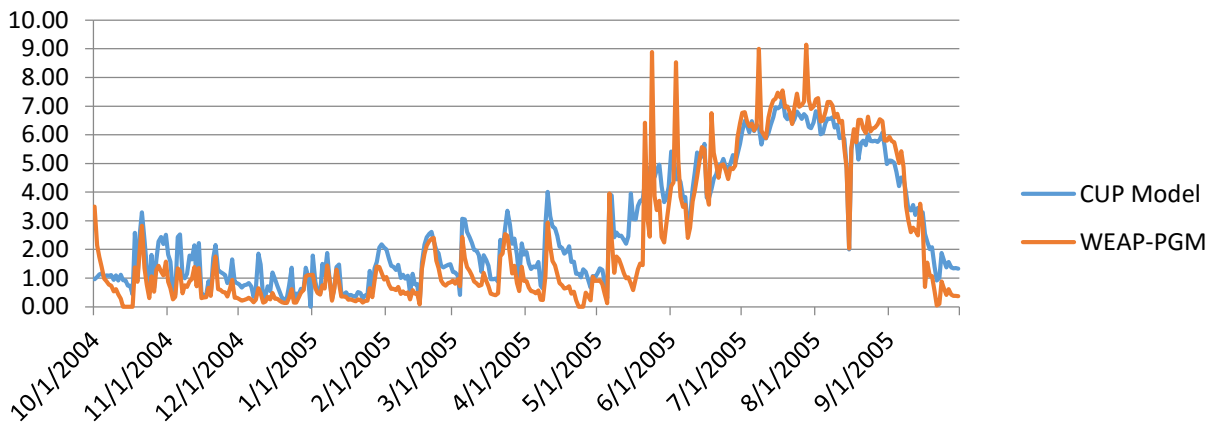
Dry Beans
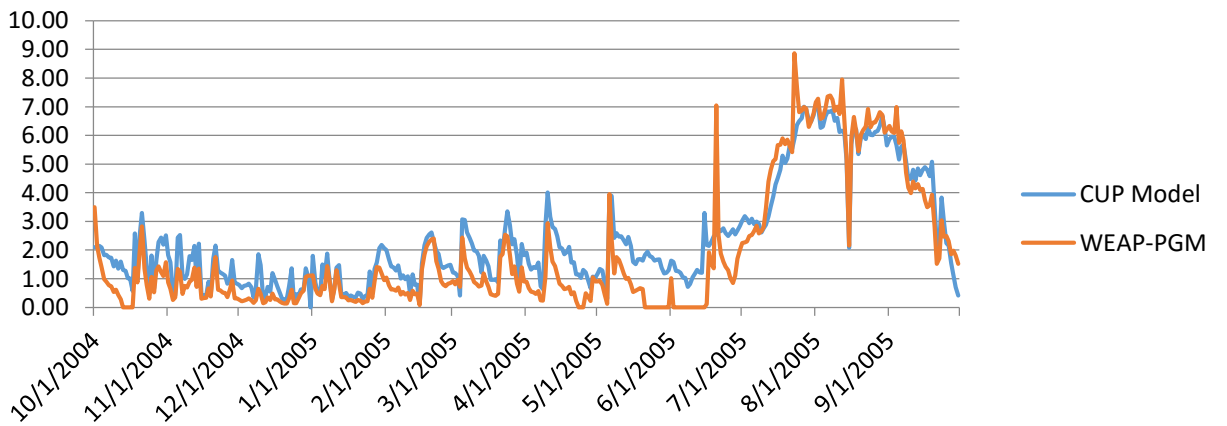
Figure C2-4b. Plots of Daily Evapotranspiration for 19 crops at the Firebaugh Location.

Grain
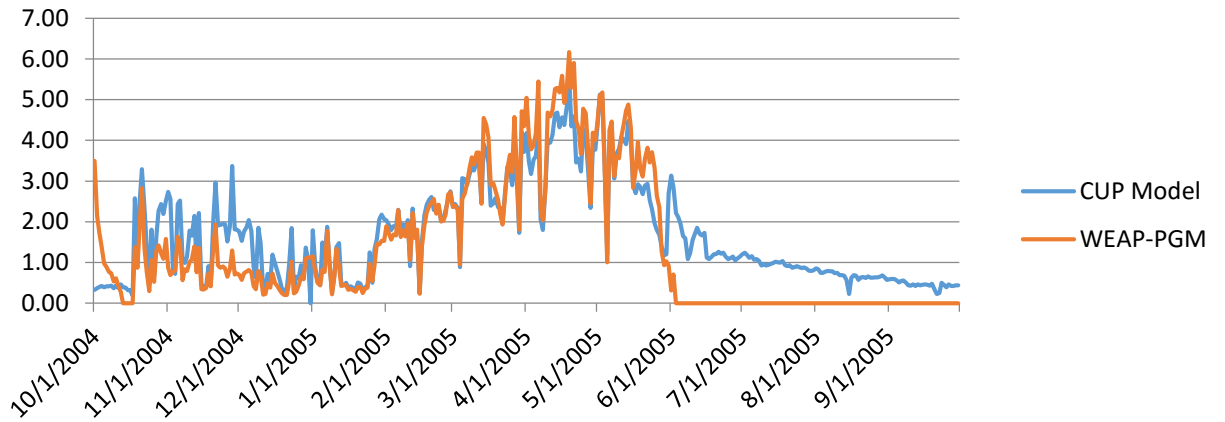
Onions and Garlic
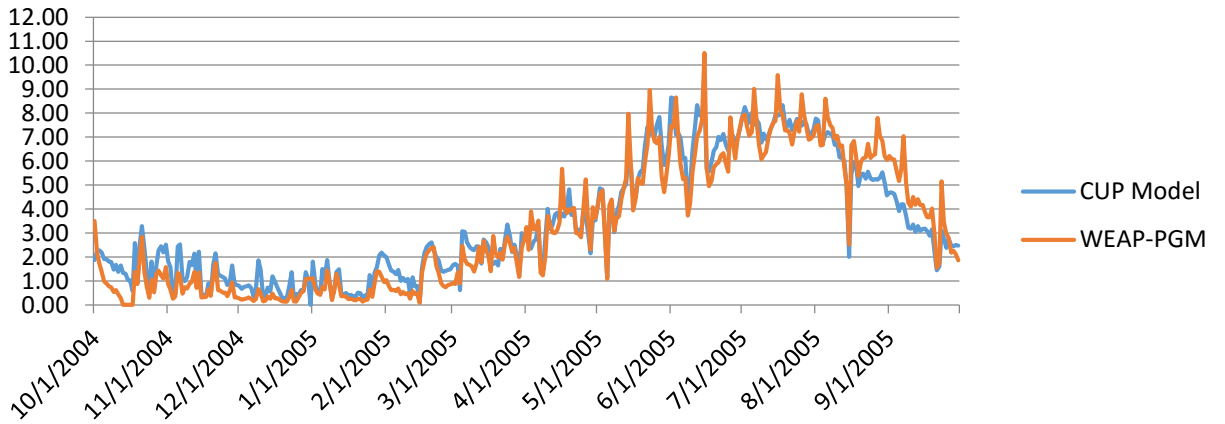
Other Deciduous
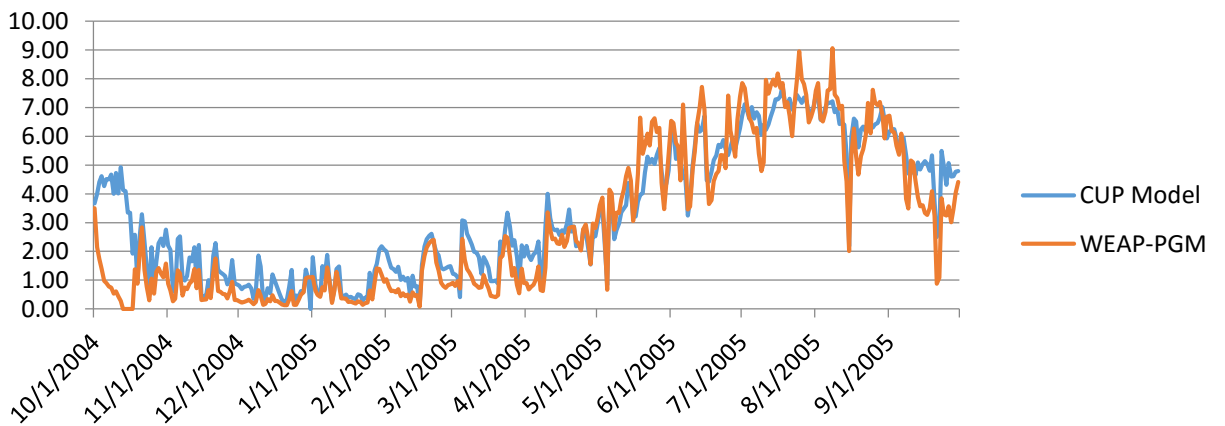
Figure C2-4c. Plots of Daily Evapotranspiration for 19 crops at the Firebaugh Location.

Other Field
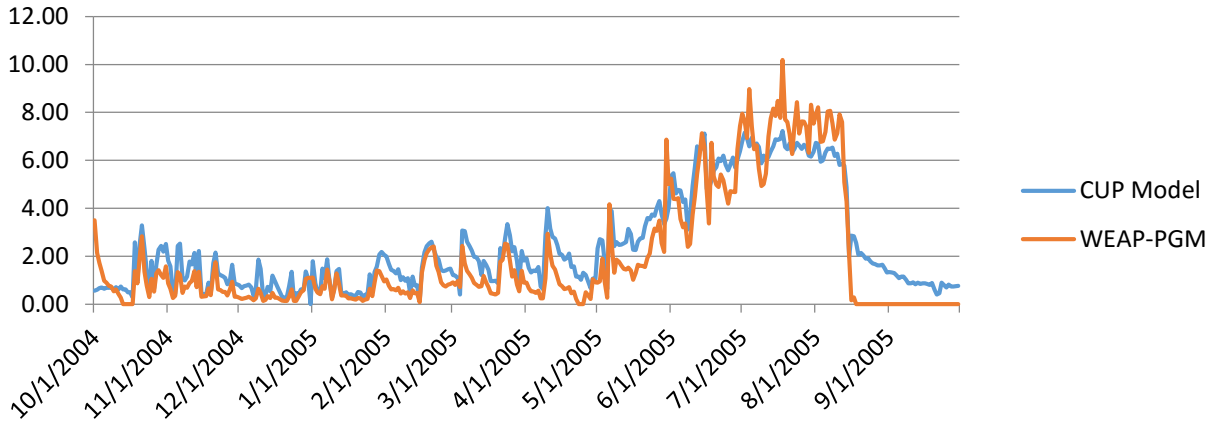
Other Truck
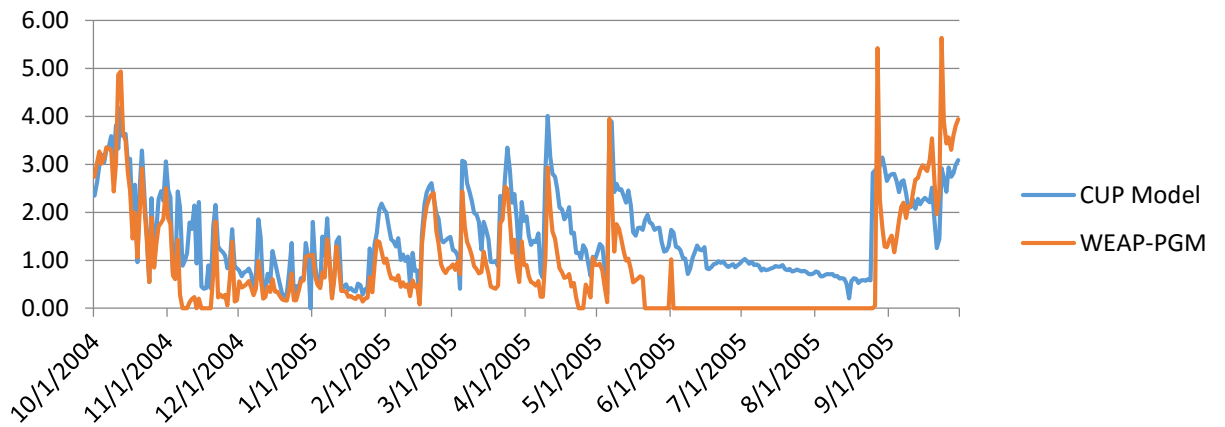
Pasture
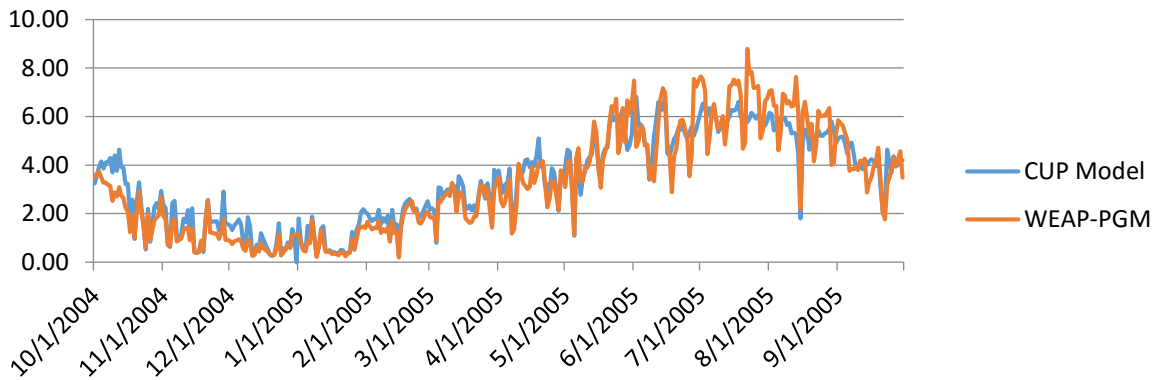
Figure C2-4d. Plots of Daily Evapotranspiration for 19 crops at the Firebaugh Location.

Potatoes
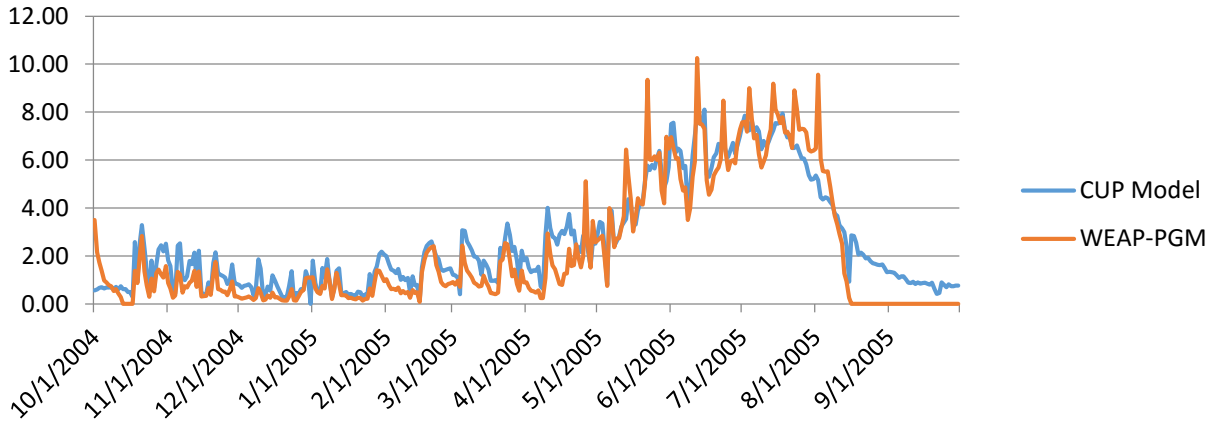
Rice
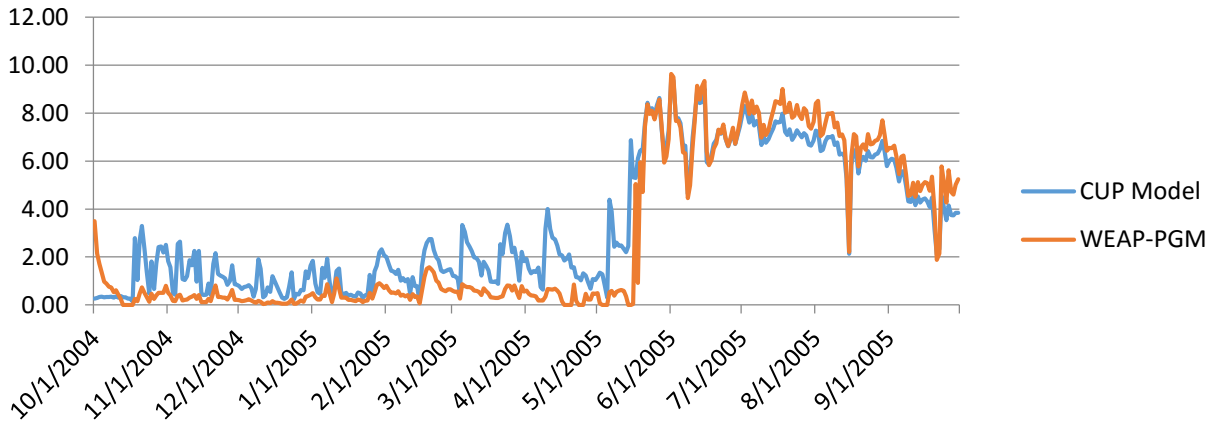
Safflower
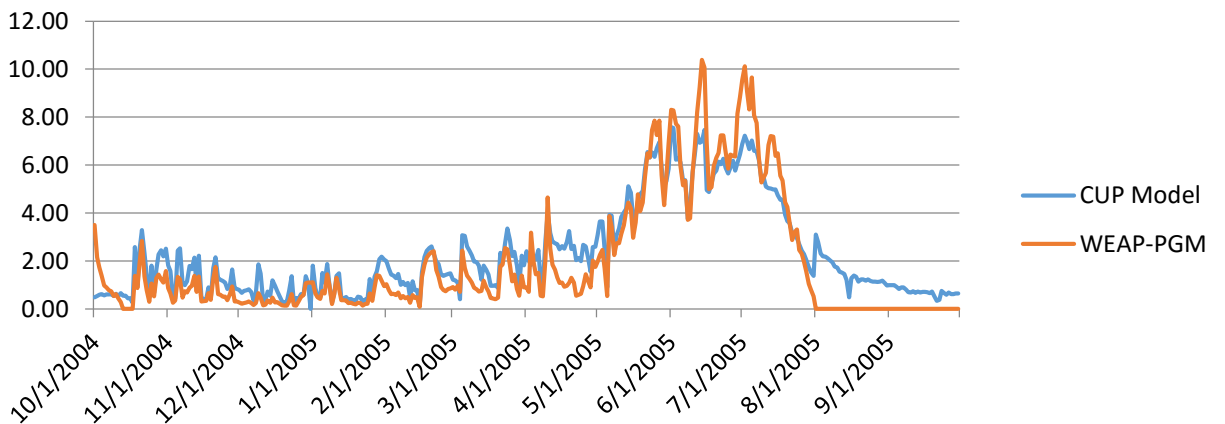
Figure C2-4e. Plots of Daily Evapotranspiration for 19 crops at the Firebaugh Location.

Subtropical
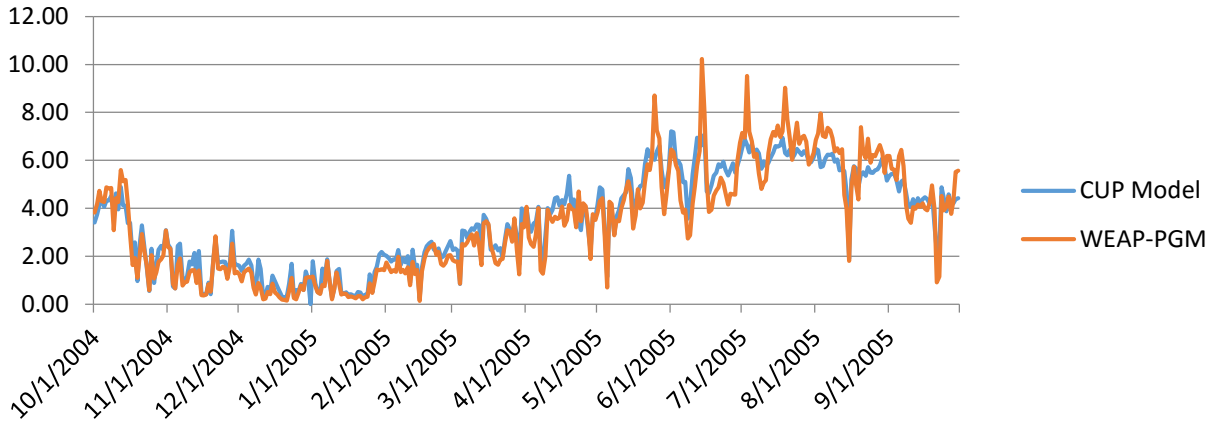
Sugar Beets
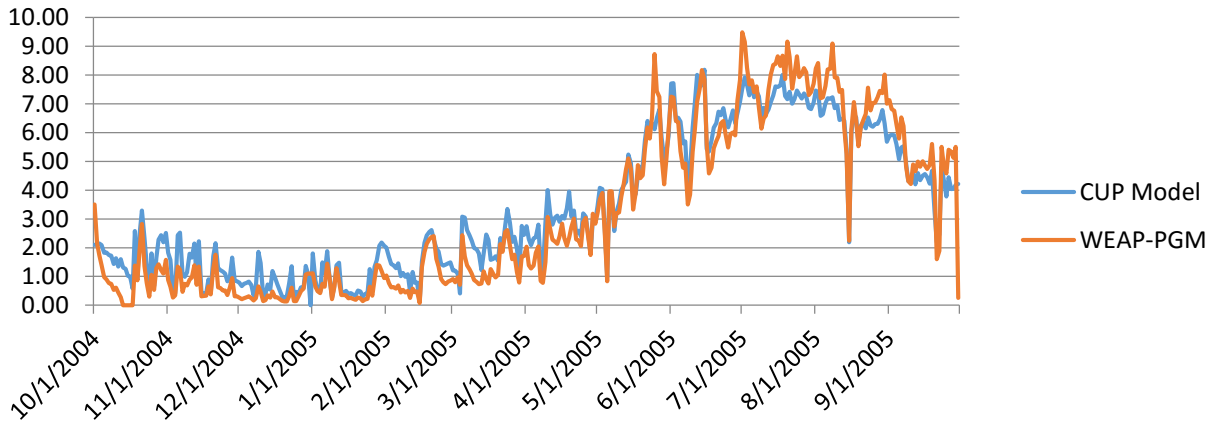
Tomatoes
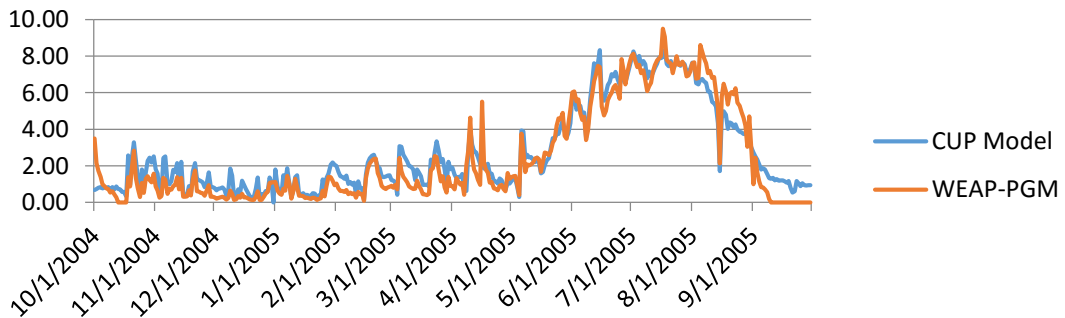
Figure C2-4f. Plots of Daily Evapotranspiration for 19 crops at the Firebaugh Location.
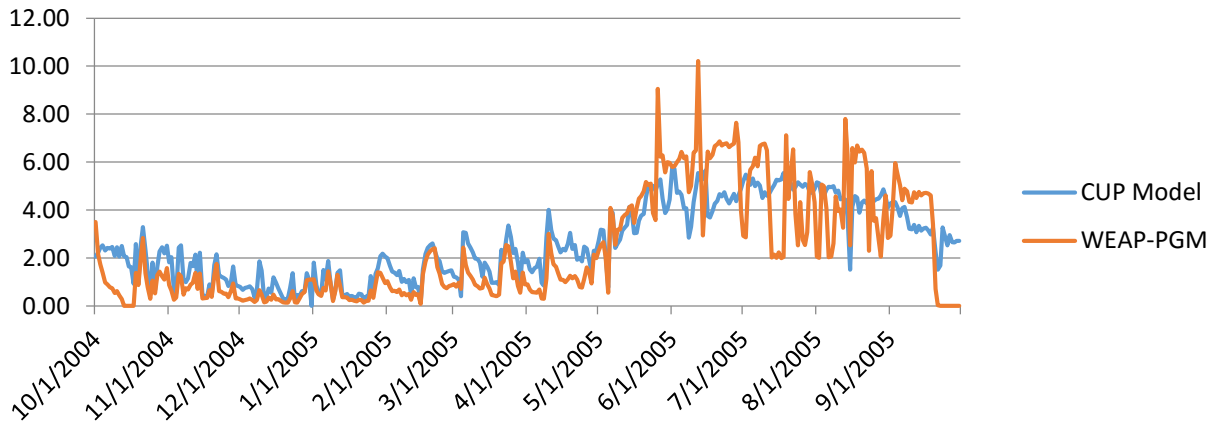
Figure C2-4g. Plots of Daily Evapotranspiration for 19 crops at the Firebaugh Location.

5.4. Shafter

The results from the Shafter location are presented in **Table 4C2-14** and Error! Reference source not found.**5a** through **C2-2g**.

Table 2-4. Seasonal ET totals from the CUP and PGM Models for the Shafter Location.

Crop	Period of Comparison	CUP ETc (mm)	PGM ETc (mm)	Percent Difference
Almonds/Pistachios	Apr 1 – Sep 30	1109	1080	-2.5
Alfalfa	Apr 1 – Sep 30	1005	1033	2.8
Corn	May 1 – Sep 30	741	741	0.0
Cotton	May 15 – Oct 15	773	792	2.4
Cucurbits – Melons	May 15 – Sep 15	634	640	0.9
Dry Beans	Jun 15 – Sep 30	535	543	1.5
Grain – Wheat	Nov 1 – May 31	581	544	-6.3
Onions	Mar 1 – Sep 30	1126	1092	-2.9
Other Deciduous – Apples	Apr 1 – Sep 30	982	989	0.7
Other Field – Corn Silage	May 1 – Aug 15	583	571	-1.9
Other Truck – Cucumber	May 15 – Aug 31	199	195	-2.1
Pasture	Apr 1 – Sep 30	955	932	-2.4

Crop	Period of Comparison	CUP ETc (mm)	PGM ETc (mm)	Percent Difference
Potatoes	Apr 15 – Aug 15	683	687	0.5
Rice	May 15 – Sep 30	866	868	0.3
Safflower	Apr 1 – Jul 31	567	558	-1.4
Subtropical - Olives	Apr 1 – Sep 30	1005	1024	1.8
Sugar Beets	Mar 15 – Sep 30	1077	1064	-1.1
Tomatoes	Apr 1 – Aug 31	736	725	-1.3
Vineyards	Apr 1 – Sep 30	755	718	-4.8

Key:
CUP = Consumptive Use Program
ETc = crop evapotranspiration
mm = millimeters
PGM = Plant Growth Model

Almonds/Pistachios
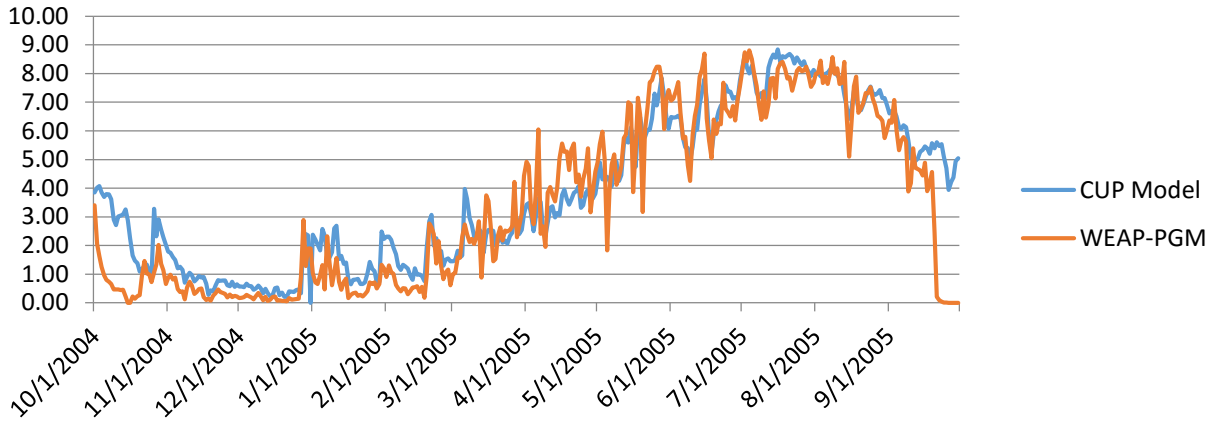
Alfalfa
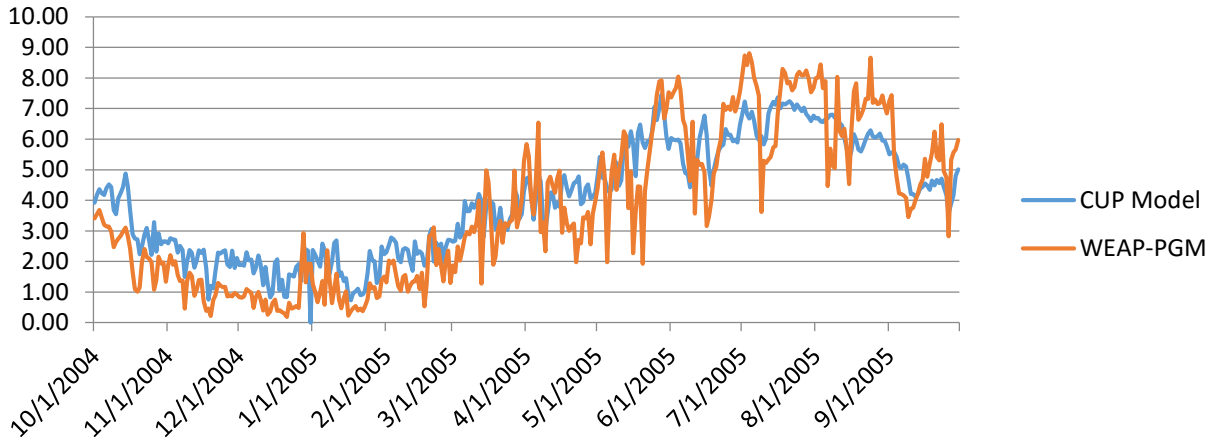
Corn
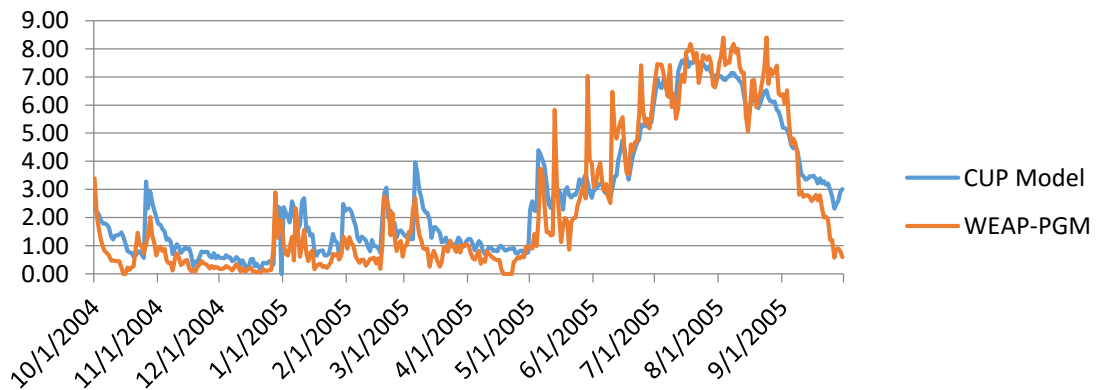
Figure C2-9a. Plots of Daily Evapotranspiration for 19 Crops at the Shafter Location.

Cotton
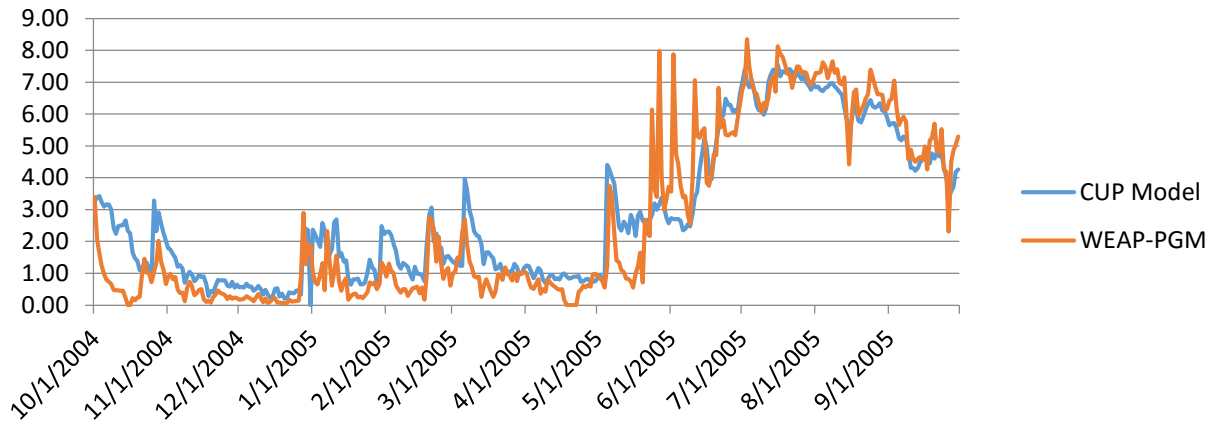
Cucurbits
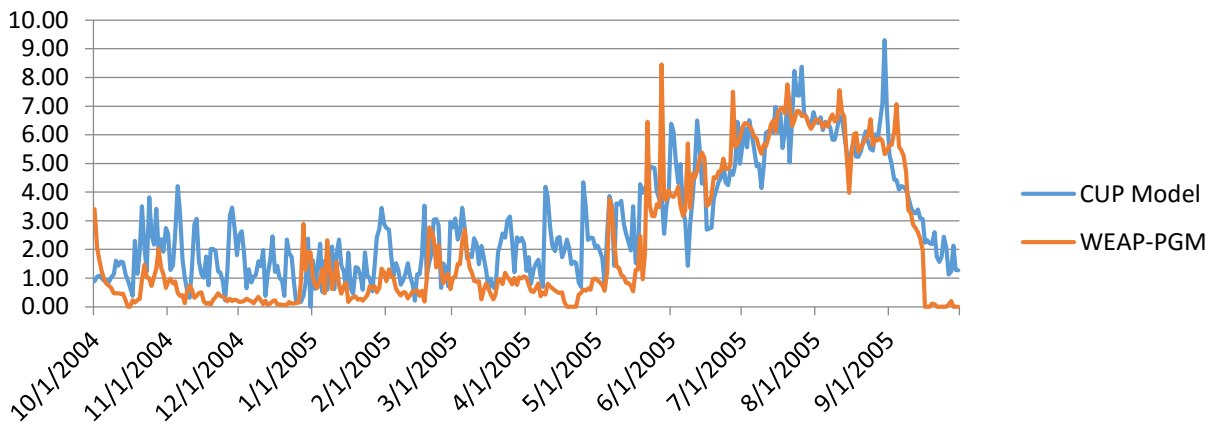
Dry Beans
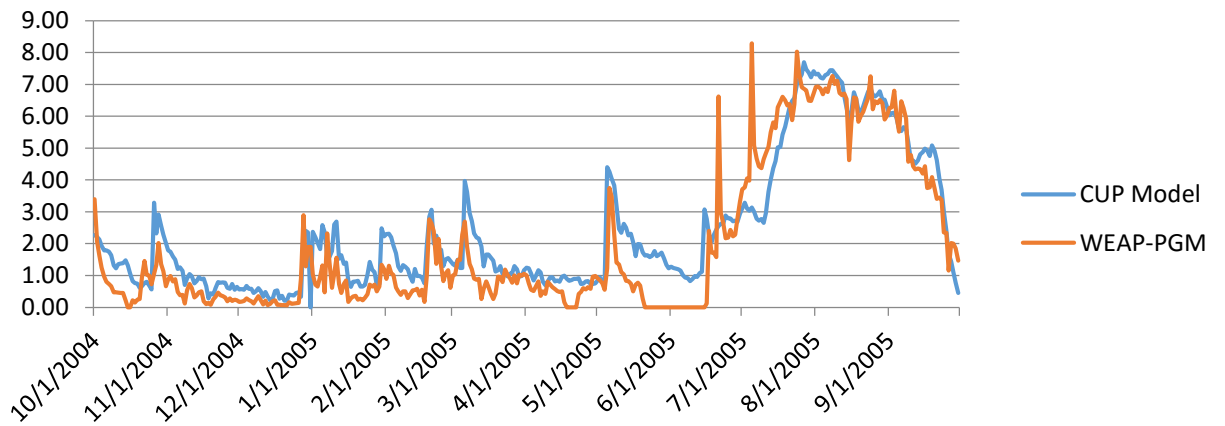
Figure C2-10b. Plots of Daily Evapotranspiration for 19 Crops at the Shafter Location.

Grain
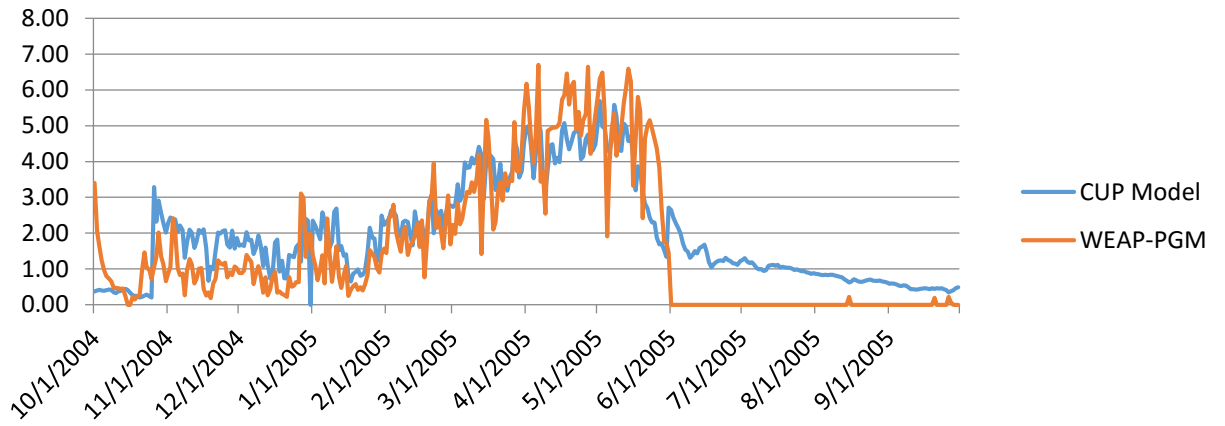
Onions and Garlic
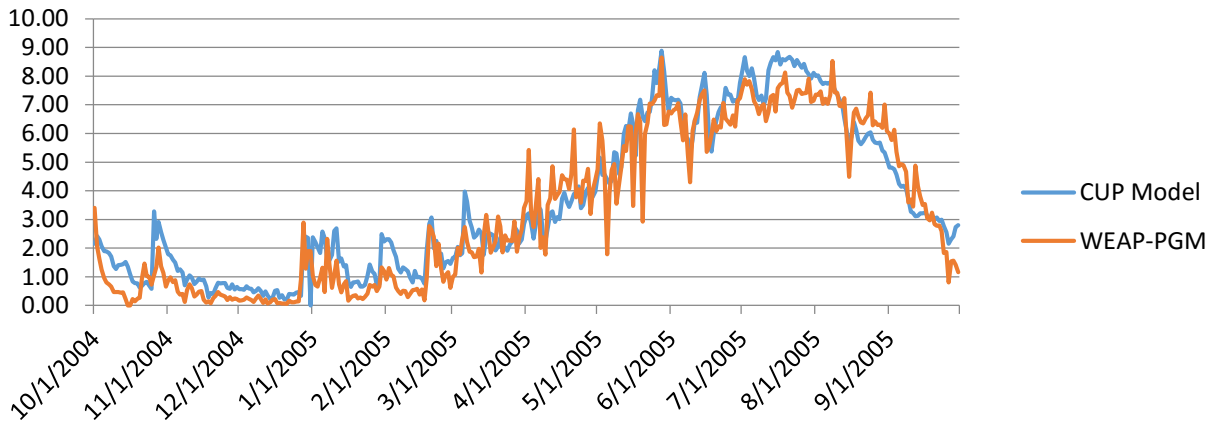
Other Deciduous
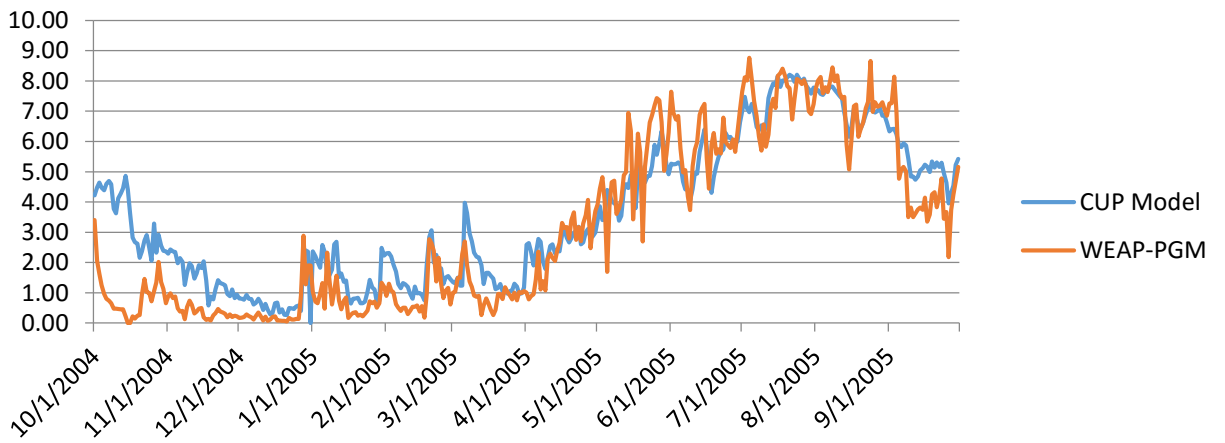
Figure C2-11c. Plots of Daily Evapotranspiration for 19 Crops at the Shafter Location.

Other Field
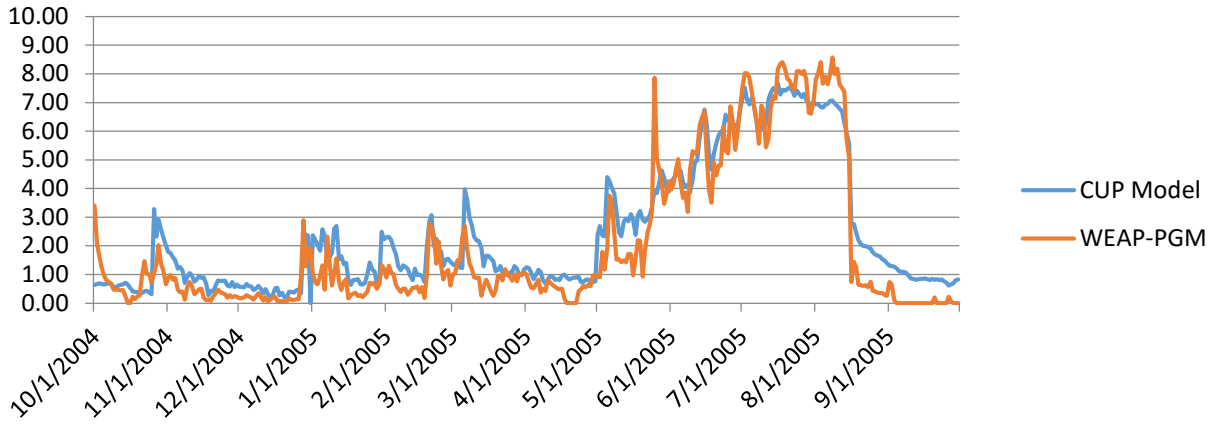
Other Truck
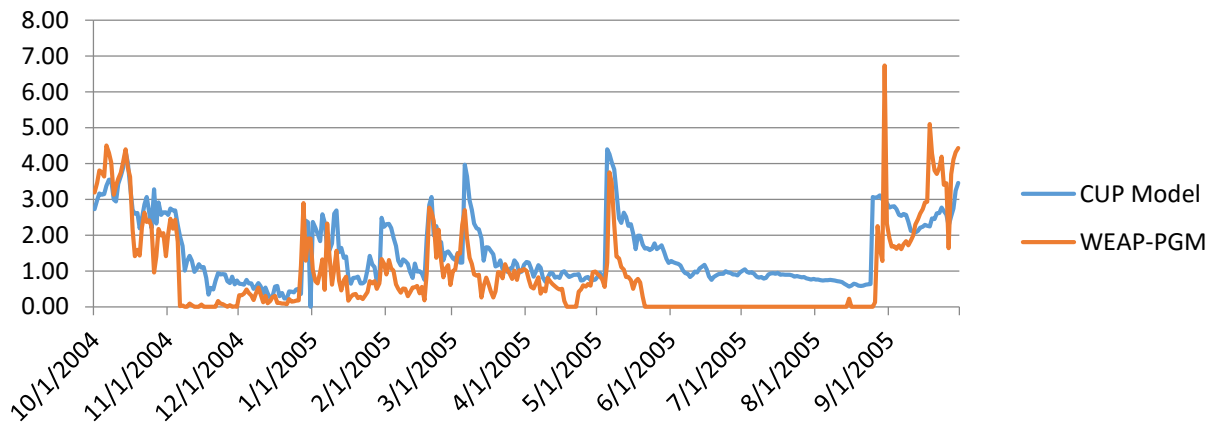
Pasture
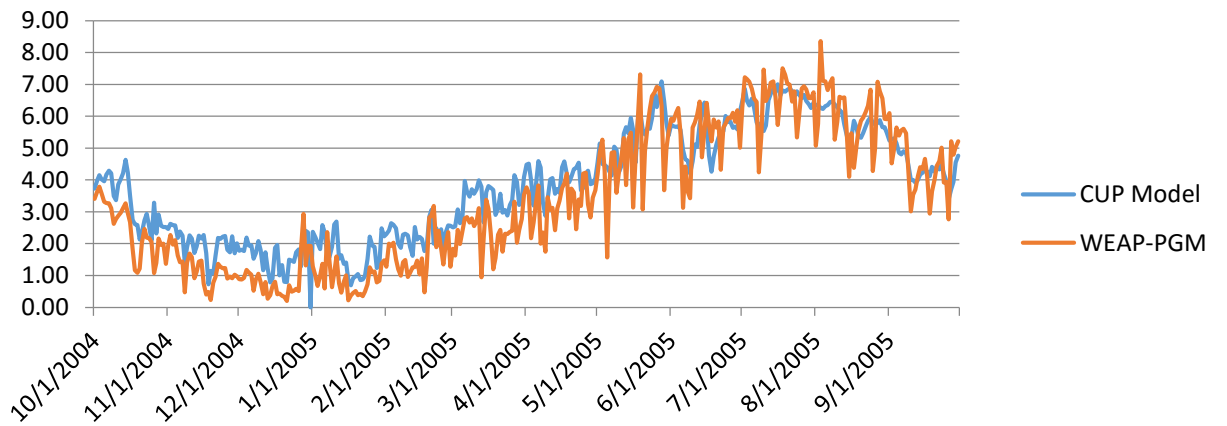
Figure C2-12d. Plots of Daily Evapotranspiration for 19 Crops at the Shafter Location.

Potatoes
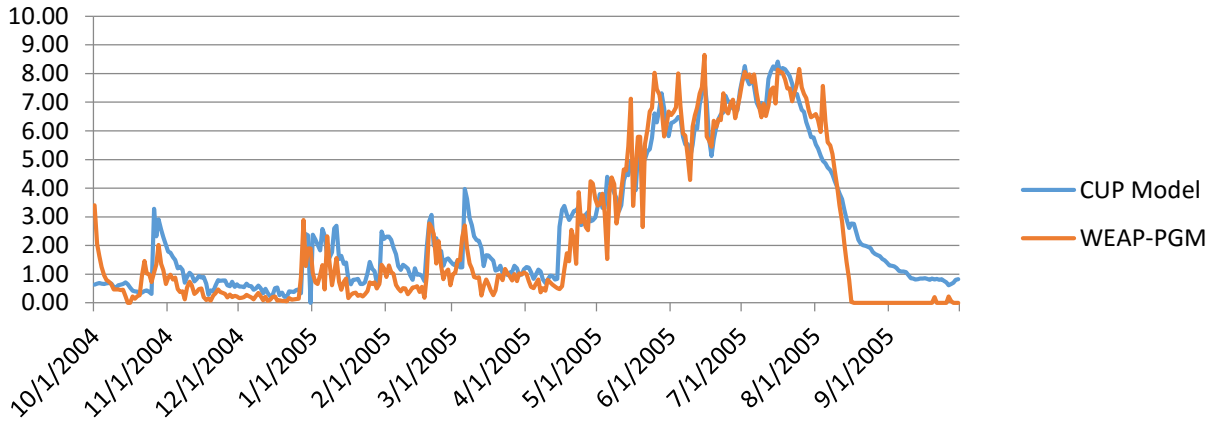
Rice
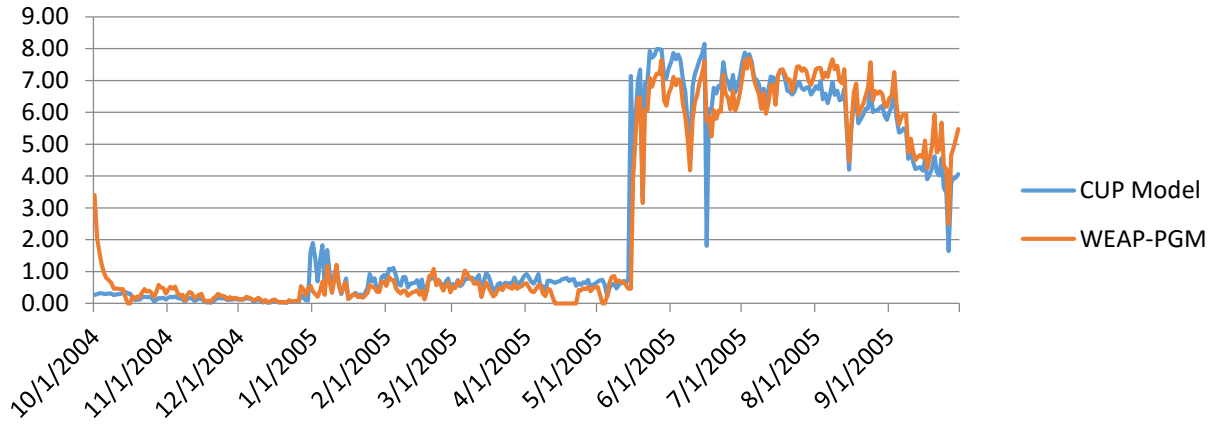
Safflower
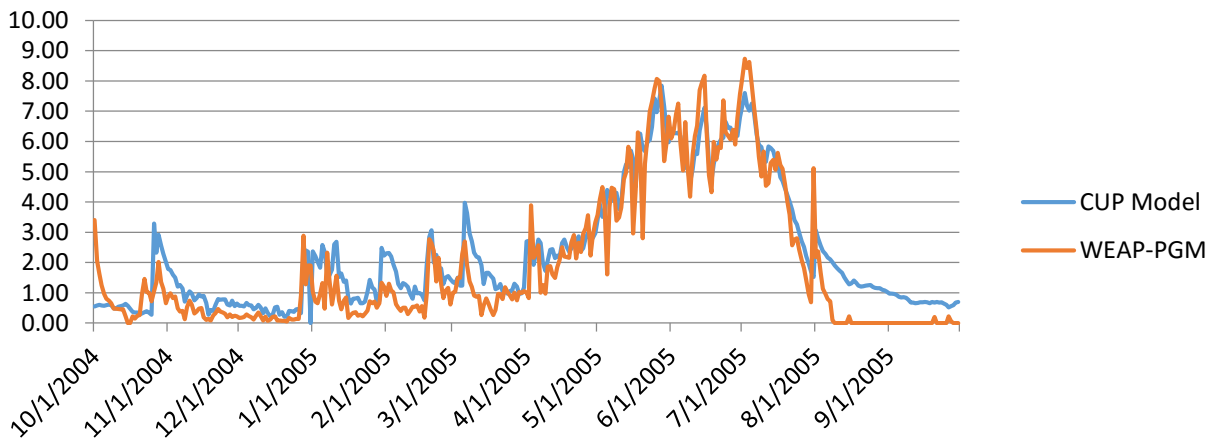
Figure C2-13e. Plots of Daily Evapotranspiration for 19 Crops at the Shafter Location.

Subtropical
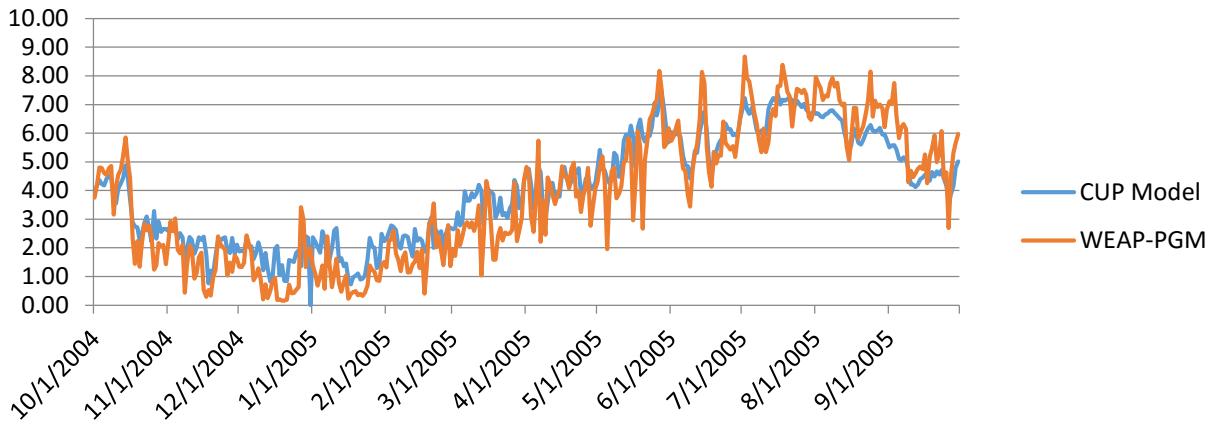
Sugar Beets
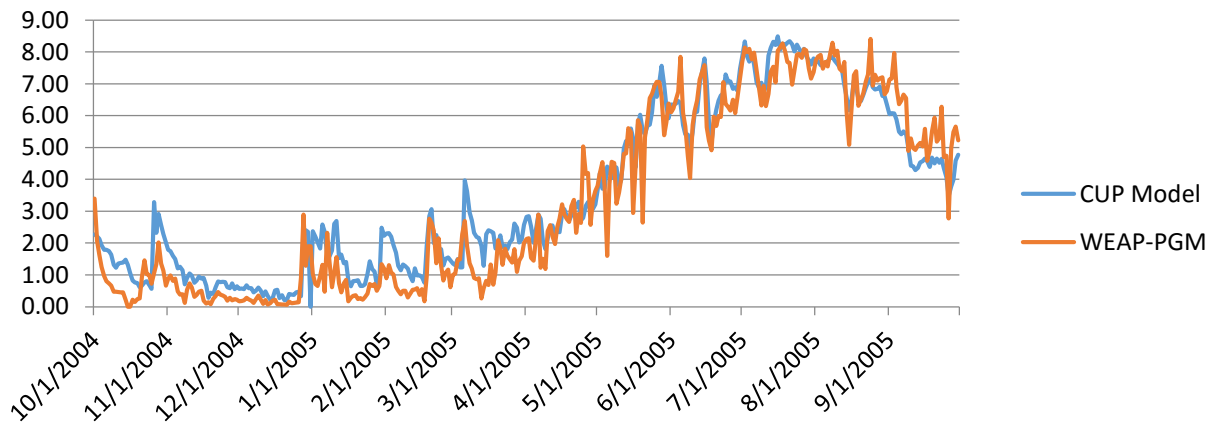
Tomatoes
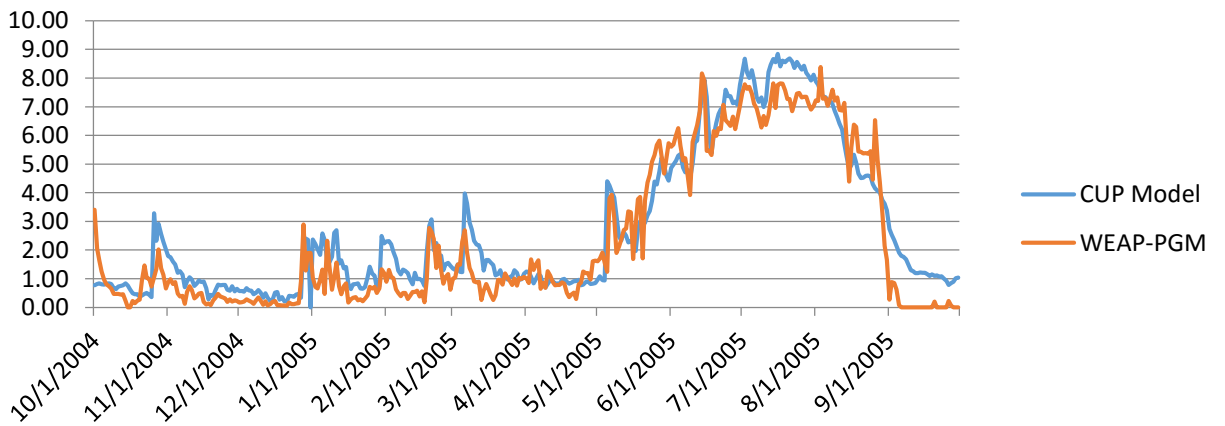
Figure C2-14f. Plots of Daily Evapotranspiration for 19 Crops at the Shafter Location.

Vineyards
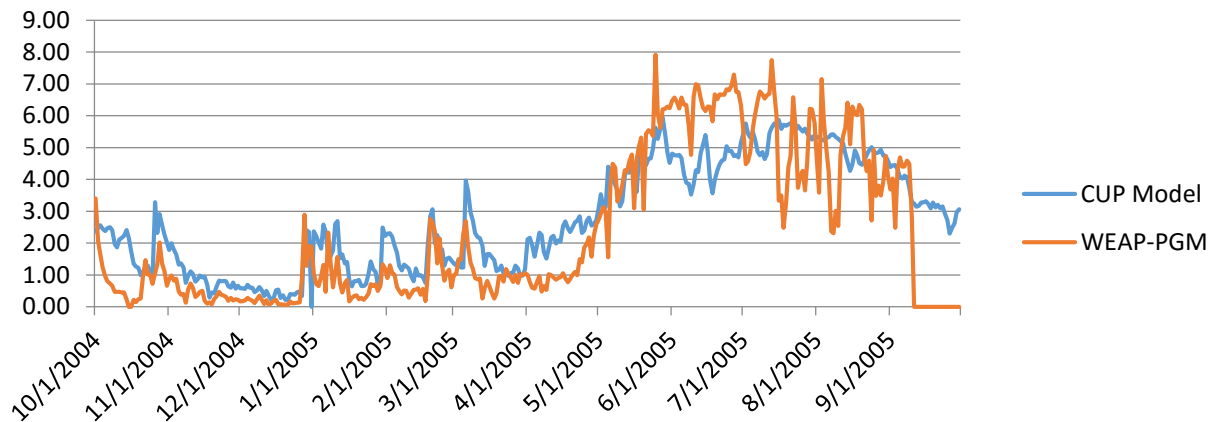
Figure C2-15g. Plots of Daily Evapotranspiration for 19 Crops at the Shafter Location.

6. ET Discussion

Comparison of simulated daily ET from the PGM and CUP models show interesting features. All but 3 of the PGM simulated crops out of 76 (4 locations and 19 crops) have a seasonal ET bias of less than 3 percent in comparison to the CUP values. In the following section potential reasons for these differences will be discussed.

One of the crops that shows a relatively large bias is grain (winter wheat) at the Shafter location. In this case the PGM value is 6.3 precent less than the CUP model. At least some of the reason for this difference is the fact that the PGM predicts less winter time bare soil evaporation then the CUP model. This pattern is seen in nearly all the graphs presented in Figures 2-2 through 2-5. Since a significant portion of the grain growing season is during the winter, when crop cover is low and bare soil evaporation dominates the ET, it is more sensitive to this difference. Analysis of the bias for grain for the other three locations reveals a similar pattern with all three having a negative bias. The discrepancy between the PGM and CUP in winter time bare soil evaporation lies in their different calculation methods and the parameterization of both models. The CUP model is sensitive to the assumed winter time crop coefficient while the PGM is sensitive to assumptions about soil physical parameters and the depth of soil that is subject to bare soil evaporation.

Another crop that shows a relatively large bias is rice at the Davis and Firebaugh locations where the bias was 6.8 percent and 4.5 percent, respectively. The reason for this discrepancy is probably related to differences in how CUP and PGM simulate the evaporation of water from ponded rice paddies. In the CUP model, the evaporation from ponded water is represented by a crop coefficient that incorporates both the plant transpiration and evaporation from the ponded water. In the PGM, the surface is effectively sub-divided into area that is covered by the

transpiring plant and by the area covered in water. The differences between the model evaporation rates has to do with the parameterization of their respective algorithms.

The final crop that has a bias larger than +/-3 percent is tomatoes at the Gerber location (-3.2 percent). As this value is not very different from the acceptable range of +/-3 percent it was felt that no further modification to the PGM calibration parameters was justified.

7. Calibrated Model ET Parameters

The calibrated values of parameters are provided in **Table C2-5**. This table includes all model parameters. The parameters that were calibrated during the exercise described above were:

1. LAI Curve Point 1 [Fraction of growing season]

2. LAI Curve Point 1 [LAI]

3. LAI Curve Point 2 [Fraction of growing season]

4. LAI Curve Point 2 [LAI]

5. Start of LAI Decline [Fraction of HU]

Table C2-5. Plant Growth Model ET parameters.

Crop or Land Cover	Evapotranspiration Parameters: Vapor Pressure Deficit (VPD) Threshold [kPa]	Evapotranspiration Parameters: Value of VPD above Threshold [kPa]	Evapotranspiration Parameters: Fraction of Maximum Stomatal [0-1]	Evapotranspiration Parameters: Maximum Canopy Interception [mm]	Growth Parameters: LAI Curve Point 1 [Fraction of growing season]	Growth Parameters: LAI Curve Point 1 [LAI]	Growth Parameters: LAI Curve Point 2 [Fraction of growing season]	Growth Parameters: LAI Curve Point 2 [LAI]	Growth Parameters: Crop-Specific Base Temperature [C]	Growth Parameters: Optimal Plant Growth Temperature [C]	Growth Parameters: Planting Date Heat Unit Threshold [HU]	Growth Parameters: Heat Units Required for Plant Maturity[HU]	Growth Parameters: Start of LAI Decline [fraction of HU]	Growth Parameters: Slope of RUE-VPD Curve [g/MJ/kPa]	Growth Parameters: Light Extinction Coefficient	Growth Parameters: Biomass Partitioning Parameter 1	Growth Parameters: Biomass Partitioning Parameter 2	Growth Parameters: Maximum Crop Height [m]	Growth Parameters: Maximum Root Depth [m]	CO2-Affected Parameters: Lower CO2 Concentration [ppm]	CO2-Affected Parameters: Higher CO2 Concentration [ppm]	CO2-Affected Parameters: Leaf Area Index (LAI) at Lower CO2	CO2-Affected Parameters: Leaf Area Index (LAI) at Higher CO2	CO2-Affected Parameters: Stomatal Conductance at Lower CO2 [m/s]	CO2-Affected Parameters: Stomatal Conductance at Higher CO2 [m/s]	CO2-Affected Parameters: Radiation Use Efficiency at Lower CO2 [g/MJ]	CO2-Affected Parameters: Radiation Use Efficiency at Higher CO2 [g/MJ]	CO2-Affected Parameters: Increase in Canopy Temperature from Lower to Higher CO2[C]	Yield Parameters: Potential Harvest Index	Yield Parameters: Minimum Value of Harvest Index	Yield Parameters: Harvest Efficiency	Yield Parameters: Residue Decomposition Coefficient	Yield Parameters: Default Management Allowed Depletion[%]
Fallow																																	
Alfalfa Davis	1	4	0.75	0	0.15	0.15	0.4	0.95	6	25	1	700	0.8	10	0.65	0.2	0.2	0.9	2	330	660	4	4.66	0.0055	0.00341	20	27	0.83	0.32	0.32	1	0.05	0.7
Alfalfa Firebaugh	1	4	0.75	0	0.15	0.15	0.4	0.95	6	25	1	700	0.8	10	0.65	0.2	0.2	0.9	2	330	660	4	4.66	0.0055	0.00341	20	27	0.83	0.32	0.32	1	0.05	0.7
Alfalfa Gerber	1	4	0.75	0	0.15	0.15	0.4	0.95	6	25	1	700	0.8	10	0.65	0.2	0.2	0.9	2	330	660	4	4.66	0.0055	0.00341	20	27	0.83	0.32	0.32	1	0.05	0.7
Alfalfa Shafter	1	4	0.75	0	0.15	0.15	0.4	0.95	6	25	1	700	0.8	10	0.65	0.2	0.2	0.9	2	330	660	4	4.66	0.0055	0.00341	20	27	0.83	0.32	0.32	1	0.05	0.7
Pasture Davis	1	4	0.75	0	0.05	0.15	0.45	0.95	12	25	1	100	0.95	10	0.65	0.2	0.2	0.5	2	330	660	4	4.66	0.0055	0.002778	35	40	0.83	0.15	0.15	1	0.05	0.7
Pasture Firebaugh	1	4	0.75	0	0.05	0.15	0.45	0.95	12	25	1	100	0.95	10	0.65	0.2	0.2	0.5	2	330	660	4	4.66	0.0055	0.002778	35	40	0.83	0.15	0.15	1	0.05	0.7
Pasture Gerber	1	4	0.75	0	0.05	0.15	0.45	0.95	12	25	1	100	0.95	10	0.65	0.2	0.2	0.5	2	330	660	4	4.66	0.0055	0.002778	35	40	0.83	0.15	0.15	1	0.05	0.7
Pasture Shafter	1	4	0.75	0	0.05	0.15	0.45	0.95	12	25	1	100	0.95	10	0.65	0.2	0.2	0.5	2	330	660	4	4.66	0.0055	0.002778	35	40	0.83	0.15	0.15	1	0.05	0.7
Corn Davis	0.5	4	0.75	0	0.15	0.2	0.5	0.99	8	25	551.4665	1925	0.8	8	0.65	0.2	0.2	2	0.8	330	660	6	6	0.0024	0.001404	40	45	2.64	0.25	0.1	1	0.05	0.7
Corn Firebaugh	0.5	4	0.75	0	0.15	0.2	0.5	0.99	8	25	551.4665	1925	0.8	8	0.65	0.2	0.2	2	0.8	330	660	6	6	0.0024	0.001404	40	45	2.64	0.25	0.1	1	0.05	0.7
Corn Gerber	0.5	4	0.75	0	0.15	0.2	0.5	0.99	8	25	551.4665	1925	0.8	8	0.65	0.2	0.2	2	0.8	330	660	6	6	0.0024	0.001404	40	45	2.64	0.25	0.1	1	0.05	0.7
Corn Shafter	0.5	4	0.75	0	0.15	0.2	0.5	0.99	8	25	551.4665	1925	0.8	8	0.65	0.2	0.2	2	0.8	330	660	6	6	0.0024	0.001404	40	45	2.64	0.25	0.1	1	0.05	0.7
Corn Silage Davis	0.5	4	0.75	0	0.15	0.1	0.5	0.99	8	25	551.4665	1800	1	7.2	0.65	0.4	0.4	2.5	0.8	330	660	5	5	0.0032	0.001878	39	45	2.64	0.823	0.823	1	0.05	0.7
Corn Silage Firebaugh	0.5	4	0.75	0	0.15	0.1	0.5	0.99	8	25	551.4665	1800	1	7.2	0.65	0.4	0.4	2.5	0.8	330	660	5	5	0.0032	0.001878	39	45	2.64	0.823	0.823	1	0.05	0.7
Corn Silage Gerber	0.5	4	0.75	0	0.15	0.1	0.5	0.99	8	25	551.4665	1800	1	7.2	0.65	0.4	0.4	2.5	0.8	330	660	5	5	0.0032	0.001878	39	45	2.64	0.823	0.823	1	0.05	0.7
Corn Silage Shafter	0.5	4	0.75	0	0.15	0.1	0.5	0.99	8	25	551.4665	1800	1	7.2	0.65	0.4	0.4	2.5	0.8	330	660	5	5	0.0032	0.001878	39	45	2.64	0.823	0.823	1	0.05	0.7
Cotton Davis	1	4	0.3	0	0.1	0.2	0.5	0.95	12.5	27.5	243.8962	1548	0.8	3	0.65	0.4	0.2	1	2.2	330	660	6	7	0.0035	0.002923	25	30	0.83	0.168	0.05	1	0.05	0.7
Cotton Firebaugh	1	4	0.3	0	0.1	0.2	0.5	0.95	12.5	27.5	243.8962	1548	0.8	3	0.65	0.4	0.2	1	2.2	330	660	6	7	0.0035	0.002923	25	30	0.83	0.168	0.05	1	0.05	0.7
Cotton Gerber	1	4	0.3	0	0.1	0.2	0.5	0.95	12.5	27.5	243.8962	1548	0.8	3	0.65	0.4	0.2	1	2.2	330	660	6	7	0.0035	0.002923	25	30	0.83	0.168	0.05	1	0.05	0.7
Cotton Shafter	1	4	0.3	0	0.1	0.2	0.5	0.95	12.5	27.5	243.8962	1548	0.8	3	0.65	0.4	0.2	1	2.2	330	660	6	7	0.0035	0.002923	25	30	0.83	0.168	0.05	1	0.05	0.7
Cucumber Firebaugh	0.5	4	0.75	0	0.15	0.1	0.5	0.95	16	32	296.1935	659	0.9	8	0.65	0.4	0.2	0.5	1.2	330	660	3	3.5	0.0042	0.002814	30	39	0.83	0.12	0.1	1	0.05	0.7

Crop or Land Cover	Evapotranspiration Parameters: Vapor Pressure Deficit (VPD) Threshold [kPa]	Evapotranspiration Parameters: Value of VPD above Threshold [kPa]	Evapotranspiration Parameters: Fraction of Maximum Stomatal [0-1]	Evapotranspiration Parameters: Maximum Canopy Interception [mm]	Growth Parameters: LAI Curve Point 1 [Fraction of growing season]	Growth Parameters: LAI Curve Point 1 [LAI]	Growth Parameters: LAI Curve Point 2 [Fraction of growing season]	Growth Parameters: LAI Curve Point 2 [LAI]	Growth Parameters: Crop-Specific Base Temperature [C]	Growth Parameters: Optimal Plant Growth Temperature [C]	Growth Parameters: Planting Date Heat Unit Threshold [HU]	Growth Parameters: Heat Units Required for Plant Maturity[HU]	Growth Parameters: Start of LAI Decline [fraction of HU]	Growth Parameters: Slope of RUE-VPD Curve [g/MJ/kPa]	Growth Parameters: Light Extinction Coefficient	Growth Parameters: Biomass Partitioning Parameter 1	Growth Parameters: Biomass Partitioning Parameter 2	Growth Parameters: Maximum Crop Height [m]	Growth Parameters: Maximum Root Depth [m]	CO2-Affected Parameters: Lower CO2 Concentration [ppm]	CO2-Affected Parameters: Higher CO2 Concentration [ppm]	CO2-Affected Parameters: Leaf Area Index (LAI) at Lower CO2	CO2-Affected Parameters: Leaf Area Index (LAI) at Higher CO2	CO2-Affected Parameters: Stomatal Conductance at Lower CO2 [m/s]	CO2-Affected Parameters: Stomatal Conductance at Higher CO2 [m/s]	CO2-Affected Parameters: Radiation Use Efficiency at Lower CO2 [g/MJ]	CO2-Affected Parameters: Radiation Use Efficiency at Higher CO2 [g/MJ]	CO2-Affected Parameters: Increase in Canopy Temperature from Lower to Higher CO2[C]	Yield Parameters: Potential Harvest Index	Yield Parameters: Minimum Value of Harvest Index	Yield Parameters: Harvest Efficiency	Yield Parameters: Residue Decomposition Coefficient	Yield Parameters: Default Management Allowed Depletion[%]
Cucumber Gerber	0.5	4	0.75	0	0.15	0.1	0.5	0.95	16	32	296.1935	659	0.9	8	0.65	0.4	0.2	0.5	1.2	330	660	3	3.5	0.0042	0.002814	30	39	0.83	0.12	0.1	1	0.05	0.7
Cucumber Shafter	0.5	4	0.75	0	0.15	0.1	0.5	0.95	16	32	296.1935	659	0.9	8	0.65	0.4	0.2	0.5	1.2	330	660	3	3.5	0.0042	0.002814	30	39	0.83	0.12	0.1	1	0.05	0.7
Cucumbers Davis	0.5	4	0.75	0	0.15	0.1	0.5	0.95	16	32	296.1935	659	0.9	8	0.65	0.4	0.2	0.5	1.2	330	660	3	3.5	0.0042	0.002814	30	39	0.83	0.12	0.1	1	0.05	0.7
Dry Beans Davis	0.5	4	0.75	0	0.2	0.05	0.5	0.85	10	27	298.3467	1378	0.85	5	0.65	0.4	0.2	0.6	1.1	330	660	2	2.33	0.0081	0.005022	25	34	0.83	0.14	0.1	1	0.05	0.7
Dry Beans Firebaugh	0.5	4	0.75	0	0.2	0.05	0.5	0.85	10	27	298.3467	1378	0.85	5	0.65	0.4	0.2	0.6	1.1	330	660	2	2.33	0.0081	0.005022	25	34	0.83	0.14	0.1	1	0.05	0.7
Dry Beans Gerber	0.5	4	0.75	0	0.2	0.05	0.5	0.85	10	27	298.3467	1378	0.85	5	0.65	0.4	0.2	0.6	1.1	330	660	2	2.33	0.0081	0.005022	25	34	0.83	0.14	0.1	1	0.05	0.7
Dry Beans Shafter	0.5	4	0.75	0	0.2	0.05	0.5	0.85	10	27	298.3467	1378	0.85	5	0.65	0.4	0.2	0.6	1.1	330	660	2	2.33	0.0081	0.005022	25	34	0.83	0.14	0.1	1	0.05	0.7
Fallow_Test																																	
Fresh Tomato Davis	0.5	4	0.75	0	0.15	0.15	0.5	0.95	10	27	272.261	1277	0.8	8	0.65	0.4	0.2	0.8	1.5	330	660	3	3.5	0.0064	0.004288	30	41	0.83	0.105	0.05	1	0.05	0.7
Fresh Tomato Firebaugh	0.5	4	0.75	0	0.15	0.15	0.5	0.95	10	27	272.261	1277	0.8	8	0.65	0.4	0.2	0.8	1.5	330	660	3	3.5	0.0064	0.004288	30	41	0.83	0.105	0.05	1	0.05	0.7
Fresh Tomato Gerber	0.5	4	0.75	0	0.15	0.15	0.5	0.95	10	27	272.261	1277	0.8	8	0.65	0.4	0.2	0.8	1.5	330	660	3	3.5	0.0064	0.004288	30	41	0.83	0.105	0.05	1	0.05	0.7
Fresh Tomato Shafter	0.5	4	0.75	0	0.15	0.15	0.5	0.95	10	27	272.261	1277	0.8	8	0.65	0.4	0.2	0.8	1.5	330	660	3	3.5	0.0064	0.004288	30	41	0.83	0.105	0.05	1	0.05	0.7
Lettuce Firebaugh	0.5	4	0.75	0	0.25	0.23	0.4	0.86	7	18	509.7799	1862	1	8	0.65	0.4	0.2	0.2	0.6	330	660	4.2	4.9	0.0042	0.002814	23	25	0.83	0.245	0.01	1	0.05	0.7
Lettuce Shafter	0.5	4	0.75	0	0.25	0.23	0.4	0.86	7	18	509.7799	1862	1	8	0.65	0.4	0.2	0.2	0.6	330	660	4.2	4.9	0.0042	0.002814	23	25	0.83	0.245	0.01	1	0.05	0.7
Onion Garlic Davis	1	4	0.75	0	0.05	0.2	0.4	0.95	2	19	4901.605	2555	0.95	10	0.65	0.4	0.6	0.5	0.6	330	660	1.5	1.75	0.0095	0.006365	30	35	0.83	0.265	0.15	1	0.05	0.7
Onion Garlic Firebaugh	1	4	0.75	0	0.05	0.2	0.4	0.95	2	19	4901.605	2555	0.95	10	0.65	0.4	0.6	0.5	0.6	330	660	1.5	1.75	0.0095	0.006365	30	35	0.83	0.265	0.15	1	0.05	0.7
Onion Garlic Gerber	1	4	0.75	0	0.05	0.2	0.4	0.95	2	19	4901.605	2555	0.95	10	0.65	0.4	0.6	0.5	0.6	330	660	1.5	1.75	0.0095	0.006365	30	35	0.83	0.265	0.15	1	0.05	0.7
Onion Garlic Shafter	1	4	0.75	0	0.05	0.2	0.4	0.95	2	19	4901.605	2555	0.95	10	0.65	0.4	0.6	0.5	0.6	330	660	1.5	1.75	0.0095	0.006365	30	35	0.83	0.265	0.15	1	0.05	0.7
Potato Davis	1	4	0.75	0	0.05	0.15	0.4	0.95	5	22	118.6567	2185	0.8	14.8	0.65	0.4	0.9	0.6	0.6	330	660	5	5.82	0.0047	0.002604	25	30	0.83	0.23	0.23	1	0.05	0.7
Potato Firebaugh	1	4	0.75	0	0.05	0.15	0.4	0.95	5	22	118.6567	2185	0.8	14.8	0.65	0.4	0.9	0.6	0.6	330	660	5	5.82	0.0047	0.002604	25	30	0.83	0.23	0.23	1	0.05	0.7
Potato Gerber	1	4	0.75	0	0.05	0.15	0.4	0.95	5	22	118.6567	2185	0.8	14.8	0.65	0.4	0.9	0.6	0.6	330	660	5	5.82	0.0047	0.002604	25	30	0.83	0.23	0.23	1	0.05	0.7
Potato Shafter	1	4	0.75	0	0.05	0.15	0.4	0.95	5	22	118.6567	2185	0.8	14.8	0.65	0.4	0.9	0.6	0.6	330	660	5	5.82	0.0047	0.002604	25	30	0.83	0.23	0.23	1	0.05	0.7
Processed Tomato Davis	1	4	0.75	0	0.15	0.1	0.4	0.95	10	22	272.261	1277	0.9	8	0.65	0.2	0.1	0.5	2	330	660	3	3.5	0.0057	0.003819	30	39	0.83	0.195	0.15	1	0.05	0.7
Processed Tomato Firebaugh	1	4	0.75	0	0.15	0.1	0.4	0.95	10	22	272.261	1277	0.9	8	0.65	0.2	0.1	0.5	2	330	660	3	3.5	0.0057	0.003819	30	39	0.83	0.195	0.15	1	0.05	0.7

Crop or Land Cover	Evapotranspiration Parameters: Vapor Pressure Deficit (VPD) Threshold [kPa]	Evapotranspiration Parameters: Value of VPD above Threshold [kPa]	Evapotranspiration Parameters: Fraction of Maximum Stomatal [0-1]	Evapotranspiration Parameters: Maximum Canopy Interception [mm]	Growth Parameters: LAI Curve Point 1 [Fraction of growing season]	Growth Parameters: LAI Curve Point 1 [LAI]	Growth Parameters: LAI Curve Point 2 [Fraction of growing season]	Growth Parameters: LAI Curve Point 2 [LAI]	Growth Parameters: Crop-Specific Base Temperature [C]	Growth Parameters: Optimal Plant Growth Temperature [C]	Growth Parameters: Planting Date Heat Unit Threshold [HU]	Growth Parameters: Heat Units Required for Plant Maturity[HU]	Growth Parameters: Start of LAI Decline [fraction of HU]	Growth Parameters: Slope of RUE-VPD Curve [g/MJ/kPa]	Growth Parameters: Light Extinction Coefficient	Growth Parameters: Biomass Partitioning Parameter 1	Growth Parameters: Biomass Partitioning Parameter 2	Growth Parameters: Maximum Crop Height [m]	Growth Parameters: Maximum Root Depth [m]	CO2-Affected Parameters: Lower CO2 Concentration [ppm]	CO2-Affected Parameters: Higher CO2 Concentration [ppm]	CO2-Affected Parameters: Leaf Area Index (LAI) at Lower CO2	CO2-Affected Parameters: Leaf Area Index (LAI) at Higher CO2	CO2-Affected Parameters: Stomatal Conductance at Lower CO2 [m/s]	CO2-Affected Parameters: Stomatal Conductance at Higher CO2 [m/s]	CO2-Affected Parameters: Radiation Use Efficiency at Lower CO2 [g/MJ]	CO2-Affected Parameters: Radiation Use Efficiency at Higher CO2 [g/MJ]	CO2-Affected Parameters: Increase in Canopy Temperature from Lower to Higher CO2[C]	Yield Parameters: Potential Harvest Index	Yield Parameters: Minimum Value of Harvest Index	Yield Parameters: Harvest Efficiency	Yield Parameters: Residue Decomposition Coefficient	Yield Parameters: Default Management Allowed Depletion[%]
Processed Tomato Gerber	1	4	0.75	0	0.15	0.1	0.4	0.95	10	22	272.261	1277	0.9	8	0.65	0.2	0.1	0.5	2	330	660	3	3.5	0.0057	0.003819	30	39	0.83	0.195	0.15	1	0.05	0.7
Processed Tomato Shafter	1	4	0.75	0	0.15	0.1	0.4	0.95	10	22	272.261	1277	0.9	8	0.65	0.2	0.1	0.5	2	330	660	3	3.5	0.0057	0.003819	30	39	0.83	0.195	0.15	1	0.05	0.7
Safflower Davis	0.5	4	0.75	0	0.15	0.25	0.4	0.95	4	25	189.6784	2174	0.65	32.3	0.9	0.4	0.2	2.5	2	330	660	3	3.5	0.0061	0.003379	26	33	0.83	0.265	0.1	1	0.05	0.7
Safflower Firebaugh	0.5	4	0.75	0	0.15	0.25	0.4	0.95	4	25	189.6784	2174	0.65	32.3	0.9	0.4	0.2	2.5	2	330	660	3	3.5	0.0061	0.003379	26	33	0.83	0.265	0.1	1	0.05	0.7
Safflower Gerber	0.5	4	0.75	0	0.15	0.25	0.4	0.95	4	25	189.6784	2174	0.65	32.3	0.9	0.4	0.2	2.5	2	330	660	3	3.5	0.0061	0.003379	26	33	0.83	0.265	0.1	1	0.05	0.7
Safflower Shafter	0.5	4	0.75	0	0.15	0.25	0.4	0.95	4	25	189.6784	2174	0.65	32.3	0.9	0.4	0.2	2.5	2	330	660	3	3.5	0.0061	0.003379	26	33	0.83	0.265	0.1	1	0.05	0.7
Sugar Beet Davis	1	4	0.75	0	0.05	0.2	0.7	0.99	4	18	138.789	2361	0.99	10	0.65	0.4	0.6	1.2	2	330	660	5.5	6.41	0.0038	0.002546	30	35	0.83	0.27	0.15	1	0.05	0.7
Sugar Beet Firebaugh	1	4	0.75	0	0.05	0.2	0.7	0.99	4	18	138.789	2361	0.99	10	0.65	0.4	0.6	1.2	2	330	660	5.5	6.41	0.0038	0.002546	30	35	0.83	0.27	0.15	1	0.05	0.7
Sugar Beet Gerber	1	4	0.75	0	0.05	0.2	0.7	0.99	4	18	138.789	2361	0.99	10	0.65	0.4	0.6	1.2	2	330	660	5.5	6.41	0.0038	0.002546	30	35	0.83	0.27	0.15	1	0.05	0.7
Sugar Beet Shafter	1	4	0.75	0	0.05	0.2	0.7	0.99	4	18	138.789	2361	0.99	10	0.65	0.4	0.6	1.2	2	330	660	5.5	6.41	0.0038	0.002546	30	35	0.83	0.27	0.15	1	0.05	0.7
Winter Wheat Davis	0.5	4	0.75	0	0.05	0.15	0.45	0.95	0	18	5682.972	2024	0.8	6	0.65	0.4	0.2	0.9	1.3	330	660	4	4.66	0.0054	0.002727	30	39	0.83	0.245	0.15	1	0.05	0.7
Winter Wheat Firebaugh	0.5	4	0.75	0	0.05	0.15	0.45	0.95	0	18	5682.972	2024	0.8	6	0.65	0.4	0.2	0.9	1.3	330	660	4	4.66	0.0054	0.002727	30	39	0.83	0.245	0.15	1	0.05	0.7
Winter Wheat Gerber	0.5	4	0.75	0	0.05	0.15	0.45	0.95	0	18	5682.972	2024	0.8	6	0.65	0.4	0.2	0.9	1.3	330	660	4	4.66	0.0054	0.002727	30	39	0.83	0.245	0.15	1	0.05	0.7
Winter Wheat Shafter	0.5	4	0.75	0	0.05	0.15	0.45	0.95	0	18	5682.972	2024	0.8	6	0.65	0.4	0.2	0.9	1.3	330	660	4	4.66	0.0054	0.002727	30	39	0.83	0.245	0.15	1	0.05	0.7
Almond Davis	2.5	4	0.75	0	0.05	0.2	0.2	0.99	6	27	229	3105	0.9	8	0.61	0.2	0.2	6	0.8	330	660	4	4	0.00305	0.002092	16.1	18	0.83	0.053	0.01	1	0.05	0.3
Almond Firebaugh	2.5	4	0.75	0	0.05	0.2	0.2	0.99	6	27	229	3105	0.9	8	0.61	0.2	0.2	6	0.8	330	660	4	4	0.00305	0.002092	16.1	18	0.83	0.053	0.01	1	0.05	0.3
Almond Gerber	2.5	4	0.75	0	0.05	0.2	0.2	0.99	6	27	229	3105	0.9	8	0.61	0.2	0.2	6	0.8	330	660	4	4	0.00305	0.002092	16.1	18	0.83	0.053	0.01	1	0.05	0.3
Almond Shafter	2.5	4	0.75	0	0.05	0.2	0.2	0.99	6	27	229	3105	0.9	8	0.61	0.2	0.2	6	0.8	330	660	4	4	0.00305	0.002092	16.1	18	0.83	0.053	0.01	1	0.05	0.3
Apple Firebaugh	0.5	4	0.75	0	0.01	0.25	0.4	0.99	7	25	240.5171	2832	0.8	3	0.65	0.2	0.2	3.5	2	330	660	3	3	0.005	0.00345	15	20	0.83	0.225	0.1	1	0.05	0.3
Apple Gerber	0.5	4	0.75	0	0.01	0.25	0.4	0.99	7	25	240.5171	2832	0.8	3	0.65	0.2	0.2	3.5	2	330	660	3	3	0.005	0.00345	15	20	0.83	0.225	0.1	1	0.05	0.3
Apple Shafter	0.5	4	0.75	0	0.01	0.25	0.4	0.99	7	25	240.5171	2832	0.8	3	0.65	0.2	0.2	3.5	2	330	660	3	3	0.005	0.00345	15	20	0.83	0.225	0.1	1	0.05	0.3
Apples Davis	0.5	4	0.75	0	0.01	0.25	0.4	0.99	7	25	240.5171	2832	0.8	3	0.65	0.2	0.2	3.5	2	330	660	3	3	0.005	0.00345	15	20	0.83	0.225	0.1	1	0.05	0.3
Forest	1	4	0.75	3	0.05	0.05	0.4	0.95	8	30	1	3000	0.99	8	0.65	0.2	0.2	6	1	330	660	6	6	0.002	0.002	16	16	0.83	0.02	0.01	1	0.05	0.7
Non-Forest	1	4	0.75	2	0.05	0.05	0.4	0.95	8	30	1	3000	0.99	8	0.65	0.2	0.2	1	1	330	660	6	6	0.002	0.002	16	16	0.83	0.02	0.01	1	0.05	0.7

Crop or Land Cover	Evapotranspiration Parameters: Vapor Pressure Deficit (VPD) Threshold [kPa]	Evapotranspiration Parameters: Value of VPD above Threshold [kPa]	Evapotranspiration Parameters: Fraction of Maximum Stomatal [0-1]	Evapotranspiration Parameters: Maximum Canopy Interception [mm]	Growth Parameters: LAI Curve Point 1 [Fraction of growing season]	Growth Parameters: LAI Curve Point 1 [LAI]	Growth Parameters: LAI Curve Point 2 [Fraction of growing season]	Growth Parameters: LAI Curve Point 2 [LAI]	Growth Parameters: Crop-Specific Base Temperature [C]	Growth Parameters: Optimal Plant Growth Temperature [C]	Growth Parameters: Planting Date Heat Unit Threshold [HU]	Growth Parameters: Heat Units Required for Plant Maturity [HU]	Growth Parameters: Start of LAI Decline [fraction of HU]	Growth Parameters: Slope of RUE-VPD Curve [g/MJ/kPa]	Growth Parameters: Light Extinction Coefficient	Growth Parameters: Biomass Partitioning Parameter 1	Growth Parameters: Biomass Partitioning Parameter 2	Growth Parameters: Maximum Crop Height [m]	Growth Parameters: Maximum Root Depth [m]	CO_2-Affected Parameters: Lower CO_2 Concentration [ppm]	CO_2-Affected Parameters: Higher CO_2 Concentration [ppm]	CO_2-Affected Parameters: Leaf Area Index (LAI) at Lower CO_2	CO_2-Affected Parameters: Leaf Area Index (LAI) at Higher CO_2	CO_2-Affected Parameters: Stomatal Conductance at Lower CO_2 [m/s]	CO_2-Affected Parameters: Stomatal Conductance at Higher CO_2 [m/s]	CO_2-Affected Parameters: Radiation Use Efficiency at Lower CO_2 [g/MJ]	CO_2-Affected Parameters: Radiation Use Efficiency at Higher CO_2 [g/MJ]	CO_2-Affected Parameters: Increase in Canopy Temperature from Lower to Higher CO_2 [C]	Yield Parameters: Potential Harvest Index	Yield Parameters: Minimum Value of Harvest Index	Yield Parameters: Harvest Efficiency	Yield Parameters: Residue Decomposition Coefficient	Yield Parameters: Default Management Allowed Depletion [%]
Vineyard Davis	1	1.5	0.75	0	0.1	0.15	0.5	0.99	8	30	279.2122	2322	0.5	8	0.65	0.2	0.2	2	2	330	660	4	4	0.005	0.0042	30	40	0.83	0.068	0.04	1	0.05	0.3
Vineyard Firebaugh	1	1.5	0.75	0	0.1	0.15	0.5	0.99	8	30	279.2122	2322	0.5	8	0.65	0.2	0.2	2	2	330	660	4	4	0.005	0.0042	30	40	0.83	0.068	0.04	1	0.05	0.3
Vineyard Gerber	1	1.5	0.75	0	0.1	0.15	0.5	0.99	8	30	279.2122	2322	0.5	8	0.65	0.2	0.2	2	2	330	660	4	4	0.005	0.0042	30	40	0.83	0.068	0.04	1	0.05	0.3
Vineyard Shafter	1	1.5	0.75	0	0.1	0.15	0.5	0.99	8	30	279.2122	2322	0.5	8	0.65	0.2	0.2	2	2	330	660	4	4	0.005	0.0042	30	40	0.83	0.068	0.04	1	0.05	0.3
Citrus Firebaugh	1	4	0.75	0					7	20	0	3600		3	0.65	0.2	0.2	3.5	2	330	660	1.6		0.0052	0.003567	15	20	0.83	0.131	0.05	1	0.05	0.3
Citrus Shafter	1	4	0.75	0					7	20	0	3600		3	0.65	0.2	0.2	3.5	2	330	660	1.6		0.0052	0.003567	15	20	0.83	0.131	0.05	1	0.05	0.3
Olive Davis	1	2	0.75	0					10	30	0	2600		8	0.61	0.2	0.2	6	3.5	330	660	2		0.0055	0.003795	16.1	18	0.83	0.058	0.01	1	0.05	0.3
Olive Gerber	1	2	0.75	0					10	30	0	2600		8	0.61	0.2	0.2	6	3.5	330	660	2		0.0055	0.003795	16.1	18	0.83	0.058	0.01	1	0.05	0.3
Rice Davis	0.5	4	0.75	0	0.3	0.2	0.6	0.99	10	25	390.9297	1657	0.99	5	0.35	0.4	0.2	0.8	0.9	330	660	4	4.62	0.005	0.0025	30	39	0.83	0.4	0.3	1	0.05	0.7
Rice Firebaugh	0.5	4	0.75	0	0.3	0.2	0.6	0.99	10	25	390.9297	1657	0.99	5	0.35	0.4	0.2	0.8	0.9	330	660	4	4.62	0.005	0.0025	30	39	0.83	0.4	0.3	1	0.05	0.7
Rice Gerber	0.5	4	0.75	0	0.3	0.2	0.6	0.99	10	25	390.9297	1657	0.99	5	0.35	0.4	0.2	0.8	0.9	330	660	4	4.62	0.005	0.0025	30	39	0.83	0.4	0.3	1	0.05	0.7
Rice Shafter	0.5	4	0.75	0	0.3	0.2	0.6	0.99	10	25	390.9297	1657	0.99	5	0.35	0.4	0.2	0.8	0.9	330	660	4	4.62	0.005	0.0025	30	39	0.83	0.4	0.3	1	0.05	0.7

8. Crop Yield Calibration

A calibration of crop yields was also performed for the 20 DWR crop groups. The calibration was performed by selecting a representative crop for each of the crop groups. The crops used in the PGM calibration for each group are presented in **Table C2-6**.

Table C2-6. Crop groups and calibrated crops.

DWR Crop Group	DWR Group Abbreviation	PGM Representative Calibration Crop
Alfalfa	ALFAL	Alfalfa
Almonds & Pistaschios	ALPIS	Almonds
OtherDeciduous	OTHDEC	Apples
Subtropical - Sacramento Valley	SUBTRP	Olives
Subtropical – San Joaquin Valley & Tulare Lake	SUBTRP	Citrus
Corn	CORN	Corn
Other field	OTHFLD	Corn Sileage
Cotton	COTTN	Cotton
Cucurbits	CUCUR	Melons
Dry Beans	DRYBN	Dry Beans
Fresh Tomatoes	FRTOM	Tomatoes
Other Truck - Sacramento Valley	OTHTRK	Cucumbers
Other Truck – San Joaquin Valley & Tulare Lake	OTHTRK	Lettuce
Onions & Garlic	ONGAR	Onion & Garlic
Pasture	PASTR	Pasture
Potatoes	POTATO	Potatoes
Processed tomatoes	PRTOM	Tomatoes
Rice	RICE	Rice

DWR Crop Group	DWR Group Abbreviation	PGM Representative Calibration Crop
Safflower	SAFLR	Safflower
Sugar Beets	SBEET	SugarBeets
Vineyards	VINE	Vineyards
Grains	GRAIN	Winter wheat

9. Crop Yield Calibration Approach

The calibration was done using observed CIMIS measured during the 1997 calender year at the same four CIMIS stations used in the ET calibration described above. The calibration target yields were based on values obtained from the State Wide Agricultural Planning (SWAP) model (Howitt et al. 2012) and County Agricultural Commissioner Reports (http://www.cdfa.ca.gov/).

The crop yield calibration was performed after the calibration of the ET parameters as described above. It was accomplished by adjusting the potential and minimum Harvest Index parameters (see Appendix D) until a reasonable agreement was obtained with the values reported values. The results are presented in Table C2-7.

Table C2-7 Crop Yield Calibration Results

Location	Gerber	Davis	Firebaugh	Shafter
Crop Group	Yield	Yield	Yield	Yield
	Short Tons / Acre (Dry Weight)			
ALFAL	4.40	4.52	5.56	5.54
ALPIS	0.79	0.82	1.17	1.07
OTHDEC	2.51	2.50	2.55	3.23
SUBTRP	1.66	1.67	1.67	1.64
CORN	4.56	4.16	4.00	3.95
OTHFLD	12.18	12.59	12.33	11.94

Location	Gerber	Davis	Firebaugh	Shafter
Crop Group	Yield	Yield	Yield	Yield
	Short Tons / Acre (Dry Weight)			
COTTN	2.20	2.20	2.73	2.61
CUCUR	1.68	1.69	3.06	3.57
DRYBN	0.88	0.92	1.15	1.30
FRTOM	0.79	0.78	0.77	0.77
OTHTRK	0.57	0.58	0.58	0.71
ONGAR	3.41	3.25	3.33	2.75
PASTR	0.79	0.30	2.25	2.19
POTATO	4.62	4.67	4.64	4.78
PRTOM	2.03	2.05	2.28	2.35
RICE	3.28	3.31	3.17	3.14
SAFLR	1.05	1.08	0.44	0.46
SBEET	6.44	6.48	6.00	6.66
VINE	1.33	1.34	1.52	1.69

In general, the calibrated yields were in very close agreement with the reported values. An example of the calibration results at the Davis location is presented presented on Figure C2-16.
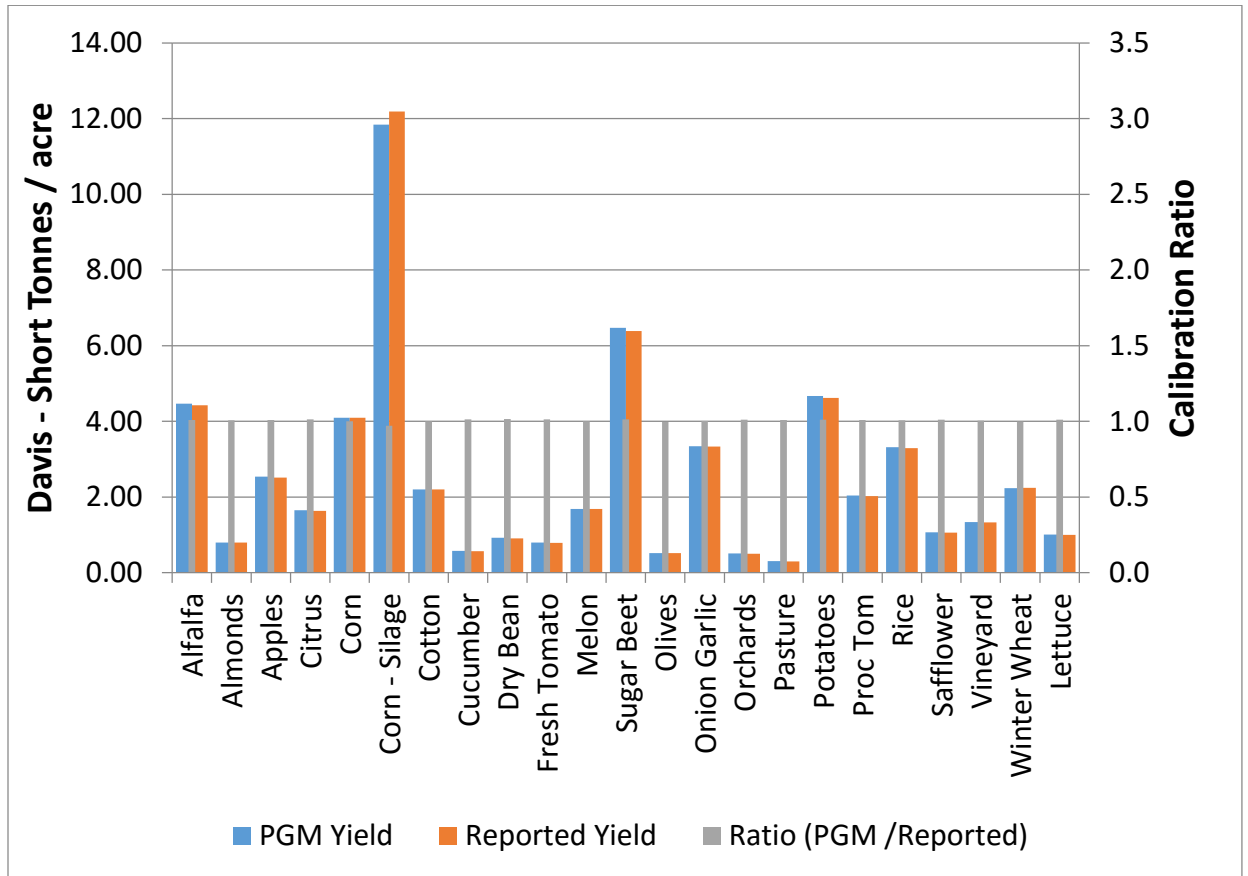
Figure C2-16. Comparison of Calibrated and Reported Crop Yields at the Davis Location.

References

Ainsworth, E.A. and S.P. Long. 2005. What we have learned from 15 years of free-air CO2 enrichment (FACE)? A meta-analytic review of the responses of photosynthesis, canopy properties and plant production to rising CO2. New Phytologist, 154(351-372).

Allen, R.G., L.S. Pereira, D. Raes, and M. Smith. 1998. Crop Evapotranspiration: Guidelines for Computing Crop Water Requirements. FAO Irrigation and Drainage Paper 56, Rome.

Allen, R.G., W.O. Pruitt, D. Raes, M. Smith, and L.S. Pereira. 2005. Estimating Evaporation from Bare Soil and the Crop Coefficient for the Initial Period Using Common Soils Information. Journal of Irrigation and Drainage Engineering. ASCE, 131(1): 14-23.

ASCE-EWRI (Environmental and Water Resources Institute of the American Society of Civil Engineers). 2005. The ASCE Standardized Reference Evapotranspiration Equation, Report 0-7844-0805-X, ASCE Task Committee on Standardization of Reference Evapotranspiration, Reston,

Virginia., American Soc. Civil Engineers. Available at http://www.kimberly.uidaho.edu/water/asceewri/

Bloom, A.J. 2006. Perspective: Rising carbon dioxide concentrations and the future of crop production. Journal of the Science of Food and Agriculture, 86(1289-1291).

Bloom, A.J., M. Burger, J.S.R. Asensio, A.B. Cousins. 2010. Carbon dioxide enrichment inhibits nitrate assimilation in wheat and Arabidopsis. Science 328(899-903).

Consoli S., N. O'Connell, and R. Snyder. 2006. Estimation of Evapotranspiration of Different-Sized Navel-Orange Tree Orchards Using Energy Balance. Journal of Irrigation and Drainage Engineering. ASCE, 132(1): 2-8.

Cooperative Extension, University of California. 1989. Using Reference Evapotranspiration and Crop Coefficients to Estimate Crop Evapotranspiration for Agronomic Crops, Grasses, and Vegetable Crops. Leaflet 21427. Division of Agriculture and Natural Resources, Davis, California.

Cooperative Extension, University of California. 1994. Using Reference Evapotranspiration and Crop Coefficients to Estimate Crop Evapotranspiration for Trees and Vines. Leaflet 21428. Division of Agriculture and Natural Resources, Davis, California.

Doorenboos, J and W.O. Pruitt. 1977. Guidelines for Predicting Crop Water Requirements. FAO Irrigation and Drainage Paper 24, Rome.

DWR. 1975. Vegetative Water Use in California. Bulletin 113-3. California Department of Water Resources, Sacramento, California. April.

———. 1976. Estimation of Monthly Crop Evapotranspiration for the Central Valley Hydrology Study. Internal Memorandum prepared by N. A. MacGillivray, San Joaquin District, California Department of Water Resources, Sacramento, California. November 3.

———. 1986. Crop Water Use in California. Bulletin 113-4. California Department of Water Resources, Sacramento, California. April.

———. 2010. Integrated Scenario Analysis for the 2009 California Water Plan Update. California Department of Water Resources, Sacramento, California. February. Available at: http://www.waterplan.water.ca.gov/cwpu2009/index.cfm. Accessed January, 2013.

Fereres E., and I. Puech. 1981. Irrigation Scheduling Guide. California Department of Water Resources, Sacramento, California.

Hansen, B.R. and D.M. May. 2006. New Crop Coefficients Developed for High-Yield Processing Tomatoes. California Agriculture, 60(2): 95-99.

Available at: http://ucce.ucdavis.edu/files/repositoryfiles/ca6002p95-69246.pdf. Accessed January, 2013.

Hatfield, J.L. 2008. The effects of climate change on agriculture, land resources, water resources and biodiversity. U.S. Climate Change Science Program: Synthesis and Assessment Product 4.3.

Howitt R.E., J. Medellín-Azuara, D. MacEwan, and J.R. Lund. 2012. Calibrating disaggregate economic models of agricultural production and water management. Environmental Modelling & Software 38: 244-258

Huntington, T.G. 2004. Climate change, growing season length, and transpiration: Plant response could alter hydrologic regime. Plant Biology, 6(651-653).

ITRC. 2002. Evaporation from Irrigated Agricultural Land in California. ITRC Report 02 – 001. Irrigation Training and Research Center, California Polytechnic State University, San Luis Obispo, California. January. Available at: http://www.itrc.org/reports/index.php. Accessed January, 2013.

———. 2003. California Crop and Soil Evapotranspiration for Water Balances and Irrigation Scheduling/Design. ITRC Report 03 – 001. Irrigation Training and Research Center, California Polytechnic State University, San Luis Obispo, California. January. Available at: http://www.itrc.org/reports/index.php. Accessed January, 2013.

Jones, D.W., R.L. Snyder, S. Eching, and H. Gomez-McPherson. 1999. California Irrigation Management Information System Reference Evapotranspiration Climate Zone Map. California Department of Water Resources, Sacramento, California. Available at: http://wwwcimis.water.ca.gov/cimis/images/etomap.jpg. Accessed January, 2013.

Kimball, B.A., K. Kobayashi, and M. Bindi. 2002. Responses of agricultural crops to Free-Air CO_2 Enrichment. Advances in Agronomy, 77(293-368).

Kimball, B.A. 2010. Lessons from FACE: CO_2 effects and interactions with water, nitrogen and temperature. Chapter 5 in "Handbook of Climate Change and Agroecosystems." Daniel Hillel and Cynthia Rosenzweig eds.

Long, S.P., E.A. Ainsworth, A.D.B. Leakey, J.Nosberger, and D.R. Ort. 2006. Food for thought: Lower-than-expected crop yield stimulation with rising CO_2 concentrations. Science, 312(1918 – 1921).

Maidment, D.R (Ed). 1993. Handbook of Hydrology. McGraw-Hill, New York, New York.

Neitsch, S.L., J.G. Arnold, J.R. Kiniry, and J.R. Williams. 2005. Soil and Water Assessment Tool Theoretical Documentation: Version 2005. http://www.brc.tamus.edu/swat/doc.html

Orang, M.N. 2013. Personal communication. Senior Engineer. California Department of Water Resources. September 18.

Orang, M.N., S.J. Matyac, and R.L.Snyder. 2004. Consumptive Use Program (CUP) Model. Acta Horticulturae. International Society for Horticultural Science. 664:461-468. Available at: http://www.actahort.org/books/664/664_58.htm. Accessed January 2013.

Orang, M.N., R.L.Snyder, S. Geng, Q.J. Hart, S. Sarreshteh, M. Falk, D. Beaudette, S. Hayes, and S. Eching. 2013. California Simulation of Evapotranspiration of Applied Water and Agricultural Energy Use in California. Journal of Integrative Agriculture: 12(13): 1371-1388. Available at: http://www.water.ca.gov/landwateruse/models/Cal-SIMETAW.pdf. Accessed December 2013.

Phene C.J., R.L. McCormick, and J.M. Miyamoto. 1985. Evapotranspiration and Crop Coefficient of Trickle Irrigated Tomatoes. Proceedings of the Third International Drip/Trickle Irrigation Congress, Nov. 18–21, 1985. Fresno, California.

PRISM. 2013. PRISM Climate Group, Oregon State University, Corvalis, Oregon. http://prism.oregonstate.edu. Accessed January 2013.

Rayej, M., R. Snyder, M. Orang, S. Geng, and S. Sarreshteh. 2011. CALSIMETAW and WEAP Models for Water Demand Planning. ICID 21st International Congress on Irrigation and Drainage. 15-23 October 2011, Tehran.

Sanden, B., P. Brown, R. Snyder. 2012. New Insights on Water Management in Almonds. Regulatory Issues Impacting California Agriculture. Visalia, California 7-8 February, 2012 Proceedings: American Society of Agronomy. 88-93. Available at: http://ucanr.org/sites/scri/files/140103.pdf. Accessed January, 2013.

Snyder, R.L, K. Bali, F. Ventura, and H. Gomez-MacPherson. 2000. Estimating Evaporation from Bare or Nearly Bare Soil. Journal of Irrigation and Drainage Engineering. ASCE, 126(6): 399-403. Available at: http://biomet.ucdavis.edu/Evapotranspiration. Accessed January, 2013.

Snyder, R., M. Orang, S. Geng, S. Matyac and S. Sarreshteh. 2005. SIMETAW (Simulation of Evapotranspiration of Applied Water). California Water Plan Update 2005. Available at: http://www.waterplan.water.ca.gov/docs/cwpu2005/vol4/vol4-cropwateruse-simetaw.pdf. Accessed January, 2013.

Snyder, R.L., M. Orang, S. Matyac, and S. Eching. 2007. Crop Coefficients. Available at: http://biomet.ucdavis.edu/Evapotranspiration. Accessed January, 2013.

Snyder, R.L., M. Orang, K. Bali, and S. Eching. 2009. Basic Irrigation Scheduling. Available at:

http://biomet.ucdavis.edu/irrigation_scheduling/bis/BIS.htm. Accessed January, 2013.

Schwankl L., L. Prichard, B.R. Hanson, and R.B. Elkins. 2007. Understanding your Orchard's water Requirements. Reducing Runoff from Irrigated Lands. Publication 8212. Division of Agriculture and Natural Resources, University of California, Davis. Available at: http://ucanr.edu/News/Healthy_crops,_safe_water/Publications_809/. Accessed January 2013.

UC Davis. 2013. Crop Current Cost and Return Studies. Department of Agricultural and Resource Economics, University of California, at Davis. Available at: http://coststudies.ucdavis.edu/current.php. Accessed January 2013.

USDA. 2010. Usual Planting and Harvest Dates for U.S. Field Crops. Agricultural Handbook Number 628. National Agricultural Statistics Service, U.S. Department of Agriculture. October. Available at: http://usda01.library.cornell.edu/usda/current/planting/planting-10-29-2010.pdf. Accessed January 2013.

Ventura, V. R.L. Snyder, and K.M. Bali. 2006. Estimating Evaporation from Bare Soil Using Soil Moisture Data. Journal of Irrigation and Drainage Engineering. ASCE, 132(2): 153-158. Available at: http://biomet.ucdavis.edu/Evapotranspiration. Accessed January, 2013.

Appendix 4D. Agricultural Water Demand Simulations with WEAP-CV PGM

This appendix provides information relevant the simulation of agricultural water use and crop yields. The appendix provides a review of existing scientific literature on data, methods and models used for computing evapotranspiration, growth and yield of major crops grown in the western United States. The potential effects of climate changes including the effects of increased carbon dioxide (CO_2) and vapor pressure deficit (VPD) on crop evapotranspiration (ET) and yields are discussed. The appendix also provides detailed information on the WEAP-CV PGM model and the algorithms employed to simulate ET and yield.

1. Climate Factors Influencing Crop Evapotranspiration and Yield

1.1 Background
An overview of interactions between climatic factors and crop responses is presented in this section. The focus of this study is on irrigated crops assuming that adequate water is supplied to meet the crop's consumptive use requirements. Other important conditions effecting ET and yield including nutrients, plant disease and weed competition; soil physical and chemical properties; cultural and irrigation management practices are also assumed to be non-limiting factors.

As shown on **Figure D-1**, a strong relationship between major climate and vegetation zones is exists at the global scale.
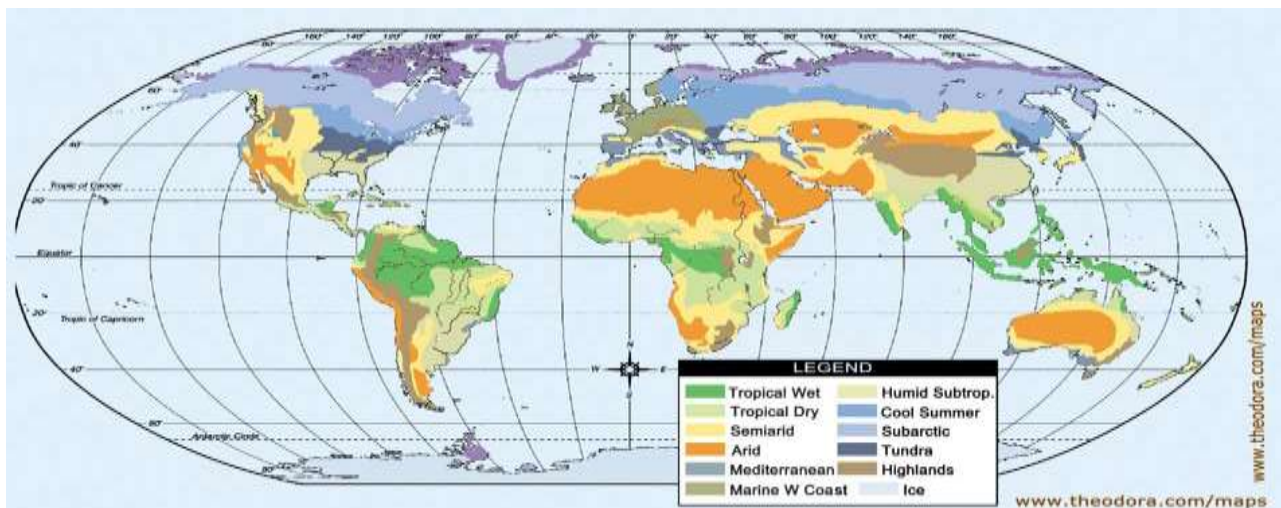
Major Global Climate Zones
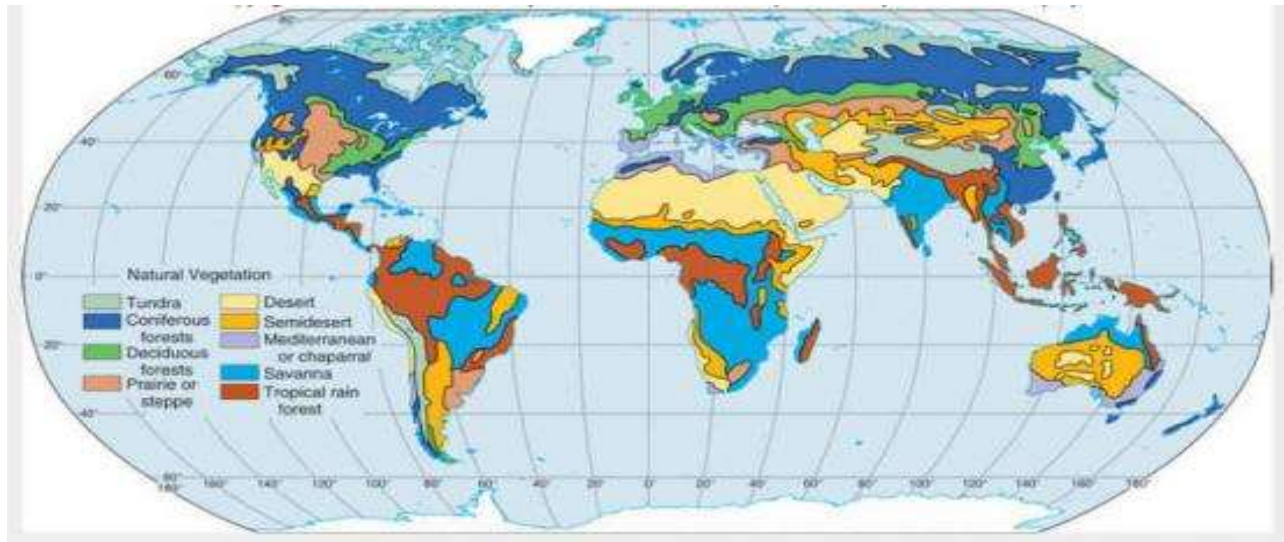
Major Global Vegetation Zones (Source: NASA)

Figure D-1. Major Global Climate and Vegetation Zones

As shown on **Figure D-2**, the relationship between vegetation zones, temperature and precipitation is of significant importance at the global, regional and local scales. However, other meteorological conditions including solar radiation, humidity and wind are well known to exert importance influences on the types and distribution of plant species. Like the native vegetation, agricultural crops have been adapted over long periods of time to grow well under a wide range of climate conditions.
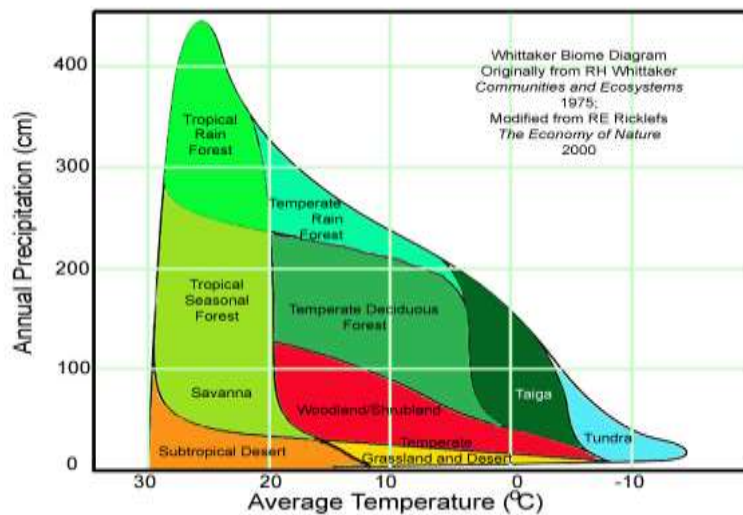
Figure D-2. Relationship between major vegetation types, temperature and precipitation

1.2 Overview of Temperature Response Effects on Crop Growth and Yields

It is well known that various plant species respond to temperature differently. Although plants are also adapted to other conditions (soil and nutrients), there exists an optimum temperature range in which plant specific biological processes such as photosynthesis and respiration are maximized. Outside of this range (either above or below), these processes decrease until mortality occurs. Depending on the balance of responses to these processes, warming can lead to either increased or decreased plant growth. Furthermore, biological responses to temperature are nonlinear, resulting in plant effects becoming increasing larger as temperature increases.

For vegetative development, there is a base temperature at which growth commences. As temperature increases, a plant's life cycle (phenological) phases occur more quickly. However, beyond the optimum temperature range, development (node and leaf appearance rate) slows. For non-perennial crops, faster development is not necessarily ideal because a shorter life cycle results in smaller plants, shorter reproductive phase duration, and lower yield potential. Consequently, the optimum temperature for yield is nearly always lower than the optimum temperature for vegetative growth. During the reproductive stage, higher temperatures affect pollen viability, fertilization, as well as grain and fruit formation. Although there is considerable genotypic variation among fruit and nut crops, winter temperatures can affect their ability to survive specific low temperature extremes (winter hardiness) and the dormancy period needed for optimum flowering and fruit set in the spring and summer (vernalization).

As global temperatures increase, the basal temperature required to initiate plant growth occurs earlier in the year. For perennial crops, this earlier spring growth combined with a corresponding extension of warmer temperatures in the fall will increase the length of the growing season. U.S. Global Change Research Program (USGCRP, 2008) estimated that the growing season in the Northern Hemisphere has already lengthened by about 1 to 4 days per decade in the last 40 years, especially at high latitudes. This lengthening may also expose plants to other changes in climatic conditions. For many plant species, day-length (photoperiod) also affects their life cycles. However, the intensity of solar radiation is less during spring and fall. Thus, warming may not result in the corresponding growth increases that temperature alone might seem to imply.

Future changes in atmospheric humidity may also affect the ability of plants to produce biomass and yield by changing the vapor pressure deficit (VPD) which is the difference between the stomatal vapor pressure (assumed to be at saturation) and vapor pressure of the surrounding atmosphere. Because the saturation vapor pressure is a nonlinear function of temperature, increasing temperature will tend to cause increases in VPD which may result in declines in biomass and yield.

Table D-1 summarizes information about temperature dependence of various life cycles phases for some major agriculture crops grown in the Reclamation project areas.

Table D-1. Temperature (0C) Dependence of various Life Cycles Phases for some Major Agriculture Crops

Crop	Base[1] Temp Veg Prod	Opt[2] Temp Veg Prod	Base[3] Temp Reprod	Opt[4] Temp Reprod	Opt Temp Range Veg Prod	Opt Temp Range Reprod Yield	Failure Temp Reprod Yield	% Yield[5] Change Per °C increase
Corn	8	34	8	34		18-22	35	-3.3
Cotton	14	37	14	28-30	34	25-26	35	-4.8
Rice	8	36	8	33	33	23-26	35-36	-10
Tomato	7	22	7	22		22-25	30	-10.5
Wheat	0	26	1	26	20-30	15	34	-5.4

Footnotes:

1. Base Temp Veg Prod = Base temperature for vegetative production
2. Opt Temp Veg Prod = Optimum temperature for vegetative production
3. Base Temp Reprod = Base temperature for reproductive phase
4. Opt Temp Reprod = Optimum temperature for reproductive phase
5. Estimated yield changes in North America relative to beginning of 21st century

Source: Synthesis and Assessment Product 4.3, Tables 2.2 and 2.6 (USGCRP, 2008)

1.3 Overview of Carbon Dioxide Response Effects on Crop Growth and Yields

The effects of carbon dioxide (CO_2) vary among various plant species. Most agricultural crops use the C3 photosynthetic pathway. Early studies of C3 plants conducted in enclosures under ideal growth conditions indicated a 33 percent increase in average yield occurred when CO2 was increased from 330 to 660 (Kimball 1983). Under similar conditions, the yield response of C4 plants such as corn increased by only about 10%. More recently, new "free-air CO_2 enrichment" (FACE) experiments have allowed evaluations of responses under experimental conditions that more closely simulate field conditions. Although some FACE results suggest yield responses that are less than previously reported (Long et al. 2006), the FACE experiments generally corroborate the previous enclosure studies (Ziska and Bunce 2007). **Table D-2** presents a summary of various plant responses to an increase of CO_2 from 330 to 660 ppm for selected major agriculture crops grown in the Reclamation project areas.

Bloom (2010) summarized multiple studies of changes in aboveground biomass when CO2 concentrations were increased from 366 to 567 ppm. For both C3 and

C4 grasses, average increases of approximately 10% occurred. Substantially larger increases were reported for legumes (75%) and trees (50%).

Table D-2. Percent change in Yield due to Increasing CO2 from 330 to 660 ppm under Ideal Growth Conditions

Crop	Carbon Fixation Pathway[1]	Leaf Photosynthesis	Total Biomass	Grain Yield
Corn	C4	3	4	4
Cotton	C3	33	46	44
Rice	C3	36	30	30
Sorghum	C4	9	3	8
Wheat	C3	35	15-27	31

Footnotes:

1. See Bloom (2010) for a detailed discussion of the C3 and C4 carbon fixation pathways.

Source: Synthesis and Assessment Product 4.3, Tables 2.7 (USGCRP, 2008)

The combined effects of increasing temperature and CO_2 can be beneficial to yields of certain leaf crops such as lettuce and spinach because increasing both CO_2 and temperature speeds the early growth phase in which these crops are harvested. However, for crops such as cotton, rice, sorghum and wheat no reported increases in yield occurred. For such closed canopy crops, increasing CO_2 at elevated temperatures caused additional increases in canopy temperatures typically ranging from 1 – 2 0C. This increased canopy temperature occurs especially in C3 plants because elevated CO2 allows reductions in leaf stomatal aperture which in turn reduces evaporative cooling of the leaves. Because the optimum temperature for yield is typically less than for vegetative growth (see Table D-1 above), the combined effects of increased CO2 and temperature tend to offset some the potential increased yields due to increased CO_2 alone.

1.4 Overview of Climate and Carbon Dioxide Response Effects on Crop Evapotranspiration

The potential effects of climate change on plant water use can be examined by an analysis of well known Penman-Monteith (PM) equation (Monteith, 1981).

$$ET = \left\{ \frac{\Delta(R_n - G) + K_t \rho_a C_p \frac{(e_s - e_a)}{r_a}}{\Delta + \gamma(1 + \frac{r_s}{r_a})} \right\} / \lambda \rho_w \quad (\text{Eqn 1})$$

Where in SI units the terms of the equation are given by:

ET = Crop evapotranspiration [mm d^{-1}]

R_n = Net solar radiation [MJ m^{-2} d^{-1}]

G = Soil heat flux [MJ m^{-2} d^{-1}]

e_s = Saturation vapor pressure of the canopy [kPa]

e_a = Actual vapor pressure of the surrounding atmosphere [kPa]

r_a = Aerodynamic resistance [s m^{-1}]

r_s = Canopy resistance [s m^{-1}]

Δ = Slope of the saturation vapor pressure-temperature curve [kPa °C^{-1}]

C_p = Specific heat capacity of moist air [MJ kg^{-1} °C^{-1}]

ρ_a & ρ_w = Mean air and water density respectively [kg m^{-3}]

γ = Psychometric constant (kPa °C^{-1})

λ = Latent heat of vaporization (MJ kg^{-1})

K_t = 86,400 s d^{-1}

The terms in Eqn. 1 depend on both biological and meteorological conditions. It is worth noting that air temperature does not appear directly in the PM equation. The ASCE PM method (Allen et al., 2005) describes relationships between several variables in Eqn. 1 and daily or hourly temperatures. Temperature dependent variables include the latent heat of vaporization λ, the mean air density, ρa, slope of the saturation vapor pressure-temperature curve, Δ, and the psychometric constant, γ. The net radiation term, Rn, also depends on temperature through the effect of surface temperature on outgoing long-wave radiation.

The saturation vapor pressure, es, is a function of air temperature and affects the stomatal vapor pressure driving diffusion of water vapor from leaves but, as discussed above, decreases in stomatal conductance caused by elevated CO_2 can increase leaf temperature which in turn increases es . Therefore, the vapor pressure deficit (VPD) defined as the difference between es and ea may increase because of the combined effects CO_2 and increased air temperature.

In the PM equation, an increase in the VPD results in an increase in ET. However, it is important to recognize that plant response to increased VPD is not as simple as represented in the PM equation. Initially, increasing VPD produces increased plant transpiration. However, when VPD increases beyond certain plant type specific thresholds, some plants respond reducing their transpiration to prevent excessive loss of cell fluids. Streck (2003) provides a comprehensive review of published research on plant responses to VPD. Although the exact mechanisms by which plants respond to VPD (Addington et al 2004) is still an area of research and it is known that not all plants exhibit the response (Ocheltree et al 2014), it is sufficiently well established and potentially significant enough that this response referred to as "apparent feedforward" is included in the WEAP-CV PGM as well as other model simulating the dynamics of plant growth processes.

Other meteorological influences on crop ET include the effects of the canopy albedo on the reflection of incoming short-wave radiation, the influence of wind speed and crop height on aerodynamic resistance, ra, and the effects of stomatal conductance and canopy development typically expressed in terms of the leaf area index (LAI) [m^2 leaf area per m^2 soil surface] on canopy resistance, rs.

Kimball (2007) performed a temperature sensitivity analysis on some of the meteorological and plant variables used in the ASCE hourly PM equation (Allen et al, 2005) using data obtained from a weather station in Maricopa, AZ during the year 1987. Results from this study are presented in **Table D-3**.

Table D-3. Sensitivity of the ASCE Hourly PM Equation to Weather and Plant Variables

Weather or Plant Variable	ET Sensitivity (% Change in ET)	
	Summer Day	Whole Year
Temperature effect per Δ°C at constant absolute humidity	2.39	3.44
Solar Radiation effect per Δ% Rs	0.58	0.40
Atmospheric vapor pressure effect per Δ% e_a	-0.16	-0.40
Wind effect per Δ% U	0.29	0.38
Stomatal conductance effect per Δ% gs	0.08	0.16
LAI effect per Δ% LAI	0.08	0.16

In **Table D-3**, the sensitivity of ET to temperature is greatest of all the variables considered. As discussed above, temperature affects many of the variables in the PM equation but its effect on the vapor pressure deficit (e_s - $e_{a)}$ is most likely the main cause of its higher significance in the results. However, increasing atmospheric humidity, ea, reduces ET by decreasing the VPD. Furthermore, it worth noting that temperature effects on growth and LAI of non-reference crops are not really represented in this analysis because reference crops are assumed to have a constant canopy height and LAI throughout the growing season which is not representative of most agricultural crops.

Future warming also has the potential to affect crop phenological characteristics related to crop ET. For perennial crops, increased warming will continue lengthening the growing season which will tend to increase total ET. For annuals, earlier warming may cause a shift in the growing season to earlier in the year. These shifts may or may not increase crop water use. As discussed above, more rapid growth due to warming may shorten the actual growth period resulting in reduced water consumption for some crops. However for those crops (either annual or perennial) exhibiting photoperiod sensitivity, earlier growing season initiation may result in slower growth in the spring when solar radiation in the northern hemisphere is less intense and consequently reduce ET during the early vegetative growth stage. Furthermore, growing season shifts may result in crops being exposed to other climatic conditions such as increased precipitation and/or humidity or decreased wind speed which would also tend to reduce crop ET.

In addition, the effects of rising CO_2 are likely to exert a significant influence on future crop ET. Based on relative gradients in concentration between the stomata and atmosphere, Bloom (2010) estimated that the rate of diffusion of water vapor out of plant is about 40 times faster than the rate of CO_2 diffusion into the leaf. For C3 plants, it was estimated 500 – 1000 water molecules are lost per molecule of CO_2 entering the leaf whereas for C4 plants due their lower internal CO_2 requirements only 200 – 300 molecules of water are lost. Under a doubling of

CO2, plants could potentially assimilate twice as many molecules of CO_2 per molecule of water lost. Plants could respond to increasing CO_2 by either decreasing their stomatal openings to maintain similar CO_2 concentrations or they could keep their stomata open and thereby lose more water while increasing the assimilation of CO_2 and potentially increasing growth. Bloom (2010) summarizes a large number of experimental studies indicating that plants actually respond using a combination of these strategies. In C3 crops, stomatal conductance was reduced by an average by 22% when CO_2 concentrations increased from 366 to 567 ppm. For C4 crops, the average reduction in stomatal conductance was about 30%. For both C3 and C4 crops, CO_2 assimilation in the leaf cells increased on average by approximately 10%. Other studies have reported similar responses to elevated CO_2 in both C3 and C4 plants. Kimball and Idso (1983) reported a 34% reduction in stomatal conductance when the CO_2 concentration was increased from 340 to 660 ppm. Based on data from FACE experiments, Ainsworth and Long (2005) reported an average reduction in stomatal conductance of between 20 - 22 percent when CO_2 concentrations were increased from 360 to 600 ppm.

1.5 Simple Assessment of the Combined Effects of Temperature and Carbon Dioxide on Future Crop ET and Yields.

A simplistic assessment of combined effects of future temperature and CO2 changes on ET and yield can be made by making assumptions about the magnitude of future changes in these climatic conditions. Reclamation (2011) estimated median temperature changes for each of its 8 major basins for the early, mid and late 21st century step change periods. Using these estimates, a reasonable consensus estimate for temperature change during the period from early to mid to late 21st century is approximately + 2 ^oC. The U.S. Climate Change Science Program's Science Assessment Product 4.2 report (2008) estimated that increasing CO2 to 700 ppm would likely increase global average surface temperature by between 1.7 and 4.4 ^oC by 2100. Thus a reasonable assumption for a CO2 concentration corresponding to a + 2 ^oC change in temperature is 660 ppm. This value is also convenient because considerable research has focused on this value and established that stomatal response remains linear for CO2 increases up to this value. For this simplistic assessment, only the effects of temperature and CO2 on ET are evaluated.

In order to estimate temperature effects on ET, average growing season crop coefficients were estimated using crop development periods and corresponding crop coefficients presented in FAO Irrigation and Drainage Paper 56 (Allen et al. 1998). These annual average Kc values for the major crops considered here were corn (0.83), cotton (0.65), rice (1.05), tomato (1.09), and wheat (0.76). These growing season averaged crop coefficients were then used to compute temperature change ET effects based on the reference crop ET change per ^oC presented in **Table D-2** above. For the simplified assessment, it was also assumed that the 10% increase in CO2 assimilation observed in both C3 and C4 (Bloom, 2010) crops would be reflected in a corresponding increase in LAI (see **Table D-3** above). The results are presented in **Table D-4** below.

Table D-4. Simplified Assessment of Combined Temperature and CO2 Changes on Major Agricultural Crops during Mid to Late 21st Century

Crop	Yield Change (%)			ET Changes (%)			
	Temp (+2°C)	CO$_2$ (660 ppm)	Combined[1] Effects	Temp (+2°C)	LAI (660 ppm)	Stomatal Response (660 ppm)	Combined[1] Effects
Corn	-6.6	4	-2.6	5.7	1.6	-30	-22.7
Cotton	-9.6	44	34.4	4.5	1.6	-25	-18.9
Rice	-20	30	10	7.2	1.6	-25	-16.2
Tomato	-21	32[2]	11	7.5	1.6	-25	-15.9
Wheat	-10.8	31	20.2	4.5	1.6	-25	-18.9

Footnotes:

1. Assumes that temperature and CO$_2$ effects are additive.
2. Assumes average yield change for C3 plants.

As can be observed in **Table D-4** above, the yield changes are variable ranging from slight decreases to significant increases depending on plant sensitivities. In contrast, ET declines are consistently greater than 15% due the significant increase in CO2 to 660 ppm and its potentially significant effects on stomatal conductance at this elevated concentration in the latter half of the 21st century. However, it must be emphasized that these effects do not consider many other factors which also have the potential to exert significant impacts either up or down on ET and yield.

2. Modeling Climate – Crop Relationships

In this section, brief discussions of various modeling approaches and a description of some of the most commonly used crop models are presented.

2.1. Overview of Modeling Approaches

Like other types of modeling, crop models range from simple to complex. The simplest are often single purpose models using statistical methods (e.g. regression) to estimate a particular output (e.g. yield) for a specific crop (e.g. corn) using a limited number of variables (e.g. temperature, precipitation, fertilizer application rates etc.). However for climate studies, such models have limitations because the included regression variables (e.g. temperature and precipitation) are likely to be correlated with non-stationary climate changes (e.g. CO2, solar radiation etc.) which were not explicitly represented in model development. Furthermore, transferability to areas outside the region where the

input variables (e.g. soil types, water table depth, etc.) have similar characteristics is another problem requiring modifications. However, simple models often have advantages in terms of the level of effort necessary to obtain data for inputs, develop the model and interpret the results. Consequently, these models can provide important information especially for initial assessments at the local to regional scales.

As the objectives of the crop modeling become more multi-purpose, more comprehensive and longer term modeling approaches that explicitly account for multiple factors are desirable. Typically, these ecophysiological models include to varying degrees representations of meteorological conditions, biogeochemical processes occurring in various plant organs, soil-plant-water interactions and management practices with explicit temporal scales ranging from minutes to days and spatial scales ranging individual plants (m^2) to fields (~100 ha). Regional and even global scale crop simulations using these models are typically performed by extrapolation of smaller scale results based on externally developed land use data.

These models are often applied to better understand the effects of a wide range of external factors such as climate, soil conditions and management actions for a variety of applications including agricultural productivity, soil and water conservation, surface and groundwater quantity and quality and ecosystem sustainability and biodiversity. In general, these models represent physical and biological processes deterministically but empirical relationships are also used when scientific knowledge and/or parameterization data are lacking or computational efficiency is necessary to accomplish study objectives. Although these models overcome various limitations of the simpler models, it must be recognized that the data requirements, expertise needed and level of effort to develop and apply them is correspondingly greater.

In ecophysiological models, plant responses to climate are typically simulated by model components that represent to varying extents plant phenology; photosynthesis and respiration; biomass accumulation, partitioning and organ growth; water balance; N-uptake and translocation and other factors (Tubiello and Ewert, 2002). Phenology is generally simulated as a function of accumulated daily temperature and day length. Photosynthetic response to light is often computed using exponential or rectangular hyperbolic functions along with various methods to determine how much of the incident solar radiation is intercepted by the canopy. A few crop models use more detailed biochemical equations. Simpler models calculate net biomass production by multiplying intercepted light by the radiation use efficiency (RUE) which is usually assumed to be constant throughout the growth period but may change as a function of CO2. In some models, biomass production may also be limited by a transpiration use efficiency (TUE) to account for the influence of low relative humidity. In models that compute maintenance and growth respiration, CO2 may affect respiration rates indirectly through changes in growth rates.

The modeling of climate effects on crop transpiration has been simulated using several different approaches. In some simpler models (Richie, 1972), actual crop transpiration is computed based on the minimum of potential evapotranspiration (PET), which may be computed by a variety of methods, and root water uptake which is computed as a function of soil water content and the root abundance. In such models, the effects of elevated CO2 may be simulated by reducing the stomatal conductance which reduces the PET rate. However, stomatal closure has been observed to elevate leaf temperature which increases water vapor diffusion rate. In simpler models, this effect may be empirically simulated by increasing air temperature which is generally assumed to equal leaf temperature. In more complex models, the simulation of photosynthetic carbon uptake is linked with calculations of stomatal conductance. In these models, the algorithms that optimize carbon fixation and transpiration reduce stomatal conductance under water stress conditions which reduces the diffusion of CO2 into the leaf. Increasing the atmospheric CO2 concentration has a similar effect on stomatal conductance. In more complex models, reduced stomatal conductance also directly affects leaf temperature and associated phonological stage development rates. In some models, the effects of elevated CO2 on increased optimum photosynthetic temperature can be simulated. However, comparisons between simple and more complex models did not show significant differences due to this effect (Tubiello and Ewert, 2002).

Biomass partitioning among roots, stems, leaves, and grain or fruit is simulated in simpler models by using constant allocation fractions that may change with crop phonological stages. More complex models dynamically allocate carbon among organ groups. In these models, elevated CO2 may dynamically modify partitioning and biomass accumulation through feedbacks between photosynthesis and organ growth known as source-sink relations. In simpler models, harvest yield is computed from final above-ground biomass using a harvest yield index coefficient that may also depend on accumulated water and heat stress. In more complex models, harvest yield is based on the dynamic feedbacks used in computing grain or fruit growth.

Other important factors that can affect crop responses to climate changes include air pollutants especially ozone, soil quality, weeds, pests and diseases. Ozone effects the assimilation of CO_2 by reducing stomatal conductance and/or decreasing biochemical activity due to cell damage (Tubiello and Ewert, 2002). Some or all of these effects are simulated to varying extents in both simple and complex models.

White et al. (2011) describe three general modeling approaches that have been implemented in crop models to simulate the effects of climate changes crop water use and yields.

1. Models that use RUE and/or TUE with various adjustments depending on the model to account for effects of CO_2, temperature, water, nutrients and

other environmental or physiological factors affecting daily net productivity.

2. Models that simulate the processes of photosynthesis and respiration at the leaf-level, scaled to canopy level considering losses through respiration and senescence. Plant temperature affects multiple processes and is either assumed equal to air temperature or obtained from simple submodels. CO_2 effects photosynthesis and stomatal conductance. Depending on the model, other environmental and physiological factors affecting growth and yield such as soil nutrients and water availability and management practices are frequently included.

3. Models that explicitly simulate the physiological effect of elevated CO_2 on reduced stomatal conductance and increased in canopy temperature. Processes of photosynthesis and respiration are simulated in ways similar to the second class of models. Other environmental and physiological factors affecting growth and yield are also included.

Typically, these models include sub-modules to represent the effects of meteorology, hydrology, plant physiology and management factors. Brief descriptions of the major data requirements and processes included in these models are provided below. Additional, model specific information is provided for some of the most commonly used models in climate studies is provided in the following section.

Meteorology requirements typically include temperature, precipitation, solar radiation, humidity and wind speed at daily to monthly time scales. Weather data requirements for computing ET by the PM method are greater than for other methods such as Preistly-Taylor (PT), Hargreaves-Semani, Blaney-Criddle (BC) and others. Because many weather stations do not collect the required solar radiation, humidity and wind speed data, many models employ estimation procedures that provide the needed weather inputs from temperature, precipitation, elevation, and latitude. For climate studies, atmospheric CO_2 concentrations are also typically required.

Hydrology modules typically provide the means to represent interactions between soil-plant-climate factors. Input data requirements include soil characteristics affecting soil evaporation (E_s), erosion, surface runoff, infiltration, redistribution of soil moisture within the soil profile, actual crop transpiration (T), and deep percolation from the root zone. Some models have the ability to simulate shallow water table effects on ET. For models that include plant – soil nutrient interactions, soil organic matter, nitrogen and phosphorus mineralization, speciation and volatilization, specific parameters representing relationships between soil concentrations and plant requirements during various life cycle stages are required. Models that include capabilities to simulate nutrients,

pesticides, herbicides and bacteria require various types of soil and constituent transport parameters.

Plant modules typically include processes that represent plant growth, biomass production and yield. Plant growth is commonly simulated based on plant specific life cycle stage dependent responses to temperature, radiation, humidity, photoperiod, plant available soil water and nutrients and CO2. Some models directly simulate the effects photosynthesis and respiration on carbohydrate and protein contents within various plant organs. In these models, yield is computed based on the availability of these substrates during the specific growth stages and may include re-translocation of substrates and nutrients between plant organs in response to environmental stresses. In other models, crop yields are computed as a function of a temperature based harvest index. Plant growth is usually partitioned into above and below biomass based on plant specific characteristics. In some models, the vertical distribution of roots includes the effects of layer specific soil water content during the growing season.

Management modules generally include capabilities to represent field operations affecting water use, crop yields, soil erosion, runoff, accumulation and transport of sediment, nutrients, herbicides and pesticides in surface and ground water. Typical management activities include crop specific dates for planting single, multi-crops and crop rotations; tillage; fertilization, herbicide and pesticide applications; plant residue management and irrigation scheduling. Most of these models allow both user defined and automated scheduling of crop management practices based on dynamic temperature and moisture conditions.

2.2. Description of Selected Models

Ecophysiological models have been applied to study the effects of climate change on agroecosystems for several decades. Using explicit search and selection criteria to identify climate change crop studies, White et al. (2011) identified 221 journal publications that addressed simulation methods, impacts and adaptations relative to climate change. Of these reviewed studies, their primary focus was impacts (66%), methods (19%) and adaptation (15%). Of the 35 crops explicitly identified, the most studied crops included wheat (35%), maize (25%), rice (11%), soybean (7%) and potato (3%). Taken together, these crops represented 80% of the studies reviewed. Tubiello and Ewert (2002) reported similar results. About 25% of the studies (55) were focused on the United States.

White et al. (2011) indicated that more than 70 models had been applied to study climate change effects on agroecosystems in the 221 studies reviewed. In these studies, the 5 most frequently used models were referenced in more than 50% of the studies. In the order of their prevalence, the top 5 models included CERES (29%), EPIC (11%), APSIM (6%), CropSyst (4%) and DSSAT - CSM+CropGro (4%). In a survey of the crop modeling community, Rivington and Koo (2010)

obtained similar results relative to the most commonly used models. Brief descriptions of the five most commonly used models are provided below:

1. CERES (Crop Environment Resource Synthesis) models have been developed for a variety of crops including wheat, maize, rice, sorghum, millet, and barley. CERES models were among the earliest crop models developed which probably influenced the prevalence of CERES references in the White's literature review. These ecophysiological models are deterministic but not overly mechanistic. Their primarily focus is on how cultivar properties, planting density, climate (including CO2), soil water, and nitrogen affect crop growth, development, and yield. Their primary purpose is to examine how alternative management practices (fertilization and irrigation) affect yield at the farm and regional scales. They have also been used to study nitrogen leaching and the effects of climate change.

CERES models account for a variety of crop development, growth and yield processes in the following:

- Phenological development stages
- Growth of leaves, stems, and roots
- Biomass accumulation and partitioning in plant organs
- Soil water balance and crop water use
- Transformations of nitrogen in the soil, uptake by roots, and partitioning between plant organs

Crop biomass accumulation is calculated independently of the plant development. Biomass production is simulated as a function of radiation use efficiency, leaf area index with reductions due to temperature and moisture stresses. Cultivar phenological development stages are computed based primarily on accumulated degree-days. Photosynthesis determines the growth rate of leaves, stems and roots. The root zone soil water content is computed based on soil characteristics affecting runoff, infiltration and drainage. Mineral nitrogen dynamics in the soil profile are also simulated.

Data inputs include:

1. Climate variables such as latitude, daily solar radiation, temperature and precipitation and atmospheric CO2 concentration and
2. Management variables such as sowing date, plant density, row spacing, sowing depth, irrigation and fertilizer schedules and
3. Crop genetic constants, phenology and growth parameters and
4. Soil parameters such as albedo, soil texture and water holding properties and profile characteristics

Many of the original CERES crop models (e.g. CERES-Wheat) have been updated for use in the DSSAT-CSM model described below.

Key references relevant to the CERES models include Jones and Kinery (1986) and Mearns et al. (1999). Additional online information for the CERES models is available at http://epicapex.brc.tamus.edu/

2. EPIC (Environmental Policy Integrated Climate) was originally developed during the 1980's to simulate effects of soil erosion on agricultural productivity in the United States. It is a deterministic, field scale, daily time step model designed to simulate drainage areas that are characterized by homogeneous weather, soil characteristics, crops, and management practices including tillage effect on surface residue, soil bulk density and nutrients as well as fertilizer and irrigation effects on crop yield.

EPIC's crop growth model uses approaches that are similar to the CERES models. One significant difference is a simpler representation of phenological stages in crop development. The biophysical processes represented in the model include:

- Solar radiation, saturation vapor pressure, canopy and soil albedo effects on potential evaporation in default method; other PET methods (5) available

- Plant evaporation computed as linear function of potential evaporation and Leaf Area Index (LAI) ; two stage soil evaporation based on soil characteristics

- Biomass production function of photosynthetically active radiation (PAR) and crop specific radiation use efficiency (RUE) with adjustment for water, temperature, nitrogen, phosphorous stresses.

- Daily adjustment of potential biomass into above ground and root growth that reflect water, temperature and nutrient stresses (nitrogen and phosphorous)

- Canopy development and senescence computed as function of biomass and crop specific maximum LAI

- Influence of atmospheric CO_2 on biomass production and canopy resistance in the Penman Monteith ET equation can be simulated

- Crop yields are computed by accumulating growing season weighted daily increments of stress adjusted biomass up to a maximum crop specific yield

EPIC requires more than 400 input data items including about three hundred climatic characteristics and 50 crop parameters (Adejuwon, 2005). However, many of these inputs can be obtained or estimated from existing EPIC databases.

Data inputs include:

1. Climate variables such as precipitation, solar radiation, relative humidity, minimum and maximum temperature, wind speed and atmospheric CO2 concentration and

2. Management variables such as details of farm operations including scheduling of tillage, type and amounts of fertilizer and pesticides applied, irrigation, density of planting, among others and

3. Crop parameters such as radiation use efficiency, crop height, canopy development and senescence, basal and optimal growth temperatures, optimum crop yield, root – shoot biomass production ratio, maximum root depth, maximum LAI and

4. Soil parameters such as bulk density, water-holding capacity, wilting point, hydraulic properties and profile characteristics

The APEX (Agricultural Policy / Environmental eXtender) model enhances the EPIC model capabilities to simulate entire farms and small watersheds. APEX has additional algorithms that route water, sediment, nutrients, and pesticides from farms through watersheds and channels. It also has groundwater and reservoir simulation capabilities. There new versions of these models (WinEPIC and WinAPEX) that have also been developed recently.

Key references relevant to the EPIC model include Williams et al. (1989) and Williams et al. (2008) and Stockle (1992). Additional online information for EPIC and APEX models is available at http://epicapex.brc.tamus.edu/

3. APSIM (Agricultural Production Systems Simulator) is an ecophysiological model designed to simulate growth, development and yield of crops, pastures and forests in relation to climate, plant genotype, soil characteristics and management practices affecting long-term productivity such as loss of soil organic matter, structural degradation, acidification and erosion. APSIM is a deterministic, multi-crop area based, daily time step model with existing capabilities to simulate more than 20 crops including wheat, maize, rice, soybean, potato, sorghum, millet, various grain legumes, safflower, sunflower, cotton, sugarcane, lucrene (alfalfa) and others.

The APSIM uses a generic crop model template (GCROP) that consists of component sub-modules for crop parameters (CPF); basic plant physiological process (CPL), crop components such as phenology and biomass (GMS) and a

standard interface (SCI) to manage interactions with other APSIM modules (e.g. soils, meteorology). The biophysical processes simulated in GCROP include:

- Transpiration – calculated as minimum of water supply (based on soil water content and root distribution) and water demand (based on radiation energy for biomass production)

- Phenology – crop growth stages computed based on accumulated thermal time (degree days) and photoperiod. Development may be reduced by water or nitrogen stress

- Biomass – calculated as minimum of either energy supply (based on intercepted radiation and RUE) or crop growth stage dependent water supply (based on transpiration efficiency and VPD) effects on daily biomass production; computes Harvest Index for yield; and retranslocates carbon between plant parts

- Leaf Area Development – calculated from thermal time effects on daily increase in number of leaves and leaf size; maybe limited by carbon and water supply and senescence

- Senescence – computed as function of age, light competition, water and temperature stresses

- Nitrogen – simulates demand, uptake, fixation and retranslocation in plant

The recently developed MICROMET module (Snow and Huth, 2004) was developed to improve capabilities to compute ET using the Penman Montheith equation in multilayer and intermingled canopies such as occur in forested, chaparral and inter-cropped field areas.

APSIM data inputs are dependent on the particular user selected modules included in the simulation. A brief description of data inputs employed by some of the modules relevant to this study is provided below:

1. Plant module inputs include basic information about crop canopy and root characteristics such as RUE, canopy light extinction, leaf senescence, max crop height and rooting depth, development stages and associated degree days, plant organ fractionation coefficients, soil water extraction limits, specific root length and others

2. Soil module includes inputs for simulating soil water, nitrogen, carbon, phosphorus and temperature; soil management practices such as fertilization, irrigation and erosion.
   i. Soil water processes can be simulated by either a cascading bucket approach (SoilWat) similar to the EPIC and CERES models or by

a numerical solution of unsaturated flow (SWIM2). Hydrologic processes simulated include runoff, drainage, soil and potential evaporation, unsaturated flow, solute flux and flow

3. Meteorology module includes station name, latitude and temperature, precipitation and radiation data at daily, monthly or annual time scales

4. Manager module allows user to control APSIM simulations user coding.

Key references relevant to the APSIM model include Wang et al. (2002) and Keating et al. (2003); Additional online information is available from the link http://www.apsim.info/Wiki/

4. CropSyst (Cropping Systems Simulation Model) is an ecophysical model developed for the purpose of simulating the effects of the effect of climate, soils, and management practices including crop rotations, cultivar selection, irrigation, nitrogen fertilization, soil and irrigation water salinity, tillage operations, and crop residue on agroecosystems. It is a multi-year, multi-crop, daily time step that simulates a single biophysically homogeneous area managed in a uniform manner. Functionality for simulating multiple land areas is available through ArcGIS.

The CropSyst modules provide algorithms that compute water and nitrogen budgets, phenology, biomass production including the effects of CO_2, canopy development, root growth, crop yield and residue. The methods used to simulate these biophysical processes are briefly described below:

- Water budget – components include precipitation, irrigation, runoff, infiltration, soil evaporation, plant transpiration, redistribution, and deep percolation
    i. Redistribution can be simulated by a simple cascading approach similar to APSIM, EPIC and CERES models or a numerical solution of the Richard's equation similar to APSIM
    ii. Potential crop ET is computed using either a Penman-Monteith or Priestly Taylor based reference crop and crop specific coefficients; actual crop ET is computed based on PET and plant available soil water

- Nitrogen budget – simulated N processes include fixation, mineralization, nitrification, and denitrification; crop N uptake is determined as the minimum of crop nitrogen demand (growth requirements plus its deficiency demand difference between the crop maximum and actual nitrogen concentration) and potential nitrogen uptake

- Phenology - daily accumulation of thermal time (daily average temperature above a base temperature and below a cutoff temperature)

during specific growth stages; vernalization and photoperiod requirements need to be considered

- Biomass – uses minimum value based on biomass-temperature-VPD and biomass-PAR-RUE relationships; nitrogen and water stresses may reduce biomass

- Canopy development – LAI is computed a function of biomass accumulated during crop growth stages including senescence

- Root growth – root depth increases to a maximum depth as canopy develops; root density is assumed zero at the current soil depth and increases linearly to a maximum density at a depth near the soil surface

- Yield – computed from total daily accumulated biomass at physiological maturity and stress adjusted Harvest Index (/harvestable yield / aboveground biomass)

CropSyst inputs depend on which modules are included in the simulation. Brief descriptions of module inputs are provided below:

1. Soil module – layer thickness and texture must be specified; bulk density, volumetric water content and unsaturated water content and water potential relationship parameters may be specified or computed by pedotransfer functions based on soil texture

2. Plant module – Phenology (basal and optimum temperatures, thermal time requirements to reach specific growth stages); Morphology (Maximum LAI, root depth, specific leaf area, leaf area duration, root characteristics and others); Biomass (growth transpiration biomass coefficient, radiation-use efficiency, nitrogen demand and root uptake parameters water, N and salinity and CO_2 sensitivity parameters); Yield harvest index; Residue decomposition and shading parameters

3. Meteorology module – requires temperature, precipitation and radiation for Priestly Taylor ET; plus wind, humidity for Penman Monteith ET method; weather generation capabilities are included in CropSyst

4. Management module – includes scheduled and automatic management events such irrigation application date, amount, and salinity concentration; nitrogen fertilization application date, amount, source, and application mode, tillage operations, and residue management; management events can be scheduled using actual date, relative date (relative to year of planting or synchronized with phenological events.

Key references relevant to the CropSyst model include Stockle et al.(1992) and Stockle et al. (2003); Additional information is available at http://www.bsyse.wsu.edu/CS_Suite/CropSyst/

5. DSSAT-CSM (Decision Support System for Agrotechnology Transfer) was designed to integrate knowledge about soil, climate, crops and management to support better decisions about transferring agricultural production technologies from one location to others. It is a deterministic ecophysiological model that simulates the effects of soil, water and management on the daily growth, development and yield of multiple crops grown in a uniform area over multiple years. The Cropping System Model (CSM) is used to simulate crops using a single soil and a single weather module. As of Version 4.5, over 28 crops are supported by DSSAT-CSM.

DSSAT-CSM simulates various biophysical processes affecting crop growth, development and yield. Methods used include the following:

- Water budget – methods include runoff using SCS approach, infiltration and redistribution using the cascading bucket approach, soil water content including upward unsaturated flow; two stage soil evaporation with actual plant transpiration computed as minimum of potential evaporation and root water uptake based on soil water content and root density, PET can be computed by PM, PT or Richie's method (see APSIM model)

- Carbon and Nitrogen budget – decomposition of soil organic matter computed as function of computed soil temperature and water content; accounts for plant senescence (above ground and subsurface) and transport by soil water

- Phenology – life cycle growth stages computed as function of temperature, photoperiod and sensitivity to N and P availability

- Plant growth – crop photosynthesis computed as function of RUE adjusted for light interception, plant density, CO_2 concentration and N, temperature and water stresses or hourly hedgerow light interception-leaf-level based on canopy development and orientation, CO2 and temperature; accounts for growth stage dependent plant organ assimilate needs and respiration effects; root growth based on growth stage dependent carbohydrate requirements

- Yield – computed based on plant growth and stresses during growth period

DSSAT-CSM inputs depend on which methods and sub-modules are included in the simulation. Brief descriptions of some of the general types of module inputs are provided below:

1. Land Use Module – includes site latitude and longitude; average annual temperature and amplitude, slope and aspect, and others

2. Weather – daily solar radiation, maximum and minimum temperature, precipitation and other simulation specifics characteristics (e.g. humidity and wind for PM ET)

3. Soil – layer thicknesses, upper and lower soil water content limits, bulk density, organic carbon, pH, rooting and drainage factors

4. Crop – photosynthesis and respiration coefficients associated with growth stages; plant organ composition parameters; carbon and nitrogen mining parameters; plant growth, senescence and dry matter partitioning parameters; phenology, crop height and width paramters

Key references relevant to the DSSAT-CSM model include Jones et al. (1989a) and Jones et al. (2003); Additional information is available at http://dssat.net/about

2.3. Crop Modeling Data

Modeling the effects of climate change on crop ET and yield requires a variety of data types to specify the fundamental interactions between crops and the agroecosystems in which they are grown. The scientific literature provides an extensive source of information about crop modeling and parameters for use in models. Some of these references are provided in the bibliography of this report. In addition, many of the most frequently used models including EPIC, APSIM, CropSyst and the DSSAT-CSM crop models have databases of crop parameters, soil, and weather information that accompany these models when they are downloaded from their websites.

Other sources of agricultural soil and a climate data are also available online. The USDA National Agricultural Statistics Service (NASS) provides downloadable GIS and spreadsheet data on crop types and acreages by county for the entire continental United States. This remotely sensed data is available on annual basis from the late 1990's up to the year previous to the current calendar year. This cropland data information can be obtained from http://nassgeodata.gmu.edu/CropScape/ . In many instances, crop models require soil data as an input. In addition to data that may be provided with various models, the USDA Natural Resources and Conservation Service (NRCS) provides downloadable geospatial soil survey data that can be used to develop soil characteristics necessary for crop modeling. A link to this data is http://soildatamart.nrcs.usda.gov/ . Crop models also provide capabilities to either directly specify or develop the weather data necessary for running the model. The

types, frequencies and time periods of these data requirements are generally dependent on the simulations to be performed. Most models provide users with the ability to generate daily or even hourly data from monthly averages using user specified site and climate characteristics. Reclamation and others have developed an archive of bias corrected and spatially downscaled climate (temperature and precipitation) and hydrology (unimpaired flows) projections for the period from 1950-2099 at the monthly and daily time scales based on the IPCC AR4 and AR5 Coupled Model Intercomparison Project (CMIP3 and CIMIP5) GCM simulations. For the continental U.S., bias-corrected, spatially downscaled (BCSD) projections from these studies may be downloaded online from http://gdo-dcp.ucllnl.org/downscaled_cmip3_projections/ . Carbon dioxide data associated with the emissions scenarios and representative concentration pathways may be downloaded from http://www.ipcc-data.org/observ/ddc_co2.html/ .

3. Climate – Crop Modeling Studies

To address the potential effects of climate change on agriculture, crop models have been employed for the past several decades. Many studies have tended to focus on the effects of particular aspects of climate change (e.g. temperature) without simultaneously considering the effects of other climatic influences (e.g. humidity). Additional difficulties occur because readily available bias corrected and spatially downscaled climate projections typically lack the climatic data needed for modeling key biophysical processes (e.g. solar radiation, wind, humidity and CO2). Furthermore, coupling plant growth and yield simulations with crop water use may not be considered or only treated as a simple sensitivity analysis (e.g. effects of CO2). Finally, due to the computationally intensive nature of crop modeling, climate changes are frequently limited to only a few projections that may neither capture the central tendency nor a representative range of future climate uncertainties (e.g. warmer-drier, warmer-wetter) relative to the central tendency of a large ensemble of future climate projections.

In the following subsections, the studies described were selected based on the criteria that they combined GCM based climate simulations with crop models based on dynamic biophysical processes affecting evapotranspiration, growth, and yield including the effects of CO2. In addition, only studies reporting results involving irrigation of crops grown in Reclamation service areas are described below.

3.1 Crop Evapotranspiration – Climate Interactions
In an early study of the sensitivity of crop ET (ETc) to potential climate changes, Rosenberg et al. (1990) calibrated the Penman Montheith (PM) equation to observations of wheat growing at Mead, NB and tall grass prairie near Manhattan, KS during their summer growth periods. The order of sensitivity of ETc to changes in climate variables was temperature $(T,+) >$ net radiation $(Rn,+) >$ absolute humidity $(ea,-) >$ canopy resistance $(rs,-) >$ leaf area index $(LAI,+)$ and $>$ wind speed $(U,+)$ where inputs followed by $(+)$ indicate direct and inverse $(-)$ proportionally respectively. The authors also examined various combinations of

changes in these variables on ETc. Of these combinations, the simulations using values of T +3 ºC, Rn +10%, ea +10%, rs +40% (~660 ppm CO2) and LAI +15% seem to be potentially the most representative of projected changes in conditions in the latter portion of the 21st century [Allen et al. 1991, Kimball (2007), Reclamation (2011)]. For these changes in input variables, the summer wheat ETc was estimated to increase by +13% and the tall grass prairie by +10%. It is important to note that these changes are estimated for a summer period at the northern hemisphere solar radiation maximum.

Kimball (2007) performed a similar type of sensitivity analysis for alfalfa growing at Maricopa, AZ. For these analyses, a PM model was calibrated to daily ET data using hourly data from nearby AZMET station during the year 1987. The calibrated PM model used to simulate temperature changes ranging from +1.2 to +5.8 ºC based on values reported in the IPCC 3rd Assessment. The ET sensitivity analysis also examined the effects of increasing stomatal resistance by 40% and LAI by 10% such as might be obtained for a crop like alfalfa at an elevated CO2 concentration around 700 ppm. For annual temperature increases in the range of +2-3.5 ºC such as estimated by the end of the 21st century in the western United States (Reclamation, 2011) and making the reasonable assumption that absolute humidity increases (Allen et al, 1991) such that relative humidity remains approximately constant, alfalfa ET during the peak growing season would increase by between 0.6% to 2.9%. Under the same assumptions, changes in annual alfalfa ET would range from -0.3% to +2.7%.

In another early study of climate change effects on crop water requirements in central and southern Great Plains (Nebraska, Kansas, Oklahoma and Texas), Allen et al (1991), employed the Penman Monteith method and unadjusted projections of changes in GCM simulated mean monthly surface air temperature, precipitation, solar radiation, humidity and wind resulting from an assumed doubling of CO2 from 330 to 660 ppm. The GCM models used for the study were the Geophysical Fluid Dynamics Laboratory (GFDL) (Manabe and Wetherald, 1987) and the Goddard Institute of Space Studies (GISS) (Hansen et al., 1988). Changes in ET and irrigation water requirements (IR) under the doubled CO2 forcing relative to the historical period from 1951-1980 were examined for alfalfa, corn and winter wheat crops. A delta change ratio method was used to create daily climate inputs based on the forced mean monthly GCM results and daily historical period records from 17 non-agricultural weather stations. Adjustments to account for differences in temperature measurements between agricultural and non-agricultural areas were applied. No adjustments in wind speed or humidity measurements were made. These measurement discrepancies would have a tendency to result in overestimates of ET. In general, both GCM models projected increases in air temperatures during the growing season on the order of +3-5 ºC. Although considerable monthly variability was projected by both models, annual precipitation changes over the region averaged about +3-5%. Considerable variation in annual wind speeds ranging -26% to +26% were reported. Humidity changes were projected to range from +32-36% and solar radiation changes during growing season months increased in a range from +1-7%.

The effects of projected temperature and solar radiation changes on the crop phenologic growth stages were used to provide estimates of changes in planting dates, acceleration of growth stages and length of the growth period. Interestingly, the authors noted that earlier and/or later growth could result in crops growing during spring and fall seasons when solar radiation was reduced thereby offsetting the effects of increased growing season length. The effects of doubled CO_2 were evaluated by assuming increases in canopy resistances of 0% (no CO_2 effects), 20%, 40%, 60% and 80%. The analyses for corn and wheat also assumed that existing basal crop coefficients (Kcb) values could be used with projected alfalfa ET as the reference crop to compute the crop ET (ETc). Soil evaporation was computed separately based on assumptions about types of irrigation systems and frequency of water applications.

For alfalfa, growing season length increased consistently throughout the region by approximately 40 days. Similarly, annual ETc increased everywhere. With no CO_2 effects on canopy resistance, the models showed significant but consistent differences with the warmer GFDL model showing greater increases in ETc (+40-60%) relative to the less warm GISS model (+30-40%). As canopy resistance was increased, a corresponding linear reduction in ETc occurred. At a 40% increase in canopy resistance similar to what has been commonly observed in many agricultural crops at 660 ppm CO_2, the projected annual ETc relative to no CO_2 effects was reduced by approximately 15% through the region. However, even at an 80% canopy resistance, alfalfa ETc increased by approximately 5-10% relative to the historic period because of the longer growth period.

For wheat winter, the growth period length was reduced by between 36-48 days throughout the region. These reductions were attributed to later fall planting and earlier spring harvest. The growth period length reductions were accompanied by corresponding reductions in annual ET. With no CO_2 effects on canopy resistance, ETc reductions ranged from -1% to -11%. At a 40% increase in canopy resistance, ETc reductions ranged from -12% to -22% (approximately - 15% relative the no CO_2 effects simulations. At an 80% increase in canopy resistance, ETc reductions ranged from -22% to -28%.

For corn, the growth period length ranged from a decrease of 80 days to an increase of 10 days. A strong latitudinal correlation was observed in the growth period length. Large decreases in the northern Great Plains were attributed to more rapid life cycle stage changes in the summer months eliminating the need for extended fall season development when reduced solar radiation and seasonal temperatures result in slower maturation. In contrast for the central and southern regions, growth period length increased slightly because reduced solar radiation during the early spring resulted in slower life cycle stage changes. These slight changes were more pronounced for the less warm GISS model. The simulated changes in annual ETc also reflected the latitudinal trends exhibited by growth period length. With no CO_2 effects on canopy resistance, ETc ranged from a 10% reduction in the northern plains to a 25% increase in the south. At a 40% increase in canopy resistance, ETc ranged from -20% in the north to +10% in the south. At

an 80% increase in canopy resistance, ETc reductions ranged from -28% in the north to -2% in the south.

In summary, this study by Allen et al. (1991) demonstrates the importance of considering the integrated effects of multiple climatic factors not just temperature and precipitation on crop ETc. Clearly, seasonal changes in other climate conditions such as solar radiation and humidity that varied with changes in planting and harvest dates exerted significant albeit potentially opposite influences on crop ETc. Finally, it is important to note that the methods used in this study simulated changes in ETc through empirical relationships between temperature (degree days) and solar radiation (photoperiod) on canopy development (LAI) without fully simulating crop growth. In the ecophysiological crop models described in the previous section, the effects in temperature, solar radiation, humidity and CO_2 on crop growth (biomass) would be explicitly simulated and could result in either increased or decreased leaf areas and stomatal conductances which in turn would affect ETc.

Izaurralde et al. (2003) used the results from the HadCM2 global climate model to assess the impacts of climate changes on agricultural production and irrigation water supplies throughout the United States for 10 year periods centered on 2030 and 2095. Projected temperatures and precipitations from the GCM were used as inputs to the EPIC crop model. However, it was not clear which of the 5 methods available in EPIC was used for estimating ETo. Furthermore, actual crop ET (ETc) is can be affected by soil properties and irrigation management which were not described. The assessment was performed at the 4 digit Hydrologic Unit Area (HUA) and only the dominant vegetation within the HUA was simulated. Although the assessments were done for individual HUAs, the reported results were combined into 10 agricultural regions of which only 4 (Pacific, Mountain, Northern Plains and Southern Plains) are located in the western United States. Because latitudinal trends in climate within the Pacific and Mountain regions are significant, the averaged results presented in this study do not reflect these important geographic differences.

The HadCM2 model was chosen because it simulates 21st century temperatures (+2.8 ºC) that are intermediate to results from several other GCM models (+1.7-5ºC) used for by the National Assessment Synthesis Team (2001). However, it is important to note the HadCM2 model projects significantly wetter conditions in California, Nevada, Utah, Arizona, New Mexico and Texas than the median values of the 112 projections presented in Reclamation's Secure Water Act Report. For example, precipitation increases ranged from 1-21% in 2030 and 12-35% in 2095. In Reclamation's report some of these same areas had decreases in precipitation ranging from 10-15% or more.

In the study, the effects of climate change on ETc were not explicitly presented. Instead, the effects of climate change on the irrigation requirements (IR) which accounts for effective precipitation were reported. For the climate sensitivity analyses, CO_2 was increased to 560 ppm corresponding to an approximately 30% increase in canopy resistance. For irrigated corn in the western region basins,

reported IR changes in 2030 ranged from -16% in the Lower Colorado to +115% in California and from -25% in the Lower Colorado to +97% in California by 2095. For irrigated alfalfa in the western region basins, reported IR changes in 2030 ranged from -3% in the Lower Colorado to +52% in Missouri and from -11% in the Lower Colorado to +71% in California by 2095.

Ficklin et al. (2009) performed an assessment of climate changes on water supplies and crop water use in the San Joaquin Valley, CA. For this assessment, the Soil Water Assessment Tool (SWAT) (Gassman et al, 2007) model was used. This model uses methods to simulate plant growth and ETc that are similar to the EPIC model that is described above. For this study, the Penman Monteith method was used to simulate crop ETc. Because SWAT simulates plant growth (biomass) and its affect on canopy resistance through LAI based on accumulated degree days, temperature exerts an additional influence on ETc beyond what is otherwise included in the PM method. However, the version of SWAT (2005) used for this study only accounts for the effects of increased CO_2 on reduced stomatal conductance but not on increased LAI. Furthermore, increased canopy temperatures that are related to stomatal closure in response to elevated CO_2 were not simulated. Consequently, the reported ETc values can be viewed as representing lower values than might actually occur if these processes had been included in the simulations.

Of the total cropland in the study area, several major crop groupings were reported by California Department of Water Resources (DWR, 2007) including fruit and nuts (38%), field crops (36%), truck crops (17%) and grains (4%). Model parameters for these crops were obtained from the SWAT model database and used without additional calibration. Soil survey data from the SSURGO database (USDA, 2007) was also used to parameterize the model. Two temperature - emission scenarios (A1F1, + 6.4 ºC - 970 ppm CO_2) and B1, +1.1 ºC - 550 ppm CO_2) were selected to represent upper limits and lower limits of future climate changes. Weather generators were used to create 50 year future daily maximum and minimum temperatures, precipitation, solar radiation and humidity time series based on climate data measured at CIMIS agrometeorology stations located in the study area.

For the lower limit B1 scenario, overall crop averaged ETc ranged from -4.2% to -13.1% as precipitation change varied from +20% to -20% relative to the current period baseline. For the upper limit A1F1 scenario, overall crop averaged ETc ranged from -35.7% to -39.7% as precipitation was changed from +20% to -20% relative to the current period baseline. If climate conditions similar to the Reclamation's median projected values of + 2.3 ºC and a -8.6 % reduction in precipitation, linear interpolation of these results indicates -27.8% change in the overall crop average ETc.

3.2 Crop Yield – Climate Interactions

In an early study using GCM results to evaluate potential climate change impacts on crop yields in the central and southern Great Plains, Rosenzwieg (1990) used the same Geophysical Fluid Dynamics Laboratory (GFDL) and the Goddard

Institute of Space Studies (GISS) temperature and precipitation outputs as Allen et al. 1991 (described above) as inputs to the CERES-Wheat and -Maize (corn) models (described above) to evaluate the effects of doubled CO_2 concentrations (660 ppm) on the yields at 14 locations in Nebraska, Kansas, Oklahoma and Texas.

In this study, future climate change was simulated by increasing CO_2 concentrations from a baseline of 330 to 660 ppm and running the models to an equilibrium climate condition. At the elevated CO_2 concentration, the GISS and GFDL simulated mean annual region-wide temperature increases were about +4.5°C and +5°C respectively. Both models projected a latitudinal trend of increased annual temperature changes (ΔT) from south to north (relative to the 1950-1980 baseline). The GISS model simulated a region-wide decrease in precipitation of about -3.3% with greater declines in the south (Rosenzweig, 1990). The GFDL model simulated a region-wide decline of only -0.8% with some precipitation increases in the south.

For the crop simulations, no downscaling or bias correction of the GCM results was performed. Daily temperature and precipitation inputs required for the CERES crop models were computed from the ratio of GCM monthly averages to observed monthly averages based on historical observations of daily data obtained from local meteorological stations. Daily solar radiation was estimated from temperature using a weather generation algorithm. A constant wind speed of 2 m s-1 was assumed in crop models. The effects of changes in humidity were not included in the study.

The CERES crop models were run for 30 year periods to compute both baseline and projected yields. Both dryland (not discussed in this report) and irrigated simulations were performed. Under irrigated conditions, water was automatically applied whenever soil moisture decreased below 80% of field capacity. To simulate the effects of CO_2 at 660 ppm on biomass, increases of 25% and 10% in daily canopy photosynthesis were assumed for wheat and corn respectively. Other assumptions described by Rosenzweig (1990) include:

- Crop parameters developed at temperatures less than those projected by the GCM simulations.

- Increased canopy temperatures due to increased stomatal resistance were not simulated.

- Overestimate of potential CO_2 yield increases because extreme climatic events, pests and nutrients were not evaluated.

In the baseline simulations, the CERES simulated yields were consistently greater than observed yields for both wheat and corn. However, no additional adjustments to the CERES model parameters were performed. Climate impact simulations were performed both with and without elevated CO_2 effects. In simulations

without the physiological effects of increased CO2, winter wheat yields typically decreased. The larger declines occurred in the southern Plains than in the northern Great Plains where annual temperature remains lower. In the GISS simulations, the projected mean yield decline was -10.9% relative to the baseline simulation with a range from +6.5% to -48.3%. In the approximately 0.5 to 1 ℃ warmer GFDL simulations without CO2 effects, the projected mean yield decline was -15.5% with a range from +0.2% to -42.7%. Wheat maturity dates occurred about three weeks earlier throughout the region because the increased temperatures caused the crop to mature more rapidly. However, this shortened growth period also resulted in less biomass production and consequently reduced yields. Including the physiological effects of CO2, increased mean wheat yields by +12% relative to the baseline in the GISS projections. This increase represents approximately a 20% increase relative to the simulations without CO2 effects (-10.9%). Increasing winter wheat yields were simulated at latitudes greater than 36° north whereas south of this latitude either no change or declines occurred. In the GFDL simulations with CO2 effects, mean wheat yields increased by +3% relative to the baseline and displayed a south to north trend ranging from -15% in the south to +15% in the north.

Similarly, simulated corn yields declined throughout the region. In the GISS simulations without the physiological effects of CO2, the projected mean corn yield decline was –16.4% with a range from -8.7% to -22.6%. In the warmer GFDL simulations, the decline in the simulated mean corn yield was -23.8% with a range from -10.9% to -37.3%. Unlike wheat, the crop yield declines were somewhat greater in north than south. In both models, corn maturity dates occurred about 2 and a half to three weeks earlier in the year due to the increased temperatures. However, simulated corn yields do not respond as much as wheat to increased atmospheric CO2 because corn's C4 photosynthetic pathway is able to accumulate sufficient photosynthetic precursors at lower ambient CO2 concentrations. Consequently, elevated CO2 does not increase yields as much as occurs in C3 plants such as wheat.

It is worth noting that Rosenzweig (1990) examined several potential adaptation strategies involving changing planting dates to earlier or later in the year and using cultivars with different vernalization requirements and photoperiod sensitivities and concluded that some improvements could be obtained but not at all locations.

In an international study of the effects of climate change on world food supply, Rosenzweig and Inglesias (1998) reported on the application of the CERES and SOYGRO (Jones et al., 1989b) models at more than 100 locations in 18 countries worldwide. In this study, GCMs including the GISS, GFDL and United Kingdom Meteorological Office (UKMO) described by Wilson and Mitchell (1987) were applied to simulate equilibrium state climate changes resulting from increased radiate forcing due to a doubling of CO2 to 660 ppm. The resulting global temperature and precipitation changes ranged from +4.2 – +5.2 ℃ and +8 - +15%, respectively.

The crop modeling involved calibration and validation using climate data for a baseline period from 1951 to 1980. Unfortunately, location specific results were aggregated to the national scale and only results for wheat were reported for the United States. For the United States, wheat yields were reported to decline between -21% to -33% without considering the effects of CO2 on photosynthesis. Including the effects of CO2, decreased the yield reduction range to -2% to -14%. The largest declines were associated with the warmest GCM (UKMO). The yield declines were reported to occur because of the combined effects of increased heat stress and a shortened of the growth period.

In the study, there was one transient simulation that explicitly included wheat, corn and soybeans yield changes in the United States. It was performed using the GISS model with results presented for 2010s, 2030s and 2050s assuming CO2 concentrations of 405, 460, and 530 ppm, respectively. For wheat, yield increases up to about 5% were reported until approximately 2040. For corn, only yield declines (-5% to -15%) occurred. However, soybean yield increases of approximately +15% to +20% occurred throughout the simulation period. Because results for both irrigated and dryland cropping were not explicitly reported, the typically beneficial effects of irrigation cannot be accessed in these results. However, it is clear from these results that significant differences in yield effects occur between C3 (wheat and soybeans) and C4 (corn) crops and that crop specific characteristics are important determinants in the crop's response to the combined effects of temperature and CO2 changes. Finally, this study demonstrates the importance of transient simulations in order to evaluate when climate change impacts become may be become significant.

Brown and Rosenberg (1999) used the results of GCM simulations to assess climate change impacts to major wheat and corn producing regions throughout the United States. The EPIC crop growth model was calibrated at representative farms using daily weather records from National Weather Service Cooperative Climate Network Stations during the baseline period (1968 – 1989). Climate generators were used to estimate daily values of solar radiation, relative humidity, and wind speed for both the baseline and climate change scenarios. At each representative farm, the EPIC model was calibrated with local yield, soil and management data obtained from variety sources.

The GISS, UK Meteorological Office Transient (Murphy, 1995) and Australian Bureau of Meteorology Research Center (McAveney et al., 1991) GCMs were used to obtained gridded temperature and precipitation over a range of projected global mean temperatures (GMTs) from +1 to +5 $^{\circ}$C. Atmospheric CO2 concentrations of 365, 560, and 750 ppm were used in the EPIC crop simulations.

In most the western United States, wheat was the only crop simulated at the representative farms. In addition, the crop production was simulated only under dryland conditions. In this region under dryland conditions, yields are typically less than under irrigated conditions. However, the GCMs projected generally wetter conditions. At a GMT increase of +1 $^{\circ}$C, winter wheat yields declined very slightly at a CO2 concentrations of 365 ppm but increased by approximately

+25% and +50% at CO2 concentrations of 560 and 750 ppm, respectively. At a GMT increase of +2.5 $^{\circ}$C, yield declines averaged about -15% at a CO2 concentrations of 365 ppm; remained slightly positive at 560 ppm CO2 and at 750 ppm ranged from about +25% to + 50% for the 3 GCMs. At a GMT increase of +5 $^{\circ}$C, yield declines ranged -5% to -75% with the greatest declines at the lowest CO2 enrichments. The effects on corn yields were similar albeit much less dramatic. The authors attributed the yield declines to early crop maturation caused by elevated temperatures.

As part of the U.S. National Assessment Study, Izaurralde et al. (2003) used climate change results from a transient simulation from the HadGM2 (formerly referred to as the UKTR model) that included the entire continental United States. This run assumed a 1% per year increase in atmospheric CO2 concentrations during the period from 1994 – 2100. In the Pacific, Mountain, Northern and Southern Plains regions, simulated minimum daily temperature increases ranged from +1.1 to +1.9 $^{\circ}$C in 2035 and +3.5 to +4.7 $^{\circ}$C by 2095 with the smallest increases along the Pacific Coast and the largest increases in the interior Mountain region. Precipitation changes ranged from +1% in the Southern Plains to +21% in the interior Mountain region by 2035 and +12% in the southern Plains to +35% in the interior Mountain region by 2095. Unlike Reclamation's projections, no declines in precipitation were reported anywhere in the western United States during the 21st century.

The EPIC model was used to simulate climate change impacts on several crops including corn and alfalfa at representative farms under both dry land and irrigated growing conditions as well as wheat and soybeans under dry land conditions. CO_2 effects on yield were simulated at 365 and 560 ppm for baseline (1961-1990), 2035 and 2095 climate conditions. Under irrigated conditions without CO2 effects, alfalfa yields relative to the baseline increased in both 2035 and 2095. The yield increases ranged from +11% to +26% in 2035 and +13% to +28% in 2095 with the largest increases occurring in the Southern Plains region. With CO2 effects at 560 ppm, yield increases ranged from +32% to 46% in 2035 and +34% to +50% in 2095 with the largest increases occurring in the Southern Plains region.

Under irrigated conditions without CO2 effects, corn yields increased relative to the baseline in both 2035 and 2095 in all regions except in the Southern Plains in 2095 where yields declined by -6%. The largest yield increase (+27%) occurred in the interior Mountain region in 2095. With CO2 at 560 ppm in 2095, the yield was increased to +38% in 2095 in the Mountain region and the largest decline decreased to -5% in the Southern Plains. The authors indicated that elevated CO2 effects were largely derived from reductions in the temperature and water stresses experienced by the crop. Because of the wetter conditions simulated by the HadGM2, decreases in water stress should be anticipated and presumably the decrease in temperature stress is associated with more rapid phonological development due to increased temperatures. However, more rapid crop development is usually associated in decreased rather than increased yields.

For winter wheat which was only simulated under dry land conditions, yields without CO_2 effects increased in both 2035 and 2095 relative to the baseline in all regions except the Southern Plains. With CO_2 effects included, simulated wheat yields increased relative to the baseline without CO_2 in all regions in both 2035 and 2095.

The authors also provided assessments of the effects of climate change on basin water yields (essentially runoff) and irrigation requirements. In general they concluded that elevated CO_2 will reduce watershed transpiration losses and result in increased water yields which combined with decreased crop transpiration will contribute to an improvement in water supply-demand imbalances. However due to with the dependence of the results on a single GCM that projects consistently wetter conditions throughout the 21st century, their quantitative projections have considerable uncertainty.

4. Description of the WEAP-CV PGM Algorithms

The WEAP-CV PGM was developed to aid planners and researchers in analyzing the balance between water supplies and water demands in light of growing concerns over climate change. The algorithms are intended for the exploration of the effects of elevated atmospheric carbon dioxide and altered climatic variables such as temperature, humidity, and wind speed on crop water use. Additionally, the PGM module allows for an accounting of the effects climate change on crop yield. This document serves as a technical reference to explain the algorithms used to make these calculations.

In order to simulate the effects of climate changes on crop water use and yield, algorithms simulate the following processes were selected for inclusion in the PGM.

- Increase in soil evaporation and plant transpiration caused by increased temperature.

- Increase or decrease in temperature stress caused by increased temperature.

- Increase in radiation use efficiency caused by elevated CO2 (fertilization effect).

- Increase in leaf area caused by elevated CO2.

- Reduction in stomatal conductance caused by elevated CO2.

- Reduction in stomatal conductance and radiation use efficiency caused by increases in vapor pressure deficit.

- Initiation, senescence, and termination of the growth period based on accumulated heat units.

- Plant growth rate and harvest yield driven by accumulation of degree day heat units.

These processes are discussed in more detail in several publications (Kimball et al., 2002; Huntington, 2004; Neitsch, et al., 2005; Long et al., 2006; Ainsworth and Long, 2005; Hatfield et al., 2008; Kimball, 2010; Bloom, 2009; Streck , 2003; Addington et al., 2004; and Ocheltree et al., 2014). At this time, there are no algorithms for the interactions between plants and nutrients in the PGM.

As described in Section 2 above, there are multiple approaches representing varying levels of bio-physical interactions. For this study, the objective was to primarily simulate crop water use and secondarily yield recognizing the need to perform century long simulations a large basin scale. The algorithms implemented in the PGM model were drawn from three main sources. The evapotranspiration calculations were largely extracted from the ASCE EWRI standardized reference crop ET calculations (Allen et al., 2005). In the case of variables related to crops other than the standard reference crops described in ASCE EWRI, the algorithms found in SWAT version 2005 were utilized (Neitsch, et al., 2005). Calculations of crop growth and yield were based on the routines described in the SWAT and APEX models (Neitsch, et al., 2005; Williams et al., 2008) with modifications to simulate an increase in leaf area index caused by elevated CO_2 concentration (Eckhardt, et al., 2002). Soil water balance calculations are similar to those found in the SWAT and APEX models (Neitsch, et al., 2005; Williams et al., 2008). Details of these models are described in section above.

4.1 Potential Evapotranspiration

In WEAP-CV PGM, a tall grass (alfalfa) reference, as described in Allen et al. (2005) is used as the reference crop. In the description of the evapotranspiration (ET) algorithm that follows, the source of each equation is provided. Equations were taken from the ASCE EWRI standardized reference evapotranspiration document (Allen et al., 2005) and SWAT documentation (Neitsch, et al., 2005, Eckhardt et al 2002).

The model estimates potential evapotranspiration (PET) for each daily time step using the approach found in SWAT:

1. The potential evapotranspiration is initially estimated for the alfalfa reference crop (PETDAY) using the Penman-Monteith method.

2. The maximum plant evapotranspiration (EPMAX) is estimated using the Penman-Monteith method for specific crops such as annuals, and

deciduous and non-deciduous perennial crops.

3. Evaporation from the crop canopy is calculated as a function of the size of the crop canopy and available moisture.

4. Potential bare soil evaporation is calculated as a function of canopy cover and crop residues.

5. The sum of canopy evaporation, crop transpiration, and bare soil evaporation is compared to PETDAY. If the sum exceeds PETDAY, then potential bare soil evaporation and maximum plant transpiration (EPMAX) are reduced, in that order.

4.2 Potential Evapotranspiration for the Alfalfa Reference Crop (PETDay)

$$PETDay = \frac{DLT * RN + rho * cp * 86400 * VPD / AR}{HV * (DLT + GMA * [1 + CR / AR])}$$

Eq. 1

Where

$PETDay$: potential plant transpiration in mm d^{-1} *[Eq. 2:2.2.1 in SWAT 2005]*

DLT: slope of the saturation vapor pressure curve in kPa ℃$^{-1}$

RN: net radiation in MJ m^{-2} d^{-1}

rho: air density in kg m^{-3}

cp: specific heat of moist air at constant pressure in MJ kg^{-1} ℃$^{-1}$

VPD: vapor pressure deficit in kPa

AR: aerodynamic resistance for heat and vapor transfer in s m^{-1}

HV: latent heat of vaporization in MJ kg^{-1}

GMA: psychrometer constant in kPa ℃$^{-1}$

CR: canopy resistance for vapor transfer in s m^{-1}

To calculate potential evapotranspiration, the Penman-Monteith method must be solved for a reference crop. The model uses alfalfa at a height of 40 cm with a minimal leaf resistance of 100 s m-1. The terms necessary to solve the Penman-Monteith equation for the alfalfa reference crop are as follows:

a) The slope of saturation vapor pressure curve is calculated using the following equation:

$$DLT = \frac{4098 \; \exp\left(\dfrac{17.27 * T}{T + 237.3}\right)}{(T + 237.3)^2}$$

Eq. 2

Where

DLT: slope of saturation vapor pressure curve in kPa °C^{-1} *[Eq. 5 in ASCE EWRI]*

T: daily mean air temperature ($[T_{min} + T_{max}] / 2$) in °C

b) The net radiation for PET is calculated using the following equation:

$$RN\_PET = ralb + rout$$

Eq. 3

Where

RN_PET: net radiation for PET in MJ m^{-2} d^{-1} *[Eq. 15 in ASCE EWRI]*

ralb: net short-wave radiation for PET in MJ m^{-2} d^{-1}

rout: net outgoing long-wave radiation in MJ m^{-2} d^{-1}

$$ralb = ra * (1.0 - 0.23)$$

Eq. 4

Where

ralb: *[Eq. 16 in ASCE EWRI]*

ra: extraterrestrial radiation in ASCE EWRI or daily mean short-wave radiation in MJ m^{-2} d^{-1}

Note: Surface albedo is assumed to be a constant value of 0.23 characteristic of a standardized short or tall reference crop.

$$rout = rbo * rto * 4.9\text{E-}9 * \left[\frac{T_{K\,max}^{4} + T_{K\,min}^{4}}{2} \right]$$

Eq. 5

Where

rout: [Eq. 17 in ASCE EWRI]

$T_{K\,max}$: maximum absolute temperature during the 24-hour period [K] (K=°C+273.16)

$T_{K\,min}$: minimum absolute temperature during the 24-hour period [K] (K=°C+273.16)

Note: 4.9E-9 is the Stefan-Boltzman constant

$$\mathbf{rbo} = -(0.34 - 0.139 * \sqrt{\mathbf{ED}})$$
Eq. 6

Where

rbo: net emissivity [Eq. 17 in ASCE EWRI]

ED: actual vapor pressure [kPa]

There are two options for calculating the actual vapor pressure. One takes into consideration the min and max relative humidity, the second option determines the vapor pressure using dew point temperature. If the dew point temperature data are available, it is the preferred method (Allen et al., 2005).

Option 1. Min and Max Relative Humidity approach for determining vapor pressure

$$\mathbf{ED} = \frac{\mathbf{svpmin} * \mathbf{maxRH}/100 + \mathbf{svpmax} * \mathbf{minRH}/100}{2}$$
Eq.7

Where

ED: [Eq. 11 in ASCE EWRI]

svpmin: minimum saturation vapor pressure using the ASCE EWRI approach in kPa

svpmax: maximum saturation vapor pressure using the ASCE EWRI approach in kPa

maxRH: maximum relative humidity in percent

minRH: minimum relative humidity in percent

$$\mathbf{svpmin} = \mathbf{0.6108} * \mathbf{e}^{17.27*MinTemp/237.3+MinTemp}$$
Eq.8

$$\mathbf{svpmax} = \mathbf{0.6108} * \mathbf{e}^{17.27*MaxTemp/237.3+MaxTemp}$$
Eq.9

$$\mathbf{SVP} = \frac{\mathbf{svpmin + svpmax}}{\mathbf{2}}$$
Eq. 10

Where:

svpmin: [Eq. 7 in ASCE EWRI]

svpmax: [Eq. 7 in ASCE EWRI]

SVP: saturation vapor pressure in kPa *[Eq. 6 in ASCE EWRI]*

MinTemp: minimum temperature in °C

MaxTemp: maximum temperature in °C

Option 2. Dew Point Temperature approach for determining actual vapor pressure

ED: Actual vapor pressure using dew point temperature in kPa

$$\mathbf{ED} = \mathbf{0.6108} * \mathbf{e}^{17.27*Dew\ Point\ Temp/237.3+Dew\ Point\ Temp}$$ **Eq.11**

Where:

ED: [Eq. 8 in ASCE EWRI]

Dew Point Temp: dew point temperature in °C

Note: Dew point temperature can be measured directly or computed from relative humidity and air temperature

The cloudiness function is estimated as follows:

$$\mathbf{rto = 1.35 * (\frac{Rs}{RMx}) - 0.35}$$
Eq. 12

Where

rto: Cloudiness function [dimensionless] (limited to 0.05≤rto≤1.0)
        [Eq. 18 in ASCE EWRI]

Rs/RMx: relative solar radiation (limited to limited to 0.3≤Rs/Rso≤1.0)

Rs: measured or calculated solar radiation for the day in MJ m^{-2} d^{-1}

RMx: calculated clear-sky radiation in MJ m^{-2} d^{-1}

The ratio Rs/RMx in Eq. 12 represents relative cloudiness and is limited to 0.3 < Rs/RMx ≤ 1.0 so that rto has limits of 0.05 ≤ rto ≤ 1.0.

To calculate the maximum possible radiation for the day, the solar declination, the relative distance of the earth from the sun, the sine and cosine of the site's latitude, and the corresponding Julian day have to be known.

Solar declination:

$$\mathbf{sd = 0.409 * Sin\left(\frac{JulianDay}{58.09} - 1.39\right)}$$
Eq. 13

Where

sd: solar declination in radians *[Eq. 24 in ASCE EWRI]*

The eccentricity of the orbit is calculated as:

$$\mathbf{dd = 1 + 0.033 * Cos}\left(\frac{\mathbf{JulianDay}}{\mathbf{58.09}}\right)$$

Eq. 14

Where

dd: inverse relative distance factor (squared) for the earth-sun [unitless]

[Eq. 23 in ASCE EWRI]

Sine and Cosine of the site's latitude (Lat):

$$\mathbf{latsin = Sin\ (Lat * 2\pi/360)}$$

Eq. 15

$$\mathbf{latcos = Cos\ (Lat * 2\pi/360)}$$

Eq. 16

The sunset hour angle, h, is given by:

$$\mathbf{h = ArcCos[-tan\ (lat)\ tan(sd)]}$$

Eq. 17

$$\mathbf{ys = latsin * Sin\ (sd)}$$

Eq. 18

$$\mathbf{yc = latcos * Cos\ (sd)}$$

Eq. 19

Where

h: *[Eq. 27 in ASCE EWRI]*

Extraterrestrial radiation, ra, is defined as short-wave solar radiation in the absence of an atmosphere. It is a well-behaved function of the Julian Day of the year and latitude. It is needed for calculating RMx, which is in turn used in calculating Rn. For daily (24-hour) periods, ra can be estimated from the solar constant, the solar declination and the julian day of the year as follows:

$$ra = 37.586 * dd * (h * ys + yc * Sin(h))$$
  Eq. 20

Where

  ra: [Eq. 24 in ASCE EWRI]

When a dependable, locally calibrated procedure for determining RMx is not   available, RMx, for purposes of calculating Rn, can be computed as:

$$RMx = (0.75 + 2 * 10^{-5} \, Elev) \, ra$$
  Eq. 21

Where

  RMx: [Eq. 19 in ASCE EWRI]

  Elev: station elevation above sea level in m

The net radiation for maximum plant evapotranspiration (ET) is calculated by the following equation:

$$RN\_ET = ralbl + rout$$
Eq. 22

Where:

  RN_ET: net radiation for maximum plant ET in MJ m^{-2} d^{-1} *[Eq. 42 in ASCE EWRI]*

ralb1: net short-wave radiation for maximum plant ET in MJ m^{-2} d^{-1}

$$\mathbf{ralb1 = ra * (1.0 - albday)}$$
Eq. 23

Where:

ralb1: [Eq. 43 in ASCE EWRI]

albday: surface albedo for the day

To calculate the albedo for the day, the residue on soil surface for current day has to be determined.

$$\mathbf{SolCov = Max\ (0.8 * [PBio + Residue], 0.0)}$$
Eq. 24

$$\mathbf{eaj = Exp\ (cej * [SolCov + 0.1])}$$
Eq. 25

$$\mathbf{albday = 0.23 * (1.0 - eaj) + \ salb * eaj}$$
Eq. 26

If the crop type is non-deciduous and completely covers the soil, albedo is constant:

$$\mathbf{albday = 0.23}$$
Eq. 27

Where:

SolCov: aboveground biomass and residue for current day in Tonnes/ha   *[SWAT 2005]*

PBio: potential biomass production for current day in Tonnes/ha (Computed in PGM)

Residue: crop residue on soil surface after harvest in Tonnes/ha

eaj: soil cover index *[Eq. 1:1.2.16 in SWAT 2005]*

cej: constant $(-5*10^{-5})$

salb: soil albedo for wet bare soil (0.08)

albday: [Eq. 1:1.2.15 in SWAT 2005]

The psychrometric constant is calculated by the following equation:

$$GMA = \frac{1.013E-3 * PB}{0.622 * HV}$$
Eq. 28

Where:

GMA: [Eq. B.12 in ASCE EWRI]

Specific capicity of moist air = 1.013E-3

Ratio of molecular weight of water vapor to dry air = 0.622

The atmospheric pressure is calculated by the following equation:

$$PB = 101.3 \left(1.0 - 2.21E - 5 * ELEV\right)^{5.257}$$
Eq. 29

Assuming reference temperature of 293K – see ASCE EWRI Eq. 3

PB: atmpposheric pressure in kPa *[Eq. 3 in ASCE EWRI]*

ELEV: elevation of the site in meters [m] above mean sea level

$$HV = 2.501 - 2.361E - 3 * TX$$
Eq. 30

HV: latent heat of vaporation in MJ/kg *[Eq. B.7 in ASCE EWRI]*

TX: average daily air temperature in ºC

The specific heat of moist air at constant pressure is as follows in MJ kg-1 °C-1:

$$cp = 1.013E - 3$$
Eq. 31

The air density, rho, (kg/m3) is calculated by the following equation:

$$\text{rho} = 3.486 * PB / Tkv$$
Eq. 32

Where:

   rho: [Eq. B.10 in ASCE EWRI]

$$Tkv = \frac{TX + 273.16}{1.0 - 0.378 * \left(\frac{ED}{PB}\right)}$$
Eq. 33

Tkv: virtual temperature (°K) [Eq. B.11 in ASCE EWRI]

Vapor pressure deficit (kPa) is calculated by the following equation:

$$\text{VPD} = SVP - ED$$
Eq. 34

Where:

   VPD: vapor pressure deficit in kPa *[Eq. 1:2.3.5 in SWAT 2005]*

   SVP: saturation vapor pressure at mean air temperature in kPa

   ED: actual vapor pressure at mean air temperature in kPa

The aerodynamic resistance is calculated by the following equation:

$$AR = \frac{109.6}{U2}$$

Eq. 35

Where

> *AR:* aerodynamic resistance in s/m *[Constant 109.6 is derived from ASCE EWRI Eq. B.2 for 0.5 m alfalfa reference crop and 2 m shelter height]*

> *U2:* mean daily wind speed at 2 m height in m s^{-1}

Note: This equation is similar to Eq. B.2 in ASCE EWRI when the measurement height is 2 m and the reference crop height is 0.5 m as assumed for the tall reference crop (alfalfa). When equation B.2 is used the value in the numerator is 109.6.

The canopy resistance is calculated by the following equation:

$$CR = \frac{45}{1.4 - 0.4 * (CO2 / 330)}$$

Eq. 36

Where:

> *CR:* canopy resistance in s/m *[Constant 45 based on alfalfa reference crop in ASCE EWRI Table 2]*

> *CO2:* atmospheric carbon dioxide concentration in ppm

Note: This equation is similar to Eqs. B.3 to B.6 in ASCE EWRI. In the ASCE standardized reference eqn., the tall crop (alfalfa) canopy resistance is assumed to be 45 s m-1.

4.3. Maximum Plant Evapotranspiration (EPMax)

To calculate the maximum plant evapotranspiration (EPMax) for a specific crop, the Penman-Monteith method is solved as follows:

$$\mathbf{EPMax = \frac{DLT * RN\_ET + rho * cp * 86400 * VPD / ARMxET}{HV * (DLT + GMA * (1 + CRMxET / ARMxET))}}$$

Eq. 37

Where

> *EPMax:* maximum plant evapotranspiration for a specific crop in mm d^{-1} *[Eq. 2:2.2.1 in SWAT 2005]*

> *DLT:* slope of the saturation vapor pressure curve in kPa ºC^{-1}

RN_ET: net radiation for maximum plant ET in MJ m^{-2} d^{-1} *[Eq. 42 in ASCE EWRI]*

rho: air density in kg m^{-3}

cp: specific heat of moist air at constant pressure in MJ kg^{-1} °C^{-1}

VPD: vapor pressure deficit in kPa

ARMxET: aerodynamic resistance for maximum plant ET in s m^{-1}

HV: latent heat of vaporization in MJ kg^{-1}

GMA: psychrometric constant in kPa °C^{-1}

CRMxET: Canopy resistance for maximum plant ET in s m^{-1}

To make sure maximum ET is not greater than potential ET (reference crop: Alfalfa)

EPMax = Min (EPMax, PETDay)
    Eq. 38

Where:

EPMax: Maximum evapotranspiration for a specific crop in mm d^{-1} *[SWAT 2005 Code]*

The wind speed and height of wind speed measurement is calculated by the following equations based on the approach taken in SWAT.

If the crop height is less than 1.0 m (CPHT<1.0) in height, the wind speed is adjusted as follows:

UZZMxET = U2
    Eq. 39

ZZMxET = 200
    Eq. 40

ZOM = 0.123 * CHZ
    Eq. 41

If the crop height is greater than 1.0 m and less than or equal to 2.5 m (1.0<CPHT≤2.5) in height, the wind speed is adjusted as follows:

ZZMxET = CPHT * 100 + 100
    Eq. 42

ZOM = 0.123 * CHZ
    Eq. 43

$$UZZMxET = U2 * \left(\frac{Log\left(\frac{ZZMxET - D}{ZOM}\right)}{Log\left(\frac{200 - D}{ZOM}\right)} \right)$$

Eq. 44

If the crop height is greater than 2.5 m (CPHT>2.5) in height, the wind speed is adjusted as follows:

ZZMxET = CPHT * 100 + 100

Eq. 45

UZZMxET = U2 * (ZZMxET/200)^0.2

Eq. 46

ZOM = 0.058 * CHZ^1.19

Eq. 47

Where:

UZZMxET: wind speed (m s^{-1}) at height *ZZ* (cm) *[Eq. B.14 in ASCE EWRI]*

ZZMxET: height at which wind is determined in cm *[Eq. B.14 in ASCE EWRI]*

CPHT: canopy height in m

ZOM: roughness length for momentum transfer in cm *[Eq. B.14 in ASCE EWRI]*

CHZ: canopy height in cm

The canopy height is calculated by the following equation. If crop height is less than 0.01 m, canopy height is as follows:

CHZ = 1.0

Eq. 48

Otherwise

CHZ = CPHT * 100

Eq. 49

Where

CHZ: [SWAT 2005 Code]

The roughness length for vapor transfer is calculated by the following equation.

ZOV = 0.1 * ZOM
   Eq. 50

Where:

ZOV: roughness length for vapor transfer in cm *[Eq. 2:2.2.6 in SWAT 2005]*

The zero-plane displacement of wind profile is calculated by the following equation.

D = 0.667 * CHZ
   Eq. 51

Where:

D: displacement height for plant type in cm *[Eq. 2:2.2.7 in SWAT 2005]*

The aerodynamic resistance for maximum plant ET is calculated by the following equation.

$$\text{ARMxET} = \frac{\ln[\frac{(\text{ZZMxET}-\text{D})}{\text{ZOM}}] * \ln[\frac{\text{ZZMxET}-\text{D}}{\text{ZOV}}]}{(0.41^{\wedge}2) * \text{UZZMxET}}$$
   Eq. 52

Where:

ARMxET: aerodynamic resistance for maximum plant ET in s m^{-1}

 [Eq. 2:2.2.3 in SWAT 2005]

The stomatal conductivity is adjusted for high vapor pressure according to Figure 1 and it is calculated by the following equations.

$$\text{FvpdMxET} = \text{Max} \ (0.1, \ 1.0 - \text{bx} * \text{XX}) \qquad \text{if} \qquad \text{XX} > 0$$
Eq. 53

$$\text{FvpdMxET} = 1.0 \qquad\qquad\qquad\qquad \text{if} \qquad \text{XX} < 0$$

$$\text{gsi\_adj} = \text{gsi} * \text{FvpdMxET}$$
Eq. 54

Where:

XX: VPD – vpth
Eq. 55

bx = (1 – vpd2) / (vpdabth – vpth)
Eq. 56
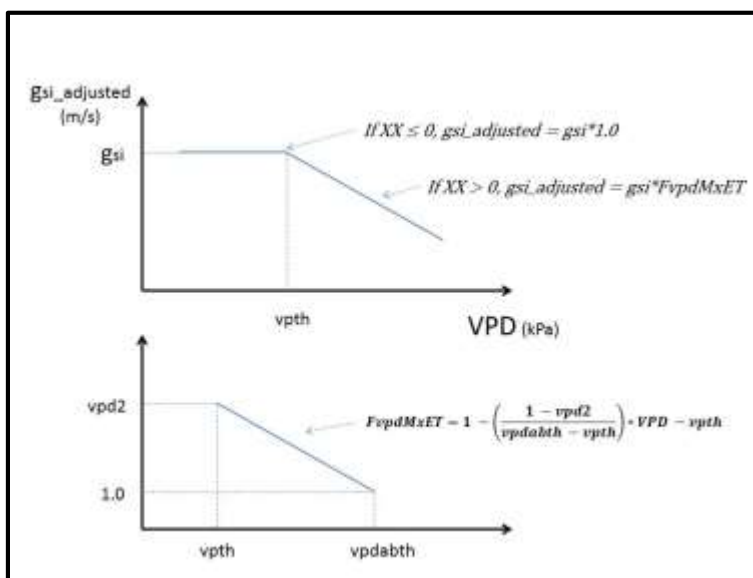
Figure D-3. Stomatal conductivity adjustment for high vapor pressure

FvpdMxET: [SWAT 2005 Code]

gsi_adj: adjusted stomatal conductivity for high vapor pressure in m s^{-1}

[SWAT 2005 Code]

gsi: maximum stomatal conductance in m s^{-1}

bx: rate of decline in leaf conductance per unit increase in VPD (m s^{-1} kPa^{-1})

[Eq. 2:2.2.16 in SWAT 2005]

vpd2: corresponding fraction of the maximum stomatal conductance at the value   of VPD

vpdabth: value of VPD above vpth

vpth: threshold VPD above which the stomatal conductivity is adjusted in kPa

The canopy resistance for maximum plant ET is calculated by the following equation.

$$\textbf{CRMxET} = \frac{\frac{\textbf{1.0}}{\textbf{gsi\_adj}}}{(\textbf{0.5} * \textbf{LAI}) * (\textbf{StomResp1} - \textbf{StomResp2} * \frac{\textbf{CO2}}{\textbf{330}})}$$

Eq. 57

Where:

CRMxET: Canopy resistance for maximum plant ET in s m^{-1}

[Eq. 2:2.2.15 in SWAT 2005]

LAI: Leaf area index of canopy

StomResp1: Stomatal response value 1 at elevated CO_2 concentration (C3/C4   crop parameter dimensionless)

StomResp2: Stomatal response value 2 at elevated CO_2 concentration (C3/C4   crop parameter dimensionless)

CO2: Carbon dioxide concentration in the atmosphere (ppm)

4.4. Canopy Interception

Canopy interception is the portion of rainfall that remains in the canopy and does not contribute to surface runoff or infiltration. PGM allows the maximum amount of water that can be held in canopy storage to vary from day to day as a function of the leaf area index as follows:

$$CanMxl = CanMx * \frac{LAI}{XLAI330}$$

<div align="center">

Eq. 58

</div>

Where:

CanMxl: maximum amount of water that can be trapped in the canopy on a given day in mm of H_2O *[Eq. 2:2.2.1 in SWAT 2005]*

CanMx: maximum amount of water that can be trapped in the canopy when the canopy is fully developed in mm of H_2O

LAI: leaf area index for a given day (dimensionless)

XLAI330: maximum leaf area index for the plant at 330 ppm of CO_2 (dimensionless)

When precipitation falls on any given day, the canopy storage is filled before any water is allowed to reach the ground and infiltrate or become surface runoff.

When rainfall is less than the difference between CanMxl and CanStor:

$$CanStor = CanStor + RF$$

Eq. 59

$$RF = 0$$

Eq. 60

Otherwise

$$CanStor = CanMxl$$

Eq. 61

$$RF = RF – (CanMxl – CanStor)$$

Where

CanStor: amount of free water held in the canopy on a given day in mm

[Eq. 2:2.1.2 in SWAT 2005]

RF: rainfall reaching the ground on a given day in mm *[Eq. 2:2.1.3 in SWAT 2005]*

Once the potential evapotranspiration is determined, the actual evaporation is calculated. This model first evaporates any rainfall intercepted by the canopy. Next, the model calculates the maximum amount of transpiration and the maximum amount of soil evaporation.

The model removes as much water as possible from canopy storage when calculating actual evaporation. If potential evapotranspiration, PETDAY, is less than the amount of free water held in the canopy, CanStor, then

CanStor = (CanStor - PETDAY)
Eq. 62

CanET = PETDAY
Eq. 63

EPMax = 0
Eq. 64

ESMax = 0
Eq. 65

Otherwise

CanET = CanStor
Eq. 66

CanStor = 0
Eq. 67

Where:

CanET: Plant canopy evapotranspiration in mm

4.5. Potential Soil Evaporation

To calculate the potential soil evaporation (ESMax), PETDay from the Penman-Monteith method is used as follows:

ESMax = PETDay * eaj
Eq. 68

Eos1 = PETDay / (ESMax + EPMax)
Eq. 69

Eos1 = ESMax * Eos1
Eq. 70

$$\textbf{ESMax = Min (ESMax, Eos1)}$$
Eq. 71

Where:

 eaj: soil cover index. See Eqn 25.

To be sure that maximum plant and soil evapotranspiration do not exceed potential ET, the following equations and conditions are used.

IF PETday – CanET < EPMax + ESMax THEN
 Eq. 72

ESMax = PETDay * ESMax / (ESMax + EPMax)
 Eq. 73

EPMax = PETDay * EPMax / (ESMax + EPMax)

ELSE

ESMAX = ESMAX

EPMAX = EPMAX
 Eq. 74

5. Soil Water Balance & Actual Evapotranspiration

5.1. Soil Water Movement

Precipitation that is not intercepted by the canopy can become either surface runoff or infiltrates into the soil. Water in the soil exits the model domain through either transpiration, evaporation, or deep percolation out the bottom of the root zone.

Of these different pathways, plant uptake of water removes the majority of water that enters the soil profile. The potential plant uptake as a function of depth is calculated using:

$$\textbf{UXLayers(i)} = \frac{\textbf{EPMax}}{\textbf{1} - \textbf{Exp}(-\textbf{bw})} * \left(\textbf{1} - \textbf{Exp}\left(-\textbf{bw} * \frac{\textbf{TotLayDepth(i)}}{\textbf{RDepth}}\right)\right)$$
 Eq. 75

Where:

 UXLayers(i): potential transpiration from soil layer between the ground surface and the bottom of layer (i) in mm d^{-1} *[Eq. 5:2.2.1 in SWAT 2005]*

 bw: water-use distribution parameter (10 by default),
dimensionless

TotLayDepth(i): distance from the soil surface to the bottom of layer (i) in mm

RDepth: depth of root development in the soil in mm

The potential water uptake from a particular soil layer can be calculated by solving the previous equation for the depth at the top and bottom of the soil layer and taking the difference between the values. Since root density is greatest near the soil surface and decreases with depth, the water uptake from the upper layer is assumed to be much greater than that in the lower layers. The water-use distribution parameter, bw, is set to 10 in PGM. With this value, 50% of the water uptake will occur in the upper 6% of the root zone.

As the water content of the soil decreases, the water in the soil is held more and more tightly by the soil particles. To reflect the effect this has on a plant's ability to extract water the following equation is used:

IF   SWLayer(i) < (AWCLayer(i) / 4) THEN

$$\mathbf{F(i) \; = \; Exp\left(5 * \frac{4*SWLayer(i)}{AWCLayer(i)} - 1\right)}$$

Eq. 76

ELSE

F(i) = 1.0

Eq. 77

Where:

F(i): water availability factor (dimensionless) for layer (i) *[Eq. 5:2.2.4 in SWAT 2005]*

SWLayer (i): amount of water in the soil layer on a given day in mm

AWCLayer(i): available water capacity for layer (i) in mm

AWCLayer(i) = SWCFC(i) – SWCWP(i) [Eq. 5:2.2.6 in SWAT 2005]

SWCFC(i): soil water content at field capacity for layer (i) (fraction)

SWCWP(i): soil water content at welting point for layer (i) (fraction)

The soil layers' thickness and the number of layers defined in the model are shown in Figure 2. In PGM, there are 13 layers in total (i = 13). The

top layer, which is the evaporation layer (Z[1]), is the only layer that is defined by the user in the interface.
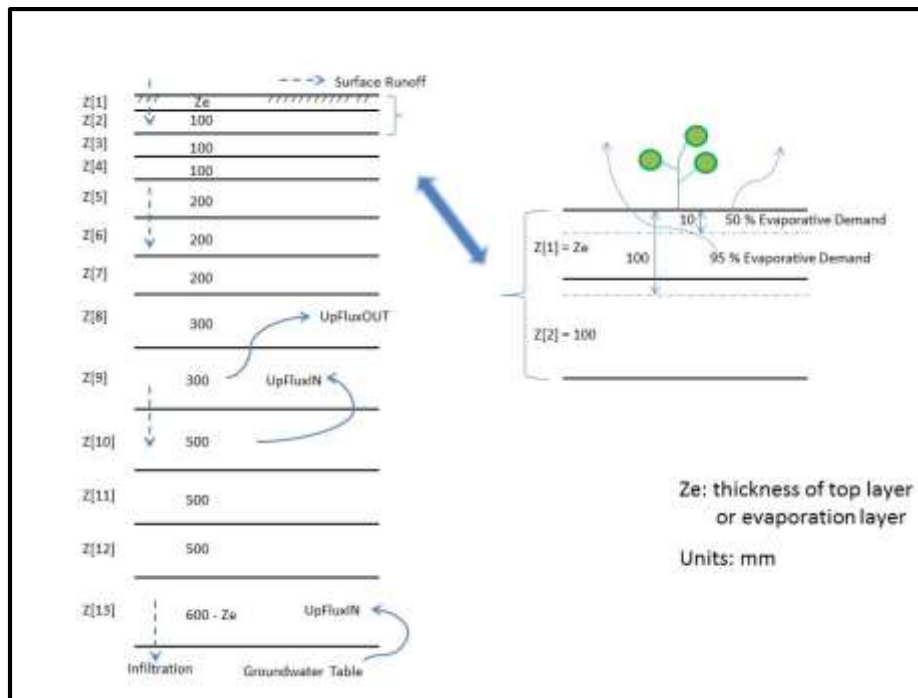
Figure D-4. Soil layer profile

Once the potential water uptake and water availability factor have been obtained for soil water conditions, the actual amount of water uptake from the soil layer is calculated.

$$\mathbf{TALayer(i) = (UXLAyer(i) + \ TRemain * epco) * \ F(i)}$$
    Eq. 78

$$\mathbf{TRemain = UX - TA}$$
    Eq. 79

Where:

   TALayer(i): actual water uptake from soil layer in mm *[Eq. 5:2.2.3 in SWAT 2005]*

   TRemain: water uptake remaining in mm

   epco: plant uptake compensation factor: 0 to 1.0 (dimensionless)

   UX: potential water use rate for the whole soil profile in mm d^{-1}

   TA: actual water uptake from the whole soil profile in mm d^{-1}

The plant uptake compensation factor (epco) allows plants to compensate for water deficiencies in dry layers by using water from other layers for

soils with good rooting environments (epco near 1.0). However, compensation is reduced and finally is not allowed as epco approaches 0.0.

The total sum of the actual water uptake from all soil layers is the actual plant transpiration for the day. Once total actual plant transpiration is calculated, actual soil evaporation must be calculated. When an evaporation demand for soil exists, the model must first partition the evaporative demand between the different layers. The depth distribution used to determine the maximum amount of water allowed to be evaporated is:

$$\textbf{EPlayer(i)} = \textbf{ESMax} * \frac{\textbf{TotLayDepth(i)}}{\textbf{TotLayDepth(i)} + \textbf{Exp(2.374} - \textbf{0.00713} * \textbf{TotLayDepth(i))}}$$
$\qquad$ **Eq. 80**

Where:

$\qquad$ *EPLayer(i):* potential evaporation demand for the soil between the soil surface and the bottom of layer (i) *[Eq. 2:2.3.16 in SWAT 2005]*

$\qquad$ *ESMax:* potential soil evaporation in mm

$\qquad$ *TotLayDepth(i):* total depth from the soil surface to bottom of layer (i) in mm

The coefficients in equation (80) were selected so that 50% of the evaporative demand is extracted from the top 10 mm of the soil and 95% of the evaporative demand is extracted from the top 100 mm of soil (Figure 2). The amount of evaporative demand for a particular soil layer is determined by taking the difference between the evaporative demands calculated at the upper and lower boundaries of the soil layer.

To reflect the decrease in soil water content in the evaporative water demand from drier soils, an evaporative water demand factor is determined based on the soil physical properties and estimated with the function:

$$\textbf{EFactor(i)} = \textbf{Min}\left(\textbf{1.0}, \textbf{Exp}\left(\textbf{2.5} * \frac{\textbf{SWLayer(i)} - \textbf{SWCFC(i)}}{\textbf{AWCLayer(i)}}\right)\right)$$
$\qquad$ **Eq. 81**

Where:

$\qquad$ *EFactor(i):* evaporative water factor for layer (i) (dimensionless) *[Eq. 2:2.3.18 in* $\qquad\qquad$ *SWAT 2005]*

$\qquad$ *SWLayer (i):* amount of water in the soil layer on a given day in mm

$\qquad$ *SWCFC(i):* soil water content at field capacity for layer (i) in mm

AWCLayer(i): available water capacity for layer (i) in mm

Once the potential evaporative soil demand has been obtained for soil water conditions, the actual amount of soil evaporation from the soil layer is calculated.

$$\mathbf{EALayer(i) = EPLayer(i) * EFactor(i)}$$
      Eq. 82

Where:

    EALayer(i): actual amount of soil evaporation from the layer (i) in mm *[Eq.   2:2.3.18 in SWAT 2005]*

In addition to limiting the amount of water removed by evaporation in dry conditions, the model defines a maximum value of water that can be removed at any time. This maximum value is 80% of the plant available water on a given day where the plant available water is defined as the total water content of the soil layer minus the water content of the soil layer at wilting point.

$$\mathbf{EALayer'(i) = Min(EALayer(i), 0.8 * (SWLayer(i) - SWCWP(i)))}$$
      Eq. 83

Where:

    EALayer'(i): amount of water removed from layer (i) by evaporation in mm   *[Eq. 2:2.3.20 in SWAT 2005]*

The amount of water removed from soil layers is determined by taking the difference between the actual evaporative demands calculated at the upper and lower boundaries of the soil layers. Even further the model limits soil evaporation to some specific soil depth. The maximum soil depth from which evaporation is allowed to occur is set to 0.5 m.

5.2. Infiltration

Infiltration is determined using the Philip Equation. The root zone sorptivity is calculated if irrigation, rainfall or water ponding is greater than 0.0.

$$\mathbf{CapDrive = \frac{0.46*m + 2.07*m^2 + 19.5*m^3}{1 + 4.7*m + 16*m^2 * 1/\alpha}}$$
      Eq. 84

$$\beta = 1.3$$

Eq. 85

$$RZSorp = (2*(SWCS - ThRZ)*Ksat*\frac{CapDrive}{\beta})^{1/2}$$

Eq. 86

$$MaxInfil =$$

$$(RZSorp*\sqrt{InfilEnd} + Ksat*InfilEnd) - (RZSorp*\sqrt{InfilStart} + Ksat*InfilStart)$$

Eq. 87

Where:

CapDrive: capillary drive

m = 1 -1/n

n: van Genuchten parameter

α: inverse of the air-entry value (bubbling pressure)

β: assumed to be 1.3

SWCS: soil water content at saturation, dimensionless

ThRZ: soil water content in root zone, dimensionless

Ksat: saturated hydraulic conductivity in length/time

RZSorp: The root zone sorptivity in lenth/time

MaxInfil: maximum infiltration rate in length/time [PGM Internal Code]

InfilEnd: time of infiltration end

InfilStart: time of infiltration start

Upflux coming into layer (i) from underneath layer (see **Figure D-4** above) is calculated with the function:

$$UpFlux(i) = KUpFlux(i)*\frac{(\psi A + CLayDepth(i-1) - \psi B + CLayDepth(i)}{CLayDepth(i-1) - CLayDepth(i)}$$

Eq. 88

Where:

UpFlux(i): Upflux coming into layer (i) in mm

KUpFlux(i): upflux hydraulic conductivity in mm s^{-1}

ψA: Pressure head at point A

ψB: Pressure head at point B

CLayDepth(i): center layer depth point for layer (i) in mm

The main assumption is that ψB is greater than ψA for upflux to happen.

If the depth of the center of layer (i) is below the groundwater table depth, the soil water content is adjusted to saturation.

if   CLayDepth(i) > WTDepth

$$\mathbf{Th(i) = SWCS(i)}$$
        Eq. 89

Where:

WTDepth: water table depth in mm [PGM Internal Code]

The ponded water mass balance is computed only for the top layer when there is water ponding (DSP > 0).

If the potential soil evaporation (ESMax) is greater or equal than total depth of applied water and ponded surface water:

$$\mathbf{Infilt(i) = 0.0}$$
        Eq. 90

$$\mathbf{EvapRemain = ESMax - DSP + TWDAL}$$
        Eq. 91

$$\mathbf{SurfEvap = DSP + TWDAL}$$
        Eq. 92

$$\mathbf{DSP = 0.0}$$
        Eq. 93

$$\mathbf{SWRO = 0.0}$$
        Eq. 94

If the potential soil evaporation (ESMax) is smaller than total applied water and depth of ponded water:

Infilt(i) = Min(DSP + TWDAL – ESMax, MaxInfil)
   Eq. 95

EvapRemain = 0.0
  Eq. 96

SurfEvap = ESMax
  Eq. 97

DSP = Min(MaxPond, DSP + TWDAL – ESMax – Infilt(i))
   Eq. 98

SWRO = DSP + TWDAL - ESMax - Infil(i) - MaxPond
  Eq. 99

Where:

  Infilt(i): infiltration into soil layer (i) in mm

  EvapRemain: evaporation remain in mm

  SurfEvap: surface evaporation in mm

  DSP: depth of surface ponding in mm

  SWRO: surface water runoff in mm

  MaxPond: maximum depth of surface ponding in mm

  TWDAL: total water depth applied to land in mm

If surface ponding is not present, runoff may still occur. In this case the model first determines if the total applied water depth is greater than the maximum infiltration and the maximum ponding depth. If so,

SWRO = TWDAL – (MaxInfilt + MaxPond)
  Eq. 100

DSP = MaxPond
  Eq. 101

Infilt(i) = MaxInfilt
  Eq. 102

EvapRemain = EA + TA
  Eq. 103

SurfEvap = 0.0
  Eq. 104

If the opposite condition is reached, the model uses the following relationships.

SWRO = 0.0
  Eq. 105

DSP = TWDAL - MaxInfilt
  Eq. 106

Infilt(i) = MaxInfilt
  Eq. 107

EvapRemain = EA + TA
  Eq. 108

SurfEvap = 0.0
  Eq. 109

Where:

> *MaxPond:* maximum ponding depth in mm
>
> *EA:* actual soil evaporation in mm
>
> *TA:* actual plant transpiration in mm

When the total applied water depth is less than the maximum infiltration rate, the model determines the following:

SWRO = 0.0
  Eq. 110

DSP = 0.0
  Eq. 111

Infilt(i) = TWDAL
  Eq. 112

EvapRemain = EA
  Eq. 113

SurfEvap = 0.0
  Eq. 114

And finally when there is no water applied at all, PGM determines the following:

SWRO = 0.0
> Eq. 115

DSP = 0.0
> Eq. 116

Infilt(i) = 0.0
> Eq. 117

EvapRemain = EA
> Eq. 118

SurfEvap = 0.0
> Eq. 119

The following steps are used to compute the soil layer water mass balance. There are two potential conditions.

1.   **The first condition is when there is infiltration at the soil surface.**

For soil layers below the groundwater table:

If CLayDepth(i) is greater than WTDepth:

$$\mathbf{Infilt(i) = \ Min\ (Ksat, infilt(i) - \ UpFluxOut(i))}$$
> Eq. 120

For cases in which there is infiltration:

> For the case where infiltration fills the soil in excess of saturation:

$$\mathbf{Infilt(i) = \big(Infilt(i-1) + UpFluxIn(i-1) - UpFluxOut(i-1) +}$$
$$\mathbf{Th(i-1) - evap - TALayer(i-1) - SWCS(i-1)\big)}$$
> Eq. 121

> For the case in which infiltration fills soil between field capacity and saturation:

$$\mathbf{Infilt(i)} = (\mathbf{Infilt(i-1)} + \mathbf{UpFluxIn(i-1)} - \mathbf{UpFluxOut(i-1)} +$$
$$\mathbf{Th(i-1)} - \mathbf{evap} - \mathbf{TALayer(i-1)} - \mathbf{SWCFC(i-1)}) * (\mathbf{1-DCF})$$

<div align="center">Eq. 122</div>

For the case in which infiltration fills soil to less than field capacity:

$$\mathbf{Infilt(i)} = \mathbf{0.0}$$

<div align="center">Eq. 123</div>

2.   The second condition is for when there is no infiltration at the ground surface:

For the case when the soil water content is in excess of saturation:

$$\mathbf{Infilt(i)} = \mathbf{Min(Ksat,(SWCS(i-1) - SWCFC(i-1)) * (1-DCF))}$$

<div align="center">Eq. 124</div>

For the case in which the soil water content is between field capacity and saturation:

$$\mathbf{Infilt(i)} = \mathbf{Min(Ksat, (\,Infilt(i-1) + UpFluxIn(i-1) -}$$
$$\mathbf{UpFluxOut(i-1) + Th(i-1) - evap - TALayer(i-1) -}$$
$$\mathbf{SWCFC(i-1)) * (1-DCF)} \qquad\qquad \text{Eq. 125}$$

For the case in which irrigation fills soil to less than field capacity:

$$\mathbf{Infilt(i)} = \mathbf{0.0}$$

<div align="center">Eq. 126</div>

Where:

> *Infilt(i):* infiltration into soil layer (i) in mm
>
> *UpFluxIn(i):* upflux going in to layer (i) in mm
>
> *UpFluxOut(i):* upflux going out from layer (i) in mm
>
> *Th(i):* soil water content for layer (i) in mm

evap: soil evaporation in mm

TALayer(i): actual plant water uptake from soil layer (i) in mm

SWCS: soil water content at saturation in mm

SWCFC: soil water content at field capacity in mm

DCF: soil water content decline factor (dimensionless) *[Eq. 2:3.2.3 in   SWAT 2005]*

Where:

$$\mathbf{DCF} = \mathbf{1} - \mathbf{Exp}(-\frac{1}{\mathbf{TT}})$$
Eq. 127

and

$$\mathbf{TT} = \frac{\mathbf{SWCS} - \mathbf{SWCFC}}{\mathbf{Ksat}}$$
Eq. 128

$$\mathbf{evap} = \mathbf{Min}(\mathbf{EALayer(i)}, \mathbf{EvapRemain})$$
Eq. 129

Where:

TT: travel time for percolation (hrs) *[Eq. 2:3.2.4 in SWAT 2005]*

evap: evaporation in mm

The model checks that plant transpiration and soil evaporation won't reduce the soil water content below wilting point. If the soil water available for transpiration and evaporation is less than what is demanded, both evaporation and transpiration are reduced using relative weights as follows:

$$\mathbf{EFrac} = \frac{\mathbf{evap}}{\mathbf{evap} + \mathbf{TALayer(i)}}$$
Eq. 130

$$\mathbf{TFrac} = \frac{\mathbf{TALayer(i)}}{\mathbf{TALayer(i)} + \mathbf{evap}}$$
Eq. 131

$$\textbf{TALayer(i)} = \textbf{TFrac} * \left(\begin{array}{c} \left(\textbf{Th(i)} - \textbf{SWCWP(i)}\right) + \textbf{Infilt(i)} + \textbf{UpFluxIN(i)} \\ - \textbf{UpFluxOUT(i)} \end{array} \right)$$

Eq. 132

$$\textbf{EALayer(i)} = \textbf{EFrac} * \left(\begin{array}{c} \left(\textbf{Th(i)} - \textbf{SWCWP(i)}\right) + \textbf{Infilt(i)} + \textbf{UpFluxIN(i)} \\ - \textbf{UpFluxOUT(i)} \end{array} \right)$$

Eq. 133

The model may allow evaporation to decrease the soil water content below wilting point.

$$\textbf{EALayer(i)} = \textbf{EALayer(i)} + \textbf{Min(EvapLeft, P5} * \textbf{SWCWP(i))}$$

Eq. 134

Where:

EFrac: fraction of evaporation to evaporate (dimensionless) [PGM Internal Code]

TFrac: fraction of transpiration to transpire (dimensionless) [PGM Internal Code]

EvapLeft: evaporation that was not met in mm [PGM Internal Code]

P5: maximum water content that can be removed below welting point (0.0≤ P5 ≤1) in the top 0.5 m of soil and it is set to 1.0 below 0.5 m (dimensionless)

Thus, model can be adjusted to allow the top 0.5 m of soil to dry down to any fraction of wilting point.

Finally the model recalculates the new soil water content by doing a soil water mass balance for each soil layer.

$$\textbf{Th(i} - \textbf{1)} = \textbf{Th(i} - \textbf{1)} + \textbf{Infilt(i} - \textbf{1)} + \textbf{UpFluxIn(i} - \textbf{1)} - \\ \textbf{UpFluxOut(i} - \textbf{1)} + \textbf{EALayer(i} - \textbf{1)} - \textbf{TALayer(i} - \textbf{1)} - \textbf{Infilt(i)}$$

Eq. 135

Also the model checks that no layer has a water content greater than saturation. If such a condition exists, then the water in excess of saturation is transferred to the layer above.

$$\textbf{Transfer(i)} = \textbf{Th(i)} - \textbf{SWCS(i)} \qquad \textbf{if} \qquad \textbf{Th(i)} > \textbf{SWCS(i)}$$
   Eq. 136

$$\textbf{Th(i)} = \textbf{SWCS(i)} \qquad \textbf{if} \qquad \textbf{Th(i)} > \textbf{SWCS(i)}$$
   Eq. 137

$$\textbf{Transfer(i)} = \textbf{0.0} \qquad \textbf{if} \qquad \textbf{Th(i)} \leq \textbf{SWCS(i)}$$
   Eq. 138

If there is a correction for excess water in the top layer, the surface runoff is adjusted.

$$\textbf{SWRO} = \textbf{SWRO} + \textbf{Transfer(i)}$$
   Eq. 139

Where:

>   *Transfer(i):* excess water transfer to layer (i) in mm
>
>   *SWCS(i):* soil water content at saturation in layer (i) in mm
>
>   *SWRO:* surface runoff in mm

5.3. Crop Growth and Yield

Crop growth is simulated with a single model using different parameters for different crop types. Due to the similarities with the APEX and SWAT models, the model can be parameterized using the databases provided with those models. The growth period for annual crops can be initiated at a user specified planting date or once a user specified number of heat units has accumulated. Leaf senescence occurs when a crop specific fraction of the heat units required to reach maturity (PHU) is reached. Harvest can be specified as a date or as a function of heat unit accumulation. Perennial crops initiate growth once the daily average air temperature exceeds the crop specific base temperature.

Phenological development of the crop is based on daily heat unit accumulation. It is computed using the equation:

$$\textbf{HU} = \textbf{0.5} * (\textbf{TMX} + \textbf{TMN}) - \textbf{TBSC} \qquad \text{HU} > 0$$
   Eq. 140

Where:

HU: number of heat units accumulated during a day *[Eq. 5:1.1.1 in SWAT 2005]*

TMX: maximum temperatures for the day in ºC

TMN: minimum temperatures for the day in ºC

TBSC: crop-specific base temperature of all variables in ºC (no growth occurs at or below TBSC)

A heat unit index is calculated by dividing the accumulated heat units by the total HU required to reach maturity (HUI = $\sum$ HU / Potential HU). The HUI ranges from 0.0 at germination to 1.0 at harvest. The timing of harvest, leaf area growth and senescence, and partitioning of dry matter among roots, shoots, and economic yield are affected by HUI.

5.4. Potential Growth

Potential growth is calculated using the following formula. Potential growth is the growth that can occur if there is no temperature, water, or nutrient stress. In this version model, only temperature and water stress are simulated.

$$Bio = 0.001 * PAR * (RUE - WAVP * X1)$$
Eq. 141

Where:

Bio: daily potential increase in biomass in t ha^{-1} d^{-1} *[Eq. 275 in APEX 2008]*

PAR: intercepted photosynthetic active radiation in MJ m^{-2} d^{-1}

RUE: radiation-use efficiency factor for converting energy to biomass (kg ha^{-1})/(MJ m^{-2})

WAVP: crop specific parameter relating RUE and VPD (kg ha^{-1})/(MJ m^{-2}/kPa)

X1: See Eq. 144 (kPa)

$$PAR = 0.5 * RA * (1.0 - exp(-0.65 * LAI))$$
Eq. 142

Where:

PAR: *[Eq. 5:2.1.1 in SWAT 2005]*

RA: solar radiation in MJ m^{-2} d^{-1}

LAI: leaf area index (dimensionless)

Constant 0.5: used to convert solar radiation to photosynthetically active radiation

Constant 0.65: light extinction coefficient (dimensionless)

$$\mathbf{RUE} = \frac{\mathbf{100 * CO_2}}{\mathbf{CO_2 + \exp(bc1 - bc2 * CO_2)}}$$

Eq. 143

Where:

RUE: [Eq. 5:2.1.4 in SWAT 2005]

CO_2: atmospheric CO_2 concentration in ppm

bc1, bc2: crop specific parameters obtained from two known values on the RUE-CO_2 curve

Note: The calculation of the parameters bc1 and bc2 from two known values on the RUE-CO_2 curve is described in the SWAT documentation (Neitsch, et al., 2005).

$$X1 = \max(0.0, \text{VPD} - VPD_{th})$$

Eq. 144

Where:

X1: [Eq. 275b in APEX 2008]

VPD: vapor pressure deficit in kPa

VPD_{th}: threshold vpd (default = 1.0)

LAI is simulated as a function of heat units, crop stress, and crop development stage. During the crop growth stages from emergence to leaf senescence, LAI is estimated with the following equations:

$$LAI = LAI_0 + dHUF * XLAI * (1.0 - Exp(5.0 * LAI_0 - XLAI) * sqrt(REG)$$
Eq. 145

$$HUF = \frac{HUI}{HUI + exp(\ell(1) - \ell(2) * HUI)}$$
Eq. 146

Where:

LAI: leaf area index value of the crop at the end of the day, dimensionless   *[Eq. 5:2.1.16 in SWAT 2005]*

LAI$_0$: leaf area index value of the crop at the beginning day, dimensionless

dHUF: daily change in HUF, dimensionless

HUF: heat unit factor, dimensionless *[Eq. 5:2.1.10 in SWAT 2005]*

XLAI: maximum leaf area index of the crop, dimensionless

REG: value of the minimum crop stress factor, dimensionless

HUI: heat unit index (0 at planting to 1 at physiological maturity) of the crop,   dimensionless

ℓ1 and ℓ2 coefficients: crop parameters relating HUF and HUI for crop

$$HUI = \frac{Acc\ daily\ HU}{Potential\ HU}$$
Eq. 147

Where:

HUI: [Eq. 5:2.1.11 in SWAT 2005]

Acc Daily HU: Cumulative heat units

Potential HU: Number of heat units required to reach maturity

From leaf senescence to the end of the growing season, LAI is estimated with the equation:

$$\mathbf{LAI = XLAI *} \left[\frac{\mathbf{1.0 - HUI}}{\mathbf{(1.0 - HUI_D)}} \right]$$

Eq. 148

Where:

LAI: [Eq. 5:2.1.19 in SWAT 2005]

HUI_D: value of HUI when LAI starts declining

5.5. Crop Height

Crop height is estimated with the relationship:

$$\mathbf{CPHT = HMX * sqrt(HUF)}$$

Eq. 149

Where:

CHT: crop height in m *[Eq. 5:2.1.14 in SWAT 2005]*

HMX: maximum height for crop

HUF: heat unit factor (see Eq. 146)

5.6. Root Growth

In the PGM, it is assumed that the portion of total biomass production allocated to the roots declines from a value of 0.4 at germination to 0.2 at maturity. The root allocation fraction is computed with the equation:

$$\mathbf{Fr_{root} = 0.40 - 0.20 * HUI}$$

Eq. 150

Where:

Fr_{root}: Fraction of total biomass partitioned to roots on a given day in the growing   season, *[Eq. 5:2.1.21 in SWAT 2005]*

HUI: Fraction of potential heat units accumulated for the plant by a given day in the growing season

5.7. Above-ground Biomass

The potential above-ground biomass is estimated as a fraction of the total crop biomass production that considers the fraction of biomass partitioned to the root system.

$$\mathbf{Bio_{above} = (1.0 - Fr_{root}) * Bio}$$
Eq. 151

Where:

Bio_{above}: potential aboveground biomass on a given day in t ha^{-1}, *[Eq. 5:2.4.4 in SWAT 2005]*

5.8. Root Depth

Rooting depth is simulated as a function of heat units and potential root zone depth:

$$\mathbf{RD = min(2.5*RDMX*HUI, RDMX, RZ)}$$
Eq. 152

Where:

RD: root depth in m for crop *[Eq. 5:2.1.23 in SWAT 2005]*

RDMX: maximum root depth in m for crop

HUI: heat unit index of the crop

RZ: soil profile depth in m

6. Growth Constraints

In the PGM, plant growth can be limited by water and/or temperature stresses.

6.1. Water Stress Factor:

The water stress factor is computed by considering the potential transpiration which is a function of the leaf area, stomatal conductance, and atmospheric conditions (EPMax). This value is compared to the moisture constrained transpiration (TALayers) that accounts for the moisture status of the soil.

$$\mathbf{WS} = \frac{\mathbf{TALayers}}{\mathbf{EPMax}}$$

Eq. 153

Where:

> *WS:* water stress factor for a specific crop (dimensionless) *[Eq. 5:3.1.1 in SWAT 2005]*

> *TALayers:* actual plant water uptake from soil layers in mm d^{-1} (See Eq. 78)

> *EPMax:* maximum plant transpiration in mm d^{-1} (See Eq.38)

6.2. Temperature Stress Factor:

The plant temperature stress is computed with the following constraints and equations:

$$\mathbf{TS} = \mathbf{Exp}\,(-\mathbf{0.1054*RTO}) \qquad \mathbf{RTO} \leq \mathbf{200\,and\,TGX} > \mathbf{0.0}$$

Eq. 154

$$\mathbf{TS} = \mathbf{0.0} \qquad \mathbf{RTO} > \mathbf{200\,or\,TGX} \leq \mathbf{0.0}$$

Eq. 155

Where:

$$\mathbf{RTO} = \frac{\mathbf{TOPC - TX}}{\mathbf{2 * TGX}}$$

Eq. 156

$$\mathbf{TGX} = \mathbf{TX - TBSC} \qquad \mathbf{TX} \leq \mathbf{TOPC}$$

Eq. 157

Where:

> *TS:* plant temperature stress factor (dimensionless) *[Eq. 5:3.1.2 to Eq. 5:3.1.5 in SWAT 2005]*

> *TX:* average daily air temperature in °C

> *TBSC:* base temperature for corresponding crop in °C

TOPC: optimal temperature for corresponding crop in °C

Finally, the plant stress factor is determined as the lowest value of the WS and TS stress factors.

$$\textbf{REG} = \textbf{Min}\ (\textbf{TS}, \textbf{WS})$$
Eq. 158

Where:

REG: plant stress factor due to either *TS* and *WS,* dimensionless

6.3. Actual Growth

Actual growth is calculated as a function of the potential growth and the plant stress factor:

$$\textbf{ActBio} = \textbf{Bio} * \textbf{REG}$$
Eq. 159

Where:

ActBio: actual plant biomass on a given day in t ha^{-1} *[Eq. 5:3.2.1 in SWAT 2005]*

Bio: potential increase in biomass in t ha^{-1} d^{-1} (See Eq. 141)

REG: plant stress factor due to TS and WS, dimensionless

For the above-ground biomass the following equation is used.

$$\textbf{ActBio}_{\textbf{above}} = \textbf{Bio}_{\textbf{above}} * \textbf{REG}$$
Eq. 160

Where:

ActBio$_{above}$: actual above-ground biomass on a given day in t ha^{-1}*[Eq. 5:3.2.1 in SWAT 2005]*

Bio$_{above}$: potential increase in above-ground biomass in t ha^{-1} d^{-1} (See Eq. 151)

7. Economic Yield

In PGM, economic yield is calculated using a harvest index. The harvest index specifies the portion of the plant mass that is harvested. This value is relatively stable for a range of plant types (SWAT 2005):

Harvest Index is calculated for each day of the plant's growing season using the relationship:

$$\mathbf{HI} = \mathbf{HI_{opt}} * \frac{\mathbf{100 * HUI}}{\mathbf{(100 * HUI + exp(11.11 - 10 * HUI)}}$$
Eq. 161

Where:

> *HI:* Potential harvest index on the day of harvest, dimensionless *[Eq. 5:2.4.1 in SWAT 2005]*
>
> *HI$_{opt}$:* potential harvest index for the plant at maturity given ideal growing conditions
>
> *HUI:* heat unit index (fraction of potential heat units accumulated for the plant on   a given day in the growing season

The potential crop yield is calculated using the following equations and constraints:

$$\mathbf{yld} = \mathbf{Bio_{above}} * \mathbf{HI} \qquad\qquad \textbf{when HI} \leq \textbf{1.00}$$
Eq. 162

$$\mathbf{yld} = \mathbf{Bio} * \left(1 - \frac{1}{\mathbf{(1 + HI)}} \right) \qquad\qquad \textbf{when HI} \geq \textbf{1.00}$$
Eq. 163

Where:

> *yld:* crop yield in t ha^{-1} *[Eq. 5:2.4.2 & Eq. 5:2.4.3 in SWAT 2005]*
>
> *Bio$_{above}$:* above-ground biomass on the day of harvest t ha^{-1}
>
> *HI:* harvest index on the day of harvest

7.1. Actual Crop Yield

In this model an actual harvest index is calculated during the second half of the crop growth season. The actual harvest index accounts for the potential impact of cumulative water stress on crop yield.

$$YLD_{Actual} = HI_{Actual} * ActBio_{Above}$$
Eq. 164

$$HI_{Actual} = (HI - HI_{Min}) \frac{WS}{WS + \exp(6.13 - 0.0883 * WS)} + HI_{Min}$$
Eq. 165

where:

YLD_{Actual} : actual crop yield in t ha^{-1} *[Eq. 281 in APEX 2008]*

HI_{Actual} : actual harvest index used to compute crop yield, dimensionless *[Eq. 5:3.3.1 in SWAT 2005]*

HI : potential harvest index on the day of harvest, dimensionless

HI_{Min} : minimum harvest index for a specific crop, dimensionless

7.2. Rice Specific Algorithms

Accurately reproducing water management practices can be one of the most complicated portions of modeling. Because water management affects the hydrologic balance, it is critical that the model is able to accommodate management practices like those used in rice production. In this section the rice ponding algorithm is described starting with pond evaporation.

The volume of water lost to evaporation from the pond is calculated using a factor, n (0.875), for free surface evaporation. The factor 0.875 is the ratio of the crop coefficient found in FAO56 for open water less than 2 m deep (1.05) and the conversion from the alfalfa reference (PETDay) to the short grass reference (1.2) (Allen et al., 2005). The total potential evaporation is then further reduced by the transpiration (EPMax) which accounts for the growth of the rice crop:

$$EPond = n * PETDay - EPMax$$
Eq. 166

where:

$EPond$: evaporation from water surface in mm

n : evaporation coefficient (0.875), dimensionless

$EPMax$: Maximum plant evapotranspiration in mm (See Eq. 38)

The volume of water lost to transpiration from a rice field:

$$TaRice = EPMax + CanET$$
Eq. 167

where:

TaRice : transpiration from rice in mm

7.3. Rice Ponding

Rice ponding is controlled by parameters that specify the depth of ponding required during various growth stages of rice crop development. The timing of ponding depth requirements is specified either using heat units or calendar dates. If using heat units to determine planting date and crop stage development (HU-HU), the following equations and constraints are employed:

$$MaxPondD = MaxPondD_1 \qquad \textit{if accHU} < \textit{Pre\_1}$$
Eq. 168

$$MaxPondD = MaxPondD_2 \qquad \textit{if Pre\_1} \leq \textit{accHU} < \textit{Pre\_2}$$
Eq. 169

$$MaxPondD = MaxPondD_3 \qquad \textit{if Pre\_2} \leq \textit{accHU} < \textit{Initial}$$
Eq. 170

$$MaxPondD = ((MaxPondD_4 - (MaxPondD_3 + 0.0833)) * (\frac{CropHU}{Develop})) + MaxPondD_3 + 0.0833$$

If JulianDay $\geq$ Initial and CropHU $<$ Develop
Eq. 171

$$MaxPondD = ((MaxPondD_5 - MaxPondD_4) * (\frac{CropHU - Develop}{Mid - Develop}) + MaxPondD_4$$

If Develop $\leq$ CropHU $<$ Mid
Eq. 172

$$MaxPondD = ((MaxPondD_6 - MaxPondD_5) * (\frac{CropHU - Mid}{Late - Mid}) + MaxPondD_5$$

If Mid $\leq$ CropHU $<$ Late
Eq. 173

$$MaxPondD = ((MaxPondD_7 - MaxPondD_6)$$
$$* (\frac{CropHU - Late}{EndLate - Late}) + MaxPondD_6$$

If Late ≤ CropHU < EndLate
   Eq. 174

where:

   MaxPondD : maximum ponding depth in mm [PGM Internal Code]

   MaxPondD_1 : maximum ponding depth before pre-flooding stage in ft

   MaxPondD_2 : maximum ponding depth during pre-flooding stage in ft

   MaxPondD_3 : maximum ponding depth during non-flooding stage in ft

   MaxPondD_4 : maximum ponding depth during Initial stage in ft

   MaxPondD_5 : maximum ponding depth during Develop stage in ft

   MaxPondD_6 : maximum ponding depth during Mid-stage in ft

   MaxPondD_7 : maximum ponding depth during Late stage in ft

   MaxPondD_8 : maximum ponding depth for EndLate stage in ft

   Pre_1 : heat units required for pre-stage_1 of flooding since January 1,   dimensionless

   Pre_2 : heat units required for pre-stage_2 of non-flooding since January 1,   dimensionless

   Initial : heat units required for initial growing stage or planting date heat units   threshold since January 1, dimensionless

   Develop : heat units required for development growing stage since planting day,   dimensionless

   Mid : heat units required for mid growing stage since planting day, dimensionless

   Late: heat units required for late growing stage since planting day, dimensionless

   EndLate : heat units required for end growing stage since planting day,   dimensionless

> *CropHU:* accumulated heat units since rice planting ^0C

> *accHU*: accumulated heat units since January 1 using a base temperature of 0 ^0C.

If using FIX-HU approach (User specified planting date with accHU determining growth stages) is employed, then the previous algorithms from Eq. 168 to Eq. 174 apply as well. The only difference is how the timing of the initial stages is determined. In the FIX-HU approach the stages prior to planting are fixed and determined based on Julian Days and then heat units are the driver for the developmental stages. The way that these stages are determined for the FIX-HU approach is described below:

> *Pre_1 :* julian day for pre-stage_1 of flooding, dimensionless (Eq. 168)

> *Pre_2 :* julian day for pre-stage_2 of non-flooding, dimensionless (Eq. 169)

> *Initial :* julian day for initial growing stage or planting date, dimensionless (Eq. 170)

> *Develop :* heat units required as a fraction of PHU (heat units required to reach maturity) for development growing stage since planting day, dimensionless (Eq. 171)

> *Mid :* heat units required as a fraction of PHU for mid growing stage since planting day, dimensionless (Eq. 172)

> *Late:* heat units required as a fraction of PHU for late growing stage since planting day, dimensionless (Eq. 173)

> *EndLate :* heat units required as a fraction of PHU for end growing stage since planting day, dimensionless (Eq. 174)

To better understand the different ponding depths and growing stages for the complete rice growing season a scheme of them is shown in **Figure D-5**. As observed in the figure, the different stages can be determined based on heat units (HU-HU approach) or a combination of Julian days and heat units (Fix-HU approach). Both approaches determine when a specific stage starts and ends.

1. Initially there is a five-day flood-up stage (Pre_1) where a ponding depth of 3 inches is reached.

2. A non-ponding period of 10-days follows the flood-up stage (Pre_2).

3. Seeding occurs at the beginning of the Initial stage (May 1) with a gradually flood-up period until 5 inches of ponding is reached by the beginning of the Develop stage.

4. Flood-up continues up to 8 inches of ponding at the beginning of Mid stage.

5. Pond depth remains constant at 8 inches until the Late stage is reached.

6. From Late stage to the EndLate stage the pond depth is gradually reduced down to zero pond depth. During this stage there are no more irrigation applications. Harvest may occur any time after the EndLate stage.
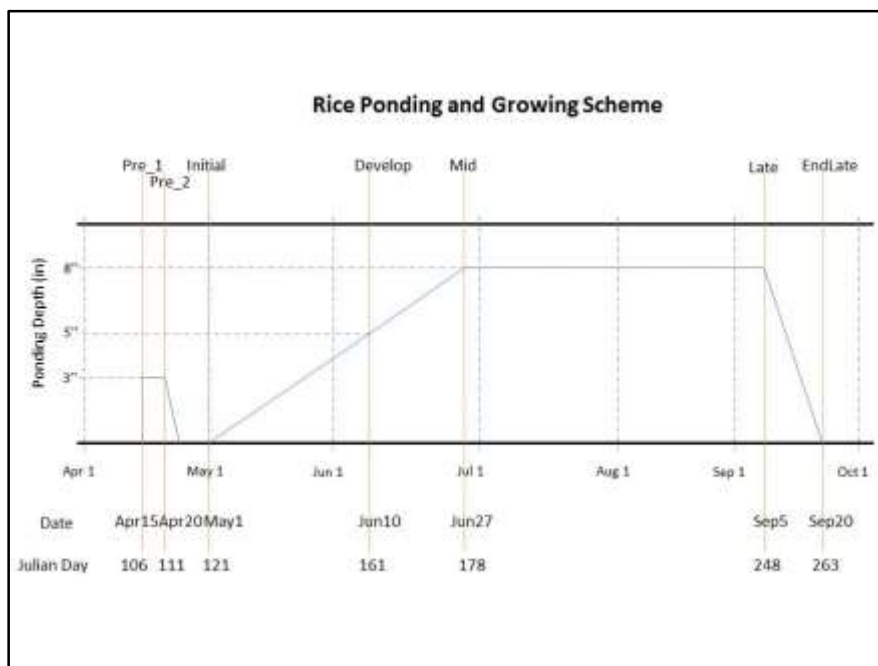
Figure D-5. Schematic representation of rice field pond depth during growing season

7.4. Deciduous Crop Algorithms

In the fall, deciduous crops lose all their leaves and become dormant for a period of time. Almonds, apples and vineyards are examples of these types of crops. For such deciduous crops some specific crop management practices must be specified including the time when irrigation ceases and the time when leaves start to fall. Specifying when irrigation ceases is necessary because after harvest occurs, deciduous crops are typically given reduced amounts of irrigation water which eventually ceases completely as the weather cools. To determine the exact day when irrigation should be stopped for each year, a temperature threshold is used. In PGM, several conditions may be applied. These conditions include temperature and Julian day of the year conditions. Finally the Julian Days may vary depending on the crop to be modeled. In PGM, the **JulianDay** and **NumDaysTempOct1** variables are hardwired into the code.

If   MinTemp < StopIrrMinTemp
        Eq. 175

        JulianDay > 274 (Oct 1)

        NumDaysTempOct1 > 3

Then

$$StopDecidIrrig = true$$
        Eq. 176

Where:

        MinTemp: minimum temperature on a specific day in °C

        StopIrrMinTemp: temperature threshold for which irrigation stops in °C

        NumDaysTempOct1: number of days with minimum temperature is lower than the   temperature threshold, dimensionless

        StopDecidIrrig: flag that indicates that irrigation must be stopped

A similar approach is used to determine the day when the "fall" starts. When this occurs, it means that the deciduous trees lose their leaves and the transpiration ceases.

If   MinTemp < FallLeavesMinTemp
        Eq. 177

        JulianDay > 305 (Nov 1)

        NumDaysTempNov1 > 3

Then

$$StartFall = true$$
        Eq. 178

Where:

        FallLeavesMinTemp: temperature threshold for which fall starts in °C

        NumDaysTempNov1: number of days with minimum temperatures lower than the   temperature threshold, dimensionless

         StartFall: flag that indicates that fall starts and leaves fall [PGM Internal Code]

7.5. Perennials Crop Algorithms

Simulation of non-deciduous perennial crop management also may require some additional conditions . Examples of some non-deciduous perennial crop include alfalfa, pasture and urban lawns. For these plant types, a specific number of cuttings can be defined. For alfalfa , up to 7 fixed cuttings are defined, and they are scheduled to happen each year based on a regular defined schedule and using Julian Days as shown below.

        Cutting 1: Julian Day 105 (Apr 15)
            Eq. 179

        Cutting 2: Julian Day 133 (May 13)

        Cutting 3: Julian Day 161 (Jun 10)

        Cutting 4: Julian Day 189 (Jul 8)

        Cutting 5: Julian Day 217 (Aug 5)

        Cutting 6: Julian Day 245 (Sep 2)

        Cutting 7: Julian Day 288 (Oct 15)

For pasture and urban lawn plant types, a slightly different approach can be used. For these crops the regularly scheduled intervals between cuttings can be employed to simulate cattle grazing and lawn mowing.

7.6. Winter Wheat Specific Algorithms

For annuals crop types, winter wheat is the only crop that is treated differently than the rest. The reason for this treatment is because winter wheat is planted in the late fall and is harvested in the late spring or early summer. To simulate these conditions, PGM only starts accumulating heat units for winter wheat beginning on June 1 of each year and continues accumulating them until May 31 of the following year. If winter wheat starts growing on December 15 as it is set up by default, it continues growing until it accumulates sufficient heat units to be harvested. On May 31, all PGM variables related to winter wheat are set up back to zero in order to start another crop cycle. Consequently during the 1st year for a model simulation run, there is not a winter wheat crop growing until the 2nd year.

References

Addington, R.N., R.J. Mitchell, R. Oren, & L.A. Donovan. 2004. Tree Physiology. 24,561-569.

Adejuwon, J. 2005. Assessing the suitability of the EPIC crop model for use in the study of impacts of climate variability and climate change in West Africa. Singapore. Trop. Geog. 26(1): 44-60.

Ainsworth, E.A. and S.P. Long. 2005. What we have learned from 15 years of free-air CO_2 enrichment (FACE)? A meta-analytic review of the responses of photosynthesis, canopy properties and plant production to rising CO_2. New Phytologist, 154(351-372).

Allen, R. G., Walter, I. A., Elliott, R., Itenfisu, D., Brown, P., M. Jensen, and R.L. Synder. 2005. ASCE Standardized Reference Evapotranspiration Equation. American Society of Civil Engineers. p. 58.

Allen, R.G., L.S. Pereira, D. Raes, M. Smith. 1998. Crop Evapotranspiration – Guidelines for computing crop water requirements – FAO Irrigation and Drainage Paper 56. United Nations FAO, Rome, Italy, 330 p.

Allen, R.G., F.N. Gichuki & C. Rosenzweig 1991. CO2-Induced Climatic Changes and Irrigation Water Requirements. Journal of Water Resources Planning and Management. Vol. 117, No. 2 pp. 157-178.

Borg, H. and D.V. Grimes. 1986. Depth development of roots with time: An empirical description. Trans. ASAE 29:194-197.

Bloom, A.J. 2010. Global Climate Change: Convergence of Disciplines. Sinauer Assoc., Sunderland, MA, 420 pp.

_____. 2009 Responses of crop plants to rising atmospheric carbon dioxide concentrations. California Agriculture 63:67-72.

Brown, R.A. and N.J. Rosenberg. 1999. Climate change impacts on the potential productivity of corn and winter wheat in their primary United States growing regions. Climate Change 41:73-107.

California Department of Water Resources (DWR). 2007. Land Use Survey Data. http://www.water.ca.gov/landwateruse/anaglwu.cfm

Hansen, J., G. Russell, D. Rind, P. Stone, A. Lacia, S. Lebedeff, R. Ruedy & L. Travis. 1988. Global climate changes as forecast by the GISS 3-D model. Journal of Geophysical Research 93:9341-9364.

Doorenbos, J. and A.H. Kassam. 1979. Yield response to water. Irrigation and Drainage Paper 33. Food Agric. Org. United Nations, Rome.

Eckhardt, K. N. Fohrer & H.G. Frede. 2002. SWAT-G, a version of SWAT99.2 modifed for application to low mountain range catchments. Phys. Chem. Earth. 27:641-644.

Ficklin, D.L., Y. Luo, E. Luedeling & M. Zhang. 2009. Climate change assessment of a highly agricultural watershed using SWAT. Journal of Hydrology. 374:16-29.

Gassman, P.W., M.R. Reyes, C.H. Green, and J.G. Arnold. 2007. The Soil and Water Assessment Tool: historical development, applications, and future research directions. Transactions of the ASABE. 50 4:1211-1250

Hatfield, J.L. 2008. The effects of climate change on agriculture, land resources, water resources and biodiversity. U.S. Climate Change Science Program: Synthesis and Assessment Product 4.3.

Huntington, T.G. 2004. Climate change, growing season length, and transpiration: Plant response could alter hydrologic regime. *Plant Biology*, 6(651-653).

Izaurralde, R.C., N.J. Rosenberg, R.A. Brown,, & A.M. Thomson. 2003. Integrated assessment of Hadley Center (HadCM2) climate-changee impacts on agricultural productivity and irrigation water supply in the conterminous United States Part II. Regional agricultural production in 2030 and 2095. Agricultural and Forest Meteorology. 117:97-122.

Jensen, M.E., R.D. Burman, and R.G. Allen (ed). 1990. Evapotranspiration and irrigation water requirements. ASCE Manuals and Reports on Engineering Practice No. 70. ASCE, N.Y. 332 pp.

Jones, J.W. and Kinery, J.R. 1986. CERES-Maize: a simulation model of maize growth and development. Texas A&M Press, College Station, Texas.

Jones, J.W., G. Hoogenboom, C.H. Porter, K.J. Boote, W.D. Batchelor, L.A. Hunt, P.W. Wilkens, U. Singh, A.J. Gijsman, & J.T. Richie. 2003. The DSSAT cropping system model.Europ. J. Agronomy. 18:235-265.

Jones, J.W., G.Y. Tsuji, G. Hoogenboom, L.A. Hunt, P.K. Thornton, P.W. Wilkens, D.T. Imamura, W.T. Bowen & U. Singh. 1989a. Decision support system for agrotechnology transfer; DSSAT v3. In: G.Y. Tsuji, G. Hoogenboom, & P.K. Thornton (Eds.). Understanding Options for Agricultural Production. Kluwer Academic, Dordrecht, the Netherlands, pp 157-177.

Jones, J.W, K.J. Boote,G. Hoogenboom, S. Jagtap & G. Wilkerson. 1998b. SOYGRO v5.42: soybean crop growth simulation model. User's Guide. Dept. of Agr. Eng. & Agro., University of Florida, Gainsville, Fl.

Keating, B.A., P.S. Carberry, G.L. Hammer, M.E. Probert, M.J. Robertson, D. Holzworth, N.I. Huth, J.N.G. Hargreaves, H. Meinke, Z. Hochman, G. McLean, K. Verburg, V. Snow, J.P. Dimes, M. Silburn, E. Wang, S. Brown, K.L. Bristow, S. Asseng, S, Chapman, R.L. McCown, D.M. Frebairn, & C.J. Smith. Europ. J. Agronomy. 18:267-288.

Kimball, B.A. 2010. Lessons from FACE: CO_2 effects and interactions with water, nitrogen and temperature. Chapter 5 in "Handbook of Climate Change and Agroecosystems." Daniel Hillel and Cynthia Rosenzweig eds.

_____. 2007. Global Change and Water Resources. In: Irrigation of Crops, 2nd ed., Agronomy Monograph no. 30, American Society of Agronomy, Madison, WI.

_____. 1983. Carbon dioxide and agricultural yield: An assemblage and analysis of 770 prior observations. Water Conservation Laboratory, Report No. 14. USDA/ARS Phoenix, AZ.

Kimball, B.A. and S.B. Idso. 1983. Increasing CO2: Effects on crop yield, water use and climate. Agricultural Water Mangement. 7:55-72.

Kimball, B.A., K. Kobayashi, and M. Bindi. 2002. Responses of agricultural crops to Free-Air CO_2 Enrichment. *Advances in Agronomy*, 77(293-368).

Long, S.P., E.A. Ainsworth, A.D.B. Leakey, J.Nosberger, and D.R. Ort. 2006. Food for thought: Lower-than-expected crop yield stimulation with rising CO2 concentrations. Science, 312:1918 – 1921.

Manabe, S. and R. Wetherald. 1987. Large-scale changes in soil wetness induced by increase in atmospheric carbon dioxide. Journal of Atmospheric Science, 44:1211-1236.

McAveney, B.J., R. Coleman, J.F. Fraser & R.R. Dhani. 1991. The Response of the BMRC AGCM to a Doubling of CO2. BMRC Technical Memorandum N. 3., Melborne, Australia.

Mearns, L.O., T. Mavromatis, E. Tsvetsinskaya, C. Hays, and W. Easterling. 1999. Comparative response of EPIC and CERES crop models to high and low resolution climate change scenarios. J. Geophys. Res. 104: 6623-6646.

Monteith, J.L., 1981. Evaporation and Surface Temperature. Quarterly Journal Royal Meteorological Society, 107, 1-27.

Murphy, J.M. 1995. Transient Response of the Hadley Center Coupled Ocean-Atmosphere Model to Increasing Carbon Dioxiode. Part I. Control; Climate and Flux Correction. J. Clim. 8:35-56.

National Assessment Synthesis Team. 2001. Climate Change Impacts on the United States. U.S. Global Change Research Program. Report for the US Global Change Research Program, Cambridge University Press,Cambridge UK, pp. 620

Neitsch, S.L., J.G. Arnold, J.R. Kiniry, and J.R. Williams. (2005) Soil and Water Assessment Tool Theoretical Documentation: Version 2005. http://www.brc.tamus.edu/swat/doc.html

Ocheltree, T.W., J.B. Nippert, & P.V.V. Prasad. 2014. Stomatal responses to changes in vapor pressure deficit reflect tissue-specifc differences in hydraulic conductance. Plant, Cell and Environment. Vol. 37, Issue 1, p. 132–139.

Penman, H.L. 1956. Evaporation: An introductory survey. Netherlands Journal of Agriculture Science 4:7-29.

Reclamation. 2011. SECURE Water Act Section 9503(c) – Reclamation Climate Change and Water 2011. Prepared by U.S. Department of the Interior, Bureau of Reclamation, Technical Services Center, Denver, Colorado.

Rosenberg, N.J., B.A. Kimball, P. Martin, & C.F. Cooper. 1990. Climate change, CO2 Enrichment and evapotransiration. In: P.E. Waggoner (Ed)), Climate Change and US Water Resources. Wiley, New York, p. 151-175.

Rosenzwieg, C. 1990. Crop Response to Climate Change in the Southern Great Plains: A Case Study. Professional Geographer. 41 1:20-37.

Rosenzweig, C. and A. Inglesias. 1998. The use of crop models for international climate change impact assessment. In: Understanding Options for Agricultural Production. G.Y. Tsuji et al. (eds). pp.267-292. Kluwer Academic Publishers. Great Britain.

Snow, V. and N. Huth. 2004. The APSIM – MICROMET module. HortResearch Internal Report No. 2004/12848. Auckland, New Zealand.

Stockle, C.O., M. Donatelli & R. Nelson. 2003. CropSyst, a cropping systems simulation model. Europ. J. Agronomy. 18:289-3007.

Stockle, C.O., J.R. Williams, N.J. Rosenberg, and C.A. Jones. 1992. A method for estimating the direct and climatic effects of rising atmospheric carbon dioxide on growth and yield of crops: Part I--Modification of the EPIC model for climate change analysis. Agric. Systems 38:225-238.

Streck, N. A. 2003. Stomatal Response to Water Vapor Pressure Deficit: An Unsolved Insolved Issue. Revista Brasileira Agrocienia. Vol. 9, No.4. p.317-322.

Thornthwaite, C. W. 1948. An approach toward a rational classification of climate. Geographical Review 38:55-94.

Tubiello, F.N. and F. Ewert. 2002. Simulating the effects of elevated CO2 on crops: approaches and applications for climate change. European Journal of Agronomy. 18:57-74

Uchijima, Z., T. Udagawa, T. Horie, and K. Kobayashi. 1968. The penetration of direct solar radiation into corn canopy and the intensity of direct radiation on the foliage surface. J. Agron. Meteorol. Tokyo 3:141-151.

U.S. Global Change Research Program, USGCRP. Scientific Assessment of the Effects of Global Change on the United States. A Report of the Committee on Environment and Natural Resources National Science and Technology Council. May 2008.

Wang, E., M.J. Robertson, G.L. Hammer, P.S. Carberry, D. Holzwoorth, H. Meinke, S.C. Chapman, J.N.G. Hargreaves, N.I. Hith & G. McLean. Europ. J. Agromony. 18:121-140.

White, J.W., G. Hoogenboom, B.A. Kimball, & G.W. Wall. 2011. Methodologies for simulating impacts of climate change on crop production. Field Crops Research. 124: 357-368.

Williams, J.W., R.C. Izaurralde, and E.M. Steglich. 2008. Agricultural Policy/Environmental Extender Model: Theoretical Documentation, Version 0604. Blackland Research and Extension Center, Temple, Texas.

Williams, J.R., C.A. Jones, J.R. Kiniry, and D.A. Spanel. 1989. The EPIC crop growth model. Trans. ASAE 32(2): 497-511.

Wilson, C.A. and Mitchell J.F.B, Mitchell. 1987.

Ziska, L.H., and J.A. Bunce. 2007. Predicting the impact of changing CO2 on crop yields: some thoughts on food. New Phytologist 175:607-618.

APPENDIX 5E. ECONOMICS PERFORMANCE ASSESSMENT TOOLS

1. Introduction

The economics performance assessment tools (EPAT) were developed as part of the Central Valley Project Integrated Resources Plan and updated for the Sacramento/San Joaquin Basin Study. Included in the EPAT is a set of economic models and assumptions that produce performance metric results for trade-off analysis. This document summarizes the key economic analysis tools for evaluation of municipal and industrial (M&I) water supply and quality and agricultural water supply.

Each economics model was modified to allow for analysis of three development scenarios (Slow Growth, Current Trends and Expansive Growth) and three levels of development (2025, 2055, and 2085). The latest models in use by U.S. Bureau of Reclamation (Reclamation) and the Department of Water Resources (DWR) were adopted and adapted to develop these modified versions. The list of economics models include:

- Municipal and Industrial Water Supply and Quality
- Least Cost Planning Simulation model (LCPSIM)
- Other Municipal Water Economics model (OMWEM)
- South Bay Water Quality model (SBWQM)
- Lower Colorado River Basin Water Quality Model (LCRBWQM)
- Agricultural Water Supply
- Statewide Agricultural Production model (SWAP)

Each of these models is briefly discussed in this document, including variables in the models that are used to establish the demand and supply conditions in the three development scenarios and three levels of development, 2025, 2055, and 2085.

[Note, completion of EPAT development is dependent on full simulation of all development scenarios at each level of development. For example, water transfer prices in LCPSIM are determined with SWAP simulations, specific to development scenario and level of development.]

2. Municipal and Industrial Water Supply and Quality

2.1 Least Cost Planning Simulation Model (LCPSIM)

The Least Cost Planning Simulation Model (LCPSIM) is an annual time-step urban water service system reliability management model (DWR 2009a). Its objective is to estimate the least-cost water supply management strategy for an area, given the mix of available supplies. The model uses a shortage loss function derived from contingent valuation studies and water agency shortage allocation strategies. It accounts for the ability of shortage management (contingency) measures, including water transfers, to reduce regional costs and losses associated with shortage events. It also considers long-term regional demand reduction and supply augmentation measures in conjunction with regional carryover storage opportunities that can reduce the frequency, magnitude, and duration of those shortage events.

A shortage event, or foregone use, is the most direct consequence of water supply unreliability. Foregone use occurs when, for example, residential users or businesses have established a lifestyle or a level of economic production based on expected availability of water that is not met in a particular year or sequence of years.

Assuming that long-term supply augmentation measures are adopted in order of their cost, with lowest cost measures adopted first, LCPSIM finds the water management strategy that minimizes the sum of the total annual cost of the adopted long-term measures and the total expected annual shortage costs and losses remaining after their adoption. The value of the availability of a supply from a proposed project of future condition, can be determined from the change it produces in this least-cost mix of supply measures and shortages.

It was assumed that regions being evaluated in LCPSIM have the facilities and institutional agreements in place to move water as needed to minimize the economic effect of shortage events. Water demands and supplies were estimated using data from the DWR, local agencies' planning studies and Urban Water Management Plans, and CalLite. LCPSIM currently evaluates two hydrologic regions, the San Francisco Bay – South and the South Coast Hydrologic Region (See Figures 1 and 2). Counties analyzed in the regions are shown in the figures.
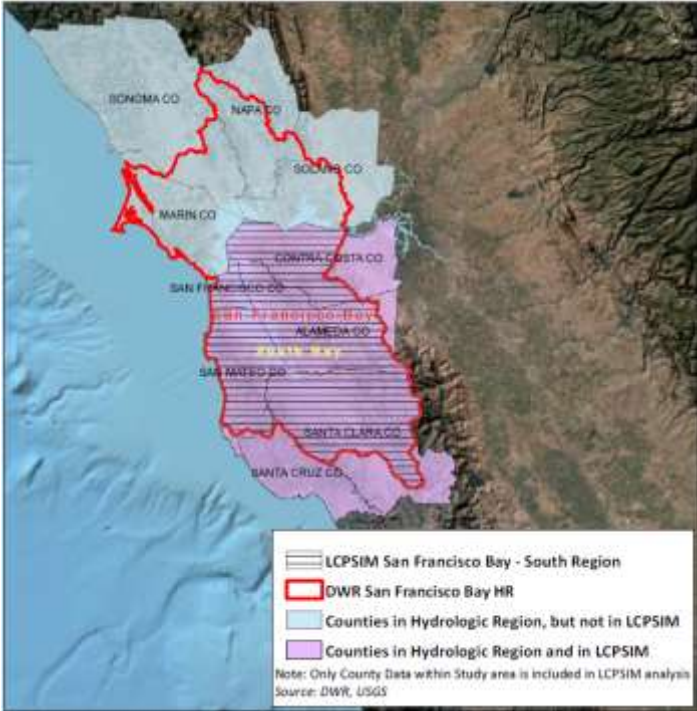
Figure 1. LCPSIM San Francisco Bay Area - South Region

Figure 2. LCPSIM South Coast Region

The LCPSIM, San Francisco Bay - South and South Coast Hydrologic Region models were updated for three development scenarios at the 2025, 2055, and 2085 levels of development. Model preparation primarily involved updating model parameters with available population and water portfolio information from Reclamation and DWR's Water Plan Update (2009b/2013). Parameters pertinent to the level of development not available from the Water Plan Update were estimated using the existing 2025 and 2055 models. Model preparation also included any necessary adjustment to the model analysis period to accommodate CalLite model outputs. Parameters in LCPSIM pertinent to the level of development and the approach proposed to update the parameters are listed in Tables 1A through 8 for the San Francisco Bay – South and Tables 1B through 8 for the South Coast HR. All costs are reported in 2007 dollars.

Regional supplies in the San Francisco Bay – South include a combination of local and imported sources. Imported supplies are delivered through the Hetch Hetchy Aqueduct, Mokelumne Aqueduct, and SWP and CVP facilities. Estimated regional supply quantities are reported in Table 1A.

TABLE 1A. LCPSIM REGIONAL SUPPLIES: SAN FRANCISCO BAY REGION–SOUTH

Regional Supplies	Baseline
Local	
Average local surface supply	38 TAF/year for all levels of development and development scenarios
Average local groundwater supply	203 TAF/year for all levels of development and development scenarios
Imported	
Hetch Hetchy Aqueduct deliveries	Annual time series from SFPUC PEIR Study WSIP1LT[a] for all levels of development and development scenarios
Mokelumne Aqueduct deliveries	Annual time series from EBMUD Freeport Regional Water Project EIS/EIR With Project EBMUDSIM study #6292[a] for all levels of development and development scenarios
SWP deliveries	Annual time series from CalLite simulation
CVP deliveries	Annual time series from CalLite simulation

[a] Time series extrapolated to 2003 using average value for water year type

Regional supplies in the South Coast Hydrologic Region include a combination of local and imported sources. Imported supplies are delivered through the LA Aqueduct, Colorado River Aqueduct and SWP and CVP facilities. Estimated regional supply quantities are reported in Table 1B.

TABLE 1B. LCPSIM REGIONAL SUPPLIES: SOUTH COAST REGION

Regional Supplies	Baseline
Local	
Average local surface supply	257 TAF/year average delivery over time-series for all levels of development and development scenarios [a].
Average local groundwater supply	1160 TAF/year for all levels of development and development scenarios
Imported	
Colorado River Deliveries	1050 TAF/year for 2010, 954.8, 846.7, and 846.7 TAF/year for 2025, 2055, and 2085 respectively [a].
LA Aqueduct	246 TAF/year average delivery over time-series for all levels of development and development scenarios [a].
SWP deliveries	Annual time series from CalLite simulation
CVP deliveries	Annual time series from CalLite simulation

Source: NODOS Study- IRPSIM output

Water management actions, including recycling, desalination, and single-year transfers, are estimated for the San Francisco Bay – South in Table 2A and South Coast Region in Table 2B. Recycling and desalination estimates reflect the reasonable and foreseeable water management actions in future conditions. Single-year transfers represent the cost of additional supply from fallowing agricultural land in the Sacramento and San Joaquin Valleys. These costs vary depending on the water supply condition.

Table 2a. LCPSIM Water Management Actions (CalFED): San Francisco Bay Region–South

Water Management Actions (CALFED)		Baseline
Local recycling		51 TAF/year for all levels of development and development scenarios
Desalination		0 TAF/year for all levels of development and development scenarios
Single-year Transfers[a]		
San Joaquin Valley		
	Wet	$188, $223, and $300 per AF for 2025, 2055, and 2085, respectively
	Dry	$211, $250, and $334 per AF for 2025, 2055, and 2085, respectively
	Critical	$211, $250, and $334 per AF for 2025, 2055, and 2085, respectively
Sacramento Valley		
	Wet	$126, $156, and $222 per AF for 2025, 2055, and 2085, respectively
	Dry	$135, $166, and $233 per AF for 2025, 2055, and 2085, respectively
	Critical	$171, $211, and $297 per AF for 2025, 2055, and 2085, respectively

[a] The cost shown is acquisition cost; delivered cost is higher because of Delta salinity and other operational losses.

Table 2B. LCPSIM Water Management Actions (CALFED): South Coast Region

Water Management Actions (CALFED)	Baseline
Local recycling	345 TAF/year for all levels of development and development scenarios
Desalination	51 TAF/year for all levels of development and development scenarios
Single-year Transfers[a]	
San Joaquin Valley	
Wet	$223, $289, and $354 per AF for 2025, 2055, and 2085, respectively
Dry	$250, $322, and $395 per AF for 2025, 2055, and 2085, respectively
Critical	$250, $322, and $395 per AF for 2025, 2055, and 2085, respectively
Sacramento Valley	
Wet	$156, $213, and $269 per AF for 2025, 2055, and 2085, respectively
Dry	$166, $224, and $282 per AF for 2025, 2055, and 2085, respectively
Critical	$211, $284, and $358 per AF for 2025, 2055, and 2085, respectively

[a]. The cost shown is acquisition cost; delivered cost is higher because of Delta salinity and other operational losses.

Table 3A. LCPSIM Regional Base Operations Cost: San Francisco Bay Region–South

Regional Base Operations Cost	Baseline
Distribution cost	$62, $98, and $135 per AF for 2025, 2055, and 2085, respectively from CALFED Bay-Delta Program Economic Evaluation of Water Management Alternatives: Screening Analysis and Scenario Development
Treatment cost	$99, $102, and $105 per AF for 2025, 2055, and 2085, respectively from CALFED Bay-Delta Program Economic Evaluation of Water Management Alternatives: Screening Analysis and Scenario Development
Cost of Reuse and Deep Percolation	$50, $78, and $106 per AF for 2025, 2055, and 2085, respectively from Electricity Price Forecasts (DWR) for all development scenarios
SWP aqueduct conveyance	
Groundwater bank	$58, $122, and $186 per AF for 2025, 2055, and 2085, respectively from Electricity Price Forecasts (DWR) for all development scenarios
Regional conveyance	$99, $209, and $319 per AF for 2025, 2055, and 2085, respectively from Electricity Price Forecasts (DWR) for all development scenarios
CVP conveyance	
Groundwater bank	$0/AF for all levels of development and development scenarios
Regional conveyance	$98, $206, and $315 per AF for 2025, 2055, and 2085, respectively from Electricity Price Forecasts (DWR) for all development scenarios

The cost of water supply operations, including conveyance, treatment, and distribution, for the San Francisco Bay – South are listed in Table 3A and in Table 3B for the South Coast Region. Water supply operation costs are determined, primarily, by the change in real energy prices.

South Coast Region costs of delivery from the Colorado River Aqueduct and the East Branch Canal are included in Table 3B. South Coast Region has access to groundwater banking of Colorado River water. No CVP conveyance or CVP groundwater banking options exist in the South Coast Region. Regional base distribution, treatment, and cost of reuse and deep percolation are identical to

those of the San Francisco Bay – South Region. Regional conveyance costs are clearly higher when delivering to the South Coast Region.

Annual regional base use (demand) is estimated for urban, agricultural, and environmental water use in the San Francisco Bay – South (Table 4A). Urban demand estimates are estimated using the county population projections developed for the CVP IRP for the three development scenarios. Demand in the San Francisco Bay – South is effectively reduced by conservation measures and annual precipitation levels. Conservation estimates reflect the reasonable and foreseeable water management actions in future conditions.

Table 3B. LCPSIM Regional Base Operations Cost: South Coast Region

Regional Base Operations Cost	Baseline
Distribution cost	$62, $98, and $135 per AF for 2025, 2055, and 2085, respectively from CALFED Bay-Delta Program Economic Evaluation of Water Management Alternatives: Screening Analysis and Scenario Development
Treatment cost	$99, $102, and $105 per AF for 2025, 2055, and 2085, respectively from CALFED Bay-Delta Program Economic Evaluation of Water Management Alternatives: Screening Analysis and Scenario Development
Cost of Reuse and Deep Percolation	$50, $78, and $106 per AF for 2025, 2055, and 2085, respectively from Electricity Price Forecasts (DWR) for all development scenarios
SWP aqueduct conveyance	
Groundwater bank	$58, $122, and $186 per AF for 2025, 2055, and 2085, respectively from Electricity Price Forecasts (DWR) for all development scenarios
Regional conveyance	$260, $541, and $796 per AF for 2025, 2055, and 2085, respectively from Electricity Price Forecasts (DWR) for all development scenarios
East Branch Conveyance	
	$350, $542, and $733 per AF for 2025, 2055, and 2085, respectively
Colorado River Aqueduct conveyance	
Groundwater bank	$135, $283, and $416 per AF for 2025, 2055, and 2085, respectively
Regional conveyance	$107, $355, and $523 per AF for 2025, 2055, and 2085, respectively from Electricity Price Forecasts (DWR) for all development scenarios

Table 4A. LCPSIM Annual Regional Base Use: San Francisco Bay Region–South

Annual Regional Base Use		Baseline
Regional Population		
	Slow Growth	6,909,861, 7,797,001, 8,615,836 people for 2025, 2055, and 2085, respectively
	Current Trends	1,219,596, 1,566,642, and 1,927,041 people for 2025, 2055, and 2085, respectively
	Expansive Growth	8,234,521.5, 11,492,008, 15,533,297 people for 2025, 2055, and 2085, respectively
Water Use per person		
		162.2, 168, and 171.4 gallons per day per person for 2025, 2055, and 2085, respectively
Urban demand target		
	Slow Growth	1,055.4, 965.4, 850.5 TAF/year for 2025, 2055, and 2085, respectively
	Current Trends	1,084.0, 1,341.9, and 1,531.0 TAF/year for 2025, 2055, and 2085, respectively
	Expansive Growth	1,346.9, 2,021.1, 2,850.3 TAF/year for 2025, 2055, and 2085, respectively
Regional demand reductions		
Conservation		142.3, 166.5, and 166.5 TAF/year for 2025, 2055 and 2085, respectively for all development scenarios from Water Use Efficiency Comprehensive Evaluation
Precipitation		Four station average annual rainfall 1884-2003 from National Weather Service[a]
Agricultural use		30 TAF/year for all levels of development and development scenarios from DWR Water Portfolio (on-farm applied water net of reuse) 1998-2005
Environmental use		5 TAF/year for all levels of development and development scenarios from DWR Water Portfolio (managed wetlands) 1998-2005

[a] Historical rainfall records starting in 1883 are used to create a stochastic sequence for the hydrologic study period to estimate urban demand targets.

South Coast Region not only has a higher per-capita water use than the San Francisco Bay Region- South, but also higher population projections, leading to a substantially greater urban demand target each year. Table 4B displays the regional population, urban demand targets and other users for the South Coast Region.

Table 4B. LCPSIM Annual Regional Base Use: South Coast Region

Annual Regional Base Use		Baseline
Regional Population		
	Slow Growth	22,001,121, 21,953,012, and 21,180,881 people for 2025, 2055, and 2085, respectively
	Current Trends	22,230,713, 26,001,538, and 28,848,985 people for 2025, 2055, and 2085, respectively
	Expansive Growth	26,302,856, 36,047,247, and 49,282,219 people for 2025, 2055, and 2085, respectively
Water Use gal/person/day		
		186.7, 189.5, and 193 gallons per day per person for 2025, 2055, and 2085, respectively
Urban demand target		
	Slow Growth	4,601.1, 4,659.9, 4,579.0 TAF/year for 2025, 2055, and 2085, respectively

Table 4B. LCPSIM Annual Regional Base Use: South Coast Region

Annual Regional Base Use	Baseline
Current Trends	4,649.1, 5,519.3, and 6,236.8 TAF/year for 2025, 2055, and 2085, respectively
Expansive Growth	5,500.7, 7,651.6, 10,654.2 TAF/year for 2025, 2055, and 2085, respectively
Regional demand reductions	
Conservation	463, 650, and 950 TAF/year for 2025, 2055 and 2085, respectively for all development scenarios from Water Use Efficiency Comprehensive Evaluation
Precipitation	Four station average annual rainfall 1884-2003 from National Weather Service[a]
Agricultural use	772, 652, and 389 TAF/year for 2025, 2055, and 2085 respectively and development scenarios from DWR Water Portfolio (on-farm applied water) 1998-2005
Environmental use	33.6 TAF/year for all levels of development and development scenarios from DWR Water Portfolio (managed wetlands) 1998-2005

[a] Historical rainfall records starting in 1883 are used to create a stochastic sequence for the hydrologic study period to estimate urban demand targets.

In addition to the reasonable and foreseeable future levels of conservation, desalination, and recycling, the San Francisco Bay – South LCPSIM allows regional reliability management options to be added if additional options reduce total costs. Table 5A lists the available quantity and cost of regional reliability management options. Similarly, the South Coast Region's options are displayed in Table 5B.

Table 5A. LCPSIM Regional Reliability Management Options : San Francisco Bay Region–South

Regional Reliability Management Options	Baseline
Conservation	108 TAF/year interior and 163 TAF/year exterior increasing in cost up to $1,800/AF for 2025 and 90.0 TAF/year interior and 156 TAF/year exterior increasing in cost up to $1,800/AF for 2055 and 2085 for all development scenarios
Water recycling	407 TAF/year increasing in cost from $738/AF to $4,245/AF for 2025 and from $760 to $4,276/AF for 2055 and 2085 for all development scenarios
Desalination	134 TAF/year at $1,527/AF for 2025 and $1,692/AF for 2055 and 2085 for all development scenarios

Unlike the San Francisco Bay Region-South, the South Coast Region increases in Desalination capacity and options in later levels of development. Price increases from 2025 to later levels of development, but so does capacity. See Table 5B for numbers.

Table 5B. LCPSIM Regional Reliability Management Options : South Coast Region

Regional Reliability Management Options	Baseline
Conservation	392 TAF/year interior and 444 TAF/year exterior increasing in cost up to $1,900/AF for 2025 and 285 TAF/year interior and 299 TAF/year exterior increasing in cost up to $2,000/AF for 2055 and 2085 for all development scenarios
Water recycling	973 TAF/year increasing in cost from $692 to $1507/AF for 2025 and 2276 TAF/year from $723 to $1538/AF for 2055 and 2085 for all development scenarios
Desalination	280 TAF/year at $1,984/AF for 2025 and 1171 TAF at $2149/AF for 2055 and 2085 for all development scenarios

Regional ground and surface carryover storage operation constraints are listed in Tables 6A and 6B. The annual put, take, and total storage specifications are included for each facility utilized by the San Francisco Bay – South Region and the South Coast region in the subsequent table.

Table 6A. LCPSIM Regional Ground and Surface Carryover Storage : San Francisco Bay Region–South

Regional Ground and Surface Carryover Storage	Baseline
Groundwater spreading operations	30 TAF of storage, put limit of 30 TAF/year and take limit of 10 TAF/year for all levels of development and development scenarios
California Aqueduct groundwater banking operations	565 TAF of storage, put limit of 178 TAF/year, and take limit of 130 TAF/year from MWD for all levels of development and development scenarios
Arvin-Edison Project delivery constraint[a]	155 TAF of Table A allotment, 22 TAF of reserve Table A, 56% share of the bank, and 0 TAF base take available for all levels of development and development scenarios

[a] The take limit for MWD from Arvin Edison is reduced for each consecutive year for which a take is made.

Table 6B. LCPSIM Regional Ground and Surface Carryover Storage : South Coast Region

Regional Ground and Surface Carryover Storage	Baseline
Reserve Reservoir Operations	154 TAF of storage, put limit of 154 TAF/year and take limit of 154 TAF/year for all levels of development and development scenarios
In-Region Reservoir Operations	653.6 TAF of storage, put limit of 631 TAF/year, and take limit of 231 TAF/year from MWD for all levels of development and development scenarios
IRP GW Program	140 TAF of storage, put limit of 140 TAF/year and take limit of 114 TAF/year for all levels of development and development scenarios
Prop 13 & Raymond Basin GW	211 TAF of storage, put limit of 51.5 TAF/year and take limit of 68.3 TAF/year for all levels of development and development scenarios
North Los Posas Banking	210 TAF of storage, put limit of 33 TAF/year and take limit of 47 TAF/year for all levels of development and development scenarios
San Bernardino Banking	50 TAF of storage, put limit of 20 TAF/year and take limit of 22 TAF/year for all levels of development and development scenarios
Colorado River Aqueduct GW Banking Operations	1400 TAF of storage, put limit of 240 TAF/year and take limit of 395.6 TAF/year for all levels of development and development scenarios

Table 6B. LCPSIM Regional Ground and Surface Carryover Storage : South Coast Region

Regional Ground and Surface Carryover Storage	Baseline
DWA & CVWD Adv. Deliv. Pgm.	800 TAF of storage, put limit of 250 TAF/year and take limit of 45.4 TAF/year for all levels of development and development scenarios
Kern-Delta WD & North Kern WSD	250 TAF of storage, put limit of 56.2 TAF/year and take limit of 25 TAF/year for all levels of development and development scenarios
Semitropic WSD	350 TAF of storage, put limit of 35.2 TAF/year and take limit of 63.9 TAF/year for all levels of development and development scenarios
Mojave WSD	75 TAF of storage, put limit of 75 TAF/year and take limit of 33.9 TAF/year for all levels of development and development scenarios
Arvin-Edison WSD	350 TAF of storage, put limit of 111 TAF/year and take limit of 75 TAF/year for all levels of development and development scenarios

A shortage management strategy dictates the operation and costs associated with inadequate supply conditions in the San Francisco Bay – South and the South Coast Region. These rules include constraints on transfers, rationing, and associated costs, listed in Table 7.

Table 7. LCPSIM Shortage Management Strategy: San Francisco Bay Region–South and South Coast Region

Shortage Management Strategy[a]	Baseline
Contingency conservation campaign	5.0% for all levels of development and development scenarios
Point at which transfers to depleted carryover storage are triggered	80% of each facility's annual take capacity for all levels of development and development scenarios
Shortage allocation rule cut ratio	Industrial user 25%, commercial user 50%, multi-family residential 60%, landscape user 200%[b,c] for all levels of development and development scenarios
Demand hardening factor	33 in 2025 and 25%[b,d] in 2055 and 2085
Rationing program threshold	80% non-interruptible shortage triggers rationing cost of $0.50/person[b] for all levels of development and development scenarios
Take call ratio for using contingency conservation	100% call on available carryover to meet net delivery with conservation reduction[b] for all levels of development and development scenarios
Capacity use ratio for using contingency conservation	20% of capacity[b,e] for all levels of development and development scenarios
Threshold for shortage allocation	Below a 95.0% level of shortage, all users will experience the same percentage reduction[b] for all levels of development and development scenarios
Inverse power function exponent for loss value adjustment	Inverse power function of 1.0[b] for all levels of development and development scenarios

Industrial customer size (% of total use)

San Francisco Bay Region–South	2.3%, 1.7%, and 1.3% for 2025, 2055 and 2085 from DWR
South Coast Region	2.2% in 2025 and 1.7% in 2055 and 2085 from DWR

Commercial customer size (% of total use)

San Francisco Bay Region–South	23.8% in 2025 and 25.3% in 2055 and 2085 from DWR

Table 7. LCPSIM Shortage Management Strategy: San Francisco Bay Region–South and South Coast Region

Shortage Management Strategy[a]	Baseline
South Coast Region	25.5% in 2025 and 25.6% in 2055 and 2085 from DWR
Landscape customer size (% of total use)	
San Francisco Bay Region–South	8.5%, 7.8%, and 7.4% for 2025, 2055 and 2085 from DWR
South Coast Region	5.5%, 5.3%, and 5.1% for 2025, 2055 and 2085 from DWR
Multi-family customer size (% of total use)	
San Francisco Bay Region–South	21.4% in 2025 and 21.2% in 2055 and 2085 from DWR
South Coast Region	16.8% for all development scenarios from DWR

Notes:

[a] Shortage management strategies were developed using Metropolitan Water District's Water Surplus and Drought Management Plan.

[b] A specified reduction in use can be expected upon implementation of a contingency conservation program that includes such measures as increased watering regulations, increased water waste patrols, emergency water pricing programs, and intensive public education campaigns. Contingency measures to meet shortages are implemented only after shortages exceed 5% of total urban use.

[c] User shortage percentage limited to the specified percent of overall shortage percentage.

[d] Percentage increase in conservation (compared to base use levels) makes shortages effectively larger by 50% times the percentage increase in conservation.

[e] Limit on the fraction of carryover storage capacity filled before triggering contingency conservation.

Costs associated with shortage conditions are determined by an economic loss function (Table 8). The loss function is intended to approximate willingness-to-pay at the water user level, derived from contingent valuation studies and water agency shortage allocation strategies, assigning a cost to forgone use.

Table 8. LCPSIM Economic Loss Function: San Francisco Bay Region–South and South Coast Region

Economic Loss Function	Baseline
Polynomial loss function[a]	$1,036 (intercept), coefficients $b_1 = 21,995$, $b_2 = -14,781$, $b_3 = -3,149$ for 2025; $1,574 (intercept), coefficients $b_1 = 21,255$, $b_2 = -15,018$, $b_3 = -3,150$ for 2055; $2,357 (intercept), coefficients $b_1 = 20,105$, $b_2 = -15,377$, $b_3 = -3,151$ for 2085 for all levels of development and development scenarios from MWD 2005 RUWMP

[a] This model element assigns economic loss to foregone use.

2.2 Other Municipal Water Economics Model (OMWEM)

Several relatively small M&I water providers are not covered by LCPSIM. A set of individual spreadsheet models, collectively called Other Municipal Water Economics Model (OMWEM), is used to estimate economic benefits of changes in SWP or CVP supplies for potentially affected M&I water providers outside the San Francisco Bay – South region. The model includes CVP M&I supplies north of Delta, SWP and CVP supplies to the Central Valley and the Central Coast, SWP supplies or supply exchanges to the desert regions east of the South Coast hydrological region, and American River contractors. The model estimates the

economic value of M&I supply changes in these areas as the change in cost of shortages and alternative supplies (such as groundwater pumping or transfers).

Data from available 2010 Urban Water Management Plans were used to estimate 2025 water demand and supplies for an average condition and a dry condition, and to identify additional water supply options and their costs. Water demand estimates for 2055 and 2085, at the three development scenarios, are based on population projections developed by the CVP IRP. For each level of development and development scenario OMWEM uses project water supplies to match supply to demand. If supply is insufficient to meet demand in years categorized as below normal water supply or greater, the model calculates the cost of additional water supplies.

 If the water supply year is categorized as dry or critical, the model allows for shortfalls, up to 5 percent, to be initially managed with dry/critical supply sources and end-user shortage, before the cost of additional water supplies are calculated. Then, providers can acquire dry-year supplies to eliminate shortfalls up to fifty percent. These supplies have unit costs specific to the dry and critical condition. Thereafter, it is assumed that end-users must take additional shortage.

If the marginal water supply for the provider is not a water transfer, then the 5 percent end-use shortage is not required first. The provider can eliminate a shortfall of up to fifty percent of demand using the dry/critical supply, but end-user shortage is used to cope with any larger shortfalls.

The model calculates shortage costs based on a constant elasticity of demand (CED) loss function with a demand elasticity of -0.1. This form of shortage loss function has been used in California as long ago as the CVPIA Programmatic EIR/S (Reclamation, 1999b). More recently, a description of this shortage cost function was provided by M.Cubed (2007). This shortage function generates very high costs at high shortage levels. The marginal value of water from the CED function can be capped. The current cap is set at $7,000 per acre-foot year (AFY) more than the provider's retail water price.

Two model runs are required to compare a baseline and an alternative future condition. Results from a baseline scenario are saved as values and compared to results from the alternative future condition. The cost of water supplies required to obtain water balance in the baseline do not influence the incremental cost of supplies in the alternative future condition. In the dry and critical condition, however, marginal costs of shortage increase with shortage. Therefore, the marginal value of additional supplies decline as supply increases.

Supply estimates in OMWEM for SWP contractors in average conditions are listed in Table 9. The supply estimates are based on 2010 UWMP documentation and represent projected supply conditions across development scenarios and levels of development.

Table 9. OMWEM SWP Contractor Average Year Supply Estimates (TAF/Year)

SWP Table A holder	Surface Water	Groundwater	Recycled Water	Other
Antelope Valley – East Kern Water Agency	0	0	0	0
Coachella Valley Water District	404,000	124,200	27,585	11,000
Crestline – Lake Arrowhead Water Agency	433	0	0	0
Desert Water Agency	2,800	7,250	8,000	13,800
Mojave Water Agency	0	65,500	0	0
San Luis Obispo County FCWCD	1,199	1,900	0	0
County of Santa Barbara FCWCD and CCWA	31,777	16,449	2,500	23,209
Kern County Water Agency (SWP) ID #4	0	0	0	0
Napa County FCWCD	20,914	0	0	3,105
Solano County Water Agency	207,350	0	0	0

Note: The same values are assumed for all development scenarios in 2025, 2055, and 2085

Supply estimates in OMWEM for CVP contractors in average conditions are listed in Table 10. The supply estimates are based on 2010 UWMP documentation and represent projected supply conditions across development scenarios and levels of development.

Table 10. OMWEM CVP Contractor Average Year Supply Estimates (TAF/Year)

CVP Contract Holder	Surface water	Natural Groundwater	Recycled Water	Other
City of Redding	0	19,000	0	0
City of Shasta Lake and Shasta CWA	0	0	0	0
City of West Sacramento	5,520	0	0	0
San Benito County	0	49,925	0	0
City of Tracy	10,000	2,500	0	9,500
City of Avenal	0	0	0	0
City of Coalinga	0	0	0	0
City of Huron	0	0	0	0

Note: The same values are assumed for all development scenarios in 2025, 2055, and 2085

Supply estimates in OMWEM for American River contractors in average conditions are listed in Table 11. The supply estimates are based on 2010 UWMP

documentation and represent projected supply conditions across development scenarios and levels of development.

Table 11. OMWEM American River Contractor Average Year Supply Estimates (TAF/Year)

American River Contractors (CVP)	Surface water	Groundwater	Recycled Water	Transfers	Other
City of Folsom	27,000	3,250	0	9,540	0
San Juan W.D.	58,000	0	0	0	0
El Dorado I.D.	59,640	0	7,730	7,500	30,000
City of Roseville	34,000	0	2,980	0	0
Placer County W.A.	248,800	0	5,936	0	573

Note: The same values are assumed for all development scenarios in 2025, 2055, and 2085

Supply estimates in OMWEM for SWP contractors in dry conditions are listed in Table 12. The supply estimates are based on 2010 UWMP documentation and represent projected supply conditions across development scenarios and levels of development.

Table 12. OMWEM SWP Contractor Dry Year Supply Estimates (TAF/Year)

WP Contract Holder	Surface water	Groundwater	Recycled Water	Other
Antelope Valley – East Kern Water Agency	0	0	0	0
Coachella Valley Water District	404,000	124,200	27,585	11,000
Crestline – Lake Arrowhead Water Agency	0	0	0	0
Desert Water Agency	2,800	7,250	8,000	13,800
Mojave Water Agency average	0	65,500	0	35,420
San Luis Obispo County FCWCD	1,199	1,900	0	0
County of Santa Barbara FCWCD and CCWA	23,603	16,449	2,500	14,300
Kern County Water Agency (SWP) ID #4	0	75,000	0	0
Napa County FCWCD normal	6,165	0	0	9,390
Solano County Water Agency	186,615	0	0	0

Note: The same values are assumed for all development scenarios in 2025, 2055, and 2085

Supply estimates in OMWEM for CVP contractors in dry conditions are listed in Table 13. The supply estimates are based on 2010 UWMP documentation and represent projected supply conditions across development scenarios and levels of development.

Table 13. OMWEM CVP Contractor Dry Year Supply Estimates (TAF/Year)

CVP Contract Holder	Surface water	Groundwater	Recycled Water	Other
City of Redding	0	19,000	0	0
City of Shasta Lake and Shasta CWA	0	0	0	0
City of West Sacramento	0	0	0	0
San Benito County	0	49,925	0	0
City of Tracy	9,000	2,500	0	7,425
City of Avenal	0	0	0	0
City of Coalinga	0	0	0	0
City of Huron	0	0	0	0

Note: The same values are assumed for all development scenarios in 2025, 2055, and 2085

Supply estimates in OMWEM for American River contractors in dry conditions are listed in Table 14. The supply estimates are based on 2010 UWMP documentation and represent projected supply conditions across development scenarios and levels of development.

Table 14. OMWEM American River Contractor Dry Year Supply Estimates (TAF/Year)

American River Contractors (CVP)	Surface water	Groundwater	Recycled Water	Transfers	Other
City of Folsom	21,870	2,633	0	9,540	0
San Juan W.D.	0	0	0	0	0
El Dorado I.D.	58,094	0	7,730	5,625	15,000
City of Roseville	30,000	0	2,980	0	0
Placer County W.A.	184,400	0	5,936	0	573

Note: The same values are assumed for all development scenarios in 2025, 2055, and 2085

Demand estimates in OMWEM for SWP contractors are listed in Table 15. The supply estimates are based on individual contractor 2010 UWMPs and represent projected supply conditions across development scenarios and levels of development. Demand estimates in OMWEM for CVP contractors are listed in Table 16. The supply estimates are based on individual contractor 2010 UWMPs and represent projected supply conditions across development scenarios and levels of development.

Table 15. OMWEM SWP Contractor Demand Estimates (TAF/Year)

SWP Contractor	Development Scenario	2025	2055	2085
Antelope Valley – East Kern Water Agency	Slow Growth	102,184	94,519	85,504
	Current Trends	107,599	131,448	155,725
	Expansive Growth	119,331	200,108	251,518
Coachella Valley Water District	Slow Growth	597,572	653,559	714,414
	Current Trends	625,567	727,521	797,527
	Expansive Growth	627,415	760,310	953,918
Crestline – Lake Arrowhead Water Agency	Slow Growth	5,663	6,653	7,573
	Current Trends	6,100	8,335	9,867
	Expansive Growth	6,536	10,000	14,741
Desert Water Agency	Slow Growth	61,120	82,311	107,145
	Current Trends	70,400	108,991	138,136
	Expansive Growth	71,012	121,315	199,625
Mojave Water Agency average	Slow Growth	116,099	132,826	147,934
	Current Trends	124,100	161,860	186,870
	Expansive Growth	132,079	190,613	268,783
San Luis Obispo County FCWCD	Slow Growth	5,974	6,198	6,204
	Current Trends	6,350	7,878	9,747
	Expansive Growth	7,113	10,333	15,234
County of Santa Barbara FCWCD and CCWA	Slow Growth	75,858	68,729	58,841
	Current Trends	76,255	87,053	92,166
	Expansive Growth	91,961	123,841	165,401
Kern County Water Agency (SWP) ID #4	Slow Growth	45,563	65,221	83,256
	Current Trends	52,785	98,794	146,340
	Expansive Growth	53,439	103,557	164,897
Napa County FCWCD normal	Slow Growth	27,151	30,045	30,965
	Current Trends	30,877	46,106	59,840
	Expansive Growth	33,356	53,743	78,603
Solano County Water Agency	Slow Growth	228,873	280,780	319,481
	Current Trends	255,106	409,538	607,107
	Expansive Growth	271,533	451,825	682,147

Table 16. OMWEM SWP Contractor Demand Estimates (TAF/Year)

CVP Contractor		2025	2055	2085
City of Redding	Slow Growth	31,083	38,751	46,663
	Current Trends	36,000	51,685	65,425
	Expansive Growth	35,346	55,238	83,892
City of Shasta Lake and Shasta CWA	Slow Growth	6,994	8,719	10,499
	Current Trends	8,100	11,629	14,721
	Expansive Growth	7,953	12,429	18,876
City of West Sacramento	Slow Growth	26,144	25,795	20,679
	Current Trends	29,120	37,152	37,403
	Expansive Growth	32,151	46,147	58,109
San Benito County	Slow Growth	92,954	94,406	95,448
	Current Trends	95,000	102,086	109,516
	Expansive Growth	94,775	100,393	107,312
City of Tracy	Slow Growth	23,367	34,064	44,129
	Current Trends	28,200	49,926	71,052
	Expansive Growth	28,273	51,931	79,955
City of Avenal	Slow Growth	3,084	4,042	5,499
	Current Trends	3,500	5,748	7,750
	Expansive Growth	3,740	6,734	12,296
City of Coalinga	Slow Growth	10,425	12,705	14,225
	Current Trends	12,000	18,937	27,686
	Expansive Growth	11,950	19,844	29,627
City of Huron	Slow Growth	2,606	3,176	3,556
	Current Trends	3,000	4,734	6,921
	Expansive Growth	2,987	4,961	7,407

Demand estimates in OMWEM for American River contractors are listed in Table 17. The supply estimates are based on individual contractor 2010 UWMPs and represent projected supply conditions across development scenarios and levels of development.

Table 17. OMWEM American River Contractor Demand Estimates (TAF/Year)

American River Contractors (CVP)		2025	2055	2085
City of Folsom	Slow Growth	32,376	35,099	37,601
	Current Trends	34,458	45,669	57,374
	Expansive Growth	37,710	55,367	79,582
San Juan W.D.	Slow Growth	72,066	104,957	155,643
	Current Trends	84,140	144,134	204,632
	Expansive Growth	84,486	156,794	289,477
El Dorado I.D.	Slow Growth	52,944	63,426	76,073
	Current Trends	60,028	83,875	107,234
	Expansive Growth	61,706	96,134	148,986
City of Roseville	Slow Growth	40,693	59,264	87,884
	Current Trends	47,510	81,386	115,546
	Expansive Growth	47,705	88,534	163,454
Placer County W.A.	Slow Growth	182,476	265,758	394,097
	Current Trends	213,048	364,956	518,142
	Expansive Growth	213,923	397,012	732,974

2.3 South Bay Water Quality Model (SBWQM)

For M&I salinity assessment, the South Bay Area Water Quality Economics Model (SBWQM), includes the portion of the Bay Area region from Contra Costa County in the North to Santa Clara County in the South. The model was originally developed and used for the economic evaluation of a proposed expansion of Los Vaqueros Reservoir (Reclamation 2006). It uses estimated relationships between salinity and damages to residential appliances and fixtures to estimate the benefits from changes in salinity. Specific model outputs compare change in average salinity and change in annual salinity costs.

The model inputs include project water supply and chloride concentrations in mg/L from CalLite. Separate calculations were provided for CCWD and agencies that utilize the South Bay Aqueduct. For CCWD, water quality estimates were based on diversion volume and water quality at Old River and Rock Slough. For the other areas, water quality is based on diversion volume and salinity at Banks Pumping Plant. Changes in water quality at the City of Antioch's diversion were used to estimate additional cost of treatment or replacement supply.

The SBWQM was updated for three development scenarios at three levels of development, 2025, 2055, and 2085. Model preparation involved updating available population and water portfolio information from Reclamation and DWR's Water Plan Update (2010). Parameters in the SBWQM pertinent to the level of development and the approach proposed to update the parameters is listed in Table 18.

Table 18. South Bay Water Quality Model Level of Development Parameters

Parameter	2025	2055	2085
Regional Supplies (AF/Year)			
Contra Costa Water District	CalLite	CalLite	CalLite
Santa Clara Water District	CalLite	CalLite	CalLite
Local Supplies (AF/Year)			
Contra Costa Water District	22,930	22,930	22,930
Santa Clara Water District	449,200	449,200	449,200
Local Water Quality (Average Chlorides, mg/L)			
Santa Clara Water District	62	62	62

Note: The same values are assumed for all development scenarios

Household estimates were estimated using population projects for the region over the three development scenarios and levels of development. The water quality damage functions that are part of the model require household estimates to estimate total water quality damages. The households estimates are listed in Table 19.

Table 19. South Bay Water Quality Model Household Estimates

Parameter	2025	2055	2085
Strategic Growth			
Contra Costa Water District	209,481	183,202	160,937
Santa Clara Water District	781,359	683,339	600,291
Current Growth			
Contra Costa Water District	244,568	304,382	376,072
Santa Clara Water District	847,548	1,054,834	1,303,276
Expansive Growth			

Table 19. South Bay Water Quality Model Household Estimates

Parameter	2025	2055	2085
Contra Costa Water District	249,048	333,092	441,201
Santa Clara Water District	949,174	1,269,484	1,681,510

Note: The same values are assumed for all development scenarios

2.4 Lower Colorado River Basin Water Quality Model (LCRBWQM)

LCRBWQM was developed by Reclamation (Lower Colorado Region) and Metropolitan Water District of Southern California (Metropolitan) in 1998. This model was updated as part of Metropolitan's and Reclamation's 1999 Salinity Management Study. The current version of the model was updated with population data from the Department of Water Resources (DWR) and costs have been updated to 2007 levels. For a detailed description of LCRBWQM, see Metropolitan and Reclamation (1999). The model inputs from CalLite are SWP East and West Branch deliveries and TDS of these deliveries in mg/L, respectively. Some water diverted at Banks Pumping Plant (PP) is conveyed directly to southern California; other supplies are mixed in San Luis with water diverted at Jones PP.

LCRBWQM divides Metropolitan's service area into 15 sub areas. The division of the south coast region into sub areas provides detail regarding sources of water and salts in each area. This detail is necessary because each region obtains very different shares of supply from different sources, and some sources, the Colorado River and groundwater, in particular, have higher salinity than others. Table 20 shows the sub areas and estimates of population in each. Table 21 shows average salinity levels and water sources for the 2025 condition.

Table 20. South Coast Regions in LCRBWQM and Population Estimates under Current Trends

Region	County	2010	2025	2055	2085
North West	Ventura	646,810	734,209	957,633	1,062,505
San Fernando Valley – West	Los Angles	2,610,532	2,941,222	3,276,951	3,635,813
San Fernando Valley – East	Los Angles	1,523,967	1,632,428	1,818,764	2,017,938
San Gabriel Valley	Los Angles	3,386,605	3,525,574	3,928,006	4,358,165
Central Los Angeles -	Los Angles	1,555,402	1,801,696	2,007,353	2,227,179
Central and West Basins	Los Angles	616,334	695,185	774,538	859,358
Coastal Plain	Los Angles	311,610	353,985	394,391	437,581
North West Orange County	Orange	195,881	220,847	237,972	264,032
South East Orange County	Orange	3,159,564	3,414,825	3,679,621	4,082,579

Table 20. South Coast Regions in LCRBWQM and Population Estimates under Current Trends

Region	County	2010	2025	2055	2085
North West	Ventura	646,810	734,209	957,633	1,062,505
San Fernando Valley – West	Los Angles	2,610,532	2,941,222	3,276,951	3,635,813
Western MWD	Riverside	845,728	1,223,698	1,743,761	1,934,722
Eastern MWD	Riverside	682,340	897,778	1,279,328	1,419,428
Upper Chino	San Bernardino	486,737	522,328	657,308	729,290
Lower Chino	San Bernardino	372,501	568,530	715,449	793,798
North San Diego	San Diego	311,648	426,583	522,555	579,780
South San Diego	San Diego	2,873,548	3,271,825	4,007,909	4,446,818
Total		19,579,208	22,230,713	26,001,538	28,848,985

Table 21. Average LCRBWQM Salinity and Water Supply Shares for the 2025 Condition

		Average Percent of Regional Supply from Each Source						
Region	Avg Salinity, mg/l	Ground water Recovery	Ground-water	Surface Water	LA Aque-duct	SWP East	Co. River Aque-duct	SWP West
North West	319	0%	11%	0%	0%	88%	0%	0%
San Fernando V. W	275	0%	14%	0%	54%	32%	0%	0%
San Fernando V. E	444	23%	19%	0%	0%	37%	21%	0%
San Gabriel Valley	352	1%	57%	6%	0%	0%	13%	23%
Central Los Angeles	318	0%	12%	0%	24%	49%	8%	7%
Central & W Basins	427	2%	36%	0%	0%	40%	22%	0%
Coastal Plain	528	23%	21%	0%	0%	36%	20%	0%
NW Orange County	423	1%	42%	0%	0%	0%	21%	37%
SE Orange County	432	11%	12%	0%	0%	0%	28%	50%
Western MWD	333	2%	39%	0%	0%	0%	9%	50%
Eastern MWD	525	2%	27%	4%	0%	0%	52%	15%
Upper Chino	223	1%	24%	5%	0%	0%	0%	70%
Lower Chino	464	21%	62%	0%	0%	0%	3%	14%
North San Diego	553	1%	3%	4%	0%	0%	67%	24%
South San Diego	538	2%	6%	12%	0%	0%	59%	22%

Table 20. South Coast Regions in LCRBWQM and Population Estimates under Current Trends

Region	County	2010	2025	2055	2085
North West	Ventura	646,810	734,209	957,633	1,062,505
San Fernando Valley – West	Los Angles	2,610,532	2,941,222	3,276,951	3,635,813

The model is designed to assess the average annual salinity benefits or costs based on demographic data, water deliveries, TDS concentration, and cost functions that define the relationship between TDS and costs in a number of categories. Cost information was developed based on technical studies, consumer surveys, interviews of contractors and experts, and engineering judgment. All of the cost data (such as the price of water heaters, water rates, reverse osmosis costs, etc.) were obtained from retail stores, warehouses, available reports and publications, and engineering cost estimates. For a complete reference of the data and their source material see MWDSC and Reclamation's Salinity Management Study (1999).

The cost categories are shown in Table 22 below. Salinity costs can be classified generally as those incurred privately, and those incurred by utilities. Private cost categories are residential, irrigation, commercial, and industrial. Utility costs include recycled water costs, water utility costs, and groundwater recharge costs.

Table 22. Categories of Costs Counted by LCRBWQM

Private	Utility
Residential	Recycled Water and Wastewater Costs
• Life of Water Pipes	• RO Cost for Replenishment
• Life of Water Heaters	• RO Cost for Indirect Recharge
• Life of Faucets	Commercial / Industrial
• Life of Garbage Grinders	• RO Cost for NPDES
• Life of Clothes Washers	• RO Cost for Impacts of Water Softeners on POTWs
• Life of Dish Washers	Water Utility
• Houses using Bottled Water	• Production
• Houses with Water Softeners	• Distribution
• Cost of Cleaning Products ($)	Salt Removal in Groundwater Recharge
Irrigation – by Crop Type	• Direct Recharge
Commercial	• Indirect Recharge

Table 22. Categories of Costs Counted by LCRBWQM

Private	Utility
Residential	Recycled Water and Wastewater Costs
• Life of Water Pipes	• RO Cost for Replenishment
• Sanitary, cooling, irrigation, kitchen, laundry, misc	
Industrial	
• Process Water – Softening, minor, demineralization	
• Cooling Towers	
• Boiler Feed	
• Sanitation & Irrigation	

The types of salinity benefits (reduced costs) in each category include:

- Residential: Residential benefits from reduced salinity levels include an increase in appliance and residential plumbing life along with a reduction in use of bottled water and water softener products. Equations estimate expected life as a function of salinity; see Table 4 below for representative equations. Residential benefits account for the costs of appliance and water softener products.

- Agricultural: Benefits from reduced salinity levels are increased crop yield (Ayers 1985). The total damages incurred by agriculture are a function of crop area, total yield, and the reduction in yield from salinity levels.

- Commercial and Industrial: Benefits from reduced salinity levels include decreased costs for water softening and treatment, water for cooling, and extended equipment life. Costs are estimated using a dollar per mg/l per unit of water used. Economic damages are also a function of water use, cost of treatment and maintenance.

- Water Utility: Utility benefits from reduced salinity levels include an increased life of treatment and distribution facilities. The total economic damages from salinity are a function of population and useful life of facilities.

- Groundwater Recharge: Groundwater benefits from reduced salinity level are a reduction in salt removal costs. The total economic damages from salinity levels are also a function total water pumped.

- Recycled Water: Recycled water benefits from reduced salinity levels are leeching costs and salt removal costs. Total economic damages from salinity include additional salinity added by increased use of water softeners.

Table 23 shows equations that are used for household costs and the life of household features.

Table 23. Equations for Household Costs and Life of Household Features as a Function of TDS or Total Hardness

Customer Cost Category	Measure (Dependent Variable)	Equation Constant	Parameter on TDS (mg/l)	Parameter on Total Hardness (mg/l $CaCO_3$)
Bottled water usage	% households that use bottled water	5.7	+0.04	
Soap and detergent use	1982 $/household/yr	85		0.12
Water softeners	1983 $/household/yr	-4.7		0.11
Water softeners	% households that use softeners	-7.13		0.094
Water heaters	Life yrs	13.1	-0.00415	
Galvanized waste water pipe	Log Life yrs	1.549	-0.000797	
Galvanized water pipe	Life yrs	16.56	-0.0067	
Brass faucets	Log Life yrs	1.304	-.0007	
Dishwashers	Log Life yrs	1.03	-0.00034	
Clothes washers [1]	Life yrs	14.42	-0.011+ .0000046TDS	
Garbage disposals [1]	Life yrs	9.2	-0.004 + .000001TDS	
Faucets and fixtures	Life yrs	11.5	-0.003	

1.The parameter includes TDS because the equation is a quadratic, i.e. Yrs = a + bTDS + $cTDS^2$

The model can calculate the incremental economic benefits or costs of SWP and Colorado River Aqueduct salinity changes compared to a selected baseline condition. It also estimates the change in economic damages from a change in the volume of imported supply. Increasing deliveries of SWP supplies reduces overall economic damages in the model, because SWP deliveries are blended with the much more saline supplies such as the Colorado River. The model can be run with a 2010, 2025, 2055, or 2085 level of development for population, water use,

agricultural cropping patterns, and water supply under Current Trends, Expansive Growth and Slow Growth .

3. Agricultural Water Supply

3.1. Statewide Agricultural Production Model (SWAP)

The Statewide Agricultural Production (SWAP) model is the evolution of a series of production models of California agriculture developed by the University of California at Davis and DWR with additional funding and support provided by Reclamation. It shares some basic model structure with the Central Valley Production Model (CVPM). Relative to CVPM, SWAP allows for greater flexibility in production technology and input substitution, and it has been extended to allow for a range of analyses, including interregional water transfers and climate change effects. SWAP and CVPM have been used for numerous policy analyses and impact studies over the past 15 years, including the impacts of the Central Valley Project Improvement Act (Reclamation and USFWS 1999a), Upper San Joaquin Basin Storage Investigation (Reclamation 2008), the SWP drought impact analysis (Howitt et al. 2009), and the economic implications of Delta conveyance options (Lund et al. 2007).

3.1.1. Analytical Approach

The SWAP model is a regional model of irrigated agricultural production and economics that simulates the decisions of agricultural producers (farmers) in California. Its data coverage is most detailed in the Central Valley, but it also includes production regions in the Central Coast, South Coast, and desert areas. The model assumes that farmers maximize profit subject to resource, technical, and market constraints. Farmers sell and buy in competitive markets, and no one farmer can affect or control the price of any commodity. The model selects those crops, water supplies, and other inputs that maximize profit subject to constraints on water and land, and subject to economic conditions regarding prices, yields, and costs.

SWAP incorporates project water supplies (SWP and CVP), other local water supplies, and groundwater. As conditions change within a SWAP region (e.g., the quantity of available project water supply increases or the cost of groundwater pumping increases), the model optimizes production by adjusting the crop mix, water sources and quantities used, and other inputs. It also fallows land when that appears to be the most cost-effective response to resource conditions.

Model calibration uses Positive Mathematical Programming (PMP) which has been used in models since the 1980's and was formalized by Howitt (1995). PMP allows the modeler to infer the marginal decisions of farmers while only being able to observe limited average production data. PMP captures this information through a non-linear cost or revenue function introduced to the model. The SWAP model is specified with an increasing exponential land cost function. PMP is fundamentally a three-step procedure for model calibration that assumes farmers optimize input use for maximization of profits. In the first step a linear profit-

maximization program is solved. In addition to basic resource availability and non-negativity constraints, a set of calibration constraints is added to restrict land use to observed values. In the second step, the dual (shadow) values from the calibration and resource constraints are used to derive the parameters for an exponential "PMP" cost function and CES production function. In the third step, the calibrated CES and PMP cost function are combined into a full profit maximization program. The exponential PMP cost function captures the marginal decisions of farmers through the increasing cost of bringing additional land into production (e.g. through decreasing quality). Other input costs, (supplies, land, and labor) enter linearly into the objective function in both the first and third step

Crops are aggregated into 20 crop groups which are the same across all regions. Each crop group represents a number of individual crops, but many are dominated by a single crop. Irrigated acres represent acreage of all crops within the group, production costs and returns are represented by a single proxy crop for each group. The current 20 crop groups were defined in collaboration with DWR and updated in March 2011. For each group, the representative (proxy) crop is chosen based on four criteria: (i) a detailed production budget is available from U.C. Cooperative Extension, (ii) it is the largest or one of the largest acreages within a group, (iii) its water use (applied water) is representative of water use of all crops in the group, and (iv) its gross and net returns per acre are representative of the crops in the group. The relative importance of these criteria varies by crop. Current crop categories include alfalfa, almonds and pistachios, corn, cotton, cucurbits, dry beans, fresh tomatoes, grain, onions and garlic, other deciduous orchards, other field crops, other truck crops, irrigated pasture, processing tomatoes, potatoes, rice, safflower, sugar beets, subtropical orchards, and vineyards.

The SWAP model covers 27 agricultural subregions in the Central Valley plus an additional 10 regions in the Central Coast and Southern California. For this analysis we will only use the 27 regions in the Central Valley. The subregions are based on water budget areas, called Detailed Analysis Units, which DWR uses for water planning. The model's Central Valley configuration of subregions is shown in Figure 3.

The SWAP model is used to compare the short or long-run response of agriculture to potential changes in SWP and CVP irrigation water delivery, other surface or groundwater conditions, or other economic values or restrictions. Results from the CalLite model are used as inputs into SWAP through a standardized data linkage tool. Groundwater analysis is used to develop assumptions, estimates, and, if appropriate, restrictions on pumping rates and pumping lifts for use in SWAP. Model output includes intensive and extensive margin production response by agriculture, input use per acre and aggregate input use, respectively.

3.1.2. Assumptions and Limitations

The SWAP model is an optimization model that makes the best (most profitable) adjustments to water supply and other changes. Constraints can be imposed to simulate restrictions on how much adjustment is possible or how fast the adjustment can realistically occur. Nevertheless, an optimization model can tend to over-adjust and minimize costs associated with detrimental changes or, similarly, maximize benefits associated with positive changes.

SWAP does not explicitly account for the dynamic nature of agricultural production; it provides a point-in-time comparison between two conditions. This is consistent with the way most economic and environmental impact analysis is conducted, but it can obscure sometimes important adjustment costs.
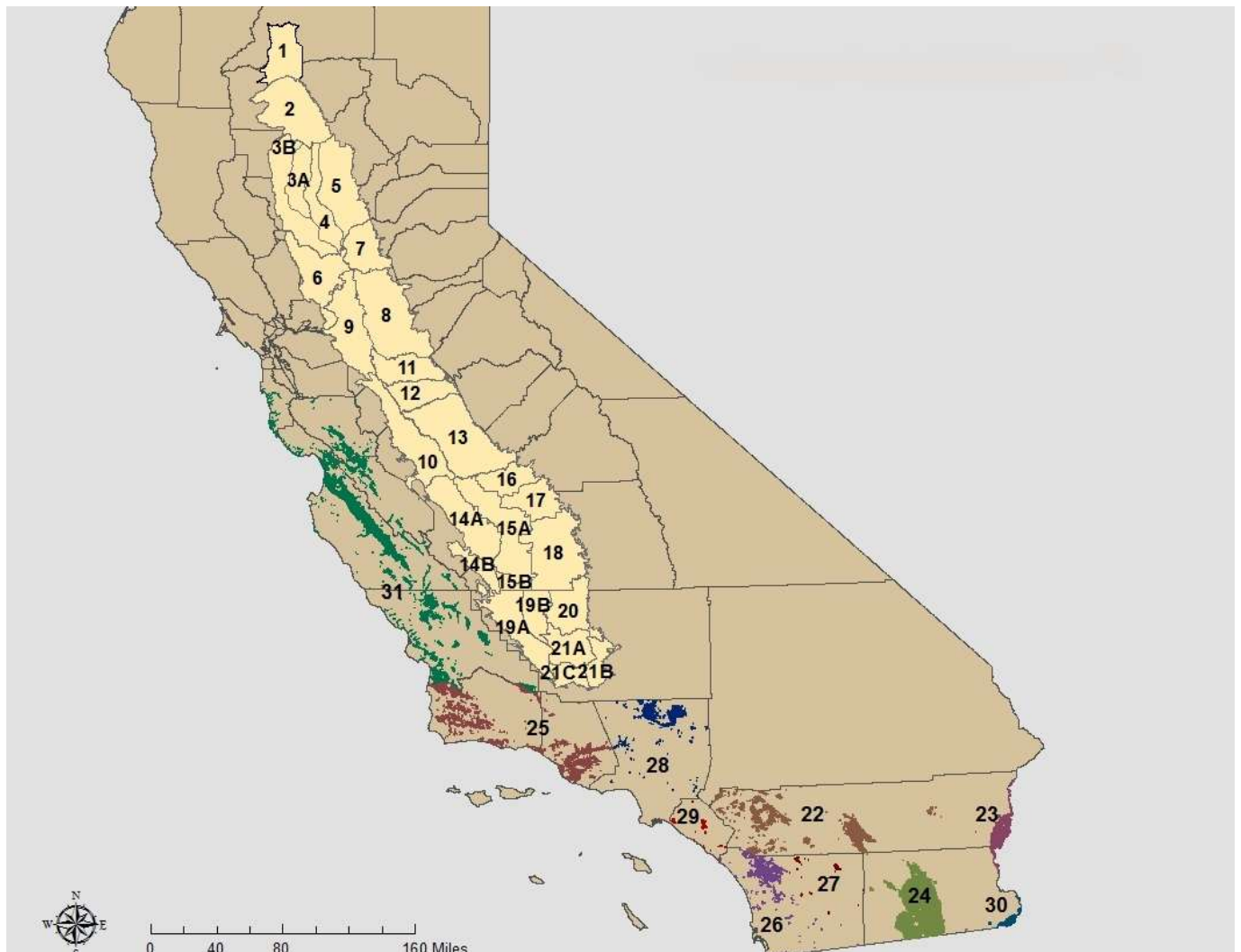
Figure 3. SWAP Region Definitions

SWAP also does not explicitly incorporate risk or risk preferences (e.g., risk aversion) into its objective function. Risk and variability are handled in two ways. First, the calibration procedure for SWAP is designed to reproduce observed crop mix, so to the extent that crop mix incorporates risk spreading and risk aversion, the starting, calibrated SWAP base condition will also. Second, variability in water delivery, prices, yields, or other parameters can be evaluated by running the model over a sequence of conditions or over a set of conditions that characterize a distribution, such as a set of water year types.

Groundwater is an alternative source to augment SWP and CVP delivery in many subregions. The cost and availability of groundwater therefore has an important effect on how SWAP responds to changes in delivery. However, SWAP is not a groundwater model and does not include any direct way to adjust pumping lifts and unit pumping cost in response to long-run changes in pumping quantities. Economic analysis using SWAP must rely on an accompanying groundwater analysis or at least on careful specification of groundwater assumptions.

3.1.3 Data Sources

SWAP calibrates to values of land and applied water using 2005 data developed by DWR for the California Water Plan Update (DWR 2009b). These data are the most recent available for a relatively normal water year (in both water and agricultural prices). SWAP includes four inputs to production: land, water, labor, and other inputs. Input costs for the proxy crops were derived from the regional cost and return studies from the University of California at Davis Extension Crop Budgets (University of California at Davis 2009). Likewise, crop yields and commodity prices for the base year (2005) in the model were obtained from the California County Agricultural Commissioner's reports (California Department of Food and Agriculture 2010). County-level data were aggregated to SWAP subregions using area-weighted averages. SWAP calibration takes place with prices and costs in 2005 dollars, consistent with the land use information, although final results can be indexed to any specified year.

Regional water supplies were specified for several sources: CVP water service contract, CVP settlement or exchange contract, SWP, CVP Friant-Kern delivery (class 1 and class 2), other local surface, and groundwater. The base year 2005 data were developed by DWR for the California Water Plan Update (2009). For future condition analysis, CalLite results from the water supply analysis of this environmental impact report/environmental impact statement (EIR/EIS) were used to provide project water deliveries.

Costs for surface water supplies are compiled from information published by individual water supply agencies. There is no central data source for water prices in California. Agencies that prepared CVP water conservation plans or agricultural water management plans in most cases included water prices and

related fees charged to growers. Other agencies publish and/or announce rates on an annual basis. Water prices used in SWAP are intended to be representative for each region, but vary in their level of detail. At least one large supplier in each region is used as the representative. In many regions, more than one supplier's price data are available. Where prices vary significantly within a region depending on the water source (e.g., CVP contractors versus local water rights diverters), these distinctions are represented in the data.

Groundwater availability is specified by region-specific maximum pumping estimates. These are determined by consulting the individual districts records and information compiled by DWR. DWR analysts provided estimates of the actual pumping in the base year and the existing pumping capacity by region. The model determines the optimal level of groundwater pumping for each region, up to the capacity limit specified. In some studies using SWAP or CVPM, the model has been used interactively with a groundwater model to evaluate short-term and long-term effects on aquifer conditions and pumping lifts. Pumping costs vary by region depending on depth to groundwater and power rates. The SWAP model includes a routine to calculate the total costs of groundwater. The total cost of groundwater is the sum of fixed, O&M, and energy costs. Energy costs are based on a blend of agricultural power rates provided by PG&E.

For CVIRP, the SWAP model was updated for three development scenarios at each level of development, 2025, 2055, and 2085. Parameters in SWAP pertinent to the level of development and the approach proposed to update the parameters are listed in Table 24.The subsequent tables and sections summarize and review the individual components.

Table 24. Statewide Agricultural Production Model Level of Development Parameters

Parameter	Approach
Water Supplies	
Regional Supplies	Base regional supplies are based on CalLite results. For each of the alternatives under any level of development, data from the CalLite model will be used.
Local Supplies	Water agency estimates of imports (e.g. Mokelumne Aqueduct) and local surface water supplies are used and held constant under all development scenarios and level of development.
Groundwater	Regional maximum groundwater pumping capacities are estimated from DWR and individual district historical data. Groundwater pumping costs reflect changes in electricity costs as estimated by PG&E data.
Crop Demand	Agricultural demand estimates are updated with Water Plan Update population and income projections. SWAP includes an endogenous price routine used to estimate region and crop-specific prices under any level of development.
Crop Yield	Agricultural yield trends due to technological innovations are estimated based on existing literature, including Water Plan Update data.

Table 24. Statewide Agricultural Production Model Level of Development Parameters

Parameter	Approach
Perennial and Silage Constraints	
Perennial Rotations	SWAP incorporates an endogenous routine for an upper-bound on perennial retirement based on the average stand life for relevant crops.
Silage (Dairy Feed) Requirements	Dairy herd feeding requirements are estimated based on a review of literature and the expected size of the future dairy herd size.
Land Use (Urban Footprint)	Land use data are based on projections in the Water Plan Update and estimates from the Landis Model.

3.1.4. Water Supplies

Regional and local water supplies under the development scenarios and levels of development will be estimated from the CalLite model and agency-specific data. These data are incorporated as inputs to the SWAP model, thus each level of development will be different.

Maximum groundwater pumping capacity estimates are from a 2009 analysis by DWR in consultation with individual districts. Groundwater pumping capacity is intended to represent the maximum that a region can pump in a year given the aquifer characteristics and existing well capacities. For long run analysis, additional pumping capacity could be installed, but careful groundwater analysis should be made to determine hydraulic feasibility. If groundwater analysis is not available, existing capacity constraints are assumed to hold.

Groundwater pumping costs are calculated as two components, the fixed cost per acre foot based on typical well designs and costs within the region, plus the variable cost per acre foot. Energy costs depend on the price of electricity, which is expected to increase in the future. Expected future power costs are calculated using the California Department of Water Resources Forward Price Projections analysis using wholesale power costs. This calculates an average power cost for each month as the average of the peak (upper bound) and off-peak (lower bound) rates. An average of the monthly costs generates an average yearly cost.

Table 25 summarizes the water supply and cost data under the three levels of development.

Table 25. Statewide Agricultural Production Model Level of Development Parameters

Parameter	2025	2055	2085
Regional Supplies	Data are based on CalLite model results for each level of development.		
Local Supplies	Estimates will vary by Region.		
Groundwater Pumping Capacity	Fixed at 2009 DWR Analyst Estimates of Maximum Groundwater Pumping Capacities by region. This assumption could be changed, but careful groundwater analysis should be completed prior to adjusting the model.		
Groundwater Pumping Cost[a]	$0.275 / Kwh	$0.382 / Kwh	$0.525 / Kwh

[a] Costs are in 2005 dollars, the baseline year in SWAP calibration runs, although simulated future condition results can be indexed to any specified year.

3.1.5 Demand Shifts

Crop demands are expected to shift in the future due to increased population, higher real incomes, changes in tastes and preferences, and related factors. An increase in real income is expected to increase demand for agricultural products. Similarly, population increase is expected to increase crop demand. Crop demands are linear in the SWAP model, and population and real income changes induce a parallel shift in demand. The change in demand for global commodity crops and California-specific crops are considered separately since there is no California-specific demand for the former. The SWAP model assumes a constant export share into the future and uses exogenous income, population, and own-price elasticities of demand to estimate the shift in demand.

Population[14] projections are based on the U.S. Census Constant Net International Migration Scenario. This provides a forecast until 2050, beyond 2050 the average percent change in population per year is used. Real income per capita[15] projections are based on BLS data and a historic rate of inflation of 3.4 percent. Table 26 summarizes the change in real income and population (U.S. average) under the three levels of development. These data are combined with elasticity estimates to generate crop-specific demand levels at 2025, 2055, and 2085.

---

[14] Data from: Table 1-C. Projections of the Population and Components of Change for the United States: 2010 to 2050 Constant Net International Migration Series (NP2009-T1-C). Available at: http://www.census.gov/population/www/projections/2009cnmsSumTabs.html.

[15] Available at: www.bls.gov/opub/mlr/2007/11/art2full.pdf

Table 26. Statewide Agricultural Production Model Level of Development Parameters

Parameter	2025	2055	2085
U.S. Average per capita Income ($)	46,571	62,770	83,767
U.S. Population (thousands)	346,655	411,590	496,254

Note: The same values are assumed for all development scenarios

For purposes of the demand shift analysis, a distinction is made between two types of crops grown in California: California specific crops and global commodities. Global commodity crops include grain rice, and corn16; all other crop groups are classified as California crops. Global commodity crops are those for which there is no separate demand for California's production. For these crops, California faces a perfectly elastic demand, and is thus a price taker. It is assumed that California's export share will continue to remain small in the future. For California specific crops, California faces a downward sloping demand for a market that is driven by conditions in the United States and international export markets. SWAP holds California's export share and international market conditions constant we are able to estimate shifts based solely on United States conditions. The model does not incorporate changes in tastes and preferences, only the shift in demand for these crops that will result from increasing population and real income.

Since California is a small proportion of global production for commodity crops, the only necessary information to estimate the shift in future demand is the long run trend in real prices. A recent report by the World Bank (2009) projects price increases (in real terms) out to 2015 for rice, corn and grains. Many experts in the field believe this is an overestimate as long run real prices have been historically declining for these crops. To deal with this contradiction, at year 2015 SWAP allows the historical downward trend in real prices to resume. The SWAP model combines the projected near-term annual increases out to 2015, with the long run trend resuming in 2015 to estimate the total percentage demand shift (change in real price) for commodity crops.

A routine in the SWAP model calculates the demand shift depending on the level of development. Average percentage shift in demand are summarized in Table 27.

---

[16] Rice demand is very elastic but not perfectly elastic. For purposes of the demand shifting analysis, it is assumed to be perfectly elastic.

Table 27. Statewide Agricultural Production Average Percentage Shift in Demand

Parameter	2025	2055	2085
Almonds and Pistachios	1.04	1.09	1.13
Alfalfa	1.05	1.10	1.15
Corn	1.43	1.29	1.17
Cotton	1.04	1.08	1.12
Cucurbits	1.41	1.83	2.23
Dry Beans	1.05	1.10	1.15
Fresh Tomatoes	1.25	1.51	1.75
Grain	1.29	1.02	0.81
Onions and Garlic	1.41	1.83	2.23
Other Deciduous	1.04	1.08	1.12
Other Field	1.05	1.10	1.15
Other Truck	1.41	1.83	2.23
Pasture	1.00	1.00	1.00
Potatoes	1.27	1.54	1.81
Processing Tomatoes	1.25	1.51	1.75
Rice	1.52	1.32	1.15
Safflower	1.05	1.10	1.15
Sugar Beet	1.00	1.00	1.00
Subtropical	1.04	1.08	1.12
Vine	1.19	1.37	1.56

Note: The same values are assumed for all development scenarios

3.1.6 Technological Innovation

Projected yield increases due to technological innovations are based on extrapolating current trends based on a review of the current literature.[17] Historically, yields have been increasing at an exceptional rate, however spending on agricultural R&D has begun to wane and there is an inherent limit to the rate of carbon fixation through photosynthesis . Thus, the SWAP model allows yield changes to level out and the technological growth rate is capped at 0.25 percent per year starting in 2020.

---

[17] Brunke, H., D. Sumner, and R. E. Howitt. 2004. "Future Food Production and Consumption in California Under Alternative Scenarios." Agricultural Issues Center, University of California, Davis, California.

Table 28 summarizes the average rate of technological change (percent per year) for the twenty crop groups in the SWAP model until 2020. Percentage yield increase is capped at 0.25 percent per year, for all crops, starting in 2020. These data are used to estimate crop yields at 2025, 2055, and 2085.

Table 28. Statewide Agricultural Production Model Level of Development Parameters

Crop Group	Average Technological Change Rate (% per year)	Crop Group	Average Technological Change Rate (% per year)
Almonds and Pistachios	1.57	Other Field	1.2
Alfalfa	1.2	Other Truck	1.01
Corn	1.01	Pasture	1.2
Cotton	1.2	Potatoes	1.01
Cucurbits	1.01	Processing Tomatoes	1.75
Dry Beans	1.2	Rice	1.35
Fresh Tomatoes	1.75	Safflower	1.2
Grain	1.2	Sugar Beet	1.2
Onions and Garlic	1.01	Subtropical	1.17
Other Deciduous	1.57	Vine	0.9

Note: The same values are assumed for all development scenarios in 2025, 2055, and 2085

Table 29 shows the resulting percentage change in yield under the three levels of development. This includes the cap in growth rate at 0.25 percent per year starting in 2020 due to agronomic production constraints.

Table 29. Statewide Agricultural Production Percentage Change in Yield

Parameter	2025	2055	2085
Almonds and Pistachios	1.20	1.21	1.22
Alfalfa	1.26	1.27	1.28
Corn	1.16	1.17	1.18
Cotton	1.20	1.21	1.22
Cucurbits	1.16	1.17	1.18
Dry Beans	1.20	1.21	1.22

Table 29. Statewide Agricultural Production Percentage Change in Yield

Parameter	2025	2055	2085
Fresh Tomatoes	1.30	1.31	1.32
Grain	1.20	1.21	1.22
Onions and Garlic	1.16	1.17	1.18
Other Deciduous	1.26	1.27	1.28
Other Field	1.20	1.21	1.22
Other Truck	1.16	1.17	1.18
Pasture	1.20	1.21	1.22
Potatoes	1.16	1.17	1.18
Processing Tomatoes	1.30	1.31	1.32
Rice	1.22	1.23	1.24
Safflower	1.20	1.21	1.22
Sugar Beet	1.20	1.21	1.22
Subtropical	1.19	1.20	1.21
Vine	1.15	1.15	1.16

Note: The same values are assumed for all development scenarios

3.1.7. Climate Change Effects

Climate change is expected to have two key effects on agriculture in California, including changing water requirements and crop yields. Climate change is expected to affect air temperatures in production regions and increase the frequency and duration of extreme weather events. Additionally, carbon dioxide levels in the atmosphere are expected to change. Temperature change will affect crop yields. Some crops, such as grains will suffer with warmer temperatures as seeds have less time to grow and mature, other crops, such as tomatoes, will benefit due to an increased growing season. Similarly, higher carbon dioxide level may increase yields in many crops but these effects exhibit diminishing marginal returns and, at some point, may negatively affect yields. Additionally, crop water requirements will change as warmer weather may require additional water application. The effects of climate change on agriculture are incorporated in the SWAP model from output from the LAWS agronomic climate model. Since SWAP is an economic model, the relevant climate effects include changes in applied water requirements per acre and yield per acre. Applied water and yield change under the three climate scenarios considered for CVPIRP.

Davis, Gerber, Firebaugh, and Shafter yield estimates under Q2, Q4, and Q5 climate scenarios are provided from the LAWS model. These regions are assigned to the corresponding SWAP model regions to estimate the percent change in crop yield under the 3 climate scenarios. Table 30 summarizes the average change

(total percent) for the twenty crop groups in the SWAP model in 2025, 2055, and 2085 under the three climate scenarios. These are incorporated as a set of adjustment constraints to the endogenously calibrated production functions in SWAP. In other words, the base calibrated production technology is allowed to hold and crop yields are adjusted by the corresponding percent, no model recalibration occurs between these steps. This is consistent with previous climate change studies using the SWAP model. All percentage change estimates are relative to the base reported in the LAWS model in order to ensure consistency.

Davis, Gerber, Firebaugh, and Shafter applied water per acre estimates under Q2, Q4, and Q5 climate scenarios are provided from the LAWS model. These regions are assigned to the corresponding SWAP model regions to estimate the percent change in crop applied water requirements per acre under the 3 climate scenarios. Table 31 summarizes the average change (total percent) for the twenty crop groups in the SWAP model in 2025, 2055, and 2085 under the three climate scenarios. These are incorporated as a set of adjustment constraints to the endogenously calibrated production functions in SWAP. In other words, the base calibrated production technology is allowed to hold and crop water requirements are adjusted by the corresponding percent, no model recalibration occurs between these steps. This is consistent with previous climate change studies using the SWAP model. All percentage change estimates are relative to the base reported in the LAWS model in order to ensure consistency.

Table 30. Average Change in Crop Yield under each Climate Scenario (Percent)

	Alfalfa	Almonds and Pistachios	Corn	Cotton	Cucurbits	Dry Bean	Fresh Tomatoes	Grain	Onions and Garlic	Other Deciduous
2025										
Q4	7.37	-0.45	-0.47	6.27	11.53	9.93	9.81	12.98	6.03	4.60
Q5	6.68	-2.72	-2.00	6.53	10.45	9.05	8.84	13.63	5.69	2.38
Q2	6.26	-4.73	-3.78	6.20	9.32	7.83	7.21	14.04	5.27	0.73
2055										
Q4	18.48	-2.30	-3.45	13.60	26.53	24.93	25.78	26.66	14.26	12.23
Q5	13.48	-5.63	-6.62	13.37	25.13	23.82	23.66	28.52	13.16	9.42
Q2	17.88	-8.69	-9.40	13.73	24.33	24.67	24.42	29.83	12.70	8.03
2085										
Q4	25.77	-6.13	-9.22	17.21	35.92	35.7	36.52	36.92	18.63	16.28

						5				
Q5	27.25	-11.60	-15.62	17.97	37.94	40.64	41.46	41.71	18.15	15.44
Q2	24.64	-19.09	-24.08	15.54	31.44	38.49	38.28	42.24	13.73	9.80

	Other Field	Other Truck	Pasture	Potato	Processing Tomatoes	Rice	Safflower	Sugar Beet	Subtropical	Vine
2025										
Q4	0.98	12.33	5.41	3.23	1.72	6.71	3.88	0.73	-0.32	3.03
Q5	-0.58	13.85	6.17	2.00	-1.68	5.06	4.12	-1.71	-4.67	0.37
Q2	-2.24	15.00	6.20	1.33	-5.63	3.28	4.52	-3.58	-8.20	-1.82
2055										
Q4	-0.35	28.42	11.37	7.89	5.38	16.18	9.39	2.14	0.06	9.12
Q5	-3.06	30.45	11.78	5.58	-1.51	13.81	8.86	-1.97	-5.81	5.92
Q2	-5.42	33.12	12.01	4.55	-5.49	12.28	9.56	-4.54	-9.79	4.44
2085										
Q4	-4.25	39.44	13.75	8.58	4.93	22.27	11.79	0.45	-1.01	12.73
Q5	-9.45	46.17	14.06	6.44	0.61	22.68	12.38	-3.91	-6.15	12.17
Q2	-17.39	48.40	11.68	0.83	-12.09	14.49	10.91	-11.91	-14.87	7.12

Table 31. Statewide Agricultural Production Model Climate % Change Applied Water Requirement Parameters

	Alfalfa	Almonds and Pistachios	Corn	Cotton	Cucurbits	Dry Bean	Fresh Tomatoes	Grain	Onions and Garlic	Other Deciduous
2025										
Q4	1.44	1.51	0.40	1.41	1.64	1.16	1.70	1.62	2.17	1.46
Q5	2.83	3.42	1.87	2.06	2.24	2.34	2.74	2.55	3.63	3.45
Q2	3.95	4.81	2.30	2.09	2.65	2.77	3.33	2.87	4.36	5.02
2055										
Q4	0.72	0.22	-0.69	2.12	2.04	0.80	2.03	0.15	2.97	0.44
Q5	2.34	2.23	0.15	2.58	3.06	1.86	3.14	1.51	4.84	2.78
Q2	3.21	3.04	-0.01	2.26	2.77	2.17	3.51	0.94	4.92	3.55
2085										
Q4	-1.04	-2.52	-6.17	-1.58	-1.47	-2.98	-0.82	-4.87	0.37	-2.98
Q5	-2.33	-3.73	-9.81	-3.06	-3.17	-4.87	-2.24	-7.78	-0.86	-4.00
Q2	-1.52	-3.60	-11.78	-5.41	-4.27	-5.49	-2.36	-10.60	-1.43	-3.07

	Other Field	Other Truck	Pasture	Potato	Processing Tomatoes	Rice	Safflower	Sugar Beet	Subtropical	Vine
2025										
Q4	1.64	1.77	0.55	1.28	0.94	0.84	0.86	1.72	-0.31	-3.68
Q5	2.46	2.56	1.77	2.35	2.00	0.58	2.19	2.87	1.01	-3.78
Q2	3.02	3.29	2.68	3.12	2.29	-0.10	2.89	3.78	1.91	-4.40
2055										
Q4	0.16	2.25	-1.25	0.75	1.10	-1.92	-1.03	2.16	-3.50	-8.71
Q5	1.30	3.30	0.09	2.24	1.67	-1.08	0.74	3.72	-2.16	-8.82

Q2	1.17	3.03	0.38	2.50	1.66	1.46	0.29	4.22	-1.92	-9.57
2085										
Q4	-5.32	-1.04	-4.82	-3.22	-1.92	-6.49	-7.41	-0.51	-7.76	-9.95
Q5	-9.02	-2.59	-7.50	-5.36	-3.53	-9.27	-11.26	-1.81	-10.18	-11.11
Q2	-11.27	-3.61	-8.88	-6.37	-4.75	-10.22	-13.24	-2.30	-10.51	-10.85

3.1.8. Perennial and Silage Constraints

A regional silage constraint for dairy herd feed is included in the model. The silage constraint forces production to meet the feeding needs of the California dairy herd, for each region. For example, each cow consumes 45 pounds of silage per day or about 8.2 tons annually and corn grain yields are 30 tons per acre thus each cow requires about 0.27 silage acres per year. Multiplying the silage acres per cow per year by the number of cows in each region yields the minimum silage requirement. Currently, the model assumes a constant herd size into the future, though additional information about future of herd sizes could be used.

Perennial crops in the SWAP model have a bearing life of between 25 and 30 years (with the exception of alfalfa). A portion of these acres will naturally be due for retirement any given season. Given the large establishment cost it is rare that farmers pull young fields out of production when facing water or other resource shortages. The SWAP model has a routine which calculates the maximum natural perennial retirement based on the time horizon of the analysis. For an analysis less than 30 years in the future only some portion of perennials will be up for natural retirement. As the time horizon of the analysis approaches the maximum bearing life of the perennial, any proportion may be removed from production.

3.1.9 Land Use Change

Urbanization and agricultural land conversion in this study follow estimates from the Landis model and analysis by Land Use Analysts at DWR for prime farming land, locally important farms, unique farms and grazing lands. Most of the land conversion from agriculture occurs south of the Sacramento Valley, where population growth is rapid. A statewide reduction in irrigated agricultural land use close to 25 percent is expected by 2085.

Table 32 shows statewide and regional land use patterns (total irrigated agricultural land) under the three levels of development by DWR hydrologic regions. PPIC developed low and expansive growth scenarios based on Landis land-use projections for 2020, 2050, and 2100. Land Use Analysts at DWR developed an intermediate scenario for 2020, 2050, and 2100 using additional data and adjustments to some of the assumptions used in the Landis model.

Estimates for 2025, 2055, and 2085 are determined by linear extrapolation using estimates from low, current, and expansive growth scenarios.

In the SWAP model, these data are disaggregated by SWAP region and included as a regional constraint on total irrigated land area. These constraints impose a reduction in irrigated agricultural land consistent with the expected future urban footprint. The data are disaggregated from hydrologic region to SWAP region and the SWAP model is used to estimate the optimal response by farmers, resulting crop mix, and intensive margin adjustments. This is consistent with expectations that farmers will adjust production in response to a shrinking total land area. This methodology has been used in numerous applications of the SWAP model, most recently for a climate change analysis which has been peer-reviewed and published (Medellin-Azuara et al. 2011).

Table 32. Statewide Agricultural Production Model Irrigated Acres

Hydrologic Region	Development Scenario	2025	2055	2085
North Coast	Slow Growth	326,209	321,907	309,764
	Current Trends	323,163	304,210	261,487
	Expansive Growth	319,101	285,939	222,026
San Francisco Bay	Slow Growth	88,956	88,808	89,175
	Current Trends	87,268	81,414	76,303
	Expansive Growth	85,118	76,041	68,569
Central Coast	Slow Growth	443,690	442,990	448,594
	Current Trends	436,341	403,246	363,730
	Expansive Growth	422,577	360,626	286,300
South Coast	Slow Growth	216,392	210,378	203,353
	Current Trends	207,071	177,258	149,967
	Expansive Growth	193,574	139,784	81,464
Sacramento River	Slow Growth	1,896,169	1,863,267	1,790,416
	Current Trends	1,876,536	1,786,251	1,600,504
	Expansive Growth	1,865,350	1,733,975	1,483,815
San Joaquin River	Slow Growth	1,882,026	1,806,036	1,719,137
	Current Trends	1,848,424	1,690,252	1,535,251
	Expansive Growth	1,827,293	1,609,503	1,357,859
Tulare Lake	Slow Growth	2,951,252	2,859,088	2,761,110
	Current Trends	2,901,425	2,661,889	2,378,904

Table 32. Statewide Agricultural Production Model Irrigated Acres

Hydrologic Region	Development Scenario	2025	2055	2085
North Lahontan	Expansive Growth	2,870,096	2,542,861	2,131,076
	Slow Growth	128,114	125,364	114,625
	Current Trends	127,294	119,805	91,718
	Expansive Growth	126,742	118,107	88,801
South Lahontan	Slow Growth	63,120	60,962	56,496
	Current Trends	61,602	57,471	48,549
	Expansive Growth	59,396	53,659	40,383
Colorado River	Slow Growth	572,069	553,791	516,215
	Current Trends	561,817	531,912	488,688
	Expansive Growth	553,376	502,737	387,454
Statewide Total	Slow Growth	8,567,998	8,332,591	8,008,885
	Current Trends	8,430,940	7,813,708	6,995,102
	Expansive Growth	8,322,624	7,423,232	6,147,748

References

Brunke, H., D. Sumner, and R. E. Howitt. 2004. "Future Food Production and Consumption in California Under Alternative Scenarios." Agricultural Issues Center, University of California, Davis, California.

County Agricultural Commissioners. Annual Crop Reports. Various years, various counties. Available at http://www.nass.usda.gov/Statistics_by_State/California/Publications/AgComm/Detail/index.asp.

DWR (California Department of Water Resources). 2009a. Least Cost Planning Simulation Model. Division of Planning and Local Assistance. Sacramento, California. Available at URL http://www.water.ca.gov/economics/downloads/Models/LCPSIM_Draft_Doc.pdf

DWR. (California Department of Water Resources). 2009b. California Water Plan Update, 2009. Bulletin 160-09. Sacramento, California

Howitt, R.E. 1995. Positive Mathematical-Programming, American Journal of Agricultural Economics, 77(2), 329-342.

Howitt, R.E., D. MacEwan, and J. Medellin-Azuara 2009a. Economic Impacts of Reductions in Delta Exports on Central Valley Agriculture, in Agricultural

and Resources Economics Update, edited, pp. 1-4, Giannini Foundation of Agricultural Economics, Davis, California.

Lund, J., E. Hanak, W. Fleenor, R. Howitt, J. Mount, and P. Moyle. 2007. Envisioning Futures for the Sacramento-San Joaquin Delta. Public Policy Institute of California, San Francisco, California.

M.Cubed. 2007. Re: Proposed Method for Calculating Customer Shortage Costs for Use in WSMP 2040 Portfolio Evaluations. October 18. http://www.ebmud.com/our-water/water-supply/projects-and-long-term-planning/water-supply-management-program/water-supply-1

Medellin-Azuara, J., Howitt, R.E., MacEwan, D., and J.R. Lund. (2011). Economic Impacts of Climate-Related Changes to California Agriculture. Climatic Change. 109 (Suppl 1), 387-205.

Metropolitan (Metropolitan Water District of Southern California) and Reclamation (U.S. Bureau of Reclamation). 1999. Salinity Management Study: Final Report, Technical Appendices. June.

Muth, R.F.: 1964, 'The Derived Demand Curve for a Productive Factor and the Industry Supply Curve', Oxfpord Economic Papers 16, 221-234.

Reclamation (U.S. Bureau of Reclamation) and USFWS (U.S. Fish and Wildlife Service). 1999a. Central Valley Project Improvement Act Programmatic Environmental Impact Statement. Mid-Pacific Region. Sacramento, California.

Reclamation (U.S. Bureau of Reclamation) and USFWS (U.S. Fish and Wildlife Service). 1999b. Central Valley Project Improvement Act Programmatic Environmental Impact Statement, Technical Appendix, Volume 8. Mid-Pacific Region. Sacramento, California.

Reclamation (U.S. Bureau of Reclamation). 2006. Initial Economic Evaluation for Plan Formulation. Los Vaqueros Expansion Investigation. Mid-Pacific Region. Sacramento, California.

Reclamation (U.S. Bureau of Reclamation). 2008. Upper San Joaquin River Basin Storage Investigation. Plan Formulation Report. Mid-Pacific Region. Sacramento, California

University of California Cooperative Extension (UCCE). Cost of Production Studies. Various Crops and Dates. Department of Agricultural and Resource Economics. Davis, California. URL = http://coststudies.ucdavis.edu.

World Bank: 2009, 'Double Jeopardy: Responding to High Fuel and Food Prices', in G8 Hokkaido-Toyako Summit, July 2.

APPENDIX 6F — DETAILED EVALUATION FACTORS AND RATINGS

			Option Characterization Rating Criteria				
			A	**B**	**C**	**D**	**E**
1	Quantity of Yield	Average af per year	> 500	> 350	> 250	> 100	< 100
2	Timing	Years before option could begin operation	< 5	< 10	< 20	< 30	> 30
3	Cost	Annual dollars per af, Present Worth	< 500	< 1000	< 2000	< 3000	> 3000
4	Technical Feasibility	5-pt qualitative scale	Regularly implemented in U.S. at scale proposed	Occasionally implemented somewhere in the world at similar scale	Regularly implemented but at smaller scales	Occasionally implemented somewhere in the world or has not been done, but peer review articles indicate promise	Has not been done and no peer review articles exist or they indicate challenges
5	Permitting	5-pt qualitative scale	Does not require an EIS or other major permits	Requires an EIS or other major permits, but similar projects of this scale have been approved in the past 20 years	Requires an EIS or other major permits, but similar projects of smaller scale have been approved in the past 20 years	Requires an EIS and no precedent exists for the option.	Requires an EIS and similar options have been declined during the permit process
6	Legal	5-pt qualitative scale	Consistent with current legal framework	Local laws may require changes, but consistent with current federal legal framework	Federal or interstate legal action is required but precedent shows item can be addressed	Federal legal action is required, no precedent exists, and timeframe or likelihood of success is unknown	Federal legal action is required and precedent shows that the legal challenges may not be overcome
7	Policy Considerations	5-pt qualitative scale	Consistent with current local and federal policies	Local policies may require changes, but precedent shows can be publicly acceptable	Changes to federal or interstate policy is required but precedent shows public acceptance is likely	Changes to local or federal policy is required, and public acceptance is unknown	Changes to local or federal policy is required, and public acceptance is unlikely
8	Implementation Risks	5-pt qualitative scale	No major implementation risks	Some implementation risks, but risks can be managed	Multiple implementation risks, but may be managed	Multiple implementation risks, ability to manage risks is unknown	Multiple implementation risks and ability to manage risks is low

			Option Characterization Rating Criteria				
			A	**B**	**C**	**D**	**E**
9	Long-term Viability	5-pt qualitative scale	No major risks	Some viability risks	Multiple, but limited risks	Multiple, moderate risks	Multiple, significant risks
10	Operational Flexibility	5-pt qualitative scale	Option can be operated/idled in any year with no financial implications	Option can be operated/idled in any year with limited financial implications	Option can be operated/idled in any year with moderate financial implications	Option can be operated/idled in any year with significant financial implications	Option does not have the flexibility to be operated or idled from year to year
11	Energy Needs	kWh/af	Requires no energy, or results in net positive generation	< 1000	< 3000	< 5000	> 5000